Dissertations - ALL   SURFACE

Crosslinked Hyaluronic Acid Hydrogel Networks Designed as Mechanical Actuators

Pushkar S. Varde
Syracuse University

Follow this and additional works at: https://surface.syr.edu/etd

Part of the Engineering Commons

Abstract

Bioengineers are in constant pursuit of solutions to problems facing the medical and pharmaceutical field by designing biomaterials that closely mimic the target natural systems. A unique collection of polymers, known as polymeric actuators, have been devised with the ability to convert an external stimulus to a change in shape, size or permeability. The current options within polymeric biomaterials with multi-functionality include matrices that are biocompatible, biodegradable, quick transitioning / shape changing, and mechanically tunable. These properties have been harnessed for application such as stents, valves, semi permeable membranes, and dynamic cell culture substrates. For such applications quick and uniform actuator response that does not need to be sustained for more than a few hours is desired. However there exist other areas of biomedical applications, such as wound closure/healing and nerve regeneration, where polymeric actuators have been underutilized. These applications however call for a polymer system that can actuate at controlled slow speeds and sustain this actuation for several days. At present there is a lack of such slow actuating polymer system. Each year over 50,000 peripheral nerve repair procedures are performed (National Center for Health Statistics, 1995). The total annual costs in U.S alone exceed $ 7 billion (American Paralysis Association, 1997). The treatment of a nerve transection is dependent on the size of the injury gap. Similarly, the extent of regeneration and re-innervation in the PNS is also governed by the size of the gap. For a smaller gap (<10 mm) the surgeon can pull the severed nerve ends closer and suture them to repair the injury. For larger gaps autologous nerve transplant is the gold standard treatment despite the inherent disadvantages. Over the past decades biomaterial researchers have tested several polymeric nerve conduits as an alternative to autologous nerve grafts. However none have been able to match the success rates of autologous grafts. There is a lack of an effective

biomaterial solution to the problem of a large gap nerve injury. For many years there has been a hypothesis that nervous tissue can be successfully elongated via application of an external mechanical force alone which could be used to treat peripheral nerve gap injuries. Mechanical actuation studies have been shown to produce successful stretch growth in individual axons and axonal bundles. This phenomenon is at play in nature during embryonic growth and development of the body of organisms to adulthood. Applying tensional forces at appropriate rates ($<$ 100 µm/hr) causes sustained axonal stretch growth. The solution we propose in this work is a biomaterial that can be programmed to perform the function of a mechanical actuator at rates suitable for axonal stretch growth. We designed, fabricated, and characterized a novel hyaluronic acid based hydrogel that shrinks over time along a pre-defined axis thereby providing the source for tension that could be used for sustained axonal stretch growth. The shear thinning property of hyaluronic acid (HA) enabled us to test if we could store a retractive stress in a rapidly crosslinked network under shear flow and then controllably release this stress and achieve shrinkage of the network scaffold along one desired axis. We investigated two strategies to achieve this goal. The retractive stress trapped in the crosslinked network was released either by manipulating the main backbone HA chains or by selectively breaking the crosslinks. The shrinkage rates obtained were within the range of stretching rates that have successfully stretched neuronal cells. We also confirmed that the material's cytocompatibility was unaffected by the chemical modifications that HA was subjected to. This polymer system is a novel addition to the existing polymeric actuators and is a step towards filling the void of a slow, long term actuating polymer.

Crosslinked Hyaluronic Acid Hydrogel Networks Designed as Mechanical Actuators

By

Pushkar S. Varde

M.S., Syracuse University, NY, 2009

Dissertation

Submitted in partial fulfillment of the requirements for the degree of Doctor of Philosophy
in the field of Biomedical Engineering in the Graduate School of Syracuse University

Syracuse University

May 2015

Acknowledgements

First and foremost I would like to thank my parents. Without their support, motivation, unconditional love, and the values they instilled in me I would not be the person I am today. Next in line would be my sister who has forever been the person I have looked up to and tried to match. She set the bar pretty high and all my life I have tried to make sure I get closer to if not someday raise that bar. My adviser Dr. Hasenwinkel deserves my heartfelt gratitude. She guided me, mentored me through my graduate school journey. There were some occasions when I had lost focus of the task at hand, due to unforeseen delays or unsuccessful experimental outcomes, however she made sure I did not stray from the path. Dr. Rebecca Bader decided to mentor a non-chemistry major student like me, answer my obvious questions, and help me transform myself into a decent polymer chemist. This dissertation would not have been possible without her guidance. For that I am thankful. I would also like to thank Dr. Sandra Hewett and her lab for generous donation of the primary cortical neurons and technical protocols for working with the cell type.

My girlfriend, Amanda Carbone, has been my rock during the entire course of my PhD education. I am extremely lucky to share my life with her. She was always the rational voice and the reason I worked harder through all the frustrations and difficulties of my research. The last couple of years have been tense in terms of my financial situation. I am forever indebted to her for standing by me when I needed her the most. The entire Carbone family made me forget that I was thousands of miles away from my home. They are some of the nicest, warm, and genuine people I have met in my life so far. Syracuse is my new home. They treated me as one of their own. I cannot thank them enough for making my life seem normal and keep me sane.

Next I would like to thank the faculty and staff that helped me during my course work and research. Sally Prasch, "The glass lady", knew soon after the first job I brought to her that my jobs would be synonymous to "new challenge". She never failed my expectations and I am thankful for that. Bill

TABLE OF CONTENTS

Chapter IV: Poly(ethylene glycol)-poly(lactic acid)-diacrylate crosslinked hydrogels

Chapter V: Study of the crosslinked HAGMa hydrogel-cell interaction

List of Figures

ends and the middle of the sample. The arrow indicates the direction of flow of the pre-crosslinking solution in the glass mold prior to rapid crosslinking. The retardance for this composition calculated from the captured spectra was 50.06 ± 10.95 nm. The magnification was 20X...64

Fig.3.12. Polarized optical micrographs of three 60 mg/ml HAGMa hydrogels crosslinked with 4:1 ratio of PEGDa after exposure to 10 µg/ml hyaluronidase for 48hrs. Images were captured at the two ends and the middle of the sample. The arrow indicates the direction of flow of the pre-crosslinking solution in the glass mold prior to rapid crosslinking. The retardance for this composition calculated from the captured spectra was 15.28 ± 1.25 nm. The decrease in the retardance compared to the value obtained before enzymatic degradation indicated loss of molecular orientation in the sample. The magnification was 20X..65

Fig.3.13. Bar graph summarizing the retardance values calculated for the PEGDa crosslinked HAGMa hydrogel samples prior to and following enzymatic degradation. The significant decrease in the retardance for the two compositions following enzymatic degradation indicated that the process of degradation reduced the molecular orientation in the hydrogels. (n=3)..........66

Fig.3.14. Bar graph summarizing the results from the negative control samples of PEGDa crosslinked HAGMa hydrogels. The negligible change in the retardance values of the samples after 2 days indicated that the reduction in molecular orientation seen in the samples exposed to the enzyme was truly on account of the degradation. (n=3)...67

Fig.3.15. Bar graph showing the predicted values of retractive stress stored in the two compositions of PEGDa crosslinked HAGMa hydrogel samples. There was no statistically significant difference observed between the two compositions although the averages seemed to scale with the increase in PEGDa concentration. (n=3)...68

Fig.3.16. Graph showing enzyme driven shrinkage profile for PEGDa crosslinked HAGMa hydrogel samples exposed to hyaluronidase for 48 hrs. The controls were not exposed to the enzyme. Panels a, c, and e show the profiles for 3:1 ratio PEGDa samples while panels b, d, and f show profiles for 4:1 ratio PEGDa crosslinked samples. Increase in concentration of the enzyme increase the magnitude of shrinkage. The composition 60 mg/ml HAGMa crosslinked with 4:1 ratio PEGDa demonstrated a linear shrinkage profile when exposed to 10 µg/ml hyaluronidase. (n=3)..69

Fig.3.17. Average sample length profiles for the negative control samples. (a, c) When the 3:1 PEGDa crosslinked HAGMa samples were exposed to hyaluronidase for duration of 48 hrs, the shrinkage was on par with control samples which were not exposed to any enzyme. (b, d) The 4:1 ratio PEGDa negative control samples showed similar insignificant shrinkage when exposed to hyaluronidase. (n=3)..71

List of Tables

CHAPTER 1

INTRODUCTION

1.1 **Polymeric actuators**: Bioengineers are in constant pursuit of solutions to problems facing the medical and pharmaceutical field by designing biomaterials that closely mimic the target natural systems. The rapid advancements in microtechnology have created demands of devices and smart materials that can function as actuators at the micro and macroscale (1, 2). Fabrication techniques, such as 3D printing, photolithography etc, have tremendously increased our capabilities of accurate micro-fabrication. In nature, the muscle tissue is the best example of an actuator where an electrical impulse stimulus causes conversion of ATP to ADP which is used to produce contraction of the muscle tissue (3). This natural system has been the inspiration to design artificial actuating polymers that could find use in robotics and as muscle prostheses (3). Polymeric actuators are defined as materials that can convert some form of stimulus to a transformation in the material (1, 3-5). This transformation is usually either a change of shape or size of the material. This change can be harnessed to perform the function of a mechanical actuator, a valve, optical modulators, or a drug delivery system (1-4, 6). The stimulus could be a change in temperature, pH, electric field, magnetic field, or crosslink density. Depending on the design of the polymer these stimuli can lead to reversible or irreversible swelling/de-swelling, bending, shrinking, or shape recovery of the polymer matrix. A homogeneous change in the polymer matrix usually leads to the swelling/de-swelling or shape recovery. The complex transformations like bending, twisting require an inhomogeneous change in the polymer matrix (1).

There are three main groups of polymeric actuators that can be used for biomedical application; hydrogel based actuators, electro active polymers (EAP), and shape memory

1

polymers (SMP) (1-3, 5). Hydrogels are three-dimensional matrices that are highly saturated with water which can reach as high as 99% of the gel mass (7). Thus swelling and de-swelling process is the most common way by which hydrogels can be actuators. The most well studied hydrogel actuator is the thermoresponsive poly (N-isopropylacrylamide) (PNIPAAm) (1, 5, 8, 9). The change in the properties of PNIPAAm is caused by the change in conformation above and below a threshold temperature called lower critical solution temperature (LCST). Above this temperature the expanded coil (soluble chains) conformation transitions to a compact (insoluble) conformation (2, 5). The LCST of PNIPAAm is 32°C which can be modulated by copolymerizing with either hydrophobic or hydrophilic segments (2). Consequently this polymer has been used quite extensively for drug delivery application.

Crosslinking PNIPAAm in the presence of proteins or drug molecules encapsulates them in the bulk of the gel. If the drug is hydrophilic then the release can be triggered below LCST where the gel's permeability is greater. However if the drug is hydrophobic then it will be squeezed out above LCST when the gel collapses (2, 8, 9). Gutowska et al. synthesized thermoresponsive PNIPAAm gels by copolymerizing with butyl methacrylate (BMA) (hydrophobic) or acrylic acid (AAc) (hydrophilic) co-monomers (10). The incorporation of hydrophobic and hydrophilic co-monomers strongly influenced the swelling/shrinking behavior of the gels. The gels were loaded with heparin below the network LCST. When the transition temperature was reached the gel demonstrated rapid de-swelling as a result of the network collapse. This collapse was very rapid and almost all of the transition occurred in less than an hour. The heparin release from swollen PNIPAAm/BMA and PNIPAAm/AAc

gels showed that release profiles correlated with de-swelling kinetics of gels. The release profile showed two distinct kinetics controlled by different mechanisms: an initial rapid release, due to the network collapse (squeezing effect) and the subsequent slow release controlled by the rate of solute diffusion within the collapsed matrix. The total network collapse, triggered by the LCST, occurred in less than 30 mins.

Polymeric actuators that respond to pH changes have also been well documented (1, 2, 5). Polyacids like poly (acrylic acid) and polybases like poly (N,N'-diethylaminoethyl methacrylate) are ideal examples of polymers that change conformation due to a change in their ionic environment. Networks designed using both thermoresponsive and pH responsive elements provide a multi-responsive actuator that is equipped to respond to subtle changes in its environment. Such networks can be deployed to release necessary proteins or antibiotics at an injury or inflammation site where the pH and temperature change based on the level of inflammation. Brazel et al. (11) synthesized poly (*N*-isopropylacrylamide-co-methacrylic acid) hydrogels and investigated pH- and temperature-triggered delivery of antithrombotic agents, streptokinase and heparin. The gels were triggered in a pulsatile on-off fashion by changing the temperature and pH. They observed that for hydrogels containing greater than 75 mol% NIPAAm, the pH and temperature sensitivity both influenced the overall swelling behavior of the networks. The transition as a result of reduction of pH or increase in temperature or both is rather quick with complete equilibrium swelling occurring within an hour. Release of the drugs occurred when the gels were in the swollen (expanded coil) state.

The swelling/de-swelling property of hydrogel based actuators has also been exploited to cause mechanical motion. Hu et al. fabricated a "bigel strip" out of polyacrylamide (PAAM) and N-isopropylacrylamide (NIPA) such that the PAAM layer is interpenetrating in to the NIPA gel block for a few millimeters (12). PAAM was unresponsive to temperature changes while NIPA changed conformation above its LCST (37°C). When the "bigel strip" was exposed to 37°C, the NIPA layer contracted while PAAM did not thereby causing the gel block to bend in the direction of the NIPA gel block to almost a complete circle. By making variations in the position of NIPA regions with respect to PAAM regions, more complex bending was also achieved. The bending was reversed by changing the solvent from water to a combination of water and acetone and reducing the temperature below LCST. The authors posited that such a polymeric actuator can find use as biological grasping tweezers. The total time for the actuation process to reach its peak was of the order of 10 to 20 mins and the maximum bending strain was calculated to be 49%. Similar efforts to fabricate bending hydrogels via pH sensitive route have been undertaken by Topham et al. They synthesized a pH sensitive triblock polymer gel strip consisting both polyacid and polybases (13). The polyacid hydrogel comprised of a poly(methyl methacrylate)-block-poly(methacrylic acid)-block-poly(methyl methacrylate) [PMMA--PMAA--PMMA] triblock copolymer, synthesized via anionic polymerization and the polybase hydrogel comprised of a poly (methylmethacrylate)-block-poly(2-(diethylamino)ethyl methacrylate)-block-poly(methyl methacrylate) [PMMA--PDEA--PMMA] triblock copolymer, synthesized via group transfer polymerization. At low pH (3.7) the bilayers bent in the direction of the polyacid as this layer shrunk while the opposite was observed at high pH (7.3). This process was successfully repeated for several cycles. The bending was very rapid. The authors believe

this phenomenon would still function even at much smaller length scale and see the use of this actuator as a pH sensitive valve in microfluidic devices. Thus the hydrogel based polymeric actuators have been successfully designed to perform macro and micro-mechanical actuations. The response time for the trigger to translate to actuation ranges between instantaneous to several minutes (2, 3, 5, 6, 8, 9, 11, 14).

Polymeric actuators that can produce even faster transition times fall in the class of electro active polymers. The basic modus operandi for the polymeric EAP's, also known as bioresponsive gels, is a microscopic or macroscopic event (swelling / de-swelling) as a direct result of an external electric stimulus. EAP's have two main categories, electronic EAP's where an electric field causes change in volume of the polymer and ionic EAP's where there is electrically-induced transport of ions and/or solvent (3). Another critical difference between the two EAP's is that the ionic EAP's operate in a liquid electrolyte medium, while the electronic EAP's are used in air. The ionic EAP's are thus particularly attractive for use within biological environments. Within each group there are a wide variety of specific actuation mechanisms. This response is manifested as an optical, chemical or mechanical signal (3). Electronic EAPs include piezoelectric polymers, electrostrictive polymers, flexoelectric polymers, and dielectric elastomers. The ionic EAPs include polymer gels, ionic polymer-metal composites (IPMC), conducting polymers, and carbon nanotubes (3). For the ionic EAP's, modifying chemical crosslinking density is the most common form of stimulus to cause a change in the property of hydrogels. This can be done by either cleaving polymer chains (irreversible) or by creating competition at the binding sites (reversible).

Liang et al. fabricated a poly (vinyl alcohol)/dimethylsulfoxide (PVA/DMSO) hydrogel which could be driven in air using a DC electric field (15). This gel is an ideal example of an electronic EAP. The physically crosslinked PVA gels were swollen in DMSO. DMSO is the component that interacts with the external electric field and is able to transfer the charges to the gel-substrate interface and act as a whole within the PVA network gel to cause motion. When the applied field exceeded a threshold value, the gel demonstrated a continuous and linear locomotion from the anode to the cathode with a maximum velocity of 1.63 mm/sec when the applied field was 275 V/mm. The locomotion is dependent on the delicate balance between the threshold field, degree of swelling, and the area of contact between the gel and the substrate. As the swelling increased, so did the area of contact which increased the frictional forces at the interface. Thus a higher field was required to produce motion. This motion behavior (speed and direction) could be well controlled by the external electric field. The mechanism put forth by the authors attributed this locomotion to the unique structure of the gel and the strong interaction between external DC field and the accumulated charges on the surface of the gel. This system could only work in air which may be desired for some industrial applications.

Miyata et al. fabricated a glucose responsive hydrogel using the formation of cross-linking complexes between poly (glucosyloxy-ethylmethacrylate) poly (GEMA) and concanavalin-A (16). When there was free glucose present in the aqueous environment that the hydrogel was placed in, the hydrogel responded by an increase in swelling. The degree of swelling was predominantly a function of the degree of crosslinking. Thus this bioresponsive gel functions as a biomolecule recognition device. This can be exploited for a drug delivery

vehicle that releases insulin based on the concentration of glucose or as a bioresponsive valve in a microfluidic device. Another example of actuation by a change in cross-linking density is the system developed by Kim et al. (17). The optical property of spherical poly (N-isopropylacrylamide-co-acrylic acid) hydrogel particles was exploited as flexible microscopic lenses that change their focus upon changes in swelling. A reaction between the biomolecule and cross-links in the hydrogel structure led to swelling at the surface of the material. Hydrogels of poly (N-isopropylacrylamide-co-acrylic acid) were prepared and functionalized with biotin and aminobenzophenone. These hydrogels were adsorbed onto a surface. Anti-biotin molecules were photo chemically cross-linked into the structure at the surface linking the biotin and aminobenzophenone. This cross-linking controlled the degree of swelling at the surface. When free biocytin, a substitute for biotin, was present in solution it knocked off the anti-biotin from the anchored hydrogel biotin thus cleaving the cross-links and changing the degree of swelling at the surface. The degree of swelling at the hydrogel surface controlled the optical properties which when actuated resulted in a change in the focus of an image projected through the material. This was documented via optical microscopy.

The final category of polymeric actuators is the shape memory polymers (SMP). SMP's are a class of polymers that are programmed to memorize a less constrained configuration, then assume a temporary strained configuration followed by returning to the less constrained form due an external stimulus (14). Traditionally SMP's are known for high percentage strain recovery and high magnitude of stress generation as a result of an external trigger. Usually this trigger is a thermal transition. The intrinsic mechanism for shape memory behavior in

thermally responsive SMPs is the reversible freezing and activation of polymeric chain motion in the network segments below and above a transition temperature, respectively. Shape memory properties have been reported in a wide range of polymers including, but not limited to, polyurethanes, epoxies, polyolefins, and polyesters. The driving force for shape recovery of an SMP is the recoiling of the polymer chains from a temporary state to a less-ordered configuration (14). Upon deformation at a higher temperature, termed as transition temperature (T_{trans}), the original orientations of the chain segments get altered, resulting in new sets of local chain-chain interactions. The temporarily deformed shape can be fixed as the material cools ($T < T_{trans}$), provided there is no elastic recoiling upon cooling. When triggered by a temperature greater than the transition temperature, the increased entropy of chain segments overcomes the constraining local chain-chain interactions, permitting the recoiling of chain segments to a more disordered state. The net-points of an SMP network, which maintain its dimensional stability, could be either covalent or physical crosslinks. The switching components that reversibly respond to temperature changes can be either amorphous or semi-crystalline. Thus the transition temperature could be glass transition temperature (Tg) characteristic of the amorphous regions or melting temperature (Tm) representative of the crystalline regions.

A majority of early SMP's that found use in biomedical applications were not designed primarily for those applications (14, 18).The very first SMP polymer system for biomedical application was adapted by Hiyashi et al. (19) in the form of a polyurethane SMP based catheter which softened at body temperature to minimize any tissue damage during surgical delivery. Since then various other systems have been devised for applications such as

coronary grafts, drug eluting stents, tissue engineering scaffolds, and dynamic cell culture substrates (14, 20). Maitland et al. (21, 22) designed a novel thermoset polyurethane (MP 5510) SMP-based micro-actuator for treating strokes by making a blend of hexamethylene diisocyanate (HDI), N,N,N',N'-tetrakis (2-hydroxypropyl) ethylenediamine (HPED), and triethanolamine (TEA) and encapsulating a nitinol backbone wire. The micro-actuator was coupled to an optical fiber and was set in a straight configuration for easy surgical insertion. Once the target clot site was reached, laser heating was applied to heat the polymer to a temperature between 65°C and 85°C to activate the SMP to form a pre-cast corkscrew shape to facilitate the capturing of the thrombus. Due to the high transition temperature there was concern about local damage to the blood vessels.

The transition temperatures for most of the SMP's are well above body temperature (14, 18). To make the polymer relevant for biomedical application, the transition temperatures in the 30° – 40° C range are necessary and have been achieved by optimizing the network composition (20, 23). A new branch of SMP's combining the properties of near body temperature T_{trans} and incorporation of degradable segments have enabled a whole new set of applications (18, 18, 24, 25). By conjugating biodegradable poly (lactic-co-glycolic acid) PLGA oligomers with shape memory component polyhedral oligosilsesqioxane (POSS), Knight et al. designed an organic-inorganic crosslinked SMP network (24). By controlling the degree of crystallinity (% POSS), the rate of degradation of the polyester segments was modulated. Both Tg and Tm were investigated for the T_{trans}. The temperature at which the temporary shape was fixed and the method of fixing the shape governed the success of shape fixing and the degree of strain recovery. If the cooling process after shape fixing was

performed slowly then that provided POSS chains time to crystallize and thus retain the temporary shape better. However the strain recovery was only 20% when Tg was used as the T_{trans}. PLGA has a Tg close to body temperature which gets further lowered in aqueous state as is common with polyesters (18, 24). When the SMP was immersed in PBS buffer at 37°C, shape recovery based on Tg trigger was observed. After the initial Tg based 20% strain recovery, further shape recovery occurred as the network degraded and the crystalline POSS was unable to hold the temporary shape. The network degraded completely on a timescale between three to fourteen weeks depending on the concentration of POSS in the network. As the POSS concentration increased, the hydrophillicity of the network decreased which also slowed the rate of PLGA degradation. This organic-inorganic crosslinked SMP network is a significant step towards increasing applicability of SMP's for biomedical applications.

An example of SMP's designed specifically for soft tissue application is surgical sutures. Langer et al. synthesized a degradable block copolymer by coupling oilgo(ε-caprolactone)diol (OCL) and oligo(p-dioxane)diol (ODX) with 2,2,(4),4-trimethylhexanediisocyanate (25). They fabricated sutures that were programmed by elongation and fixing the elongated state. The transition temperature for this SMP was 41°C. The sutures could be elongated up to 1000% before failure. When the shape memory was triggered, the force generated as the material rapidly shrunk was of the order of 1.6 N *in vitro* while *in vivo* this force was detected as 0.1 N. The degradation of the L-lactide polyesters was linear and the degradation products were cytocompatible. Thus they were able to demonstrate a possible alternative to basic sutures and a way to reduce the subjective variability in the force used to tie the knots while applying sutures. Near body temperature

transitions have also made it possible to perform fundamental science studies in order to understand behavior of cells. Substrate stiffness and topography play a major role in processes like cell division, migration, and phenotype (26, 27). Using the property of shape memory transition, substrates have been designed to understand how a dynamic change in morphology can affect the cell. Davis et al. designed polyurethane based SMP by crosslinking Norland Optical Adhesive-63 (NOA-63) and temporarily fixed a ridge and groove geometry (20). The transition temperature was between 30°C-37°C which was achieved by lowering of the Tg via fabrication conditions. The Tg of wet NOA-63 normally is 51°C. C3H/10T1/2 mouse embryonic fibroblasts were seeded on these substrates at 30°C and after 10 hours the temperature was raised to 37°C to trigger the transition. The SMP activation triggered a rapid change in morphology and almost the entire pattern was lost within an hour. The cells that had aligned to the pattern now lost their directional orientation. Despite this the cell viability still remained high (95%).

1.2 Limitations of polymeric actuators for biological applications

When it comes to biological application of polymeric biomaterials it is critical to match the mechanical properties of the polymer matrix with that of the native tissue (26-29). Hydrogels offer a good solution to this by having the property of mechanical tunability. As a mechanical actuator, the swelling/de-swelling behavior of the gel has to be used to perform actuation/locomotion. There are several design and conceptual challenges in this area, primary one being the delicate relationship between swelling phenomenon, strength of the gel, and the ability to generate forces. This relationship is also known as the force vs stroke behavior (4). Stroke is defined as the displacement achieved by the actuator. Hydrogel based

actuators like PNIPAAm generate strokes by swelling or de-swelling around the transition temperature. For a high value of stroke the swelling needs to be large which would suggest low crosslink density. This also translates to a weaker gel matrix which will be unable to produce high value of force. Thus force and stroke are inversely related. To obtain sufficient force potential, the stiffness of the ideal gel material falls outside the range of most biological soft tissues (3). The bioresponsive gels in the form of EAP's can produce high force generating displacements as a direct consequence of an external DC electric field or change in ionic makeup of the direct environment (3, 15). EAP's have found tremendous use in microfluidic devices and lab-on-chip strategies (3). However from a biomedical application perspective, their use is limited due to the requirement of maintaining a steady electric field or ionic concentration (16, 17, 30).

SMP's have been designed to be degradable, biocompatible, with transition temperatures close to body temperature, and most importantly generate high strains during the shape recovery phase. The transformation of the SMP networks after the transition temperature is reached is very rapid, usually ranging between 1.8% to 5% per minute depending on the size of the monomer used to form the crosslinked network (14, 23). The focus of a majority of investigations of polymeric actuators is in relation to microscopic applications such as sensitive valves in a microfluidic device or for localized delivery vehicles for drugs or macroscopically as coronary stents and novel tissue culture scaffolds (2, 5, 14, 18, 22, 25). For such applications quick and uniform actuator response is desired (1, 4, 5). Thus the focus of this field currently is towards designing faster responding materials. There exist other areas of biomedical applications where polymeric actuators have been underutilized. For

many years there has been a hypothesis that nervous tissue can be successfully elongated via application of an external mechanical force alone (31-34). Recently this hypothesis has been proven *in vitro* by several researchers using mechanical motors (31, 35). The principal requirement for sustained elongation of nervous tissue is a controlled slow rate of extension. In theory polymeric actuators could provide an alternative to the mechanical motors and lead to *in vivo* therapies to treat peripheral nerve gap injuries. When we inspect the current library of polymeric actuators that can be used on the macroscopic scale for such a soft tissue application there is a serious lack of available options. The rapid displacements that the current library of polymeric actuators possess, necessitate investigations into designing a new category of degradable, biocompatible, slow actuating polymer systems that can sustain actuation for several days.

1.3 Motivation for this Dissertation

Based on the discussion of the current options within polymeric actuators, it is clear that there is a lack of a slow actuating polymer system that can be used in biological environment for prolonged stress application. Our goal was to design a polymeric biomaterial that can be used *in vivo* to impart tensile force to cells akin to an *in vitro* micromotor controlled apparatus. The critical requirements for a suitable biomaterial included biocompatibility, ease of chemical modification, cell attachment, ability to generate tensile force, and biodegradation. The rationale for this work, as shown in Figure 1.1, is simple yet involves careful balancing of several parameters. We propose a system that enables us to store a retractive stress in a crosslinked network along a pre-defined axis during fabrication. Storing a retractive stress in essence means storing energy in the system. By gradually releasing this

stress we hypothesize that the crosslinked network will shrink in dimension along the pre-defined axis. Any object attached to the ends of this shrinking matrix would be similar to a micromotor applying tensile stress on that object. We chose high molecular weight, shear thinning hyaluronic acid to form our crosslinked networks. The following sections discuss the advantages of selecting this natural polysaccharide to design the polymeric actuation matrix.
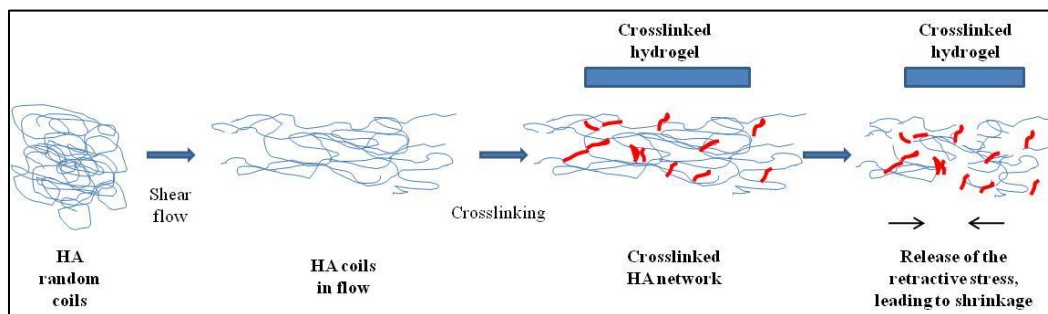
Fig.1.1. Schematic showing the rationale for fabricating hyaluronic acid based hydrogels that have retractive stress stored in the network

1.3.1 Hyaluronic Acid

Hyaluronic acid (HA) was first discovered in the vitreous humor of the eye in the year 1934 (36). The main subunit of HA is a disaccharide composed of alternating 1, 4- linked units of 1, 3-linked glucoronic acid and N-acetylglucosamine. HA is a naturally derived, non-adhesive, non-immunogenic, non-sulfated, linear viscoelastic glycosaminoglycan. HA is well known for its wound healing properties (36, 37). It exists in the human body predominantly in the synovial fluid and acts as a lubricating and shock absorbing component (37, 38). In recent past it has been used as a successful viscosupplement in eye surgeries and to relieve pain in arthritic joints (36, 37, 39). Despite its relatively high molecular weight (~ 10^6 Da) it gets degraded or turned over at a rapid pace. To counter this, researchers have crosslinked HA via different strategies (40). One of the common strategies is to attach a

photocrosslinkable moiety to the HA chain and crosslink it, thereby slowing down the degradation and considerably increasing the residence time in body. HA can be modified chemically at the hydroxy groups on both the glucoronic and N-acetylglucosamine units or the carboxyl group on the glucoronic acid unit. There has been a growing interest in the tissue engineering community for HA based scaffolds (41). HA is synthesized at the cell level without a protein core; however it interacts with many extracellular matrix molecules and cells (39). HA provides the benefit of having structural conservation, meaning there will be minimal or no immunogenic response when injected into the human body despite the source of HA.

The HA molecule in its native state is in a random coil conformation. The high molecular weight of this molecule poses some problems with ease of solubility. A solution containing HA at concentration of $1x10^6$ Da saturated the solution at a concentration of 0.4 wt% (37, 39). Beyond this, any new polymer chains dissolved in the solution causes entanglement of the coils. HA solutions are highly viscoelastic in nature. High frequency perturbations cause the solution to act like an elastic material while lower frequency forces elicit a viscous response. This is the main mechanism by which HA acts as a shock absorber in the synovial fluid in the joints. HA molecules have the advantage of being shear thinning (38, 39). Under the influence of shear flow the random coils slowly disentangle to varying degrees and align along the direction of flow. This enables even highly concentrated solutions to be injectable. The basis of this work lies in exploiting this property. If a solution of highly concentrated HA were to be sheared and then rapidly crosslinked before all the molecular chains are able to relax back to random coil conformation, then a residual retractive stress could be stored in

the network. Furthermore, if this stress were to be slowly released then we believe the process would cause the gel matrix to shrink along the original flow axis.

We investigated the shrinking mechanism by either selectively degrading the crosslinks that hold the network together or by selectively degrading the long HA backbone chains. A schematic of the two pathways used to study this crosslinked gel system is shown in Figure 1.2. To study the effect of selectively degrading the HA chains, we crosslinked the network using a nearly non-degradable crosslinker poly(ethylene glycol) diacrylate (PEGDa). In the human body HA is broken down predominantly by the enzyme hyaluronidase. The cleavage occurs at the β-N-acetyl-D-glucosaminidic linkages to yield fragments of N-acetylglucosamine at the reducing terminus and glucoronic acid at the non reducing end (36, 37, 42, 43). We used this enzyme at physiologic and elevated concentrations to simulate *in vivo* degradation at the site of injury. The breakdown products of HA have been shown to modulate wound healing (36, 37, 39). This would be an added advantage of this polymer network system that would aid in repairing the injury site while providing mechanical stimulus to the neurons to grow. To study the shrinkage induced by degrading crosslinks, we crosslinked the network using a hydrolytically degradable crosslinker poly(ethylene glycol)-poly(lactic acid) diacrylate (PEGPLADa). The degradation products are non toxic in this case as well.
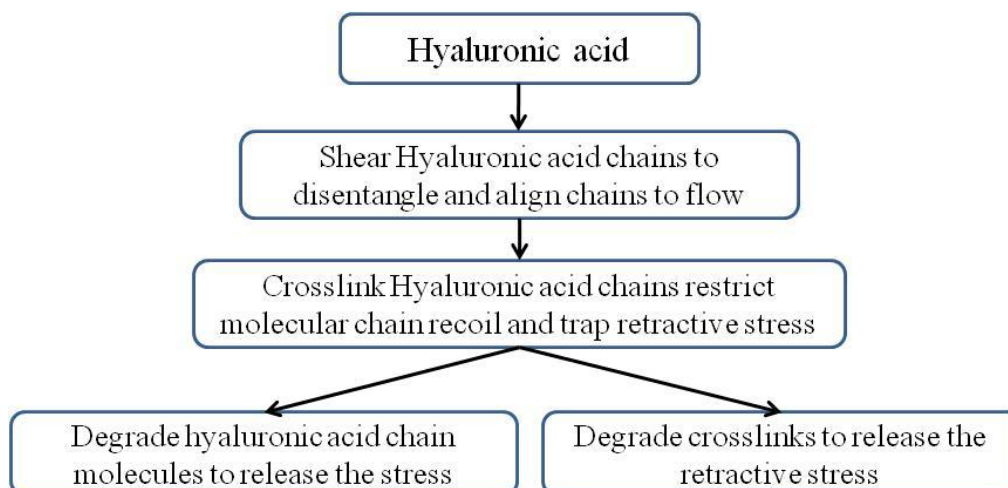
Fig.1.2. Flowchart detailing the experimental rationale

Another advantage of the HA molecule is its favorability for cell attachment. CD44 is a major cell surface receptor for HA (44). It is expressed on many different cells including neuronal cells where it is over expressed following any trauma (45). CD44 has many functions depending on the cell type. For neuronal cells it is said to be involved in directed migration. CD44 along with a receptor for hyaluronan mediated mobility (RHAMM) provide opportune sites for attachment of the crosslinked HA hydrogel to neuronal ends (46). HA has been documented as enhancing peripheral nerve regeneration (47). Rats with a sciatic nerve gap injury were implanted with a nerve guide consisting of ports to inject HA solutions. It was observed that HA helped in organizing the fibrin matrix making it more porous and favorable for regenerating axons to cross over. We believe that the versatility of HA molecule makes it an ideal candidate for application as a nerve regeneration matrix.

1.4 Targeted Application for HA Based Slow Polymeric Actuator System

1.4.1 Peripheral Nervous System

The Peripheral Nervous System (PNS) consists of cranial nerves coming out of the brain, the spinal nerves from spinal cord, and sensory nerve cell bodies and their processes (48-50). The peripheral nerves act as the cables transferring excitatory signals from and to the spinal column from the muscle tissues. Peripheral nerves are generally classified as motor or sensory nerve. However no nerve is purely sensory or purely motor. The motor nerves are myelinated while sensory are largely unmyelinated. The ratio of number of sensory nerves to number of motor nerves is around 4:1 (50). The anatomy of a peripheral nerve is shown below in Figure 1.3. A peripheral nerve is akin to a coaxial electrical cable consisting of many individual axons bundles together and insulated from each other. Individual axons are surrounded by Schwann cells that provide the necessary support for transmission of excitatory signal through the axons. Endoneurium surrounds individual axons and their ensheathing Schwann cells. The endoneurium is primarily composed of oriented collagen fibers. A group of these axons is surrounded by perineurium to form fascicles. The perineurium is composed of many layers of flattened fibroblasts. Finally, a fibrous and collagenous layer called epineurium binds many of these fascicles together to form the nerve fiber or the trunk.
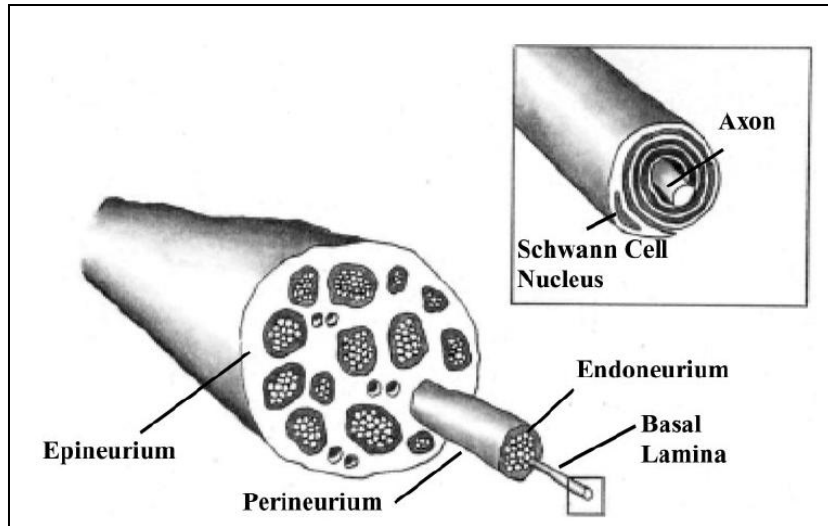
Fig.1.3. Anatomy of a peripheral nerve showing the basic architecture of a nerve (50)

1.4.2 Peripheral Nerve Injury

There are several causes for a PNS injury including but not limited to mechanical, chemical, biological, or thermal sources. The most common source is mechanical injury ranging from simple cuts to amputations. The effect of such injuries from the perspective of the nervous system is the transection of peripheral nerves. Following an injury several natural processes occur that determine the fate of the recovery from the injury. The crucial difference between a peripheral and a central nervous system (CNS) injury is that the native environment facilitates axonal regrowth for PNS, where as it is inhibitory in the case of CNS (48, 51-54). Following a complete transection nerve injury, the nerve ends move away from each other due to the inherent tension in the nervous system. Next there is retrograde degeneration of the nerve ends and the Schwann cells lose their myelin and degrade as well. The macrophages that enter the site of injury then start phagocytotic clearance of the cell and myelin debris. This also triggers release of cytokines that promote sprouting of new neurites. In the CNS the astrocytes and fibroblasts enter a hypertrophic state and form an astroglial

19

scar which is a physical barrier for the axonal sprouts to grow across the injury. In the PNS injury the absence of this scar tissue causes the neurites to re-grow and form connections to the distal end of the severed nerve or the target tissue.
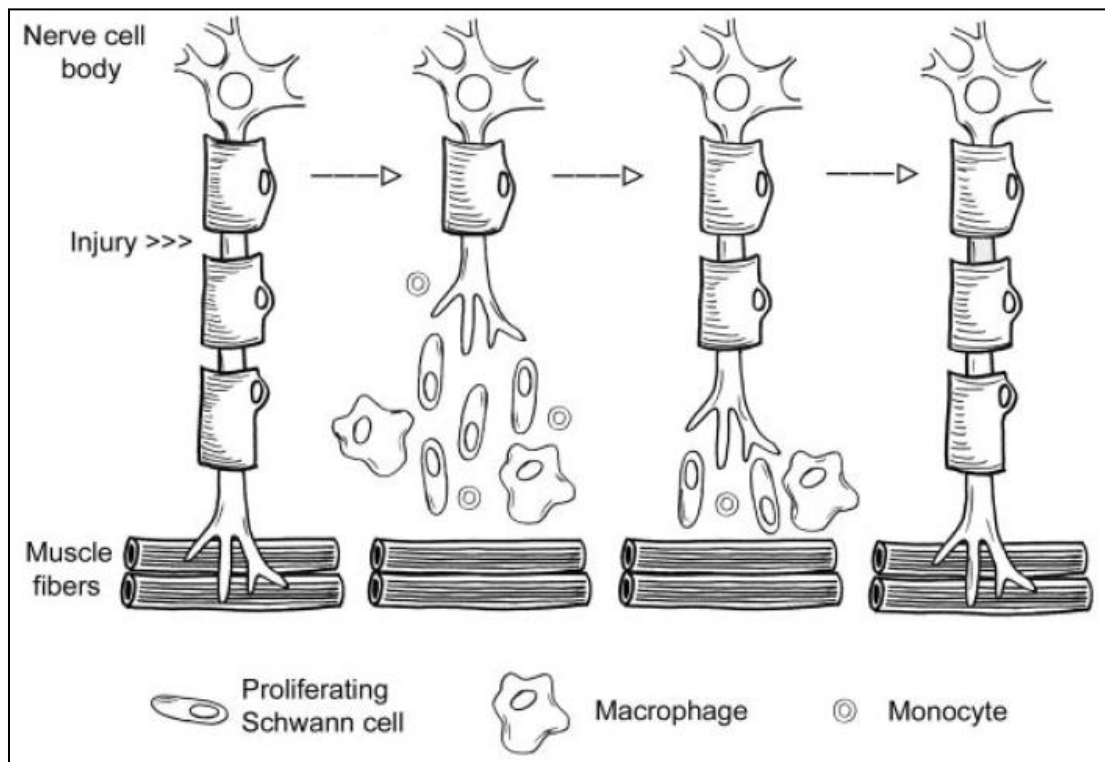
Fig.1.4. Schematic showing the sequence of events that occur at the site of a peripheral nerve injury. After a severance injury, the proximal end of the nerve starts to degrade while the Schwann cells give up their myelin coat and become phagocytic. Along with macrophages, they clear the debris at the site of injury and trigger release of cytokines which promote axonal sprouting (50)

1.4.3   Current treatments for PNS injury

The treatment of a nerve transection is dependent on the size of the injury gap. Similarly, the extent of regeneration and re-innervation in the PNS is also governed by the size of the gap. For a smaller gap (<10 mm) the surgeon can pull the severed nerve ends closer and suture them to repair the injury (36, 49). Aligning the internal fascicles into motor or sensory

20

components helps to improve the outcome. Researchers and neurosurgeons have observed that if the nerve gap is larger than 10 mm, the success of the re-innervation is low. To mitigate this issue, the current gold standard treatment is an autologous nerve graft. This means harvesting a nerve, usually sural or sensory nerves from upper extremities, and suturing it in the gap to bridge it. The recovery rate is around 80 % which is the best achieved across all available traditional and experimental treatments. Generally the surgical repair is not done immediately after the injury to reduce any unknown damage.

The main disadvantages of the surgical treatment include the availability of donor nerve tissue, multiple surgeries, and the loss of function at the donor site. Alternatives to autologous nerve grafts include allogenic or xenogenic nerve grafts, but they possess the risk of an immune reaction. Using immunosuppressant drugs is not always possible in cases involving trauma or cancer. Engineered nerve conduits were the next alternative that has been studied for the past several decades. The main requirements for a nerve conduit are easy availability, biodegradability, easy vascularization, low antigenicity, ease of oxygen diffusion, and avoiding long-term compression (49, 55). Using naturally derived materials like laminin, fibronectin to form guidance conduits have demonstrated exciting results. Batch to batch variability in these naturally derived molecules hamper their wide spread application (49). Synthetic engineered conduits provide the ability to alter the mechanical properties, biocompatibility, degradation, porosity etc. Researchers have tested constructs fabricated out of degradable biocompatible polymers like poly(lactic-co-glycolic acid) (PLGA) and poly(L-lactic acid) (PLLA) with controlled porosity (49, 56-58). Over time PLGA constructs demonstrated diminished structural rigidity leading to nerve compression. However PLLA

constructs did not show any nerve compression (49, 57). The critical limitation faced by nerve conduits is the ability to sustain axonal regeneration for gaps larger than 15 mm (49, 55). Despite promising results from all the alternate experimental forms of treatment for large gap neuronal injuries, none have managed to match the autologous nerve graft success rate.

1.4.4 Mechanical stimulation of neuronal cells

How does an axon grow? *In vitro* and *in vivo* axonal growth have slight differences in their progression, however the main framework for growth is same for both cases. *In vitro,* topographic or chemical cues guide the growth cone and cause the axonal growth. *In vivo,* the axonal growth is a two stage process where the growth cone follows the topographic and chemical cues and binds to its target and then the axon elongates grows as a result of the growth and movement of the target. The microstructural makeup of the axon, consisting of actin cytoskeleton and microtubules, is what allows the sustained and stable elongational growth of the axon. The actin cytoskeleton and microtubules exist in a balanced tension-compression environment (31, 59). As a result of various growth cues the cell secretes extracellular matrix and add new membrane along the axon. As the growth cone explores the substrate or when the target that the growth cone is attached to traverses, new actin polymerizes to sustain the movement of the growth cone. Simultaneously the addition of microtubules counters increasing tension from the actin. The transport of nutrients to sustain the addition of new membrane needs to match with the growth rate or else axonal growth is not possible and leads to retraction of the axon. Over the past several decades, *in vitro* neuronal studies have confirmed that the growth cone is the component that drives the axonal growth and elongation on a substrate (33, 60). The growth cone explores the substrate that it

is attached on and based on the chemical or mechanical guidance signals it traverses in the favorable direction. Unlike non-neuronal cells which migrate in response to favorable cues (61, 62), neuronal cell bodies generally remain stationary while the growth cone migrates and pulls the axon along with it. As for the *in vivo* growth it occurs in two phases. In the embryonic state the growth cones are in their sensing mode searching for its target. Thus the growth cone in response to matrix cues is the causative agent in the axonal growth in this phase. Once it reaches its target it no longer in control of the axonal growth/elongation. As the target moves away, on account of growth of the body, it pulls along with it the attached axons. This is a naturally occurring phenomenon. Weiss described it in 1941 (34) as a three stage process. Figure 1.5 shows a schematic of those three stages of axonal growth *in vivo*.
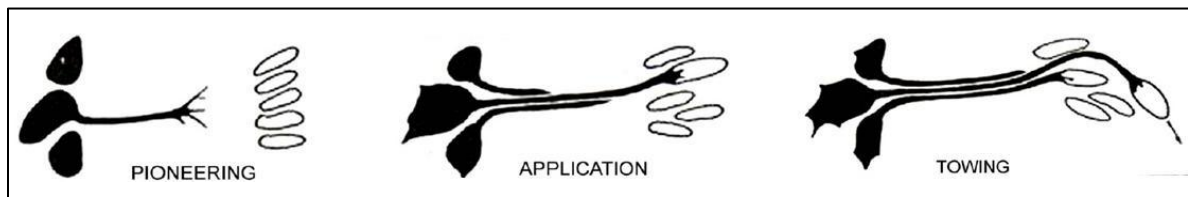
Fig.1.5. Schematic showing the three phases of in vivo neuronal growth as described by Paul Weiss. It was posited that ''the nerve is drawn out by the growth and dislocations of its terminal tissues'' (34) *(reprinted with permission from Elsevier Publishing)*

The "towing" phase presents a fascinating hypothesis that mechanical stimulation might just be enough for promoting axonal growth. It wasn't until 1984 that this was experimentally proven by Bray (31). He designed a device called a "cell puller" that consisted of a glass microelectrode attached to a micromotor. Neuronal cells obtained from dissociated chick dorsal root ganglia (DRG) were plated on glass coverslips. The microelectrodes were coated with laminin or collagen and laid in the path of growth cones. Once the growth cone attached to the microelectrode the micromotor was switched on and

the growth cone was pulled at rates ranging from 40 µm/hr to 170 µm/hr for the duration of 3 hrs to 24 hrs. What he observed was that growth cones that were extended at the rate of 100 µm/hr or less showed a net growth ranging from 100 µm to 960 µm. At higher rates the neurites initially thinned out and then detached from the glass microelectrode. Figure 1.6 shows a micrograph from one of these experiments. The cytoplasm of the extended axons appeared to be normal and an increase in volume of the axon was observed. Furthermore if the growth cone was detached and returned to the coverglass the axon continued to thrive and grow. Moreover, Bray was able to generate axons *de novo* (31). He attached the microelectrode to a round neuronal cell body devoid of any processes and by just the application of a tensile stress was able to coax the cell to generate a neurite. This extension appeared similar to a neurite but was devoid of a growth cone like structure at its point of attachment with the microelectrode. This further provided proof that towed growth did not need the growth cone.

Heidemann and Baxubaum (60), and Lamoureux et. al (63) further elaborated on this study and confirmed that mechanical tension by itself can be a potent cue for enhancing axonal growth. In towing neurites from pheochromocytoma cell (PC12 cells) and chick sensory neurons, they observed that there was a direct correlation between axonal elongational rate and tension rate and magnitude and that it was threshold dependent. They also noted that loss of tension caused retraction of the neurites. By attaching glass microspheres coated with polyethyleneimine (PEI) they were able to confirm that the new membrane gets added interstitially throughout the neurite as opposed to near the growth cone during a growth cone mediated axonal growth. They concluded that tension acts as a

regulator for axonal elongational growth by modulating the polymerization and de-polymerization of the cytoskeletal elements (60, 63).
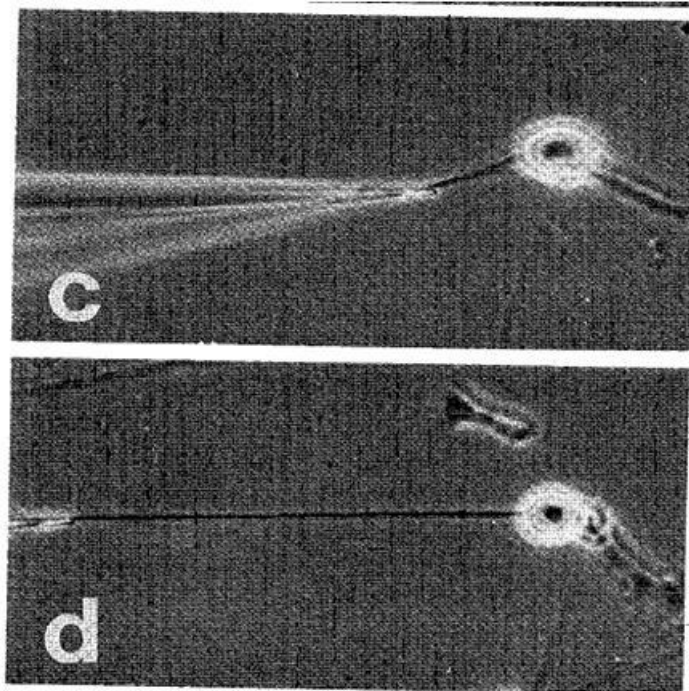
Fig.1.6. Optical micrographs showing (c) a single neuron shortly after attachment of its growth cone to a microelectrode; (d) the same neuron after being towed at 60 µm/hr for 1.9hrs (31). The process induced stretch growth of the axon. There did not seem to be any reduction in the overall thickness of the axon. *(reprinted with permission from Elsevier Publishing)*

The pioneering studies mentioned above came to the conclusion that the limiting rate for axonal stretching was about 100µm/hr for individual axons and DRG explants and it correlated with the rate at which nutrient transport vesicles can travel to support this growth. In the early 2000's, Smith et. al published a series of papers describing the effect of mechanically stretching a bundle of neurites from DRG explants (34, 35, 64, 65). Their device consisted of precision engineered overlapping Aclar membranes, one stationary and other attached to a micromotor. DRG explants were plated on the membranes and the neurites were permitted to crossover. After sufficient number of neurites had crossed over

they started to move the membranes apart using the micromotor at varying speeds. The results they obtained were astonishing. Through a controlled process of stress acclimatization, they were able to stretch the neurites at rates as high as 10 mm/day or 400 µm/hr. However they determined that at least for the first day of the stretch, the maximum rate that could successfully elicit sustained axonal elongation was 100 µm/hr. If stretched beyond this rate on the first day the neurites delaminated or appeared to have a reduced volume. Figure 1.7 shows a picture of their device with an overlaid micrograph of the stretched neurites. The neurite bundles (~10cm) they were able to get from this extreme stretching process were elctrophysiologically functional. Stretch-growth did not alter sodium (Na) channel activation, inactivation, and recovery or potassium (K) channel activation. In addition, neurons generated normal action potentials that propagated across stretch-grown axons. However, Na and K channel density showed an increase due to stretch-growth, which was hypothesized as representing a natural response to preserving the fidelity of neuronal signaling.
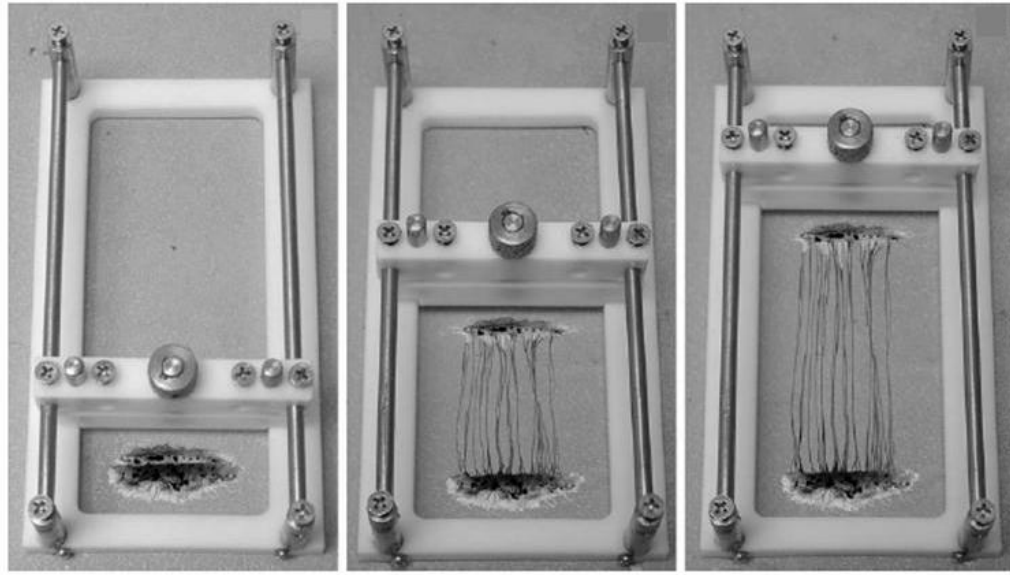
Fig.1.7. Schematic showing the mechanical device used for extreme stretch of neurite bundles. Neurons were plated on two adjoining substrates and sufficient time was given for axons to bridge the two substrates and integrate with other neurons on both sides. The membranes were pulled apart thereby stretching the interconnecting axons. The stretch rate were gradually increased to 1 cm/day leading to stretch growth to lengths of at least 10 cm. (65) *(reprinted with permission from Elsevier Publishing)*

1.5 Significance of this work

The current options within polymeric biomaterials with multi-functionality include matrices that are biocompatible, biodegradable, quick transitioning / shape changing, and mechanically tunable. These properties have all been combined in the form of actuator polymers (EAP's and SMP's) that have found application as stents, valves, semi permeable membranes, and dynamic cell culture substrates. However these matrices are not appropriate for applications requiring a slower transition and long term application of force. This work will hopefully be a step towards filling that void. We propose to design, fabricate, and characterize a novel hyaluronic acid based hydrogel actuator that shrinks over time along a pre-defined axis thereby providing the source for displacement/force. In terms of the intended application for such a

27

matrix, the goal is to provide an alternative to current autologous nerve transplant treatment. Each year over 50,000 peripheral nerve repair procedures are performed (National Center for Health Statistics, 1995). The total annual costs in U.S alone exceed $ 7 billion (American Paralysis Association, 1997). Despite the inherent disadvantages of autologous nerve transplantation, it is the most preferred treatment for a large gap peripheral nerve injury. Alternative therapies have been unable to match the success rate of this treatment. Nerve conduits have the limitation of being unable to sustain axonal growth for gaps larger than 15 mm (55). There is a lack of an effective biomaterial solution to the problem of a large gap nerve injury. The *in vitro* studies discussed in the previous sections confirm and simulate the natural *in vivo* process of tensile regulation of axonal elongation. The solution we propose is a biomaterial that can be programmed to perform the function of a mechanical actuator at rates suitable for axonal stretch growth. The inherent neuronal cell adhesive property of HA makes it an attractive scaffold for axonal regeneration. We foresee such a successful system being used inside a nerve conduit in a large gap peripheral nerve injury to stimulate and enhance axonal growth by the towed growth mechanism. Due to a finite amount of energy that can be stored in the system that translates into shrinkage, this material will transition from an active stimulator to a passive degrading bridge over the course of regeneration and recovery. The potential of shortening the gap even by a few millimeters would vastly improve the success of nerve conduit based treatments and increase their efficacy for treating large gap PNS injuries.

References

1. Ionov L. Hydrogel-based actuators: possibilities and limitations. Materials Today. 2014;17(10):494.

2. Mano J. Stimuli-responsive polymeris systems for biomedical applications. Adv Engg Mat. 2008;10(6):515.

3. Carpi F, Smela E, editors. Biomedical Applications of Electroactive Polymer Actuators. John Wiley & Sons; 2009.

4. Illeperuma W, Sun J, Suo Z, Vlassak J. Force and stroke of a hydrogel actuator. Soft Matter. 2013;9:8504.

5. Ionov L. Polymeric Actuators. Langmuir. 2014;10:1021.

6. Ishida K, Uno T, Itoh T, Kubo M. Synthesis and property of temperature-responsive hydrogel with movable cross-linking points. Macromolecules. 2012;45:6136.

7. Sperling LH. Cross-linked polymers and rubber elasticity. In: Introduction to physical polymer science. 4th ed. New Jersey: Wiley-Interscience; 2005. p. 427.

8. Cussler EL, Stokar MR, Varberg JE. Gels as size selective extraction solvents. AICHe J. 1984;30:578.

9. Huffman AS, Afrassiabi A, Dong LC. Thermally reversible hydrogels: II. Delivery and selective removal of substances from aqueous solutions. J Controlled Release. 1986;4:213.

10. Gutowska A, Bae YH, Feijen J, Kim SW. Heparin release from thermosensitive hydrogels . J Controlled Release. 1992;22:95.

11. Brazel ES, Peppas NA. Pulsatile local delivery of thrombolytic and antithrombotic agents using poly(N-isopropylacrylamide-co-methacrylic acid) hydrogels. J Controlled Release. 1996;35:57.

12. Hu Z, Zhang X, Yong L. Synthesis and application of modulated polymer gels. Science. 1995;269:525.

13. Topham PD, Ryan AJ. Antagonistic Triblock Polymer Gels Powered by pH Oscillations. Macromolecules. 2007;40:4393.

14. Song J, Xu J. Thermal Responsive Shape Memory Polymers for Biomedical Applications. In: Fazel-Rezai R, editor. Biomedical Engineering - Frontiers and Challenges. ; 2011.

15. Liang S, Xu J, Weng L, Zhang L, Guo X, Zhang X. Electrically induced linear locomotion of polymer gel in air. J Poly Sci; Part B. 2007;45:1187.

16. Miyata T, Jikihara A, Nakamae K, Hoffman AS. Preparation of poly(2-glucosyloxyethylmethacrylate) concanavalin A complex hydrogel and its glucose-sensitivity. Macromolecular Chem , and Phys. 1996;197:1135.

17. Kim JS, Singh N, Lyon LA. Displacement-induced switching rates of bioresponsive hydrogel microlenses. Chem Mat. 2007;19:2527.

18. Sokolowski W, Metcalfe A, Hayashi S, Yahia L, Raymond J. Medical applications of shape memory polymers. Biomed Mater. 2007;2:S23.

19. Hayashi S, Kondo S, Kapadia P, Ushioda E. Room-Temperature-Functional Shape-Memory Polymers. Plastics Engineering. 1995;51(2):29.

20. Davis KA, Burke KA, Mather PT, Henderson JH. Dynamic cell behavior on shape memory polymer substrates. Biomaterials. 2011;32(9):2285.

21. Small I, W., Wilson TS, Buckley P, Benett WJ, Loge WM, Hartman J, et al. Prototype fabrication and preliminary in vitro testing of a shape memory endovascular thrombectomy device. IEEE Trans on Biomed Engg. 2007;54:1657.

22. Maitland DJ, Metzger MF, Schumann D, Lee A, Wilson TS. Photothermal properties of shape memory polymer micro-actuators for treating stroke. Lasers in Surgery and Medicine. 2002;30:1.

23. Nair DP, Cramer NB, Scott TF, Bowman CN, Shandas R. Photopolymerized thiol-ene systems as shape memory polymers. Polymer. 2010;51(19):4383.

24. Knight PT, Lee KM, Qin H, Mather PT. Biodegradable thermoplastic polyurethanes incorporating polyhedral oligosilsesquioxane. Biomacromolecules. 2008;9(9):2458.

25. Lendlein A, Langer R. Biodegradable, elastic shape-memory polymers for potential biomedical applications. Science. 2002;296:1673.

26. Discher . Tissue Cells Feel and Respond to the Stiffness of Their Substrate. Science. 2005;310(5751):1139.

27. YEUNG . Effects of substrate stiffness on cell morphology, cytoskeletal structure, and adhesion. Cell motility and the cytoskeleton [Internet]. 2005;60(1):24.

28. Georges P, Miller W, Meaney D, Sawyer E, Janmey P. Matrices with compliance comparable to that of brain tissue select neuronal over glial growth in mixed cortical cultures. Biophys J. 2006;90(8):3012.

29. MA P, Elisseeff J. Scaffolding in tissue engineering. USA: CRC press; 2005.

30. Miyata T, Asami N, Uragami T. A reversibly antigen-responsive hydrogel. Nature. 1999;399:766.

31. Bray D. Axonal growth in response to experimentally applied mechanical tension. Dev Biol. 1984 4;102(2):379-89.

32. Franze K, Gerdelmann J, Weick M, Betz T, Pawlizak S, Lakadamyali M, et al. Neurite Branch Retraction Is Caused by a Threshold-Dependent Mechanical Impact. Biophys J. 2009 10/7;97(7):1883-90.

33. Dennerll T, Lamoureux P, Buxbaum R, Heidemann S. The cytomechanics of axonal elongation and retraction. J Cell Biol [Internet]. 1989;109(6):3073.

34. Smith DH. Stretch growth of integrated axon tracts: Extremes and exploitations. Prog Neurobiol. 2009 11;89(3):231-9.

35. Smith DH, Wolf JA, Meaney DF. A New Strategy to Produce Sustained Growth of Central Nervous System Axons: Continuous Mechanical Tension. Tissue Eng. 2001 04/01; 2011/05;7(2):131-9.

36. Price RD, Berry MG, Navsaria HA. Hyaluronic acid: the scientific and clinical evidence. Journal of Plastic, Reconstructive & Aesthetic Surgery. 2007 10;60(10):1110-9.

37. Laurent TC, Laurent UB, Fraser JR. Functions of hyaluronan. Annals of the Rheumatic Diseases. 1995 May 01;54(5):429-32.

38. Gibbs DA, Merrill EW, Smith KA, Balazs EA. Rheology of hyaluronic acid. Biopolymers. 1968;6(6):777-91.

39. Laurent TC, editor. The Chemistry, Biology and Medical Applications of Hyaluronan and its Derivatives. 1st ed. London and Miami: Portland Pr; 1998.

40. Luo Y, Kirker KR, Prestwich GD. Cross-linked hyaluronic acid hydrogel films: new biomaterials for drug delivery. J Controlled Release. 2000 10/3;69(1):169-84.

41. Collins MN, Birkinshaw C. Hyaluronic acid based scaffolds for tissue engineering - A review. Carbo Poly. 2013;92:1262.

42. Zhong SP, Campoccia D, Doherty PJ, Williams RL, Benedetti L, Williams DF. Biodegradation of hyaluronic acid derivatives by hyaluronidase. Biomaterials. 1994 4;15(5):359-65.

43. Roden L, Fraser JRE, Laurent TC. Enzymic pathways of hyaluronan catabolism. In: Laurent TC, editor. The Biology Of Hyaluronan. John Wiley & Sons; 1989. p. 60.

44. Lesley J, Hascall VC, Tammi M, Hyman R. Hyaluronan Binding by Cell Surface CD44. Journal of Biological Chemistry. 2000 September 01;275(35):26967-75.

45. Moon C, Heo S, Sim K, Shin T. Upregulation of CD44 expression in the spinal cords of rats with clip compression injury. Neurosci Lett. 2004 8/26;367(1):133-6.

46. Nagy J, Hacking J, Frankenstein U, Turley E. Requirement of the hyaluronan receptor RHAMM in neurite extension and motility as demonstrated in primary neurons and neuronal cell lines. The Journal of Neuroscience. 1995 January 01;15(1):241-52.

47. Wang K, Nemeth IR, Seckel BR, Chakalis-Haley DP, Swann DA, Kuo J, et al. Hyaluronic acid enhances peripheral nerve regeneration in vivo. Microsurgery. 1998;18(4):270-5.

48. Cajal R. Degeneration and Regeneration of the Nervous System. Oxford University Press. 1928:73.

49. Evans GRD. Peripheral nerve injury: a review and approach to tissue engineered constructs. Anat Rec. 2001;263:396.

50. Schmidt CE, Leach JB. Neural tissue engineering: strategies for repair and regeneration. Annu Rev Biomed Eng. 2003;5(1):293-347.

51. Bauchet L, Lonjon N, Perrin F, Gilbert C, Privat A, Fattal C. Strategies for spinal cord repair after injury: a review of the literature and information. Ann Readapt Med Phys. 2009;52(4):330.

52. Fitch M, Silver J. CNS injury, glial scars, and inflammation: Inhibitory extracellular matrices and regeneration failure. Exp Neurol. 2008;209(2):294.

53. Fawcett J. Overcoming inhibition in the damaged spinal cord. J Neurotrauma. 2006;23(3-4):371.

54. Hultborn H, Nielsen JB, Krarup C. Plasticity and regeneration of the spinal cord and peripheral nervous system. Acta Physiologica. 2007;189(2):109-10.

55. Evans GRD. Challenges to nerve regeneration. Sem Surg Onco. 2000;19:312-318.

56. Evans GRD, Brandt K, Niederbichler AD, Chauvin P, Hermann S, Bogle M, et al. Clinical long-term in vivo evaluation of Poly(L-Lactic Acid) porous conduits for peripheral nerve regeneration. J Biomater Sci Polym Ed. 2000;11:787.

57. Evans GRD, Brandt K, Widmer MS, Lu L, Meszlenyi RK, Gupta PK, et al. In vivo evaluation of poly (L-Lactic Acid) porous conduits for peripheral nerve regeneration. Biomaterials. 1999;20:1109.

58. Mikos AG, Thorsen AJ, Czerwonka LA, Bao Y, Langer R, Winslow DN, et al. Preparation of poly(glycolic acid) bonded fiber structures for cell attachment and transplantation. Polymer. 1994;35:1068.

59. Goldberg JL. How does an axon grow? Genes & Development. 2003 April 15;17(8):941-58.

60. Heidemann SR, Buxbaum RE. Tension as a regulator and integrator of axonal growth. Cell Motil Cytoskeleton. 1990;17(1):6-10.

61. Pelham RJ, Wang Y. Cell locomotion and focal adhesions are regulated by substrate flexibility. Proc Natl Acad Sci U S A. 1997;94(25):13661.

62. Hynd M, Frampton J, Turnera J, Shaina W. Directed cell growth on protein-functionalized hydrogel surfaces. J Neurosci Met [Internet]. 2007;162(1-2):255.

63. Zheng J, Lamoureux P, Santiago V, Dennerll T, Buxbaum R, Heidemann S. Tensile regulation of axonal elongation and initiation. The Journal of Neuroscience. 1991 April 01;11(4):1117-25.

64. Pfister BJ, Iwata A, Meaney DF, Smith DH. Extreme Stretch Growth of Integrated Axons. The Journal of Neuroscience. 2004 September 08;24(36):7978-83.

65. Pfister BJ, Iwata A, Taylor AG, Wolf JA, Meaney DF, Smith DH. Development of transplantable nervous tissue constructs comprised of stretch-grown axons. J Neurosci Methods. 2006 5/15;153(1):95-103.

CHAPTER 2

SPECIFIC AIMS AND HYPOTHESES

Specific Aim I: To investigate effect of crosslinker concentration on the molecular chain alignment and network properties of Poly(ethylene glycol)-diacrylate (PEGDa) crosslinked hyaluronic acid (HA) hydrogels

Hypothesis 1: Increasing the crosslinker concentration increases the degree of alignment of molecular chains in the crosslinked HA hydrogels. This is manifested as an increase in orientation birefringence (Δn) of the sample.

Hypothesis 2: As the crosslinker concentration increases, a higher degree of molecular chain alignment will be retained, resulting in increased retractive stress in the HA network.

Rationale: The HA molecular chains align along the axis of flow, to varying degrees, during the process of injecting the pre-crosslinking solution into the mold. This chain alignment can be retained to some extent by crosslinking the chains rapidly. This process traps a retractive stress in the crosslinked network. The extent to which this chain alignment is retained is a function of the crosslinker concentration. Polarized optical microscopy experiments will be performed to explore this relationship and rubber elasticity theory will help us quantify the stress that can be stored in the HA network via rapid crosslinking of the shear flow oriented HA molecular chains.

Specific Aim II: To investigate effect of glycidyl methacrylated hyaluronic acid (HAGMa) concentration on the molecular chain alignment and network properties of Poly(ethylene glycol)-poly (lactic acid)-diacrylate (PEGPLADa) crosslinked HA hydrogels

Rationale: The pre-crosslinking solution consisting of HAGMa, crosslinker, and photoinitiator is sheared while being injected into the mold. HA random coils disentangle and align along the axis of flow to varying degrees. This state of the chains can be prevented from relaxing back to random coils by rapidly crosslinking the system with excess crosslinker. The extent of retractive stress stored in the network is a function of the concentration of HAGMa chains. We hypothesize that there is a direct correlation between the concentration of HAGMa and the magnitude of stress stored in the network.

Hypothesis 1: Increasing the HAGMa concentration decreases the degree of alignment of molecular chains in the PEGPLADa crosslinked HA hydrogels. This is manifested as a decrease in orientation birefringence (Δn) of the sample.

Rationale: Shearing pre-crosslinking solution aligns the HAGMa chains to varying degree. If the shearing force is kept constant, then increasing the HAGMa concentration will decrease the extent of chain disentanglement. This would cause fewer chains to align to the flow direction.

Hypothesis 2: Increasing the HAGMa concentration increases the magnitude of retractive stress stored in the network.

Rationale: The HA molecular chains align along the axis of flow, to varying degrees, during the process of injecting the pre-crosslinking solution into the mold. This chain alignment can be retained to some extent by crosslinking the chains rapidly. This process traps a retractive stress in the crosslinked network. The extent of stress stored in network is a function of the HAGMa

35

concentration. Polarized optical microscopy experiments will be performed to explore this relationship and rubber elasticity theory will help us quantify the stress that can be stored in the HA network via rapid crosslinking of the shear flow oriented HA molecular chains.

Specific Aim III: To understand the behavior of HA hydrogel networks during degradation and measure the force generated by the networks during the degradation process.

Rationale: Crosslinking the HA chains while they are disentangled and aligned to varying degrees results in entrapment of a retractive stress in the network. This stress can be released by manipulating the network, specifically either by breaking the HA molecules or selectively cleaving the crosslinks that hold the network. The two crosslinkers selected for the study provide opportunity to independently study the two mechanisms of releasing the stress in the network. The enzymatic degradation of gels crosslinked with non-hydrolysable PEGDa will help us to study the effect of breaking the HA chains on shrinkage, while hydrolytic degradation of crosslinks in gels crosslinked with PEG-PLA-Da will help us to study the effects of cleaving just the crosslinks on shrinkage behavior.

When such a shrinking hydrogel is connected to a neuronal bundle, it will be applying a force on the bundle, in essence performing work on the tissue. We intend to study and quantify the force that the shrinking hydrogel network is capable of generating while degrading/shrinking and compare with studies that have used mechano-stimulation to elicit stretch growth in neurons. We expect to understand the effect of the species of crosslinker, its concentration in the gel, and the method of degrading the network on the shrinking behavior of the hydrogels. Comparing the results from the theoretical calculation of retractive stress in the gel network from specific aim 1

with the results from the stress measurement device, will help us to understand the limits of the shrinkage process.

Hypothesis 1: Increasing PEGDa concentration in the hydrogel increases the magnitude of shrinkage and force generated by the shrinking hydrogel.

Rationale: Higher PEGDa crosslinker concentration will increase the probability of trapping a higher volume of HAGMa molecular chains in their disentangled conformation. A higher degree of this retained alignment amounts to a higher magnitude of retractive force being stored in the network. This translates to a higher potential for the network to shrink under the influence of the enzyme hyaluronidase which causes a reorganization of the network.

Hypothesis 2: Increasing hyaluronidase concentration increases the rate of shrinkage and the rate of force generated by the shrinking PEGDa crosslinked hydrogel.

Rationale: The rate at which the crosslinked HAGMa network is reorganized due to degradation is a function of the concentration of degradation source, the enzyme. A higher concentration of the enzyme hyaluronidase should potentially speed up the rate of degradation and thus the rate of shrinkage and rate of force generated during the shrinkage.

Hypothesis 3: Increasing HA concentration in the PEGPLADa crosslinked hydrogel increases the magnitude of shrinkage and force generated by the shrinking hydrogel.

Rationale: Higher HAGMa concentration will increase the probability of trapping a higher magnitude of retractive force being stored in the network. This translates to a higher potential for the network to shrink while releasing this stored retractive stress.

Hypothesis 4: Degradation process reduces the degree of alignment of molecular chains in the crosslinked HA hydrogels.

Rationale: The basic hypothesis for this hydrogel system is that the long chain HAGMa polymer is able to disentangle under shear flow and then relax when this flow or any obstruction to relax is removed. This relaxation process in a crosslinked network causes a reorganization of the network. Hence we hypothesize that the degree of alignment will reduce as the network gets reorganized. Molecular chain alignment in a network leads to a phenomenon called birefringence. We aim to verify the above hypothesis by measuring the birefringence of the network prior and post degradation.

Specific Aim IV: To study the interaction between crosslinked hydrogel and neuronal cells using mechanical stretching device and assess the cytocompatibility of the crosslinked hydrogels

Hypothesis 1: Chemical modification and crosslinking of HAGMa will not affect the cytocompatibility of HAGMa based hydrogels.

Technical goal: To design a cell culture chamber with capability to be a mechanical stretching device.

Hypothesis 2: The potential of the shrinking hydrogels to cause axonal stretch growth can be tested using the custom-built mechanical stretching device.

Rationale: The size difference between the hydrogels crosslinked in the mold and the neuronal ends on a 2D surface, along with the issue of clamping the hydrogel under fluid without restricting its shrinking ability, make designing of a direct experiment to test the stretch growth

capability of the gel networks unfeasible. To circumvent these problems we custom-built a cell culture chamber where a micromotor can separate an interface in a controlled fashion. Score cracked glass slides can be mounted on the holders in the chamber such that one side bears a covalently crosslinked hydrogel, of desired composition, and the other slide with primary neurons cultured on adhesion protein lanes growing towards the interface of the two slides. After sufficient time has been provided for interface interaction, micromotors would separate the interface at rates corresponding to the shrinkage rate of the hydrogels in question. We aim to shed light on the following questions; can a strong bond be formed at the interface to sustain the separation motion and do the rates of separation corresponding to shrinkage rates of the hydrogel produce axonal stretch growth.

CHAPTER 3

3.1 Introduction

Polymeric actuators are a special class of materials that respond to an external trigger and undergo a transformation that can be used to perform mechanical work (1-3). Such polymers have found use in industrial applications like coatings (1) as well as biomedical applications as drug delivery devices (2, 4-6), micro-valves/switches in microfluidic devices (7, 8) and sutures (9). However their potential has been grossly underutilized. The focus of researchers with respect to actuators is reducing the response time for the polymer matrix. Certain soft tissue applications that could benefit from use of polymeric actuators include areas like wound closures and nervous tissue regeneration. The cellular processes can benefit from application of slow tensile forces at rates that the natural cell growth/division can keep up with (10-12). The inverse relation between the displacement produced by in the actuator and the resulting force generated consequently, present the greatest challenge in designing actuators for soft tissue applications (13). The polymer system should possess biodegradability, a biologically relevant trigger, controlled actuating potential that can be sustained for several days and be mechanically similar to soft tissue (10-100kPa). Presently none of the polymeric actuators can deliver all these requirements in one system. We aim to design a degradable polymeric biomaterial that can be used *in vivo* to impart tensile force to cells akin to an *in vitro* micromotor controlled apparatus. The strategy was to store a retractive stress in a crosslinked network along a pre-defined axis during fabrication. By gradually releasing this stress over time by degradative processes, we hypothesize that the crosslinked network will shrink in dimension along the pre-defined axis and produce controlled long term actuation over the course of several days.

Treatment of large gap (> 1 cm) peripheral nerve injuries has posed a significant challenge to the medical and biomedical engineering community (14-16). The nervous system is always under some degree of tension. For small gap injuries (< 1 cm) the neurosurgeon can surgically suture the nerve ends. For larger gaps the current gold standard treatment is a surgical autograph (15, 16). However this method of treatment has it pitfalls which include need for harvesting a functional nerve from somewhere else in the body, risk of infection, and loss of functionality for the donor site. The functional recovery rate is around 80% (1). Allografts and xenografts have been used as alternatives; however there is always a chance of rejection and an immune reaction. Biomaterial strategies have explored the application of polymeric conduits supplemented with growth factors or support cells like Schwann cells with promising results (14-16). However they have not been able to match the success rate of autografts.

Understanding how an axon grows could provide some guidance in improving biomaterial strategies to enhance their axonal growth. The growth cone is considered a key player in axonal growth *in vitro* (11, 17). *In vivo* however, there are two main mechanisms of axonal elongation. The first is via growth cone extension, while the second occurs after the growth cone has synapsed with its desired target and the neuron elongates as the target relocates and pulls the neuron with it (12, 18). The latter mechanical stimulation mechanism is called "stretch growth" or "towed growth". *In vitro* studies in the past decades have used calibrated micro-needles and mechanical micromotors to simulate and manipulate this phenomenon (10, 12, 19-21). The goal of such studies was to understand this mechanism and determine the limits of stretch growth. We aim to develop a hydrogel that can perform the

41

same function as a micromotor and "tug" on the neuron it is attached to, thereby providing mechanical stimulation to enhance their growth.

This work describes a crosslinked network system wherein retractive stress was stored along a pre-defined axis during fabrication and later by gradually releasing this stress we hypothesize that the crosslinked network will shrink in dimension along the same pre-defined axis. If nerve endings are attached to the ends of this shrinking matrix, it would be similar to a micromotor applying tensile stress on the neurons. Unlike the mechanized studies mentioned above, the polymer network system developed here will have a limit to its potential of being an actuator. We believe that this system will exist in two stages. During the first stage the hydrogel network will release the stored retractive stress and shrink, while in the second stage once the hydrogel has stopped shrinking it will exist as a passive scaffold that will act as a bridge for the neurites to cross over.

In order to be able to store a retractive stress in a network we needed to select a long chain biocompatible polymer. Some of the other requirements included ease of chemical modifications for the purpose of crosslinking, being a natural ligand for neuronal cells, and being naturally degradable to non-toxic byproducts. HA is a naturally occurring glycosaminoglycan that has been shown to enhance peripheral nerve regeneration (22, 23). It is a natural ligand for cell surface receptors like CD44 and RHAMM (24-27). The shear thinning property of HA would allow the molecular chains in even a highly concentrated solution to disentangle and align to the direction of flow. Rapid crosslinking of the chains in this state would allow us to store a retractive stress in the network. Releasing this stress may

lead to shrinkage of the network. We investigated the shrinking mechanism by either selectively degrading the crosslinks that hold the network together or by selectively degrading the long HA backbone chains. This chapter details our efforts at characterizing the hydrogel shrinkage as a result of degrading the HA network. To study the effect of selectively degrading the HA chains, we crosslinked the network using a almost non-degradable crosslinker poly(ethylene glycol) diacrylate (PEGDa). In the human body HA is broken down predominantly by the enzyme hyaluronidase (27-31). Enzyme concentrations simulating normal and post injury over-expression were tested. The hydrogel was characterized for its capability to shrink and to generate force in the process.

3.2 Materials and Methods

Sodium salt of HA (MW 1.6 MDa), bovine testicular hyaluronidase, poly(ethylene glycol) diacrylate (PEGDa), and glycidyl methacrylate (GMa) were purchased from Sigma Aldrich. GMa and PEGDa were filtered to remove MEHQ inhibitor. Irgacure 2959 was purchased from BASF chemicals. All other solvents and chemicals were purchased from Sigma unless stated otherwise and used without further purification.

3.2.1 **Methacrylation of HA**: Sodium salt of HA derived from *Streptococcus equi*, MW 1.6MDa, was used in the derivatization reaction. The functional unit of an HA molecule is a disaccharide consisting of *N*-acetylglucosamine and glucoronic acid. There are two main sites on an HA disaccharide suitable for modification, namely the pendant hydroxyl group on the *N*-acetylglucosamine and carboxylate on the glucoronic acid component. The derivatization method was adapted from previous work by Bader et al. with

43

poly(vinyl alcohol) gels (32). An excess of GMa was used to covalently attach the methacrylate moiety onto the HA disaccharide. Briefly, HA was dissolved in deionized water (DI H_2O) at a concentration of 3 mg/ml. A 20 molar excess of GMa was then dissolved in the HA solution, the pH was adjusted to 1.5, and the reaction was carried out at 50 °C for 2 days. Following this, the reaction mixture was dialyzed against DI H_2O for 2 days, after which the product was lyophilized and refrigerated until needed. The reaction chemistry is shown in Figure 3.1.

The degree of modification was quantified using proton NMR spectroscopy performed using a Bruker Avance-III 300 MHz spectrometer. Peaks (δ = 5.8, 6.2) representing the two protons on the methacrylate chain were used to calculate the degree of modification. The reference peak (δ = 2.0) was the peak representing protons from the methyl group on HA and methacrylate segment. The solvent used for NMR was deuterated water. The degree of methacrylation can be altered by varying the molar concentration of GMa in the reaction, and the duration of the reaction.
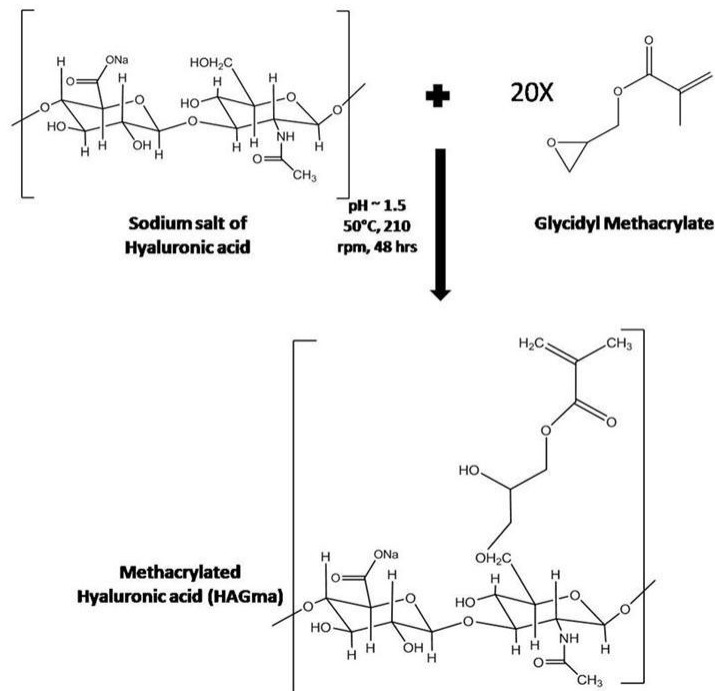
Fig.3.1 Schematic showing the reaction mechanism for methacrylation of hyaluronic acid. The reduction in pH triggered the ring opening of glycidyl methacrylate which covalently attached to the HA disaccharide.

3.2.2 **Rheological characterization**: To ensure that rapid crosslinking is able to restrain the shear flow disentangled HA molecular chains, it is imperative to know the relaxation behavior of the solution. An oscillatory strain sweep was conducted on a TA ARG2 stress-controlled rotational rheometer using parallel-plate geometry and a Peltier plate at room temperature to determine the linear viscoelastic regime. The strain was ramped from 0.1% to 10% at 25 °C. Step-strain stress relaxation experiments were conducted, where shear stress was monitored following application of a small shear strain. The diameter of the plate was 40 mm with a solvent trap and moisture chamber enclosure to prevent drying of the test solution. The strain values selected were 5%, 7%, 10% and 12%. Various compositions of HA pre-crosslinking solutions minus the photoinitiator were subjected to the stress relaxation test.

3.2.3 **Fabrication of crosslinked hydrogels**: Pre-crosslinking solutions were made consisting of methacrylated HA, PEGDa crosslinker, and 1% Irgacure 2959 (I2959). Cytocompatibility studies have showed that I2959 is one of the most cytocompatible photoinitiators (33). Irgacure 2959 is an α-cleavable type I photoinitiator or α-hydroxy phenyl ketone. It is a partially water soluble, non-yellowing compound which forms colorless solutions. The excitation frequency is 320 nm and photo-excitation produces a benzoyl and a ketyl radical of which the former is the major reactive species. One of the many advantages of this particular photoinitiator is that the excited triplet state is too short to be scavenged by oxygen, so the polymerization reaction can be carried out in air inside a fume hood (34). Experimental samples were fabricated using a mold created using glass slides as shown in Figure 3.2. The pre-crosslinking solution was injected into the mold via a 20 gauge needle at a rate of 0.5 ml/min. Rapid crosslinking was initiated by exposing the mold to a 100 W, 365 nm UV light source. The experimental samples were crosslinked immediately following injection. To make negative control samples, a delay was introduced between the injection and UV exposure to facilitate relaxation of the HA chains. Figure 3.3 shows the reaction schematic of the crosslinking chemistry.
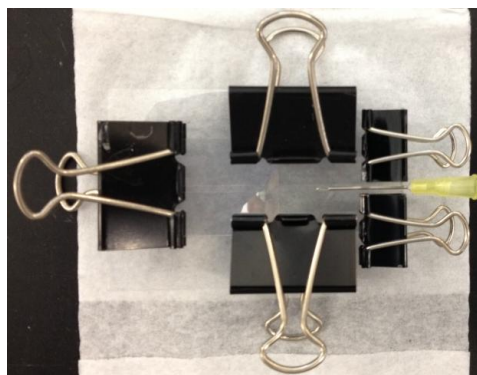
Fig.3.2. Image of the glass slide mold used to crosslink HA hydrogels. The needle shows the channel where the pre-crosslinking solution was injected prior to UV exposure.
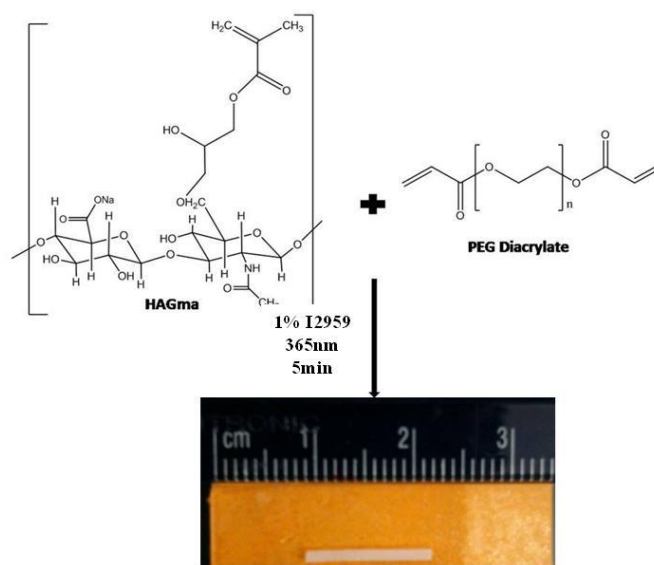
Fig.3.3. Schematic showing the crosslinking chemistry of the hydrogel. Two ratios of PEGDa (3:1 and 4:1) were used to crosslink methacrylated HA. The crosslinking solution turned from clear to opaque indicating success of crosslinking chemistry.

3.2.4 **Birefringence experiment**: Birefringence is a property that can provide evidence of a net molecular chain orientation in the crosslinked hydrogel due to rapid crosslinking of the shear aligned HAGMa chains. Crosslinked HA gels were imaged under the polarized optical light microscope (POM) to study their orientation birefringence. Since the samples were opaque in hydrated conditions, they were air dried following which they

became clear and transparent. The dried gel samples of each composition were placed between crossed polarisers and the sample stage was rotated to observe the change in optical birefringence. Since the polarisers are crossed, no light can pass through to the sensors. When an anisotropic material with some degree of net orientation is introduced between the crossed polarisers, some of the light is able to pass through the second polariser onto the sensors. The maximum intensity of this orientation induced birefringence signal can be observed when the optical axis of the sample is at 45° to the polariser. The extent of orientation in the hydrogel is a function of the how efficiently the crosslinker can arrest relaxation of the chains during crosslinking. The intensity of light was captured using a visible spectrometer and the spectral content analyzed via ocean optics OOIBase software. The raw intensity spectrum was normalized to obtain the transmittance spectrum using the following formula;

$$T(\lambda) = [I(\lambda) - I_d(\lambda)]/[I_0(\lambda) - I_d(\lambda)]$$

Where I is the intensity spectrum of the sample, I_0 is the reference bright spectrum and I_d is the dark spectrum. The transmittance spectrum, as shown in Figure 3.4, follows the relation;

$$T(\lambda) = Sin^2\left(\pi\frac{\Delta n h}{\lambda}\right) Sin^2(2\chi) \ ....(35)$$
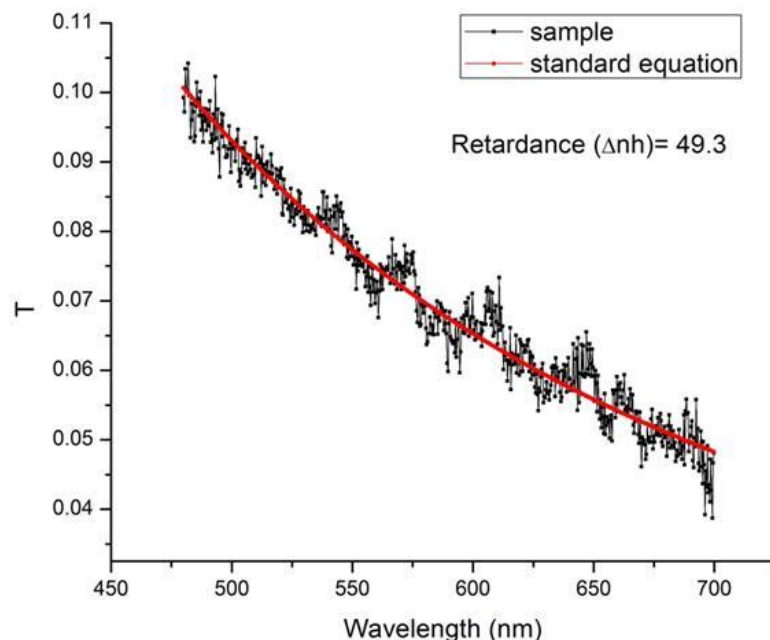
Fig.3.4. Representative transmittance spectrum from a sample within the visible light frequencies captured using the spectrometer. The black curve is from a crosslinked hydrogel sample while the red curve shows the standard equation fit curve obtained from non-linear regression.

where χ is orientation angle of sample reference axis (45°) with respect to the polariser, and h is the sample thickness. Using non-linear regression, the experimental data was fit to the above equation to get the retardance (Δnh) value. Two sets of experiments were performed to answer two different questions about this hydrogel system. Samples crosslinked with different crosslinker concentrations were compared for their retardance to determine the effect of crosslinker concentration on the degree of alignment. The second set of experiments compared the retardance of samples before and after a 48hr shrinkage experiment to confirm that the shrinkage is a result of reorganization of the molecular chains in the hydrogel network. The compositions tested were 60 mg/ml HAGMa crosslinked with 3:1 or 4:1 ratio of PEGDa. Each sample was imaged at three

separate locations representing the two ends and the middle of the sample. This was done to observe if there is any significant difference in the molecular orientation across the sample. The enzyme concentration for the degradation experiment was 10 μg/ml of hyaluronidase which simulates the over expression of the enzyme at the injury site.

3.2.5 **Calculation of predicted retractive stress in the network using rubber elasticity theory**: In order to predict the retractive stress stored in the hydrogel network, we needed to first calculate certain network parameters. Swelling experiments were performed on samples of each composition to calculate the swelling coefficient (Q_m) and crosslink density (n). HA hydrogels consisting of 60 mg/ml HAGMa were crosslinked with 3:1 and 4:1 ratio of PEGDa in the injection mold as described earlier. The gels were swollen in PBS overnight and weighed to find the wet weight (M_w). The samples were dried in a desiccator and weighed again to find the dry weight (M_d). Q_m was calculated using these masses.

$$Q_m = \frac{M_w}{M_d}$$

Using the swelling coefficient we calculated the volumetric swelling ratio (Q_v). It is related to Q_m as follows,

$$Q_v = 1 + \frac{\rho_p}{\rho_s}(Q_m - 1)$$

where ρ_p = density of dry polymer = 1.229 gm/cm^3, and ρ_s = density of solvent = 1 gm/cm^3. Applying Flory-Rehner equilibrium swelling theory (36), the crosslink density was calculated from the following equation:

$$n = \frac{-[\ln(1 - \vartheta) + \vartheta + \chi\vartheta^2]}{V\left[\vartheta^{1/3} - \frac{\vartheta}{2}\right]}$$

where υ = volume fraction of polymer in swollen mass = $1/Q_v$, V = Molar volume of solvent = 18 cm^3/mol, and χ = Flory polymer-solvent interaction parameter = 0.473. As the crosslinker concentration in the hydrogel increases, Q_m will decrease.

We adapted the rubber elasticity principles to calculate the predicted maximum retractive stress (σ_{Pr}) that can be stored in the crosslinked hydrogel network. Under normal convention when a crosslinked network is stretched by a factor α, the retractive stress in the network can be calculated using the following relation (36);

$$\sigma_{Pr} = nRT\left(\alpha - \frac{1}{\alpha^2}\right)$$

where α = extension ratio = L/L_0, R = Gas constant, and T = Temperature. In this current system we are storing a retractive stress in the network via rapid crosslinking of the oriented HA chains. So the extension ratio (α) in this case can be assumed to be the extent by which the disentangled molecular coils are retained in that state. Pre-crosslinking solution was injected into the glass mold and crosslinked to form a hydrogel. The length of this hydrogel (L) was measured. Next the same composition and volume of pre-crosslinking solution was injected into the mold but this time it was not exposed to the UV source and crosslinked. This allowed for the relaxation of the molecular chains that were previously aligned due to the shear flow. The length of the solution column in the mold channel in the absence of crosslinking provided us with L_0. The extension ratio was the ratio of the two lengths. A minimum of three samples were used for each

composition. As the crosslinker concentration in the system is increased, the restriction of chain relaxation should increase. As a result, the degree of retractive stress in the network should also increase. This predicted calculation of retractive stress was compared with the actual measured value of stress that was generated by the shrinking sample in the mechanical setup.

3.2.6 **Enzyme driven shrinkage experiment**: HA hydrogels consisting of 60 mg/ml HAGMa crosslinked with 3:1 and 4:1 ratio of PEGDa were subjected to two different concentrations of the enzyme hyaluronidase to characterize the network's ability to shrink. The concentrations we selected for this work were 5 µg/ml and 10 µg/ml. Rapidly crosslinked PEGDa hydrogels were fabricated in an injection mold as described previously. These gels were swollen in DI water overnight before testing. The hydrogels were exposed to 0 µg/ml, 5 µg/ml, and 10 µg/ml hyaluronidase for a period of 48 hrs in a 37 °C shaker. The enzyme was replenished every 4 hrs to compensate for the loss of activity. At each of these time points, images of the samples were captured, which were later measured using Image J. To confirm that the shrinkage was a result of the reorganization of polymer microstructure, we also fabricated negative control samples where we did not expect to have any stored retractive stress. This was achieved by providing the HA chains in the pre-crosslinking solution ample time to relax before being exposed to UV light source. The negative control samples were exposed to the same concentration of enzyme for the same duration and their dimensions were measured. Three samples of each composition were tested. We also conducted a 1 week long term experiment to determine how long the shrinkage continues. For this experiment, 3:1 and 4:1 ratio PEGDa crosslinked hydrogels were exposed to the over expression

concentration of 10 µg/ml of hyaluronidase for 1 week. Sample images were captured every 4hr and measured to plot the shrinkage profile. To also ensure that degradation was not a result of erosion, relative position of surface features was observed in all the images captured.

3.2.7 **Effect of solvent diffusion on shrinkage**: Diffusion is a key aspect that could affect the rate and manner of shrinkage. To ensure that the enzyme was diffusing through the bulk of the hydrogel and producing the shrinkage, samples were fabricated as described previously and then sliced longitudinally to reduce the thickness by one half. The rationale behind this was that if the enzyme was not diffusing into the bulk of the sample then the shrinkage magnitude and profile would be different than the regular samples. Three samples each of 60 mg/ml HAGMa crosslinked with 3:1 or 4:1 ratio of PEGDa were used for this experiment. The samples were exposed to 10 µg/ml of hyaluronidase at 37 °C for a period of 48 hrs. The enzyme was replenished every 4 hrs and images captured at each time point were measured using Image J.

3.2.8 **Measurement of hydrogel stiffness:** In order to determine the force generated by the shrinking hydrogel, we designed a mechanical test setup that relies on a flexible cantilever and its associated sensor. To make sure that we can accurately determine the forces, the hydrogel samples and the cantilever had to be stiffness matched. We performed surface indentation using the mesoindentation system to calculate the stiffness of the hydrogel (37). At the beginning of each indent, the tip was positioned some distance away from the sample surface and then driven into the sample until a predefined

53

maximum load was reached, as detected by the deflection of the cantilever towards the differential variable reluctance transducer (DVRT). Once the predefined load was reached, the tip was retracted from the sample until it reached its initial position. The force and displacement data were acquired during this entire process. The tip moved at a speed of 33 µm/sec. A liquid cell in the form of a Plexiglas container was incorporated in the setup along with a sample holder to submerge the sample, tip, cantilever and the DVRT. The samples were indented to a maximum load of 60 µN. Each sample was indented in at least three random locations to gauge the bulk stiffness. The stiffness was calculated from the slope of the loading portion of the load-displacement curve. Samples were tested before and after exposure to 10 µg/ml of hyaluronidase to determine the effect of degradation on hydrogel stiffness.

3.2.9 **Force measurement**: A device consisting of a flexible aluminum cantilever-DVRT pair, as shown in Figure 3.5, was custom built for measuring the force generated by HA hydrogels during the process of shrinking. The principle concept behind the design is that a shrinking hydrogel attached between a flexible calibrated cantilever and a fixed stage will deflect the cantilever. The non-contact DVRT will record this deflection and provide a way to quantify the force. The cantilever was calibrated for various known loads by attaching a string to the cantilever and hanging known weights on the other end. The cantilever was also calibrated for known displacements/deflections of the cantilever by using a calibrated micromotor. A reservoir was incorporated in the device to house the gel and keep it hydrated throughout the experiment. The gel was glued onto a fixed stage on one end and to the calibrated cantilever on the other end using epoxy glue. The non-

contact DVRT sensed any deflection in the calibrated aluminum cantilever and the data collected using data acquisition software was plotted as force versus time. The entire setup was maintained at 37 °C during the experiment by a temperature controlled water bath. HA hydrogels consisting of 60 mg/ml HAGMa crosslinked with 3:1 and 4:1 ratio of PEGDa were fabricated as described previously. Three samples of each composition were exposed to 10 µg/ml of hyaluronidase for a period of 48 hrs. Fresh enzyme was added to reservoir every 4 hrs. Control samples were not exposed to any enzyme. The raw voltage data was converted to force (mN) and displacement (µm) using calibration constants. The cross sectional area of contact of the sample with the cantilever is $1mm^2$. Using this information and the calculated force, the stress (F/A) exerted by the shrinking hydrogel on the cantilever was calculated. The work performed by the shrinking hydrogel was then calculated by multiplying the stress and the corresponding cantilever displacement.
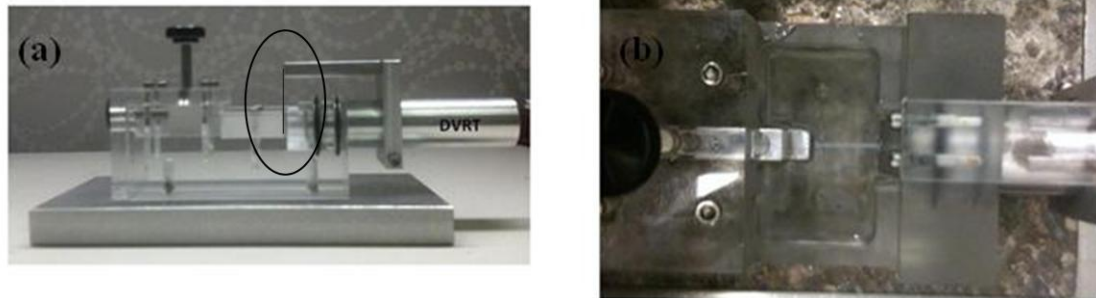
Fig.3.5. Images showing the device used to measure the force generated by the shrinking hydrogel. (a) The aluminum cantilever-DVRT pair (circled in black) is the sensing end of the device. (b) The sample is attached on one end to the calibrated flexible cantilever and to a fixed stage on the other end. The sample is kept submerged via the enclosed reservoir chamber.

3.2.10 **Statistical analysis**: For all statistical analyses, ANOVA with Tukey post-hoc analysis or a students t-test were employed as applicable using Origin Pro 8.0, with a significant

difference reported for p < 0.05. Image analysis was performed using Image J software (NIH, USA). All values are reported as mean ± standard deviation.

3.3 Results

3.3.1 **Methacrylation of HA**: Sodium hyaluronate was successfully modified and a pendant methacrylate group was added on the disaccharide thus forming methacrylated HA (HAGMa). The coupling of GMa to HA was accomplished via epoxide ring-opening mechanism. Figure 3.6 shows the NMR of the HA molecule before and after derivatization. The ratio of normalized area under either peak with the reference methyl peak shows that 79% of the potential sites on the HA molecule were successfully modified. This reaction was successfully repeated several times with the modification percentage ranging from 75% to 82%. The extent of methacrylation was controlled via the concentration of HAGMa (see appendix). A reaction consisting of 10 molar excess of glycidyl methacrylate resulted in approximately 50% methacrylation of the HA molecule. The molecular weight of the resulting HAGMa was verified using gel permeation chromatography (GPC) and was found to be 1.3 MDa.
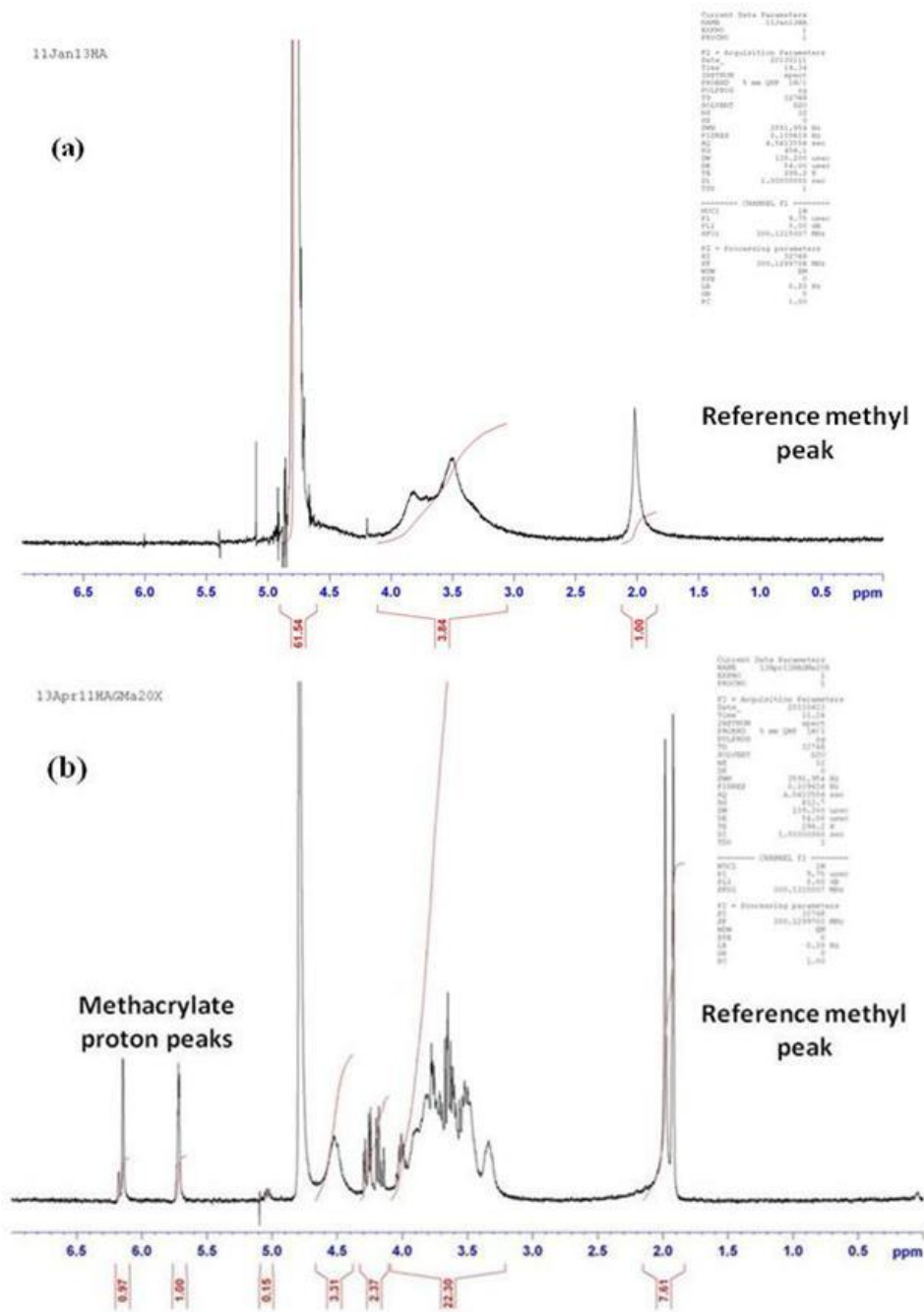
Fig.3.6. (a) Proton NMR of HA showing the peak representing methyl group (δ = 2.0) of the N-acetylglucosamine. (b) Proton NMR of methacrylated HA molecule. The two peaks (δ = 5.8, 6.2) representing the two protons on the methacrylate chain were used to calculate the degree of modification. The reference peak is a result of protons representing the methyl group on the HA backbone and the methyl group on the methacrylate segment. The solvent used was deuterated water (δ = 4.8). The degree of methacrylation was 79%.

3.3.2 **Rheological characterization**: Figures 3.7 and 3.8 show the stress relaxation plots for the compositions 60mg/ml HAGMa with 3:1 PEGDa and 60 mg/ml HAGMa with 4:1 PEGDa respectively. At time = 0 the specimen was suddenly deformed homogenously. The deformation created a stress which gradually relaxed with time. The shear stress could return to zero once the strain induced stress relaxes. Due to the high molecular weight of the HA polymer, the molecular chains may not return to the same random configuration once the stress relaxes. Instead of zero shear stress the sample could plateau out at a non-zero value as the chains may obstruct each other to prevent complete relaxation. Complete relaxation of shear stress was not observed within the test duration for any of the strain conditions. We also did not observe any plateau condition either. From pilot crosslinking tests the crosslinking time was observed to be between 45 and 55 seconds. The rheological tests indicated that the neither of the compositions, 60 mg/ml HAGMa crosslinked with 3:1 or 4:1 PEGDa, would have relaxed before the solution gets completely crosslinked. Thus these compositions would be ideal candidates for testing our hypothesis of storing a retractive stress in the crosslinked networks.
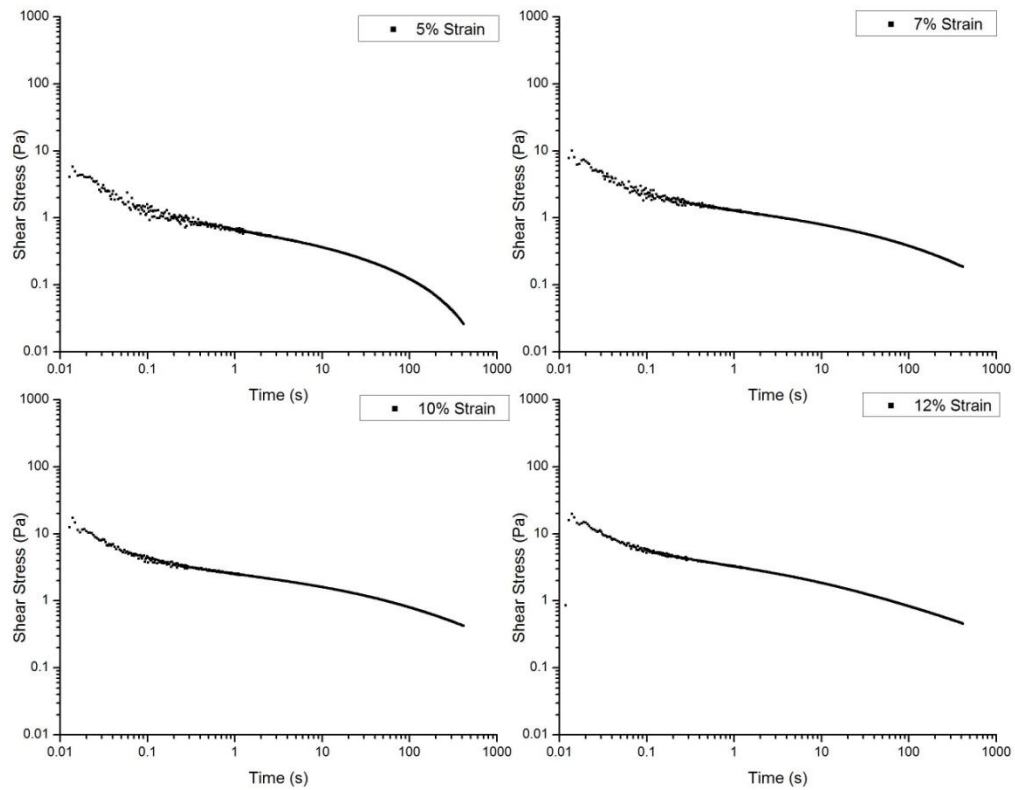
Fig.3.7.Stress relaxation curves for pre-crosslinking solutions of the composition 60mg/ml HAGMa with 3:1 PEGDa. The % strain conditions used were 5%, 7%, 10%, and 12%. The shear stress did not return to zero or plateau out within testing duration limits indicating that total molecular chain relaxation did not occur. This meant that if this solution were to be crosslinked post shearing then the crosslinking reaction would be able to trap some of the chains in the shear aligned conformation.

60mg/ml HAGMa + 4:1 PEGDa
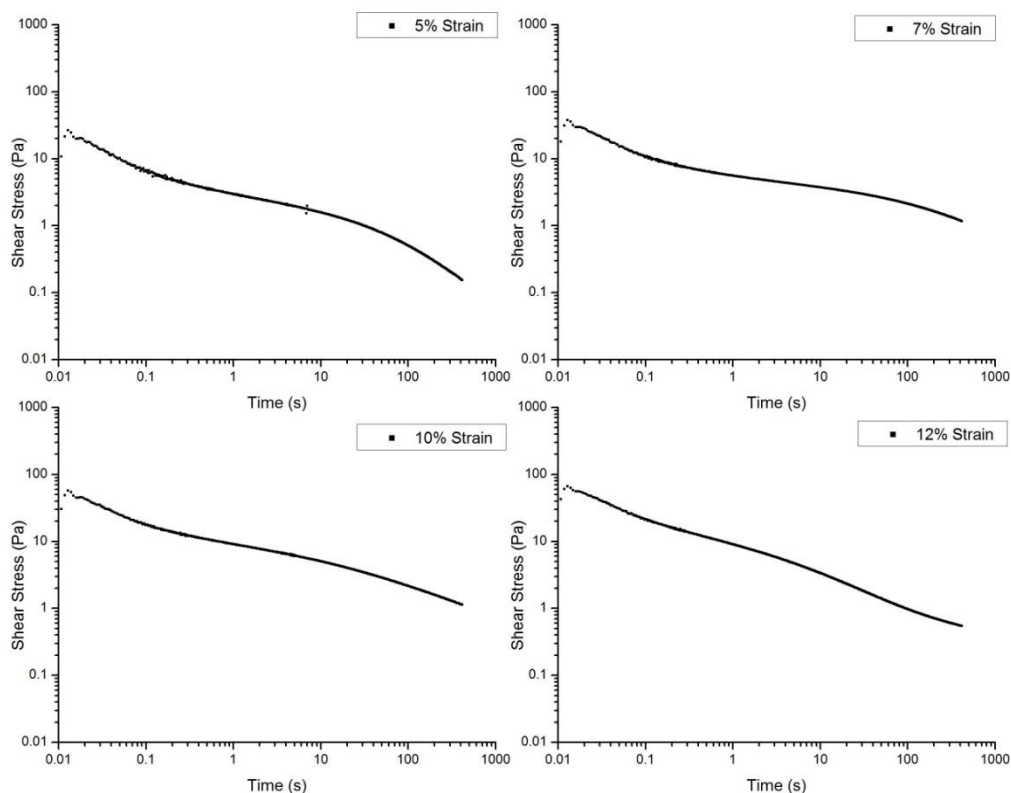
Fig.3.8.Stress relaxation curves for pre-crosslinking solutions of the composition 60mg/ml HAGMa with 4:1 PEGDa. The % strain conditions used were 5%, 7%, 10%, and 12%. The shear stress did not return to zero or plateau out within testing duration limits indicating that total molecular chain relaxation did not occur. This meant that if this solution were to be crosslinked post shearing then the crosslinking reaction would be able to trap some of the chains in the shear aligned conformation.

3.3.3 **Birefringence study**: The degree of orientation was quantified using polarized optical microscopy. Under crossed polarizers, a sample with no specific molecular orientation will appear dark while a sample possessing molecular orientation will appear bright or colorful depending on the extent of orientation and the type of the material. The brightness level is directly proportional to degree of orientation. Figure 3.9 shows optical micrographs for samples of the composition 60 mg/ml HAGMa crosslinked with 3:1 ratio of PEGDa prior to exposure to 10 µg/ml hyaluronidase. When the optical axis of the

60

sample was at 45° to the polarizers, birefringence was observed indicating presence of orientation. We calculated the retardance (Δnh) values for all the samples at three distinct locations across the sample, the middle and the two ends. After comparing the retardance values from the three locations, amongst themselves and across the samples, we concluded that there was no significant difference ($p \gg 0.05$) in the retardance values. This indicated that the crosslinking was rapid enough to preserve the shear induced molecular orientation and this orientation was nearly homogenous. The average retardance was calculated from the nine values obtained from the three samples. The average retardance for the composition 60 mg/ml HAGMa crosslinked with 3:1 PEGDa prior to enzymatic degradation was 39.71 ± 12.41 nm.

Three samples of the same composition were then exposed to 10 μg/ml hyaluronidase for a period of 48 hrs. This concentration of the enzyme was selected to simulate the over expression of the enzyme following PNS injury. The enzyme was replenished every 4 hrs. After the test duration, the samples were air dried and observed under the polarized optical microscope (POM). Figure 3.10 shows the captured micrographs. The observable brightness was significantly reduced as compared to the pre-enzyme exposure samples. This demonstrated that the enzymatic degradation caused decrease in molecular orientation within the samples. Once again we compared the retardance values along length of the sample and between samples. There was no statistically significant difference observed ($p \gg 0.05$). The magnitude of overall sample shrinkage was not measured during this experiment. The average retardance for this composition following enzymatic degradation was 8.15 ± 2.44 nm.
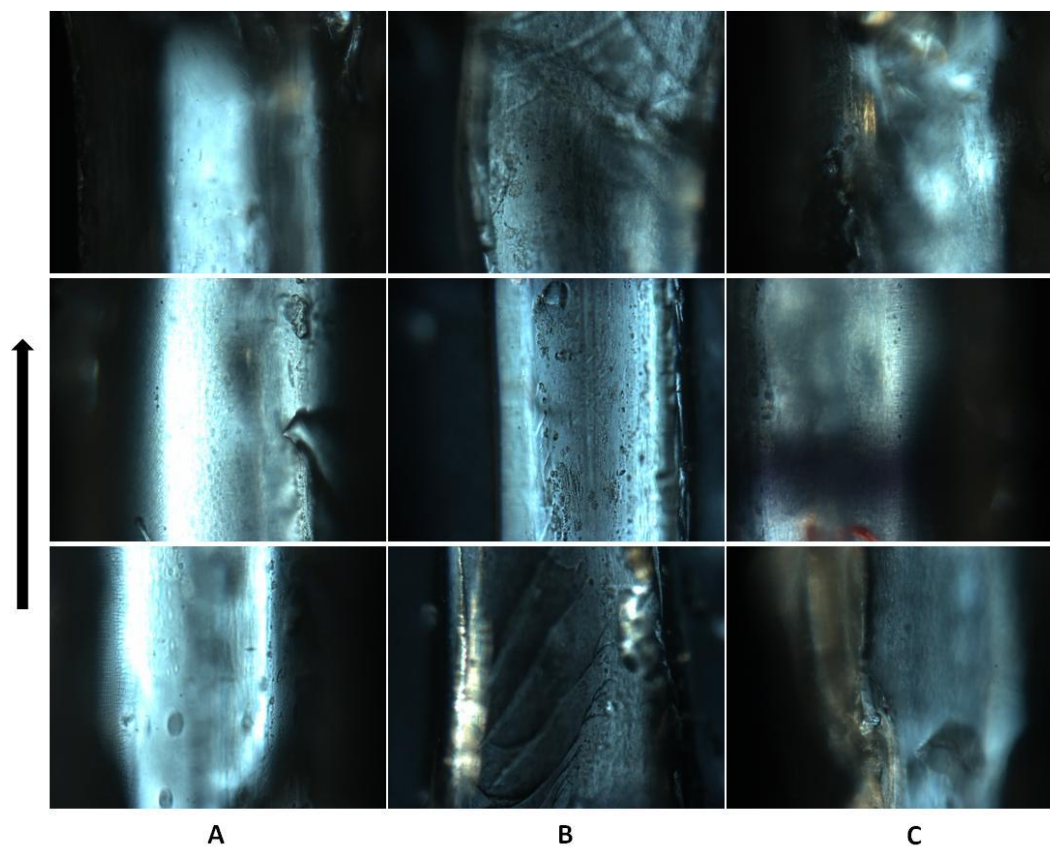
Fig.3.9. Polarized optical micrographs of three 60 mg/ml HAGMa hydrogels crosslinked with 3:1 ratio of PEGDa prior to their exposure to hyaluronidase. Images were captured at the two ends and the middle of the sample. The arrow indicates the direction of flow of the pre-crosslinking solution in the glass mold prior to rapid crosslinking. The retardance for this composition calculated from the captured spectra was 39.71 ± 12.41 nm. The magnification was 20X.
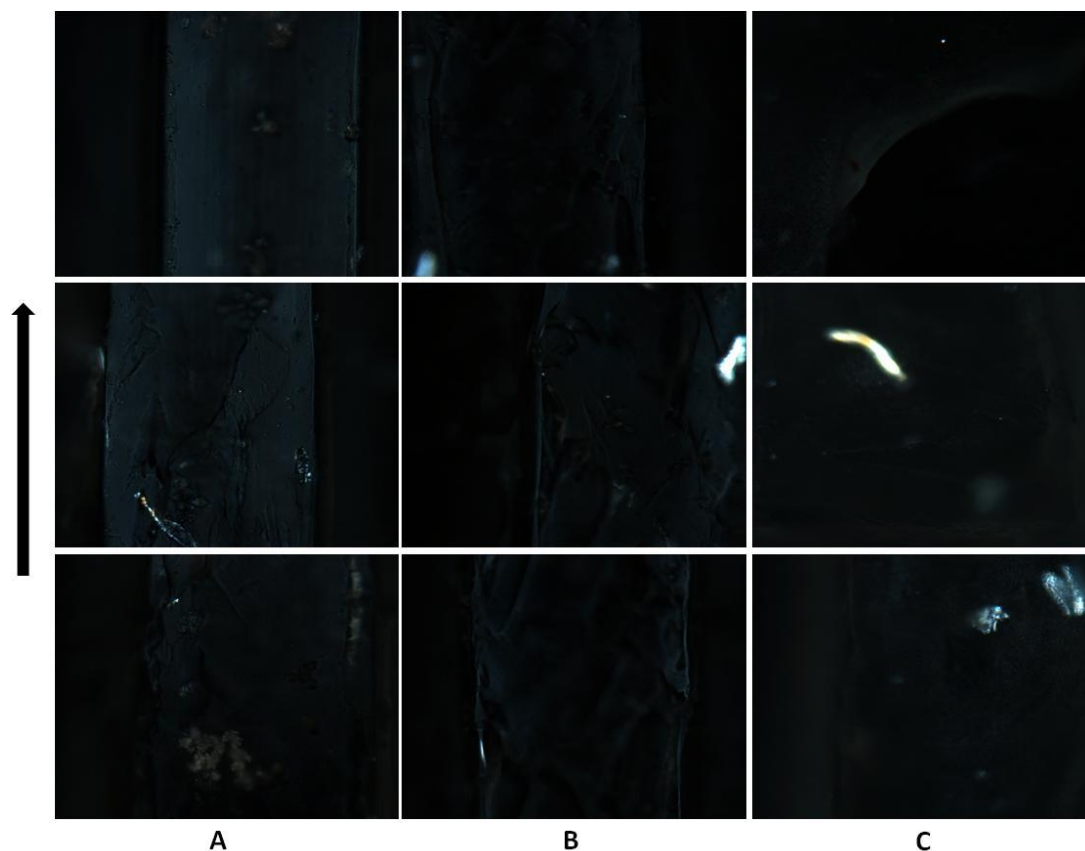
Fig.3.10. Polarized optical micrographs of three 60 mg/ml HAGMa hydrogels crosslinked with 3:1 ratio of PEGDa after exposure to 10 µg/ml hyaluronidase for 48hrs. Images were captured at the two ends and the middle of the sample. The arrow indicates the direction of flow of the pre-crosslinking solution in the glass mold prior to rapid crosslinking. The retardance for this composition calculated from the captured spectra was 8.15 ± 2.44 nm. The decrease in the retardance compared to the value obtained before enzymatic degradation indicated loss of molecular orientation in the sample. The magnification was 20X.

Similarly the second composition, 60 mg/ml HAGMa crosslinked with 4:1 ratio of PEGDa, was observed under the POM prior to and after exposure to 10 µg/ml hyaluronidase. Figure 3.11 shows the optical micrographs for the 4:1 ratio PEGDa samples prior to enzyme exposure. Each sample was imaged at the two ends and the middle to determine the homogeneity of any molecular orientation. The brightness verified the existence of molecular orientation. The average retardance was 50.06 ± 10.95

nm. Samples of the same composition were then exposed to 10 μg/ml hyaluronidase for 48 hrs and imaged to observe effect of degradation on molecular orientation. Figure 3.12 shows the polarized optical micrographs for the enzymatically degraded samples. The retardance values and the observable brightness significantly decreased ($p \ll 0.05$), as compared to values obtained from prior to degradation, indicating loss of molecular orientation. The average retardance value post enzyme exposure was 15.28 ± 1.25 nm. The magnitude of overall sample shrinkage was not measured during this experiment.
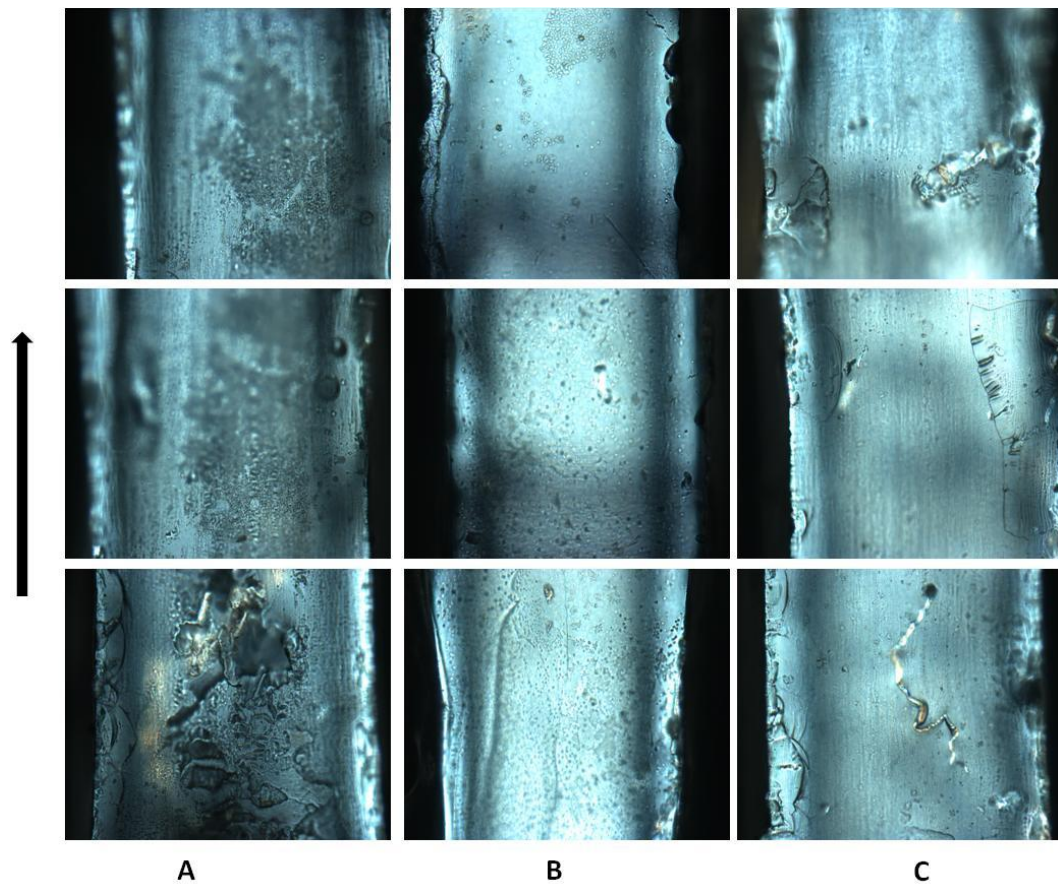
Fig.3.11. Polarized optical micrographs of three 60 mg/ml HAGMa hydrogels crosslinked with 4:1 ratio of PEGDa prior to their exposure to hyaluronidase. Images were captured at the two ends and the middle of the sample. The arrow indicates the direction of flow of the pre-crosslinking solution in the glass mold prior to rapid crosslinking. The retardance for this composition calculated from the captured spectra was 50.06 ± 10.95 nm. The magnification was 20X.

Fig.3.12. Polarized optical micrographs of three 60 mg/ml HAGMa hydrogels crosslinked with 4:1 ratio of PEGDa after exposure to 10 µg/ml hyaluronidase for 48hrs. Images were captured at the two ends and the middle of the sample. The arrow indicates the direction of flow of the pre-crosslinking solution in the glass mold prior to rapid crosslinking. The retardance for this composition calculated from the captured spectra was 15.28 ± 1.25 nm. The decrease in the retardance compared to the value obtained before enzymatic degradation indicated loss of molecular orientation in the sample. The magnification was 20X.

Figure 3.13 summarizes the results from the birefringence study for the HAGMa hydrogels crosslinked with two different ratios of PEGDa. There was a significant reduction in molecular orientation following enzymatic degradation. The retardance values, and hence the molecular orientation, scaled with an increase in crosslinker concentration. To confirm that enzymatic degradation was the sole contributor to reduction in molecular orientation, we also performed a negative control experiment

where samples were submerged for 48 hrs in PBS not containing any hyaluronidase. Figure 3.14 shows retardance results from this control experiment. There was no significant difference ($p >> 0.05$) between the retardance of the samples before and after the 48 hr PBS soak. The average values for this batch of samples were slightly lower than those described earlier, however they were within the range. The lower values could be attributed to batch variability. The lack of any significant reduction in retardance values proved that enzyme activity is required for the molecular reorganization which leads to the loss of molecular orientation.
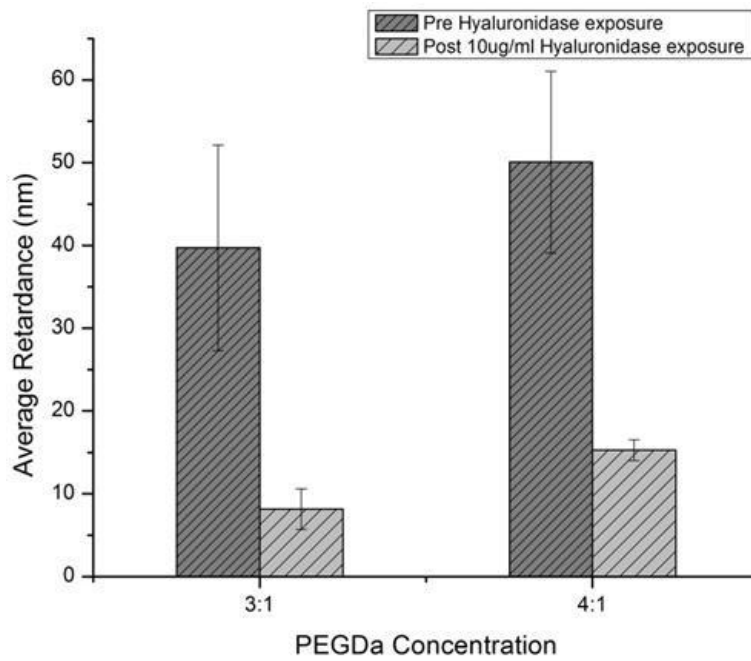
Fig.3.13. Bar graph summarizing the retardance values calculated for the PEGDa crosslinked HAGMa hydrogel samples prior to and following enzymatic degradation. The significant decrease in the retardance for the two compositions following enzymatic degradation indicated that the process of degradation reduced the molecular orientation in the hydrogels. (n=3)
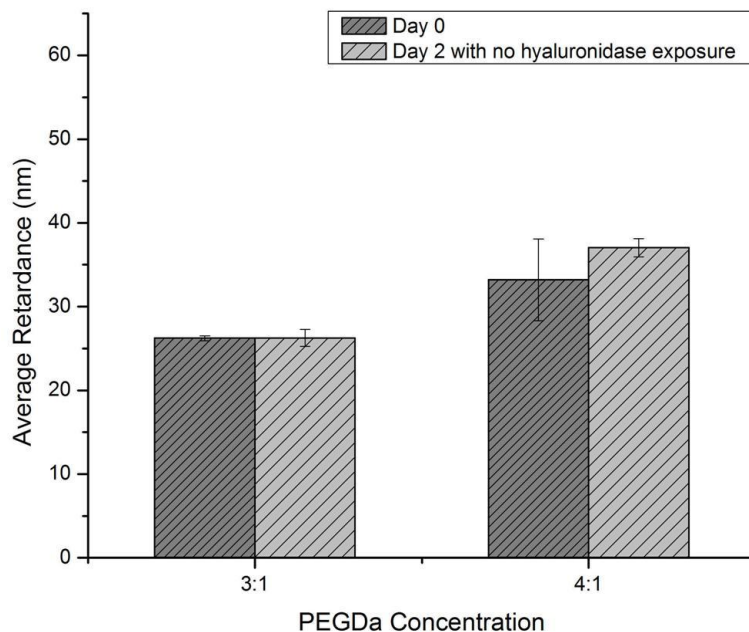
Fig.3.14. Bar graph summarizing the results from the negative control samples of PEGDa crosslinked HAGMa hydrogels. The negligible change in the retardance values of the samples after 2 days indicated that the reduction in molecular orientation seen in the samples exposed to the enzyme was truly on account of the degradation. (n=3)

3.3.4 **Estimation of retractive stress in the hydrogel:** To calculate the crosslink density of the hydrogels, swelling experiments were performed to calculate the swelling ratios. The gels with lower concentration of crosslinker showed higher average swelling; however there was no statistically significant difference in the swelling coefficients. We adapted rubber elasticity theory to estimate the retractive stress stored in a rapidly crosslinked hydrogel. Table 3.1 and Figure 3.15 show the results from these calculations. Increasing the crosslinker concentration did not significantly increase the predicted retractive stress stored in the hydrogel network.

Table 3.1. Results from the swelling experiments and retractive stress estimation study

Composition	Swelling Coefficient (Q_m)	Volumetric Swelling Ratio (Q_v)	Crosslink Density n x10^{-4}	Stretching Factor (α)	Predicted Retractive Stress (σ_{Pr}) kPa
60mg/ml HAGMa + 3:1 PEGDa	7.14 ± 0.19	8.56 ± 0.243	1.23 ± 0.08	1.01 ± 0.00	7.08 ± 0.39
60mg/ml HAGMa + 4:1 PEGDa	6.71 ± 0.74	8.07 ± 0.91	1.49 ± 0.45	1.01 ± 0.002	9.25 ± 2.21
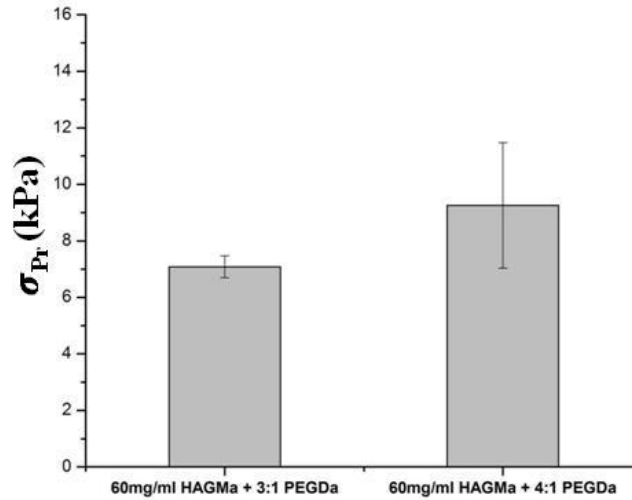
Fig.3.15. Bar graph showing the predicted values of retractive stress stored in the two compositions of PEGDa crosslinked HAGMa hydrogel samples. There was no statistically significant difference observed between the two compositions although the averages seemed to scale with the increase in PEGDa concentration. (n=3)

3.3.5 **Enzyme driven shrinkage**: Rapidly crosslinked HAGMa samples demonstrated shrinkage when they were exposed to hyaluronidase. We exposed the samples to three concentrations of hyaluronidase; 0 µg/ml, 5 µg/ml, and 10 µg/ml. The images obtained at each enzyme replenishment time point were measured and the sample lengths were normalized and plotted against time. Figure 3.16 shows the shrinkage profile for each composition. In the case of 60 mg/ml HAGMa crosslinked with 3:1 ratio of PEGDa, the control samples showed negligible reduction in their length (3%) as compared to those exposed to hyaluronidase (12%). The majority of shrinkage occurred along the long axis

of the sample which was also the axis of flow prior to crosslinking. Increasing the

enzyme concentration increased the total average magnitude of shrinkage by 2%. The

profile of the shrinkage indicated that majority of the shrinkage occurred within 30hrs.
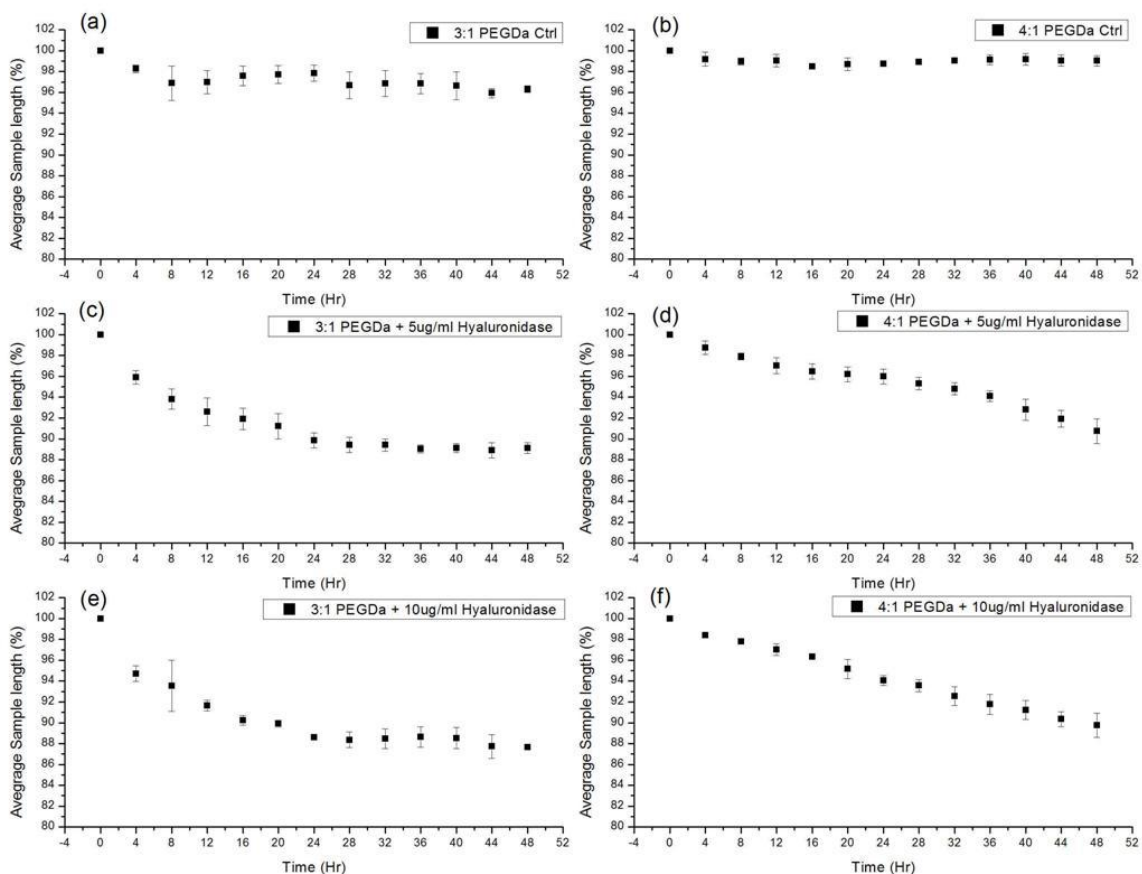
Fig.3.16. Graph showing enzyme driven shrinkage profile for PEGDa crosslinked
HAGMa hydrogel samples exposed to hyaluronidase for 48 hrs. The controls were not
exposed to the enzyme. Panels a, c, and e show the profiles for 3:1 ratio PEGDa samples
while panels b, d, and f show profiles for 4:1 ratio PEGDa crosslinked samples. Increase
in concentration of the enzyme increase the magnitude of shrinkage. The composition 60
mg/ml HAGMa crosslinked with 4:1 ratio PEGDa demonstrated a linear shrinkage
profile when exposed to 10 µg/ml hyaluronidase. (n=3)

Samples of the second composition, 60 mg/ml HAGMa crosslinked with 4:1 ratio

of PEGDa, also underwent shrinkage along their long axis when subjected to enzymatic

degradation. Compared to the controls (2%), the experimental samples shrunk on an

average about 11% - 12%. Increasing the enzyme concentration did not increase the magnitude of shrinkage; however it made the shrinkage profile almost linear. The samples indicated potential to shrink beyond 48 hrs. To test when the shrinkage stops we extended the duration of the experiment to 1 week. For each concentration of enzyme exposure, increasing the crosslinker concentration in the samples decreased the magnitude of net shrinkage achieved in 48hrs. We hypothesize that as the crosslink density increases in the gels, the freedom of motion in the network for the chains to rearrange themselves is lower as hyaluronidase cleaves the larger HA molecule into smaller segments. This led to lower shrinkage in spite of having higher retractive stress stored in the network. Samples of the composition 60 mg/ml HAGMa crosslinked with 3:1 PEGDa demonstrated the most shrinkage (2 ± 0.09 mm or 12.33 ± 0.66 %) when exposed to10 µg/ml hyaluronidase.

Enzymatic degradation caused the samples to shrink. Degradation at the surface could result in erosion of sample presenting as sample shrinkage along with the molecular reorganization. We tracked distinct features (surface asperities, visible pores) and their relative location on the sample throughout the degradation process and concluded that erosion was not responsible for the reduction in the length of the sample. To further verify the mechanism of shrinkage, we fabricated negative controls that should be devoid of any retractive stress in their crosslinked matrix. These samples made using the two PEGDa concentrations were exposed to 5 µg/ml and 10 µg/ml of hyaluronidase for 48 hrs. Figure 3.17 shows the shrinkage profiles for such samples. Comparing the results of the 48 hr shrinkage of the rapidly crosslinked samples as described above to the

negative controls it is quite evident that the latter show significantly lower shrinkage (2% - 4%) which was actually in the range of the control sample shrinkage. We attribute the shrinkage seen to the incapability of the chains to completely relax in the time provided prior to crosslinking due to physical entanglements. Thus we ascertained that the shrinkage we observed was due to the enzymatic cleavage of shear aligned backbone HA molecular chains that had their disentangled conformation preserved by rapid crosslinking process.
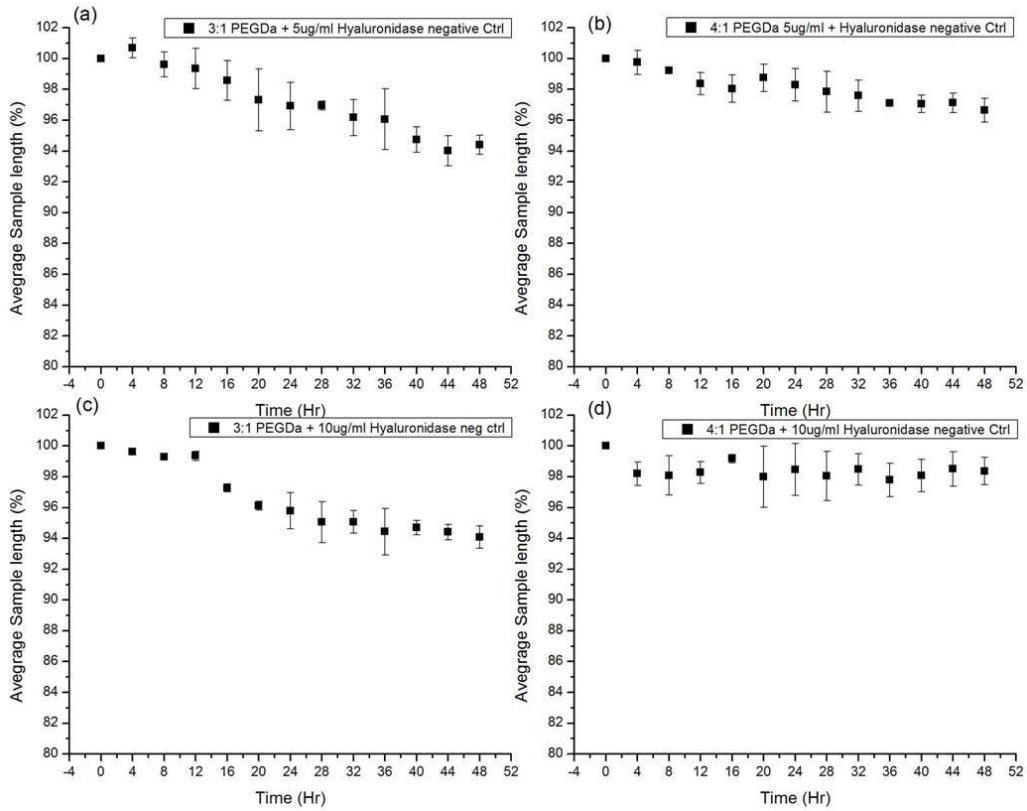
Fig.3.17. Average sample length profiles for the negative control samples. (a, c) When the 3:1 PEGDa crosslinked HAGMa samples were exposed to hyaluronidase for duration of 48 hrs, the shrinkage was on par with control samples which were not exposed to any enzyme. (b, d) The 4:1 ratio PEGDa negative control samples showed similar insignificant shrinkage when exposed to hyaluronidase. (n=3)

The long term experiment to study how long the shrinkage can be sustained showed a direct dependence on crosslinker concentration in the hydrogels. Figure 3.18 shows the average sample length profile plotted against time. For the gels crosslinked with 3:1 ratio of PEGDa, the shrinkage stopped by the end of day 2, where as for the gels crosslinked with 4:1 ratio of PEGDa the shrinkage stopped around day 3. These results verified our initial hypothesis that the gel would exist in two phases; phase 1 where it is an active stimulator and phase 2 where it is a passive scaffold. The limiting factor controlling the duration and magnitude of the shrinkage is the extent to which the molecular chains disentangle during shear flow.
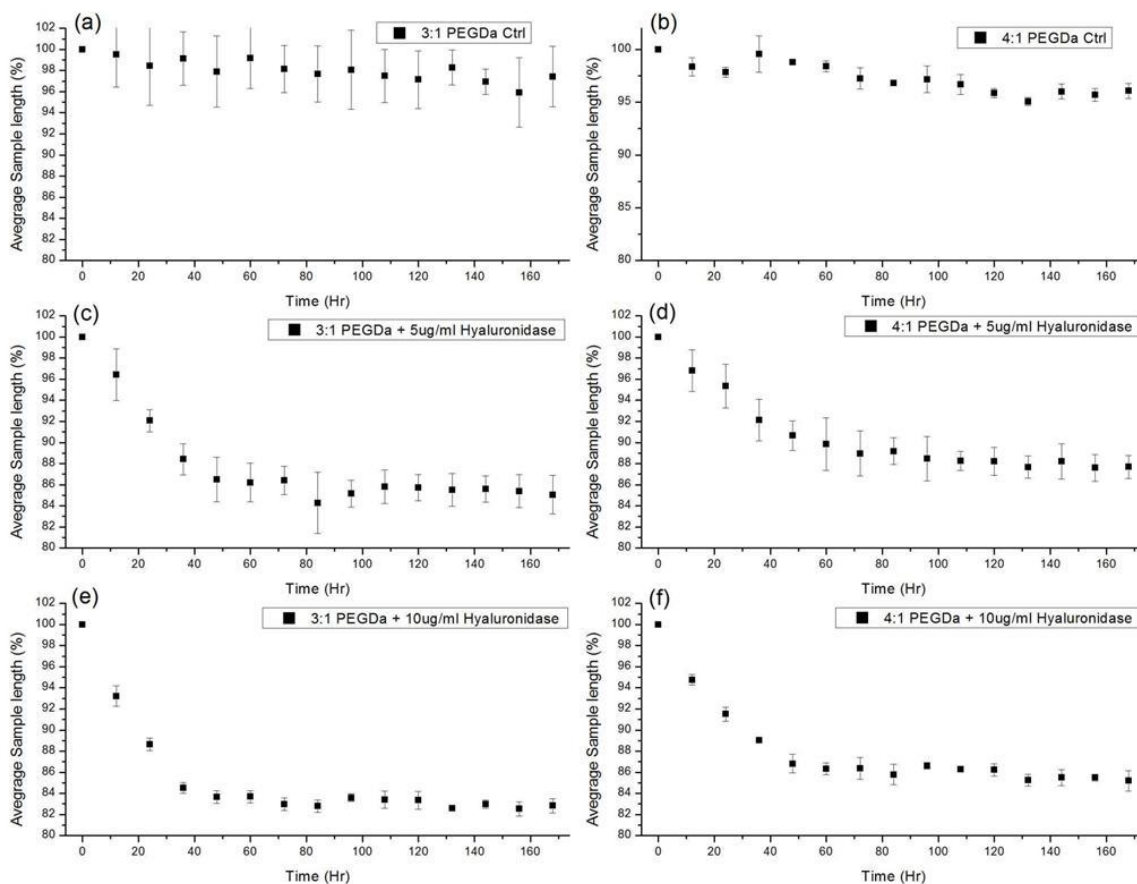
Fig.3.18. Graph showing enzyme driven shrinkage profile for PEGDa crosslinked HAGMa hydrogel samples exposed to hyaluronidase for 1 week. The controls were not exposed to the enzyme. Panels a, c, and e show the profiles for 3:1 ratio PEGDa samples while panels b, d, and f show profiles for 4:1 ratio PEGDa crosslinked samples. Increase in the concentration ratio of PEGDa seemed to slow down the shrinkage rate. The 4:1 ratio PEGDa samples sustained shrinkage for 2.5-3 days where as the 3:1 ratio PEGDa samples stopped shrinking after 1.5 days. (n=3)

We selected two concentrations of the enzyme to selectively study shrinkage induced by degradation of the backbone HAGMa chains. We observed some evidence of dependence of the rate and magnitude of shrinkage on the enzyme concentration from the overall profile of the change in sample length. We were curious if we could increase the magnitude of shrinkage by further increasing the enzyme concentration. We exposed PEGDa crosslinked samples to extremely high concentration (500 µg/ml) of

73

hyaluronidase and observed that the rate of shrinkage does increase quite dramatically. As shown in figure 3.19, almost all of the shrinkage occurred within the first 8 hours of exposure to the enzyme. However the net magnitude of sample length change remained similar to samples exposed to 5 µg/ml or 10 µg/ml hyaluronidase. This indicated that magnitude of shrinkage is dependent on the extent to which molecular orientation was retained during crosslinking, while the rate of shrinkage is dependent on the concentration of hyaluronidase and the concentration of the crosslinker. Table 3.2 summarizes the results from the constrained shrinkage experiments.
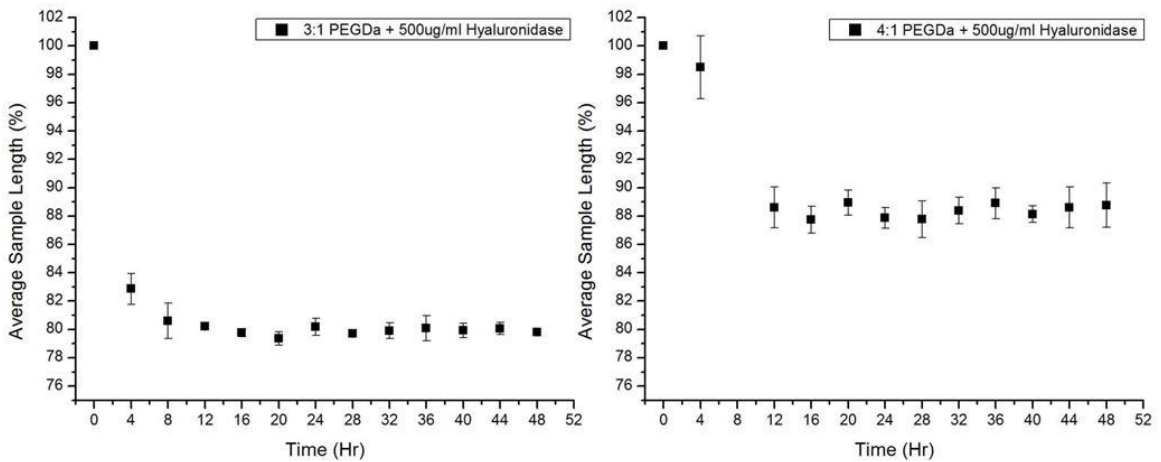
Fig.3.19. Graph showing enzyme driven shrinkage profile for PEGDa crosslinked HAGMa hydrogel samples exposed to large excess (500 µg/ml) of hyaluronidase for 48 hrs. The samples appeared to have achieved the maximum magnitude of shrinkage within the first 4-8 hours indicating that the rate of shrinkage is governed by the concentration of hyaluronidase. (n=3)

Table.3.2. Summary of the average sample shrinkage for the PEGDa crosslinked
HAGMa samples

Hyaluronidase Concentration	3:1 PEGDa		4:1 PEGDa	
	Average Sample Shrinkage (%)	Average Sample Shrinkage (mm)	Average Sample Shrinkage (%)	Average Sample Shrinkage (mm)
0 (Ctrl)	3.69 ± 0.32	0.48 ± 0.02	1.6 ± 0.33	0.17 ± 0.07
5µg/ml	10.90 ± 0.51	1.5 ± 0.15	9.2 ± 1.2	1.1 ± 0.11
10µg/ml	12.33 ± 0.06	2.00 ± 0.09	11 ± 1.9	1.4 ± 0.22
5µg/ml neg. Ctrl.	5.60 ± 0.63	0.5 ± 0.1	3.3 ± 0.7	0.5 ± 0.17
10µg/ml neg. Ctrl.	5.93 ± 0.72	0.67 ± 0.1	1.6 ± 0.8	0.28 ± 0.16

In vitro studies that have tested the effect of applying mechanical tension via micromotors or microneedles on neuronal elongation have unanimously observed that at least for the first day the rate of displacement has to be limited to 100 µm/hr (4, 7-11). Figure 3.20 shows the shrinkage rates per day for all of the compositions tested here. Increasing the enzyme concentration increased the shrinkage rates. Hydrogels of the composition 60 mg/ml HAGMa crosslinked with 3:1 and 4:1 ratio of PEGDa when degraded with hyaluronidase, generated shrinkage induced displacements at rates below the 100 µm/hr. Hydrogels exposed to 10 µg/ml hyaluronidase produced the highest magnitude of shrinkage and shrinkage rates. In contrast to a micromotor which is able to produce consistent displacements over time, our hydrogel system can cause displacements only for a finite period of time and these displacements will decrease over time due to a finite amount of energy stored in the system. However this novel concept provides the advantage of possible *in vivo* application. Further optimizations to sustain the shrinkage for an extended period of time would certainly elevate the applicability of this hydrogel system for enhancing the axonal regeneration via stretch/towed growth.
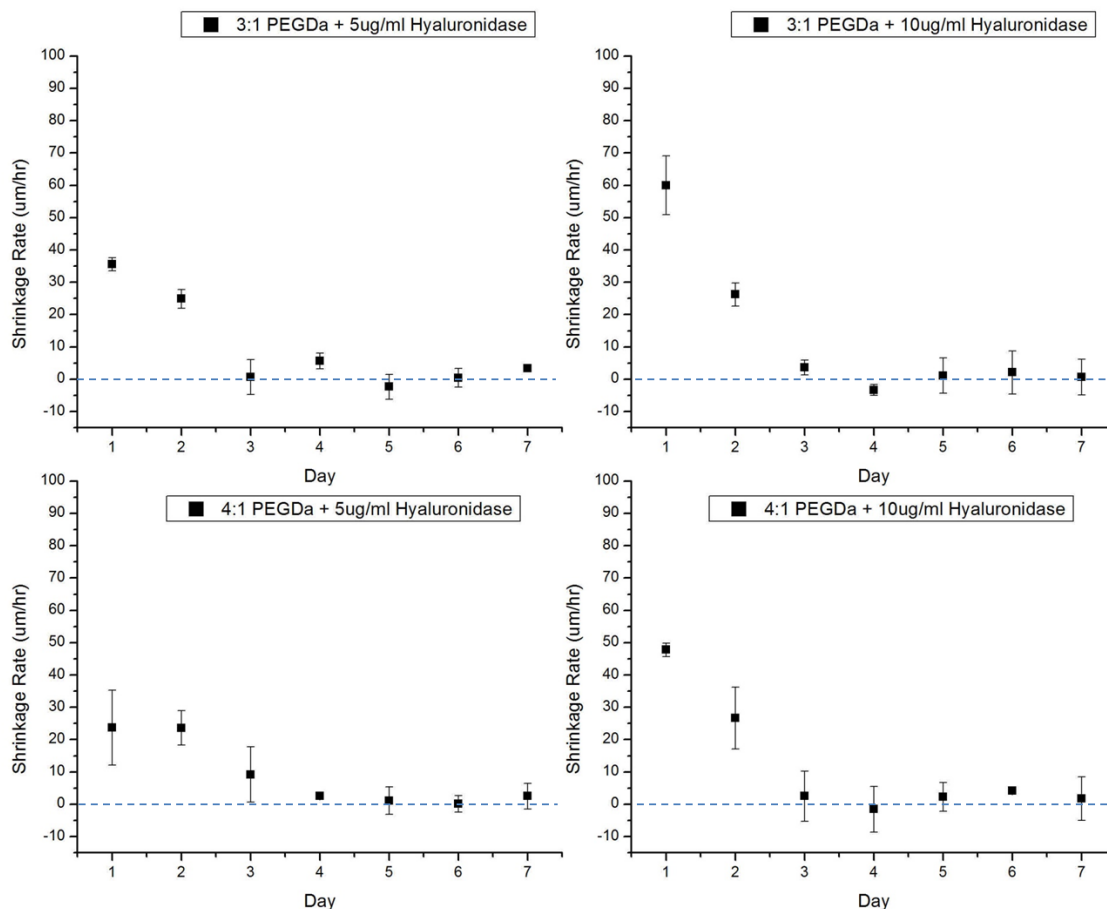
Fig.3.20. Profile of the shrinkage rates for the PEGDa crosslinked HAGMa hydrogels exposed to hyaluronidase for a period of 1 week. The shrinkage rates ranged from 25 μm/hr to 60 μm/hr for the first day. The shrinkage gradually ceased by day 3 for all the compositions. (n=3)

3.3.6 **Effect of solvent diffusion on shrinkage**: Degradation can occur either in the bulk or on the surface. To verify which mode was responsible for the results we observed, we chose to study if the enzyme was diffusing in the bulk or eroding the surface. The rationale behind using samples that were half (1 mm x 0.5 mm) the thickness of the standard samples (1 mm x 1 mm) tested was that if the degradation was occurring in the bulk we would observe similar rate of shrinkage. However if the degradation were a function of enzyme diffusion then a thinner sample would shrink faster. As shown in Figure 3.21, the

shrinkage profile was similar to standard thickness samples. The 3:1 PEGDa crosslinked samples stopped shrinking around 32 hr mark while the shrinkage for 4:1 PEGDa crosslinked samples seemed to plateau out by 48 hrs. This verified that there was no hindrance to the diffusion of the enzyme in the sample and that bulk degradation was the method by which the molecular chains were being broken down and reorganized.
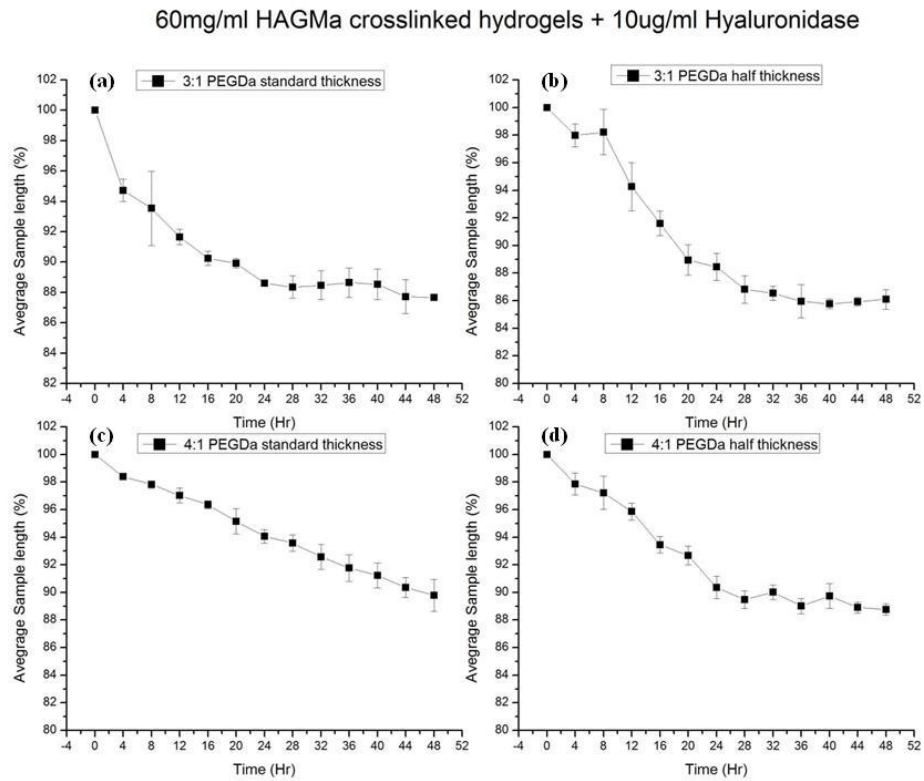
Fig. 3.21. Graph showing the enzymatic degradation driven shrinkage of PEGDa (a, b – 3:1PEGDa; c, d – 4:1 PEGDa) crosslinked hydrogels comparing effect of sample thickness on nature of sample shrinkage. The samples were exposed to 10 µg/ml hyaluronidase. The overall magnitude and the general profile of shrinkage were not affected by the thickness of the sample. (n=3)

3.3.7 **Hydrogel stiffness**: Crosslinked HAGMa samples were indented at random locations prior to and following exposure to 10 µg/ml hyaluronidase. The load-displacement curves indicated a linear elastic behavior where the loading and unloading curves overlapped.

77

The stiffness was calculated from the loading portion of the curve. Prior to exposure to the enzyme the stiffness of gels with the composition 60 mg/ml HAGMa crosslinked with 3:1 PEGDa was 3.97 ± 0.09 N/m. After exposure to hyaluronidase for 48 hrs, the stiffness dropped to 2.96 ± 0.18 N/m. Similarly the stiffness of gels made using 60 mg/ml HAGMa and 4:1 PEGDa before enzyme exposure was 5.47 ± 0.17 N/m. After exposure to the enzyme, the stiffness decreased to 3.56 ± 0.87 N/m. Figure 3.22 summarizes the results from this experiment. The stiffness values helped us in designing the aluminum cantilevers with stiffnesses specifically matched to the hydrogel composition.
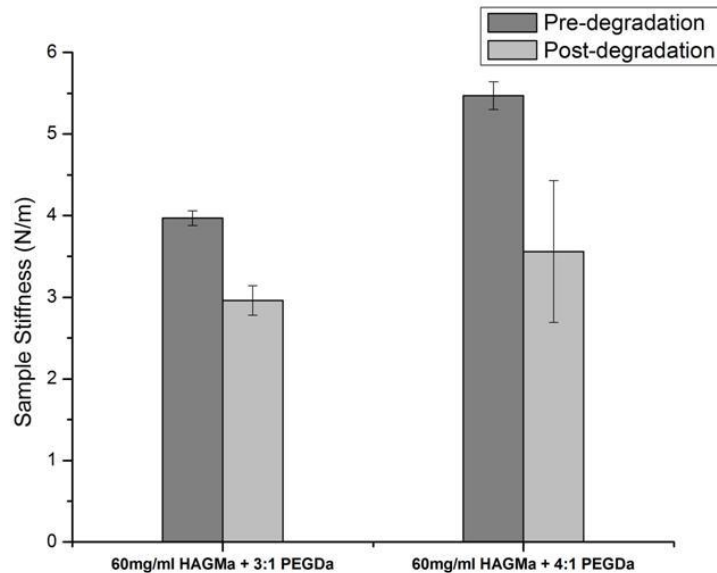
Fig. 3.22. Graph showing the measured stiffness of HAGMa hydrogels crosslinked with PEGDa before and after exposure a 48hr exposure to 10 µg/ml hyaluronidase. Degradation caused the stiffness of samples of both compositions to decrease significantly. (n=3)

3.3.8 **Measurement of shrinkage force:** Based on the stiffness values of the hydrogels before and after degradation, flexible aluminum cantilevers were fabricated to be used in the mechanical device. To ensure that we capture the entire potential of the shrinking

78

hydrogel to deliver tensile force on an attached body, it was imperative that the stiffness of cantilever be somewhere between the pre and post degradation stiffness values of the hydrogel. To test the samples made using 60 mg/ml HAGMa crosslinked PEGDa, we selected an aluminum cantilever with the stiffness 3.47 N/m. The cantilever was calibrated using known loads and known displacements (see appendix). The test was run in increments of 4 hrs for a total duration of 48 hours to ensure replenishment of the enzyme. The raw voltage values were converted to appropriate force and displacement values using the calibration constants (see appendix). Even though the DVRT signal was recorded at the rate of one point per second, the final plot only shows one data point per hour for the purpose of clarity. The cross-section of the hydrogel was 1 mm^2. The force values were then converted to their respective stress (kPa) values to compare with the previously calculated σ_{Pr} to estimate what percent of the stored predicted stress was recovered. Figure 3.23 (a, c, e) shows the force, displacement, and recovered stress curves for hydrogel samples of the composition 60mg/ml HAGMa crosslinked with 3:1 PEGDa. The average cantilever displacement measured by the end of 48 hrs for control samples was 0.5 mm which translated to a net average force of 1 mN. This is equal to 14% of the predicted stored retractive stress. We attribute the small amount of shrinkage seen in control samples to rearrangement of the gel matrix due to swelling. The cantilever displacement value was within the range of shrinkage observed for the control samples (0.48 ± 0.02 mm) of this composition during the unconstrained shrinkage experiments.

Exposing the same composition to 10 µg/ml hyaluronidase demonstrated interesting results. The average cantilever displacement achieved at the end of 48 hrs was

79

0.4 mm which was less than half (2.00 ± 0.09 mm) of what we observed in the unconstrained shrinkage experiments.

The curves for samples of the composition 60 mg/ml HAGMa crosslinked with 4:1 PEGDa are shown in Figure 3.23 (b, d, f). Once again we observed that the cantilever displacement values for control samples were similar to the unconstrained shrinkage experiments (~0.3 mm). The controls generated an average of 1.5 mN of force which correspond to a recovered stress value of 1.5 kPa or 16% of the predicted stored stress. The samples that were exposed to 10 µg/ml hyaluronidase on the other hand showed a much more significant recovery of the stored retractive stress. By the end of 48hrs, the samples applied an average of 3.47 kPa of tensile stress on the cantilever. That amounts to 37.5% of the predicted stored retractive stress. The total cantilever displacement was 1 mm which was slightly less than what was observed for the unconstrained shrinkage magnitude (1.4 ± 0.22 mm). This indicated that as the sample got weaker on account of degradation, it lost the "tug of war" battle and was no longer able to counter the resisting cantilever. The overall effect was the appearance of slowing down of the shrinking process and a lower magnitude for total recovered stress. However since the samples crosslinked with 4:1 ratio of PEGDa are stiffer than those crosslinked with 3:1 ratio of PEGDa, we did not see as large a gap between the sample shrinkage values between the constrained and the unconstrained shrinkage experiment.
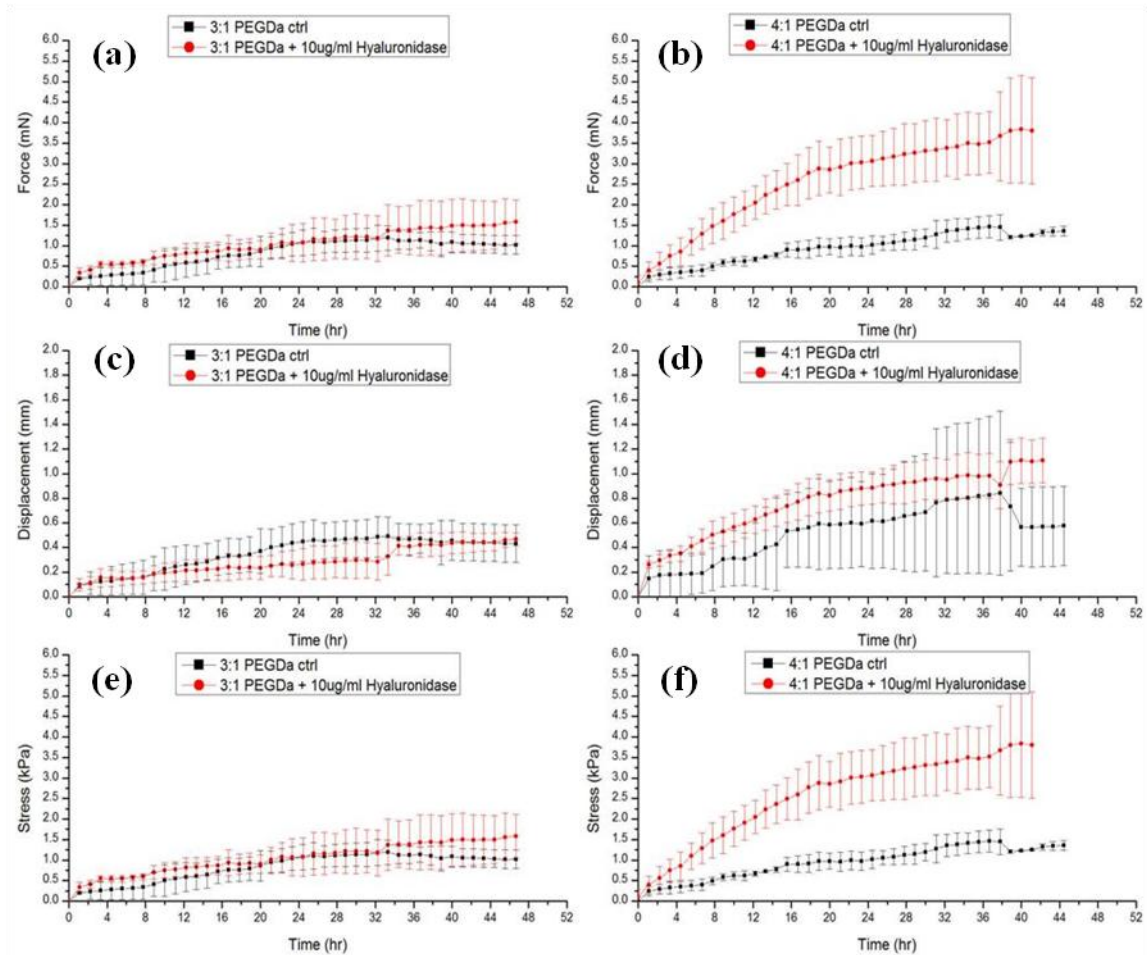
Fig.3.23. Graphs showing the force, cantilever displacement, and recovered stress curves for the HAGMa samples crosslinked with 3: 1 ratio of PEGDa (a,c,e) and 4:1 ratio of PEGDa (b,d,f). The hyaluronidase concentration used was 10 μg/ml. The control samples showed minimal shrinkage which was on par with the unconstrained shrinkage experiments. The enzymatically degraded samples that were crosslinked with 4:1 ratio of PEGDa showed the greatest recovery of the stored retractive stress (37.5%) as compared to samples crosslinked with 3:1 ratio of PEGDa (22.6%). Degradation decreased the ability of samples to continue shrinking in the constrained environment. It was more evident in case of the samples crosslinked with 3:1 ratio of PEGDa. (n=3)

Figure 3.24 shows the comparison between the predicted stored retractive stress and the measured recovered stress. It is apparent that not all of the stored stress is recovered. There is a disparity of 50 % or greater between the values.
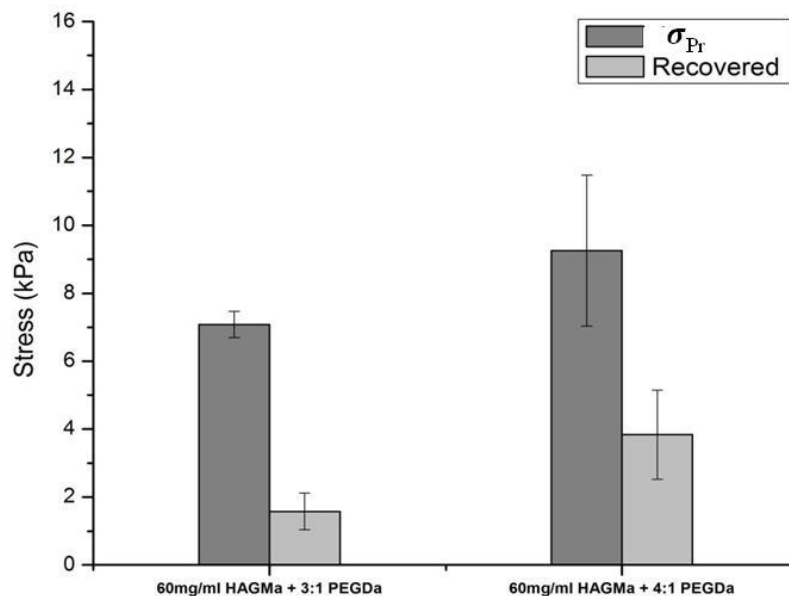
Fig.3.24. Bar graph showing the predicted and recovered values of the retractive stress stored in the two compositions of PEGDa crosslinked HAGMa hydrogel samples. The recovered stress values were significantly lower than the predicted stored retractive stress. (n=3)

3.4 Discussion

The unique properties of HA enabled us to fabricate a novel hydrogel that could be designed to shrink, via molecular reorganization, on a time scale relevant for application as a mechanical stimulator of neuronal cells. Water soluble HA has a very short half life in the body if it is injected as a solution. Derivatizing HA and crosslinking solves this problem by slowing down the degradation process. One of the clinically used HA derivatives is a solid hydrated gel called hylan-B which is implanted in soft tissues (26, 27). A 1% solution of HA when injected under the rabbit skin had a half life of 24 hours. In comparison, a 0.5% hylan-B had a half life greater than 9 months in the same scenario (26). The disaccharide subunit can be easily modified to add pendant crosslinkable moieties. We chose to methacrylate HA using GMa, as the reaction is water based and the conditions do not damage the HA molecule itself. By controlling the concentration of GMa in the reaction, we were able to affect the

extent of modification. We used several molar excesses of GMa to counter for the inaccessibility of -OH target areas on some HA molecules on account of their coiled conformation. Our main goal of storing retractive stress in the network demanded the highest modification levels and we achieved that (~82%) by using 20 molar excess of GMa.

The rheological properties of polymers are of general interest since they provide important information for designing and optimizing processing conditions. In networks made of long linear polymers, network chains impose topological constraints on each other called entanglements. HA in its ground state is in a random coil conformation. Due to its shear thinning property, under shear flow these entangled coiled chains disentangle and align to the direction of flow making it easier for even highly concentrated solutions to be injectable. Our goal for performing the rheological characterization was to observe the relaxation behavior and select compositions that relaxed slower than the time it took for the crosslinking reaction to finish. Based on the relaxation curves we selected two compositions, 60 mg/ml HAGMa with 3:1 ratio of PEGDa and 60 mg/ml HAGMa with 4:1 PEGDa. The results indicated that the solutions of these compositions would not have relaxed by the time crosslinking reaction completes. This was critical in restricting the chain conformation and storing a retractive stress in the crosslinked network.

Birefringence enabled us to verify the success of arresting the shear flow induced molecular chain alignment. Increasing the crosslinker concentration from a 3:1 ratio to 4:1 ratio increased the average retardance from 39.71 nm to 50.07 nm. The range of values we observed compare well with values reported for viscoelastic polymer solutions studied under

shear flow (38). The lack of any significant difference in retardance values calculated across the sample suggested that the crosslinking chemistry is rapid enough to trap molecular chains in similar stages of disentanglement. In order to prepare samples to be imaged under the polarized optical microscope the opaque samples needed to be air dried. This was essential to make the samples optically clear. This process shrinks the samples and may lead to under estimation of the molecular orientation. However by treating all the samples the same way, the trends we observed are a true representation of the effects of experimental conditions. To selectively study the shrinkage brought about by enzymatic degradation, we exposed the samples to the primary degradation enzyme for HA, hyaluronidase. For both compositions of samples tested we observed a significant decrease in retardance values indicating significant loss of molecular chain alignment.

The trend observed in the birefringence correlated well with our estimation of retractive stress in the crosslinked network. Traditionally when a crosslinked network is stretched by a factor α, it creates a retractive force in the network that can be calculated using rubber elasticity principles. The two states this network exists during such an experiment are the resting state and the stretched state. Drawing a parallel with our hydrogel system, we could equate the rapidly crosslinked hydrogel to the stretched state, while the resting state would be if the pre-crosslinking solution were allowed to relax in the mold without crosslinking. We measured the lengths of both these stages to calculate extension ratio α. The confinement of the mold channel and the high concentration of the solution may have hampered complete relaxation of the chains in the solution. Swelling experiments provided us an understanding of the behavior of the network in hydrated condition. Assimilating all this information, we

84

were able to generate an estimation of the magnitude of retractive stress that might get stored in the network. It is this stress that was the source of the potential energy that we planned on harnessing in order to use the network as an actuator. The results indicated that increasing the crosslinker ratio increased the average retractive stress stored in the network.

Enzymatic degradation of the rapidly crosslinked HAGMa hydrogels brought about shrinkage of the gel along its long axis, which as per the design was also the axis of flow prior to crosslinking. We observed that the crosslinker concentration and the hyaluronidase concentration affected the sample shrinkage the most. Increasing the crosslinker concentration increased the average molecular orientation and the average retractive stress stored in the network. This meant there was more potential for the network to shrink as it degraded. Enzymatic cleavage of the network increases the free volume within the network providing an opportunity for the chains to reorganize and in the process dissipate the stored retractive stress. Increasing the hyaluronidase concentration increased the magnitude of shrinkage. However increasing the crosslinker concentration also slowed down the rate at which the samples underwent change in their lengths. The denser the crosslinked network, the harder the enzymes had to work to create free volume for the network chains to reorganize. The negative control samples confirmed that molecular orientation, followed by the loss of it, was the source of sample shrinkage. The net shrinkage for all of the compositions tested was less than or equal to 1mm per day which was the upper limit of displacements that researchers have demonstrated to be successful in eliciting enhanced axonal growth (10, 12, 17, 39). The average rates of shrinkage for the first 24 hours ranged between 25 µm/hr and 60 µm/hr. These rates are well within the favorable maximum rate

100 µm/hr that have been shown to elicit enhanced axonal elongation (10, 12, 15, 21). Exposure to extremely high concentrations of enzyme failed to significantly increase the magnitude of shrinkage, although it did speed up the time it took for the sample to shrink. This result indicated that the limiting factor of this system is the degree of molecular chain alignment of the HA molecule. There is a direct correlation between the degree of orientation and the magnitude of retractive stress stored in the network, as seen from our results, and thus the magnitude of sample shrinkage. Looking at results from the mechanical device designed to measure the force generated by the shrinking hydrogel, it is evident that we are unable to recover all of the predicted stored retractive stress. As the sample gets degraded by hyaluronidase, the mechanical properties of the sample decrease. Indentation test showed that the stiffness of samples of the composition 60 mg/ml HAGMa crosslinked with 3:1 PEGDa when exposed to 10 µg/ml hyaluronidase decreased by 25%. Hence as the sample weakens, its stiffness is equal to or less than that of the aluminum cantilever. This could explain why the displacement in case of the unconstrained experiment is higher than when the samples were constrained. The net average force generated by the end of 48 hrs was 1.6 mN. This equals 22.6% of $\sigma_{Pr,}$ but the process did not appear to have ceased as seen in the unconstrained shrinkage experiment. On the contrary it appeared that due to the physical confinement and the fact that the hydrogel was now actually performing work on another body which was trying to resist it, the shrinkage profile of the sample was more gradual than the unconstrained shrinkage. The method we used to recover the stored retractive stress from the hydrogel network was by enzymatically cleaving the HAGMa chains, which are the source of the retractive stress. Hence by cleaving them in multiple locations we think that true potential of the chain to relax could not be entirely exploited. Thus the experimentally

measured recovered stress would be lower than the predicted values of retractive stress stored in the network. The hydrogel compositions we tested here performed work on the flexible cantilevers by applying tensile stress. The 3:1 PEGDa crosslinked HAGMa hydrogel when exposed to 10 µg/ml hyaluronidase applied a net stress of 1.6 nN/µm^2, while the 4:1 PEGDa crosslinked HAGMa hydrogel generated a net stress of 3.4 nN/µm^2 in the 48hr test period. Franze et al. (40) experimentally calculated an upper threshold limit for applied stress on growth cones of individual neurons that could sustain extensional growth. The value they reported was 274 ± 47 pN/µm^2, (mean ± SE). Neurite bundles are able to sustain extreme stretch rates (µm/hr) which would usually lead to detachment and retraction of individual neurites (12, 19, 21). We could draw a parallel and predict that the neurite bundles may be able to sustain higher stresses than the threshold reported for individual neurites.

In degrading the HA chains to bring about sample shrinkage we are truly not using the entire potential of the HA chain. The HA molecule is the driving force of this shrinkage phenomenon. If we observe a single HA molecule we would find it in a random coiled conformation in its ground stage. Under shear flow conditions this coil disentangles and aligns to the flow thus storing some energy. When the flow ceases to exist, the molecule starts losing this stored energy in order to return to its ground state. A shorter chain would need less energy to disentangle compared to a longer chain. Thus a longer chain would need higher energy to disentangle and will have higher potential energy that it has to lose to return to ground state. We proposed to use this principle in a crosslinked network consisting of several of such long chained HA molecules. The mechanism we explored here to make the HA molecules lose their orientation and the stored retractive stress was cleaving the HA

molecule itself. We did observe shrinkage; however we do not believe that this is the most efficient way. When we cleaved the HA molecule to shorter segments we also decreased the overall potential for shrinkage as we now have shorter segments of the HA molecule getting reorganized in the network matrix. In the next chapter we explore another technique for shrinking the crosslinked HAGMa hydrogel where we do not cleave the HA molecule but instead selectively cleave the crosslinks that hold the network together. This we believe will allow the HA molecule to expend more of its stored potential energy/retractive stress and cause a higher magnitude of hydrogel shrinkage.

At the outset of this study our main goal was to create a polymeric network based actuator to enhance axonal elongation drawing inspiration from the *in vitro* studies that used mechanical actuators. In contrast to a micromotor which is able to produce consistent displacements over time, our hydrogel system can cause displacements only for a finite period of time and these displacements decrease over time due to a finite amount of energy stored in the system. However this novel concept provides the advantage of possible *in vivo* application. Further optimizations to sustain the shrinkage for an extended period of time would certainly elevate the applicability of this hydrogel system for enhancing the axonal regeneration via stretch/towed growth.

3.5 Conclusion

Novel crosslinked hyaluronic acid based hydrogels were designed to possess the property of controlled shrinkage for the purpose of use as a potential axonal growth enhancer. The samples were characterized for their ability to shrink and ability to exert a force while

constrained during shrinkage. The composition 60 mg/ml HAGMa crosslinked with 3:1 ratio of PEGDa demonstrated the highest magnitude of shrinkage in 48 hrs (12.33%) when exposed to 10 µg/ml of hyaluronidase. However, the most linear and longest sustained shrinkage was shown by samples of the composition 60 mg/ml HAGMa crosslinked with 4:1 PEGDa (11%), when exposed to 10 µg/ml of hyaluronidase. The latter composition also allowed us to recover the highest percentage (37.5%) of the retractive stress stored in the network. This hydrogel system could prove to a viable alternate treatment for bridging large gap peripheral nerve injury.

References

1. Ionov L. Polymeric Actuators. Langmuir. 2014;10:1021.

2. Ionov L. Hydrogel-based actuators: possibilities and limitations. Materials Today. 2014;17(10):494.

3. Carpi F, Smela E, editors. Biomedical Applications of Electroactive Polymer Actuators. John Wiley & Sons; 2009.

4. Gutowska A, Bae YH, Feijen J, Kim SW. Heparin release from thermosensitive hydrogels . J Controlled Release. 1992;22:95.

5. Huffman AS, Afrassiabi A, Dong LC. Thermally reversible hydrogels: II. Delivery and selective removal of substances from aqueous solutions. J Controlled Release. 1986;4:213.

6. Miyata T, Jikihara A, Nakamae K, Hoffman AS. Preparation of poly(2-glucosyloxyethylmethacrylate) concanavalin A complex hydrogel and its glucose-sensitivity. Macromolecular Chem , and Phys. 1996;197:1135.

7. Topham PD, Ryan AJ. Antagonistic Triblock Polymer Gels Powered by pH Oscillations. Macromolecules. 2007;40:4393.

8. Hu Z, Zhang X, Yong L. Synthesis and application of modulated polymer gels. Science. 1995;269:525.

9. Lendlein A, Langer R. Biodegradable, elastic shape-memory polymers for potential biomedical applications. Science. 2002;296:1673.

10. Bray D. Axonal growth in response to experimentally applied mechanical tension. Dev Biol. 1984 4;102(2):379-89.

11. Dennerll T, Lamoureux P, Buxbaum R, Heidemann S. The cytomechanics of axonal elongation and retraction. J Cell Biol [Internet]. 1989;109(6):3073.

12. Smith DH. Stretch growth of integrated axon tracts: Extremes and exploitations. Prog Neurobiol. 2009 11;89(3):231-9.

13. Illeperuma W, Sun J, Suo Z, Vlassak J. Force and stroke of a hydrogel actuator. Soft Matter. 2013;9:8504.

14. Evans GRD. Peripheral nerve injury: a review and approach to tissue engineered constructs. Anat Rec. 2001;263:396.

15. Schmidt CE, Leach JB. Neural tissue engineering: strategies for repair and regeneration. Annu Rev Biomed Eng. 2003;5(1):293-347.

16. Wang S, Cai L. Polymers for fabricating nerve conduits. International Journal of Polymer Science. 2010;2010.

17. Heidemann SR, Buxbaum RE. Tension as a regulator and integrator of axonal growth. Cell Motil Cytoskeleton. 1990;17(1):6-10.

18. Goldberg JL. How does an axon grow? Genes & Development. 2003 April 15;17(8):941-58.

19. Pfister BJ, Iwata A, Meaney DF, Smith DH. Extreme Stretch Growth of Integrated Axons. The Journal of Neuroscience. 2004 September 08;24(36):7978-83.

20. Pfister BJ, Iwata A, Taylor AG, Wolf JA, Meaney DF, Smith DH. Development of transplantable nervous tissue constructs comprised of stretch-grown axons. J Neurosci Methods. 2006 5/15;153(1):95-103.

21. Smith DH, Wolf JA, Meaney DF. A New Strategy to Produce Sustained Growth of Central Nervous System Axons: Continuous Mechanical Tension. Tissue Eng. 2001 04/01; 2011/05;7(2):131-9.

22. Sakai Y, Matsuyama Y, Takahashi K, Sato T, Hattori T, Nakashima S, et al. New artificial nerve conduits made with photocrosslinked hyaluronic acid for peripheral nerve regeneration. Biomed Mater Eng. 2007;17(3):191-7.

23. Wang K, Nemeth IR, Seckel BR, Chakalis-Haley DP, Swann DA, Kuo J, et al. Hyaluronic acid enhances peripheral nerve regeneration in vivo. Microsurgery. 1998;18(4):270-5.

24. Borland G, Ross J, Guy K. Forms and functions of CD44. Immunology. 1998;93(2):139-48.

25. Lesley J, Hascall VC, Tammi M, Hyman R. Hyaluronan Binding by Cell Surface CD44. Journal of Biological Chemistry. 2000 September 01;275(35):26967-75.

26. Laurent TC, editor. The Chemistry, Biology and Medical Applications of Hyaluronan and its Derivatives. 1st ed. London and Miami: Portland Pr; 1998.

27. Laurent TC, Laurent UB, Fraser JR. Functions of hyaluronan. Annals of the Rheumatic Diseases. 1995 May 01;54(5):429-32.

28. Price RD, Berry MG, Navsaria HA. Hyaluronic acid: the scientific and clinical evidence. Journal of Plastic, Reconstructive & Aesthetic Surgery. 2007 10;60(10):1110-9.

29. Roden L, Fraser JRE, Laurent TC. Enzymic pathways of hyaluronan catabolism. In: Laurent TC, editor. The Biology Of Hyaluronan. John Wiley & Sons; 1989. p. 60.

30. Zhong SP, Campoccia D, Doherty PJ, Williams RL, Benedetti L, Williams DF. Biodegradation of hyaluronic acid derivatives by hyaluronidase. Biomaterials. 1994 4;15(5):359-65.

31. Menzel EJ, Farr C. Hyaluronidase and its substrate hyaluronan: biochemistry, biological activities and therapeutic uses. Cancer Lett. 1998 9/11;131(1):3-11.

32. Bader RA, Rochefort WE. Rheological characterization of photopolymerized poly(vinyl alcohol) hydrogels for potential use in nucleus pulposus replacement. Journal of Biomedical Materials Research Part A. 2008;86A(2):494-501.

33. Bryant, S J Nuttelman, C R Anseth,K S. Cytocompatibility of UV and visible light photoinitiating systems on cultured NIH/3T3 fibroblasts in vitro. Journal of biomaterials science. Polymer edition. 2000;11(5):439.

34. Allen NS, editor. Photopolymerization and photo imaging science and technology. 1st ed. New York: Elsevier Science Publishers Ltd; 1989.

35. Ward IM. Structure and Properties of Oriented Polymers. 2nd ed. Springer; 1997.

36. Sperling LH. Cross-linked polymers and rubber elasticity. In: Introduction to physical polymer science. 4th ed. New Jersey: Wiley-Interscience; 2005. p. 427.

37. Saxena T, Gilbert J, Hasenwinkel J. A versatile mesoindentation system to evaluate the micromechanical properties of soft, hydrated substrates on a cellular scale. ; 2008.

38. Schmidt G, Nakatani AI, Butler P, Karim A, Han C. Shear Orientation of Viscoelastic Polymer−Clay Solutions Probed by Flow Birefringence and SANS. Macromolecules. 2000;33(20):7219.

39. Zheng J, Lamoureux P, Santiago V, Dennerll T, Buxbaum R, Heidemann S. Tensile regulation of axonal elongation and initiation. The Journal of Neuroscience. 1991 April 01;11(4):1117-25.

40. Franze K, Gerdelmann J, Weick M, Betz T, Pawlizak S, Lakadamyali M, et al. Neurite Branch Retraction Is Caused by a Threshold-Dependent Mechanical Impact. Biophys J. 2009 10/7;97(7):1883-90.

CHAPTER 4

4.1 Introduction

The severity of a peripheral nerve gap injury is dependent on the extent of the gap created as a result of the injury. (1-3). Larger the gap, the greater is the challenge to repair it. The constant tension that the nerves exist in, make it difficult for neurosurgeons to surgically suture the nerve ends. The current gold standard treatment for large gap injury is a surgical autograph (2, 3). However there are several disadvantages of using this treatment which include need for harvesting a functional nerve from somewhere else in the body, risk of infection, and loss of functionality for the donor site. The functional recovery rate for the primary injury site is around 80% (1). The alternative strategies for autografts that have been explored over the past decades include allografts and xenografts; however the risks of rejection and an immune reaction outweigh the benefits. Biomaterial strategies have explored the application of polymeric conduits supplemented with growth factors or support cells like Schwann cells with promising results (1-3). However so far they have not been able to match the success rate of autografts.

The growth cone is a key player in axonal growth *in vitro* (4, 5). *In vivo* however, there are two main mechanisms of axonal growth. The first is via growth cone extension, while the second occurs after the growth cone has synapsed with its desired target and the neuron elongates as the target relocates and pulls the neuron with it (6, 7). The latter mechanical stimulation mechanism is called "stretch growth" or "towed growth". Bray in 1984 (8) demonstrated that short neurites could be elongated by mechanically pulling them at a limiting rate of 100 μm/hr. That study was later substantiated by Heidemann and Buxbaum

(4). Both of the studies used calibrated glass micro-needles to attach to growth cones and apply tension. Smith et al. showed experimentally that rat dorsal root ganglion (DRG) neurite bundles could be stretched successfully using micromotors at rates as high as 8 mm/day without breaking (7). They have been successful in stretching axon bundles to lengths up to 5 cm *in vitro*. The stretched axons showed normal morphological appearance and ultrastructure. These studies explored the limits of this mechanism (7-11).

There exist a group of polymers that under the influence of an external stimulus undergo a change in their shape or size (12-14). This transformation could be used to simulate the micromotors and possibly develop a therapy that can be used *in vivo* to mechanically stimulate neuronal cells. There are three main groups of polymeric actuators that have been used for biomedical application; hydrogel based actuators (13), electro active polymers (EAP) (12), and shape memory polymers (SMP) (15, 16). Hydrogel based actuators have been successfully used as drug delivery vehicles (17, 18) and as valves in microfluidic devices (19, 20). Thermoresponsive PNIPAAm gels synthesized by Gutowska et al. by copolymerizing with butyl methacrylate (BMA) (hydrophobic) or acrylic acid (AAc) (hydrophilic) co-monomers are an ideal example of utilizing the actuating mechanism to deliver drugs (21). Heparin was loaded into the gels below the network lower critical solution temperature when the gel permeability is high. When the transition temperature was reached (37°C), the gel demonstrated rapid de-swelling as a result of the network collapse. This collapse was very rapid and almost all of the transition occurred in less than an hour. Some of the most significant biomedical applications of polymeric actuators include surgical sutures and self-deploying stents. Langer et al. synthesized a novel degradable block copolymer by

coupling oilgo(ε-caprolactone)diol (OCL) and oligo(p-dioxane)diol (ODX) with 2,2,(4),4-trimethylhexanediisocyanate (22). They fabricated sutures that were programmed by elongation and fixing the elongated state. The transition temperature for this SMP was 41°C. When the triggering temperature was applied the sutures deployed and closed the incision in a mouse model. Thus they were able to demonstrate a possible alternative to basic sutures and a way to reduce the subjective variability in the force used to tie the knots while applying suture. However the response times that have been reported for polymeric actuators in the literature range between instantaneous to a few hours (12, 14, 16, 18, 19, 21-29). Predominantly the applications for these polymeric materials required quick, almost instantaneous response to the external stimulus. There is an absence of category of degradable, biocompatible, slow actuating polymer systems that can keep on actuating for several days which could benefit applications like axonal regeneration and wound healing.

This work describes a crosslinked network system wherein retractive stress was stored along a pre-defined axis during fabrication. Storing a retractive stress in essence meant storing energy in the system. By gradually releasing this stress we hypothesize that the crosslinked network will shrink in dimension along the pre-defined axis over the course of several days. If nerve endings are attached to the ends of this shrinking matrix, it would be similar to a micromotor applying tensile stress on the neurons. Unlike the mechanized studies mentioned above, the polymer network system developed here will have a limit to its potential of being an actuator. We believe that this system will exist in two stages. During the first stage the hydrogel network will release the stored retractive stress and shrink, while in

the second stage once the hydrogel has stopped shrinking it will exist as a passive scaffold that will act as a bridge for the neurites to cross over.

In order to be able to store a retractive stress in a network we needed to select a long chain biocompatible molecule. Some of the other requirements included ease of chemical modification for the purpose of crosslinking, property of being a natural ligand for neuronal cells, and being naturally degradable to non-toxic byproducts. HA is a naturally occurring glycosaminoglycan that has been shown to enhance peripheral nerve regeneration (30, 31). It is a natural ligand for cell surface receptors like CD44 and RHAMM (32-35). We investigated the shrinking mechanism by either selectively degrading the crosslinks that hold the network together or by selectively degrading the long HA backbone chains. In the previous chapter, we discussed our attempt at crosslinking HAGMa chains using PEGDa, a non-degradable crosslinker. We were able to demonstrate controlled hydrogel shrinkage by degrading the hydrogels using the enzyme hyaluronidase. The shrinkage ranged from 11% to 12.33% producing a shrinkage force as high as 3.47 mN. The method of recovering the stored retractive stress was enzymatic which cleaved the HAGMa chains. This method did not allow us to use the maximum recoiling potential of an entire uncleaved chain. This chapter details our efforts at selectively degrading the crosslinks to produce shrinkage of HAGMa hydrogels. We synthesized a hydrolysable crosslinker polyethylene glycol poly(lactic acid)-diacrylate (PEGPLADa) which helped us achieve our goal. The hydrogel was characterized for its capability to shrink and to generate force in the process.

4.2 Materials and Methods

Sodium salt of HA (MW 1.6 MDa), bovine testicular hyaluronidase, poly(ethylene glycol) diacrylate (PEGDa), and glycidyl methacrylate (GMa) were purchased from Sigma Aldrich. GMa and PEGDa were filtered to remove MEHQ inhibitor. Irgacure 2959 was purchased from BASF chemicals. All other solvents and chemicals were purchased from Sigma unless stated otherwise and used without further purification.

4.2.1   **Methacrylation of HA**: Sodium salt of HA derived from *Streptococcus equi*, MW 1.6 MDa, was used in the derivatization reaction. The functional unit of an HA molecule is a disaccharide consisting of *N*-acetylglucosamine and glucoronic acid. There are two main sites on an HA disaccharide suitable for modification, namely the pendant hydroxyl group on the *N*-acetylglucosamine and carboxylate on the glucoronic acid component. The derivatization method was adapted from previous work by Bader et al. with poly(vinyl alcohol) gels (36). An excess of GMa was used to covalently attach the methacrylate moiety onto the HA disaccharide. Briefly, HA was dissolved in deionized water (DI H_2O) at a concentration of 3 mg/ml. A 20 molar excess of GMa was then dissolved in the HA solution, the pH was adjusted to 1.5, and the reaction was carried out at 50°C for 2 days. Following this, the reaction mixture was dialyzed against DI H_2O for 2 days, after which the product was lyophilized and refrigerated until needed. The reaction chemistry is shown in Figure 4.1.

The degree of modification was quantified using proton NMR spectroscopy performed using a Bruker Avance-III 300 MHz spectrometer. Peaks (δ = 5.8, 6.2) representing the two protons on the methacrylate chain were used to calculate the degree

of modification. The reference peak ($\delta = 2.0$) was the peak representing protons from the methyl group on HA and methacrylate segment. The solvent used for NMR was deuterated water. The degree of methacrylation can be altered by varying the molar concentration of GMa in the reaction, and the duration of the reaction.
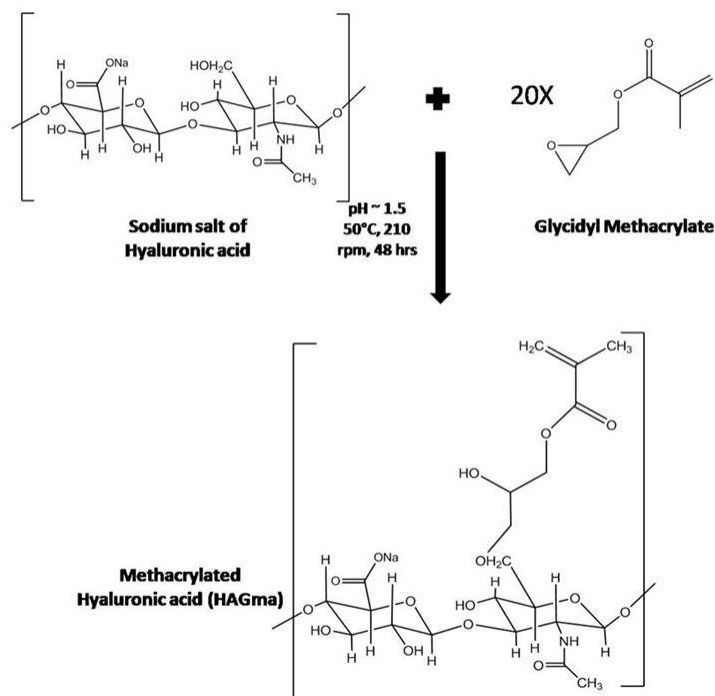
Fig.4.1. Schematic showing the reaction mechanism for methacrylation of hyaluronic acid. The reduction is pH triggered ring opening of glycidyl methacrylate. The extent of successful modification is a function of the concentration of GMa.

4.2.2 **Synthesis of PEGPLADa**: Hydrolysable PEGPLADa crosslinker was synthesized by modifying a method previously described by Sawhney et al. (37). Figure 4.2 shows the schematic of the reaction. Stage 1 of the reaction entailed adding *dl*-lactide moieties onto the α and ω hydroxyl end of PEG molecule via ring opening polymerization. Stage 2 of the reaction added photoactive acrylate terminal end to the PEG-dl lactide molecule. Poly

(ethylene glycol) (MW: 1500 Da), *dl*-lactide (MW: 180 Da) and stannous octoate were charged in a round bottom flask under nitrogen environment. The reaction mixture was stirred under vacuum for 4 hours at 200°C and 2 hours at 160°C. The reaction product was then cooled to room temperature and dissolved in methylene chloride followed by precipitation in large excess of chilled anhydrous diethyl ether. The precipitate was then dried in a vacuum dryer for 2 days. Proton NMR was used to confirm the success of the reactions. Next the PEG-*dl*-lactide molecule was dissolved in dichloromethane along with triethylamine (TEA) and acryloyl chloride. The reaction mixture was cooled to 0°C using an ice bath for 2 hours and then the reaction mixture was stirred at room temperature for an additional 22 hours. The reaction product was washed with 1M HCl and water to remove the triethanolamine hydrochloride. Methylene chloride was rotary evaporated and then the product was further dried in a vacuum oven at 70°C for 2 days. Again the reaction was confirmed using proton NMR. The solvent used for NMR was deuterated chloroform.
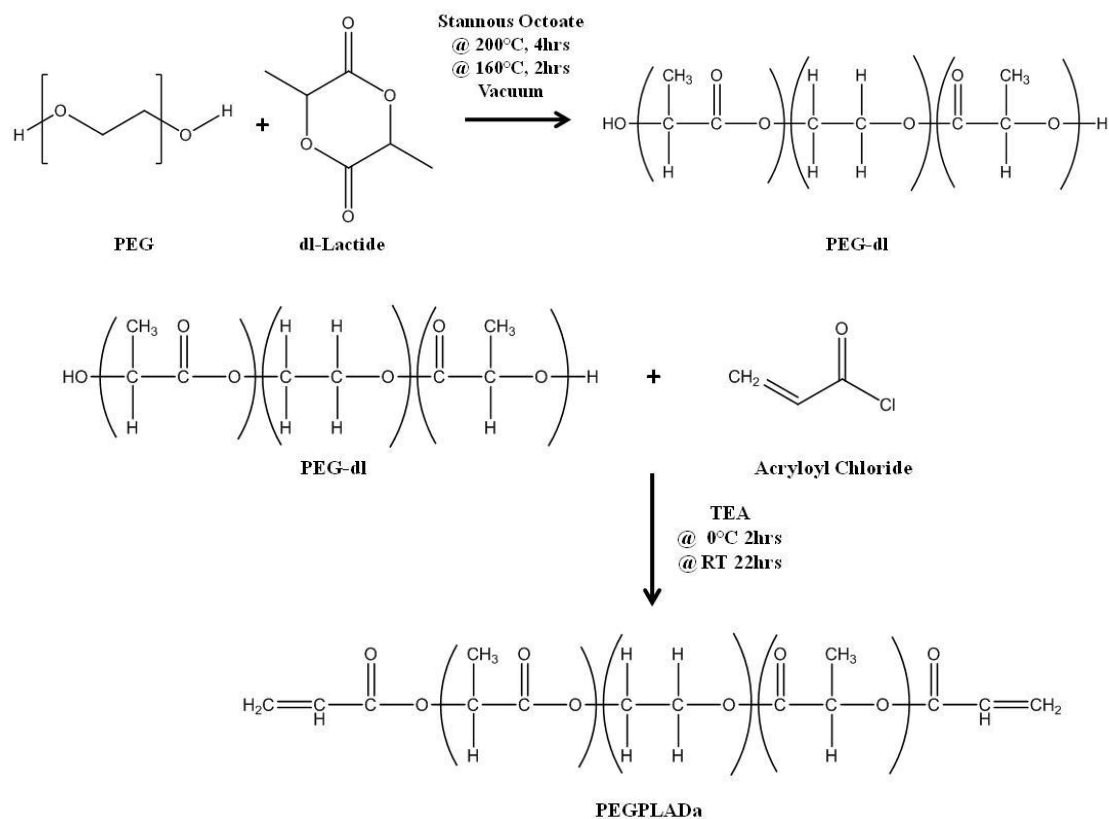
Fig.4.2. Schematic showing the synthesis of PEGPLADa. During stage 1 *dl*-lactide was reacted with PEG in the presence of tin hexanoate to obtain PEG-dl lactide. In stage 2, acrylate photo-reactive group was covalently attached to the ends of PEG-dl lactide monomer. The success of the reaction was verified using ^{1}H NMR.

4.2.3 **Rheological characterization**: To ensure that rapid crosslinking will be able to restrain the shear flow disentangled HA molecular chains, it was imperative to know the relaxation behavior of the solution. An oscillatory strain sweep was conducted on a TA ARG2 stress-controlled rotational rheometer using parallel-plate geometry and a Peltier plate at room temperature to determine the linear viscoelastic regime. The strain was ramped from 0.1% to 10% at 25 °C. Step-strain stress relaxation experiments were conducted, where shear stress is monitored following application of a small shear strain. The diameter of the plate was 40 mm with a solvent trap and moisture chamber enclosure to prevent drying of the test solution. The strain values selected were 5%, 7%, 10% and

12%. Various compositions of HA pre-crosslinking solutions minus the photoinitiator were subjected to the stress relaxation test.

4.2.4 **Fabrication of crosslinked hydrogels**: Pre-crosslinking solutions were made consisting of methacrylated HA, crosslinker, and 1% Irgacure 2959 (I2959). Cytocompatibility studies have showed that I2959 is one of the most cytocompatible photoinitiators (38). Irgacure 2959 is an α-cleavable type I photoinitiator or α-hydroxy phenyl ketone. It is a partially water soluble, non-yellowing compound which forms colorless solutions. The excitation frequency is 320 nm and photo-excitation produces a benzoyl and a ketyl radical of which the former is the major reactive species. One of the many advantages of this particular photoinitiator is that the excited triplet state is too short to be scavenged by oxygen, so the polymerization reaction can be carried out in air inside a fume hood (39). Experimental samples were fabricated using a mold created using glass slides as shown in Figure 4.3. The pre-crosslinking solution was injected into the mold via a 20 gauge needle at a rate of 0.5 ml/min. Rapid crosslinking was initiated by exposing the mold to a 100 W, 365 nm UV light source. The experimental samples were crosslinked immediately following injection. The control samples were crosslinked following a delay was introduced between the injection and UV exposure to facilitate relaxation of the HA chains. The samples were allowed to swell in DI water at 4 °C for 2 hours before any tests. The lowered temperature was utilized to minimize hydrolytic degradation. Figure 4.4 shows the reaction schematic of the crosslinking chemistry.
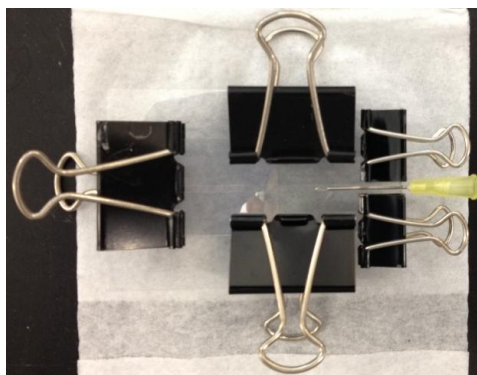
Fig.4.3. Image of the glass slide mold used to crosslink HAGMa hydrogels. The needle shows the channel where the pre-crosslinking solution was injected prior to UV exposure.
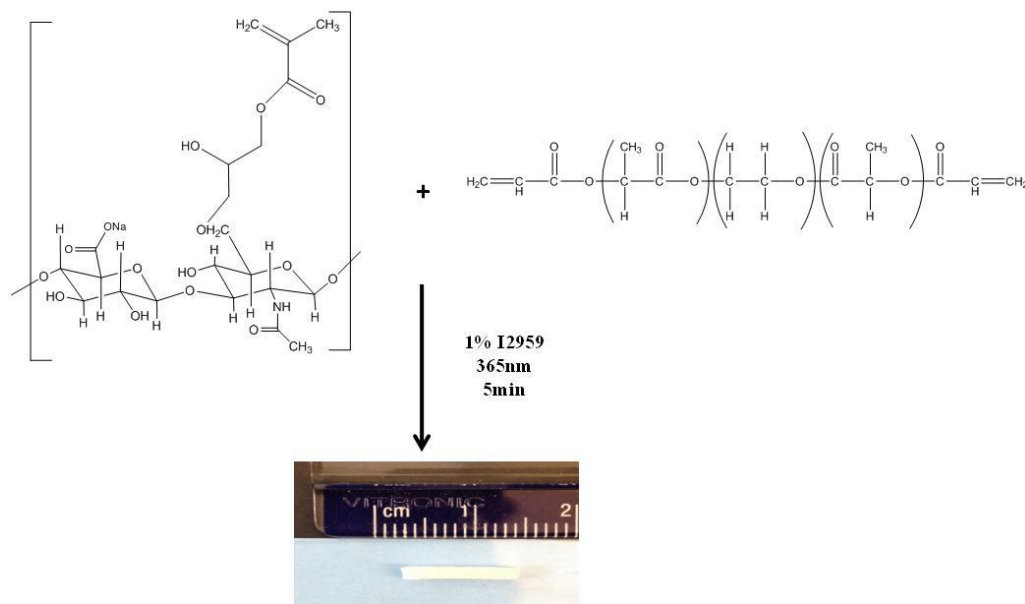
Fig.4.4. Schematic showing the hydrogel crosslinking chemistry. Two concentrations of HAGMa (60 mg/ml and 70 mg/ml) were crosslinked using 1:1 ratio of PEGPLADa. The pre-crosslinking solution turns from translucent yellow to opaque white indicating success of crosslinking chemistry.

4.2.5 **Birefringence experiment**: Birefringence is a property that can provide evidence of a net molecular chain orientation in the crosslinked hydrogel due to rapid crosslinking of the shear aligned HAGMa chains. Crosslinked HAGMa gels were imaged under the polarized optical light microscope (POM) as described in section 3.2.4 to study their

orientation birefringence. Two sets of experiments were performed to answer two different questions about this hydrogel system. Samples crosslinked with different HAGMa concentrations were compared for their retardance to determine the effect of HAGMa concentration on the degree of alignment. The second set of experiment compared the retardance of samples before and after a 48hr degradation experiment to confirm that the shrinkage is a result of reorganization of the molecular chains in the hydrogel network. The compositions tested were 60 mg/ml HAGMa crosslinked with 1:1 ratio of PEGPLADa and 70 mg/ml HAGMa crosslinked with 1:1 ratio of PEGPLADa. The sample was imaged at three separate locations representing the two ends and the middle of the sample. This was done to observe if there is any significant difference in the molecular orientation across the sample.

4.2.6 **Calculation of predicted retractive stress in the network using rubber elasticity theory**: In order to estimate the retractive stress stored in the hydrogel network, we need to first calculate certain network parameters. Swelling experiments were performed on samples of each composition to calculate the swelling coefficient (Q_m), and crosslink density (n). The compositions tested were 60 mg/ml HAGMa crosslinked with 1:1 PEGPLADa, and 70 mg/ml HAGMa crosslinked with 1:1 PEGPLADa. The gels were swollen in PBS at 4°C for a couple of hours and weighed to find the wet weight (M_w). The samples were then dried in a descicator and weighed again to find the dry weight (M_d). The swelling parameters (Q_m, Q_v, n) and the predicted maximum retractive stress in the network (σ_{Pr}) were calculated as described in section 3.2.5.

4.2.7 **Hydrolysis driven shrinkage experiment**: HA hydrogels were crosslinked with PEGPLADa as described earlier. The sample concentrations used were 60 mg/ml HAGMa crosslinked with 1:1 ratio of PEGPLADa and 70 mg/ml HAGMa crosslinked with 1:1 ratio of PEGPLADa. Crosslinked hydrogel samples were swollen to equilibrium in DI water for 2 hours at 4°C in a refrigerator to slow down any hydrolysis that may occur during the swelling process. Rapidly crosslinked hydrogel samples were then transferred into a 37°C shaker for a period of 48 hrs. As the shrinkage process is hypothesized to occur due to hydrolysis, the only form of control samples fabricated were ones with negligible retractive stress stored in the network. This was achieved by providing ample time for the HA chains in the pre-crosslinking solution to relax inside the injection mold before exposing to UV light source. Sample images were captured every 4 hrs and measured using Image J. As a long term study to determine how long the shrinkage continues to occur, samples of the above mentioned composition were kept in a 37°C shaker for a week and sample dimensions were measured form the images captured every 8 hrs.

The experiment described above tested in a controlled manner the shrinkage that is only caused by the hydrolysis process. To simulate the actual conditions at the injury site, where there would be hydrolytic as well as enzymatic degradation, PEGPLADa crosslinked hydrogels were also exposed to 10 µg/ml of hyaluronidase for duration of 48 hrs. The enzyme was replenished every 4 hrs. This experiment provided evidence of any synergistic effect that may happen on account of having both the processes occurring simultaneously.

4.2.8 **Effect of solvent diffusion on shrinkage**: Diffusion is a key aspect that could affect the rate and manner of shrinkage. To ensure that PBS was diffusing through the bulk of the hydrogel efficiently and producing the shrinkage, samples were fabricated as described previously and then sliced longitudinally to reduce the thickness by one half. The rationale behind this was that if the solvent was not diffusing into the bulk of the sample then the shrinkage magnitude and profile would be different than the regular samples. Three samples each of 60 mg/ml HAGMa crosslinked with 1:1 PEGPLADa and 70 mg/ml HAGMa crosslinked with 1:1 ratio of PEGPLADa were used for this experiment. The samples were placed in a 37°C shaker for a period of 48 hrs. Images captured at each timepoint were measured using Image J.

4.2.9 **Measurement of hydrogel stiffness:** In order to determine the force generated by the shrinking hydrogel, we designed a mechanical test setup that relies on a flexible cantilever and its associated sensor. To make sure that we can accurately determine the forces, the hydrogel samples and the cantilever had to be stiffness matched. We performed surface indentation using the mesoindentation system, as described in section 3.2.8, to calculate the stiffness of the hydrogel

4.2.10 **Force measurement protocol**: Figure 4.5 shows the custom-built device consisting of a flexible aluminum cantilever- (DVRT) pair. This device enabled us to measure the force generated by HAGMa hydrogels during the process of shrinking as described in section 3.2.8. The compositions tested were 60 mg/ml HAGMa crosslinked with 1:1 PEGPLADa, and 70 mg/ml HAGMa crosslinked with 1:1 PEGPLADa. Control samples

were made with a delay between injection into the mold and crosslinking to ensure negligible retractive stress is stored in the gel network. The raw voltage data was converted to force (mN) and displacement (µm) using calibration constants. These values were then used to determine the work performed by the shrinking hydrogel.
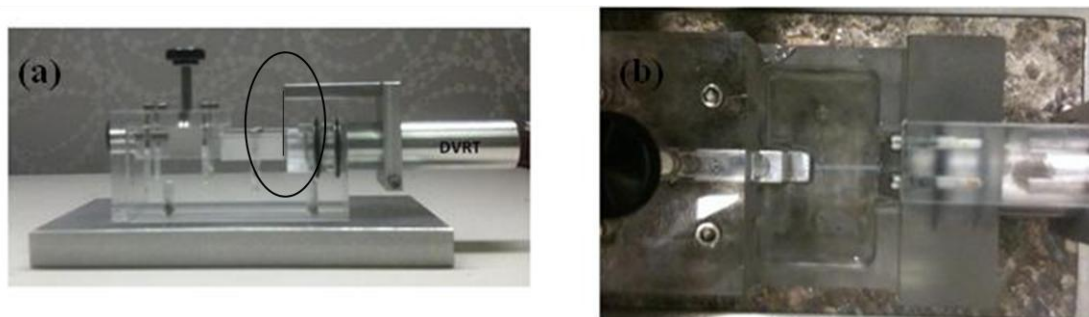
Fig.4.5. Images showing the device used to measure the force generated by the shrinking hydrogel. (a) The aluminum cantilever-DVRT pair (circled in black) is the sensing end of the device. (b) The sample is attached on one end to the calibrated flexible cantilever and to a fixed stage on the other end. The sample is kept submerged via the enclosed reservoir chamber.

5.2.10 **Statistical analysis**: For all statistical analyses ANOVA with Tukey post-hoc analysis or a students t-test were employed as applicable using Origin Pro 8.0, with a significant difference reported for $p < 0.05$. Image analysis was performed using Image J software (NIH, USA). All values are reported as mean ± standard deviation.

4.3 Results

4.3.1 **Methacrylation of HA**: Sodium hyaluronate was successfully modified and a pendant methacrylate group was added on the disaccharide thus forming methacrylated HA

(HAGMa). This reaction was successfully repeated several times with the modification percentage ranging from 75% to 82%.

4.3.2 **Synthesis of PEGPLADa**: PEG oligomer with hydroxyl end group in the form of lactidyl moiety was synthesized by ring opening of the cyclic *dl*-lactide at 200°C in the presence of the stannous octoate as the transesterification agent. The ring opening polymerization of the lactones was initiated by an alcohol in the presence of the catalyst. Figure 4.6 and 4.7 show the ^{1}H NMR of the PEG and PEG-dl lactide respectively. The lactone was added stepwise to the α and ω terminal hydroxyl group of the PEG. This resulted in a BAB copolymer having terminal hydroxyl group. The degree of polymerization depended on the ratio of the lactone concentration to the concentration of the PEG. Two mol *dl*-lactide / mol PEG resulted in a degree of polymerization of 1.9. Fig 4.8 shows the ^{1}H NMR of the stage 2 product, PEGPLADa. The terminal hydroxyl groups in the PEG-dl lactide precursor were end capped with acrylate groups by reacting with acryloyl chloride. Since the precursor has two hydroxyl end groups per molecule, the number of acrylic groups upon hydroxyl-initiated extension was expected to be two. The acrylate peaks were observed between 5.5 and 6.6 ppm.
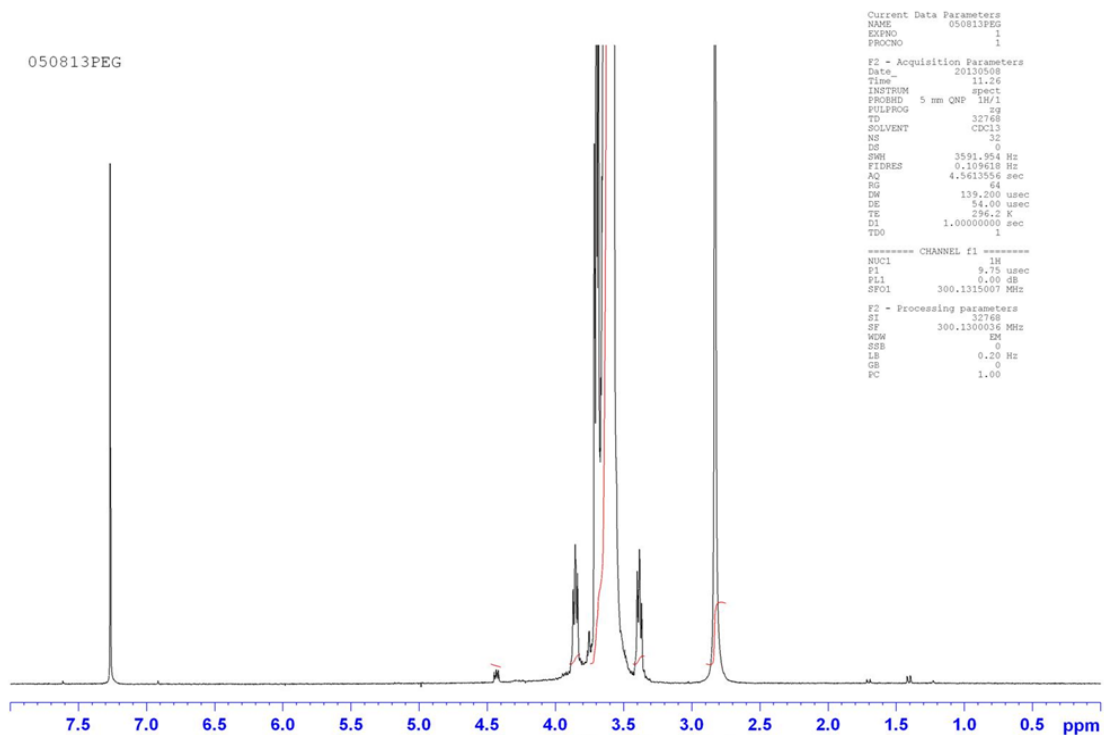
Fig.4.6. ^{1}H NMR of Poly(ethylene) glycol with molecular weight of 1500Da. The peak at 4.3 ppm represents the (-CH$_2$O) group. The solvent used was deuterated chloroform.
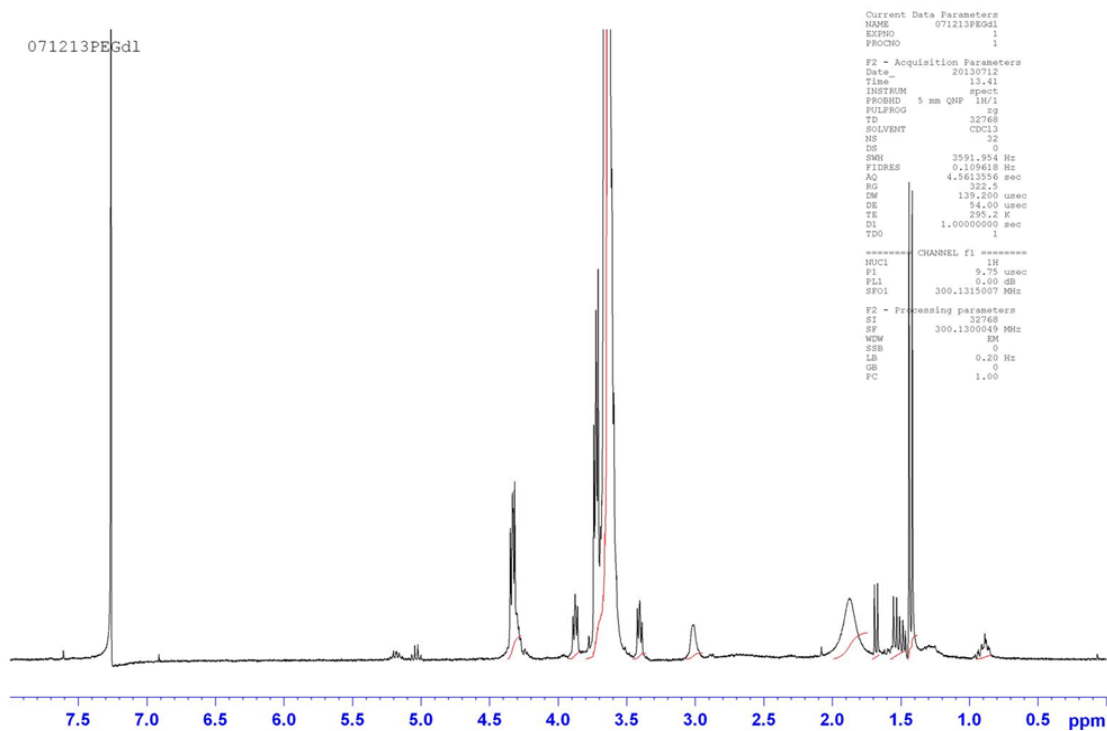
Fig.4.7. ^{1}H NMR of stage 1 product. The lactide was added onto the PEG molecule at the hydroxyl end terminals. The degree of polymerization was calculated using the reference ($-CH_2O$ = 4.3 ppm) from the PEG and the ($-CH_3$ = 1.3 ppm) of the lactide. The degree of polymerization obtained varied between 1.9 - 2.9, which was essential to synthesize a water soluble end product (19).
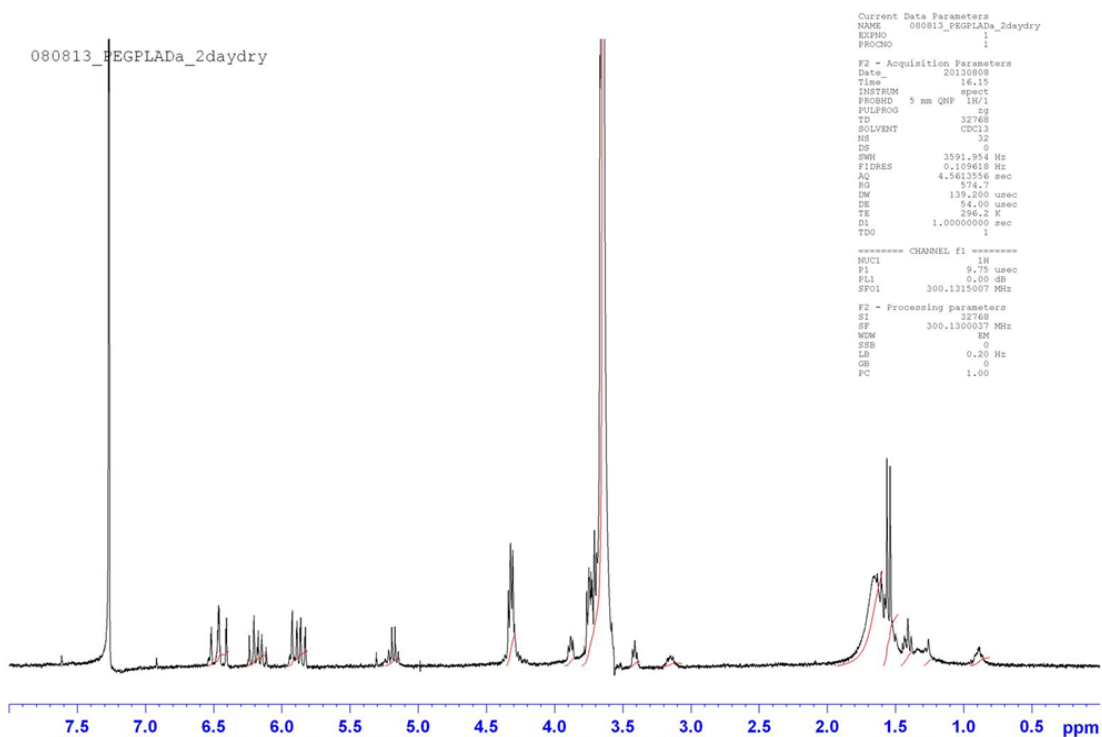
Fig.4.8. ^{1}H NMR of PEGPLADa, the end product of stage 2 reaction. The peaks seen between 5.5 and 6.6 confirmed the successful addition of the acrylate groups.

4.3.3 **Rheological characterization**: Figure 4.9 and 4.10 show the stress relaxation plots for the compositions 60mg/ml HAGMa with 1:1 PEGPLADa and 70 mg/ml HAGMa with 1:1 PEGPLADa respectively. At time = 0 the specimen was suddenly deformed homogenously. The deformation created a stress which gradually relaxed with time. The shear stress could return to zero once the strain induced stress relaxes. Due to the high molecular weight of the HA polymer, the molecular chains may not return to the same random configuration once the stress relaxes. Instead of zero shear stress the sample could plateau out at a non-zero value as the chains may obstruct each other to prevent complete relaxation. Complete relaxation of shear stress was not observed within the test duration for any of the strain conditions. We also did not observe any plateau condition either. From pilot crosslinking tests the crosslinking time was observed to be between 45

110

and 55 seconds. The rheological tests indicated that the molecular chains in neither of the compositions, 60 mg/ml HAGMa crosslinked with 1:1 PEGPLADa or 70 mg/ml HAGMa crosslinked with 1:1 PEGPLADa, would have relaxed before the solution gets completely crosslinked. Thus these compositions would be ideal candidates for testing our hypothesis of storing a retractive stress in the crosslinked networks. Another reason we selected this particular concentration of PEGPLADa was that higher concentrations of the crosslinker caused phase separation of the pre-crosslinking solution. The hydrophobic lactoyl moieties in the bifunctional crosslinker interacted with the hydrophilic HAGMa molecule and lead to the phase separation.
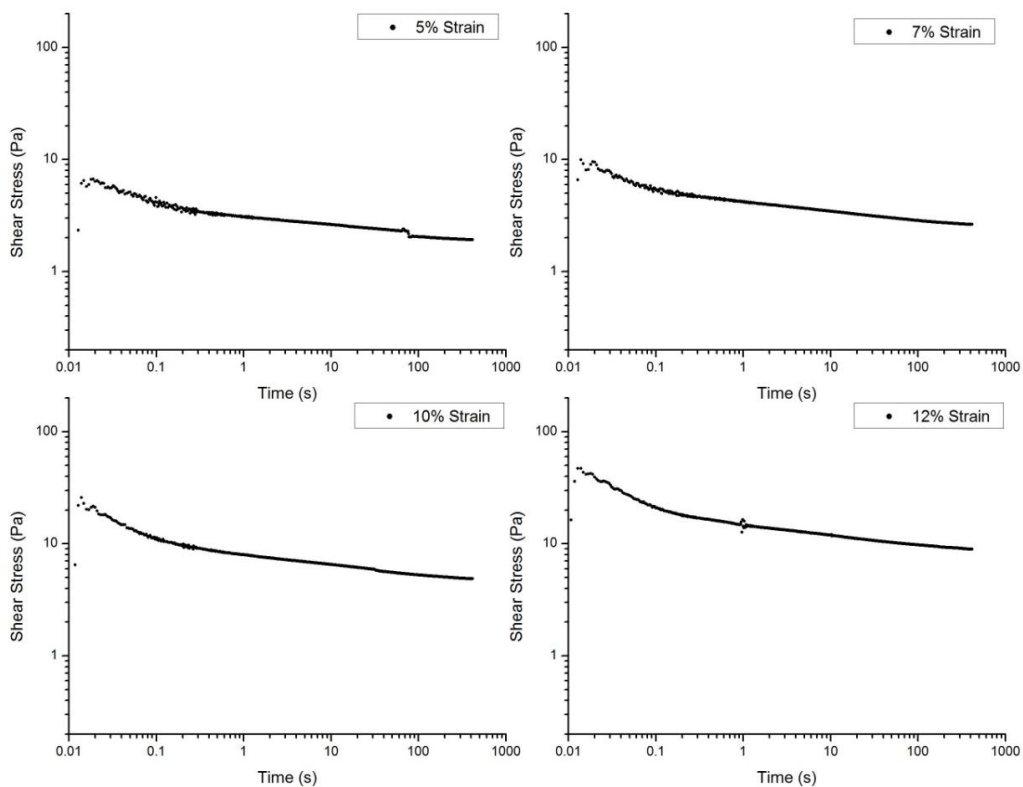
Fig.4.9. Stress relaxation curves for pre-crosslinking solutions of the composition 60 mg/ml HAGMa with 1:1 PEGPLADa. The % strain conditions used were 5%, 7%, 10%, and 12%. The shear stress curves do not return to pre-shearing zero stress or a non-zero plateau indicating that total molecular chain relaxation did not occur within testing duration limits.
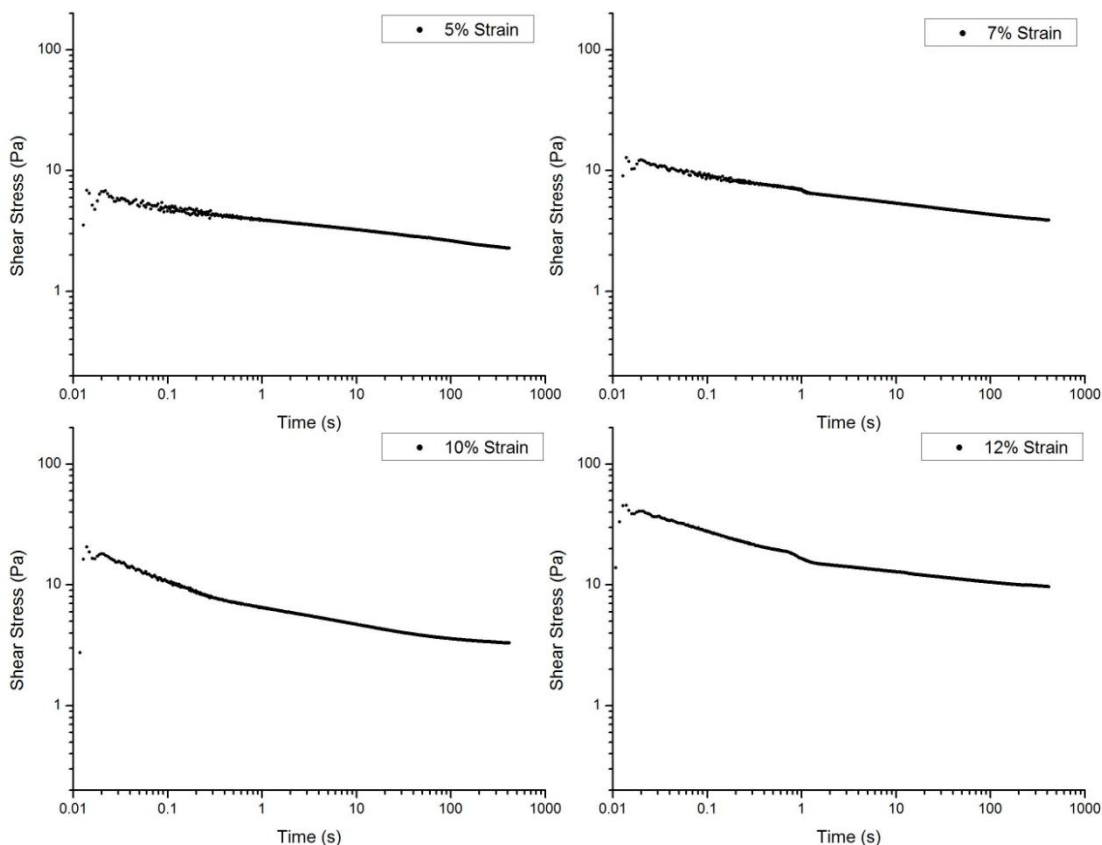
Fig.4.10. Stress relaxation curves for pre-crosslinking solutions of the composition 70 mg/ml HAGMa with 1:1 PEGPLADa. The % strain conditions used were 5%, 7%, 10%, and 12%. The shear stress curves do not return to pre-shearing zero stress or a non-zero plateau indicating that total molecular chain relaxation did not occur within testing duration limits.

4.3.4 **Birefringence study**: Figure 4.11 shows optical micrographs for samples of the composition 60 mg/ml HAGMa crosslinked with 1:1 ratio of PEGPLADa prior to hydrolytic degradation. When the optical axis of the sample was at 45° to the polarizers, birefringence was observed indicating presence of orientation. We calculated the retardance (Δnh) values for all the samples at three distinct locations across the sample, the middle and the two ends. After comparing the retardance values from the three locations, amongst themselves and across the samples, we concluded that there was no

112

significant difference (p >> 0.05) in the retardance values. This indicated that the crosslinking was rapid enough to preserve the shear induced molecular orientation and this orientation was nearly homogenous. The average retardance was calculated from the nine values obtained from the three samples. The average retardance for the composition 60 mg/ml HAGMa crosslinked with 1:1 PEGPLADa prior to enzymatic degradation was 28.60 ± 7.88 nm.

Three samples of the same composition were then immersed in PBS and placed on a shaker table at 37°C for a period of 48 hrs to facilitate hydrolytic degradation. After the test duration, the samples were air dried and observed under the polarized optical microscope (POM). Figure 4.12 shows the captured micrographs. The observable brightness was reduced as compared to the pre-enzyme exposure samples. However the retardance values did not show a significant decrease. This demonstrated that the hydrolytic degradation did not cause a significant decrease in molecular orientation within the samples. Once again we compared the retardance values along length of the sample and between samples. There was no statistically significant difference observed (p >> 0.05). The magnitude of overall sample shrinkage was not measured during this experiment. The average retardance for this composition following enzymatic degradation was 21.15 ± 3.43 nm.
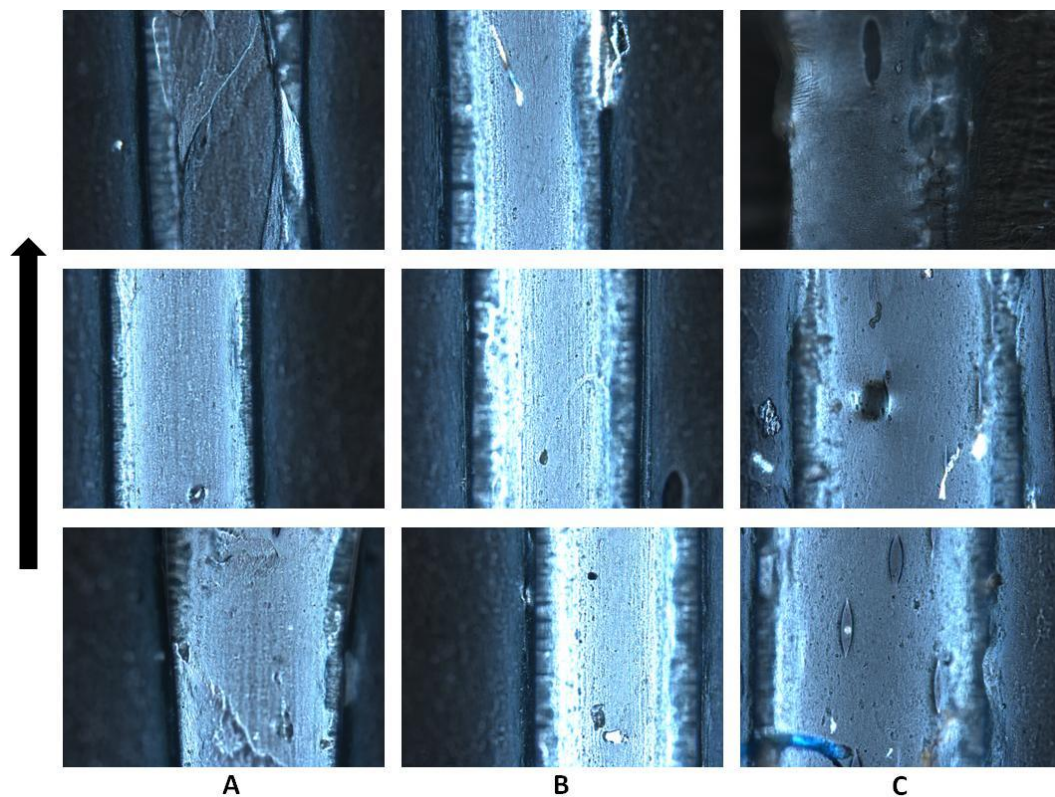
Fig.4.11. Polarized optical micrographs of three 60 mg/ml HAGMa hydrogels crosslinked with 1:1 ratio of PEGPLADa prior to their hydrolytic degradation. Images were captured at the two ends and the middle of the sample. The arrow indicates the direction of flow of the pre-crosslinking solution in the glass mold prior to rapid crosslinking. The retardance for this composition calculated from the captured spectra was 28.60 ± 7.88 nm. The magnification is 20X.
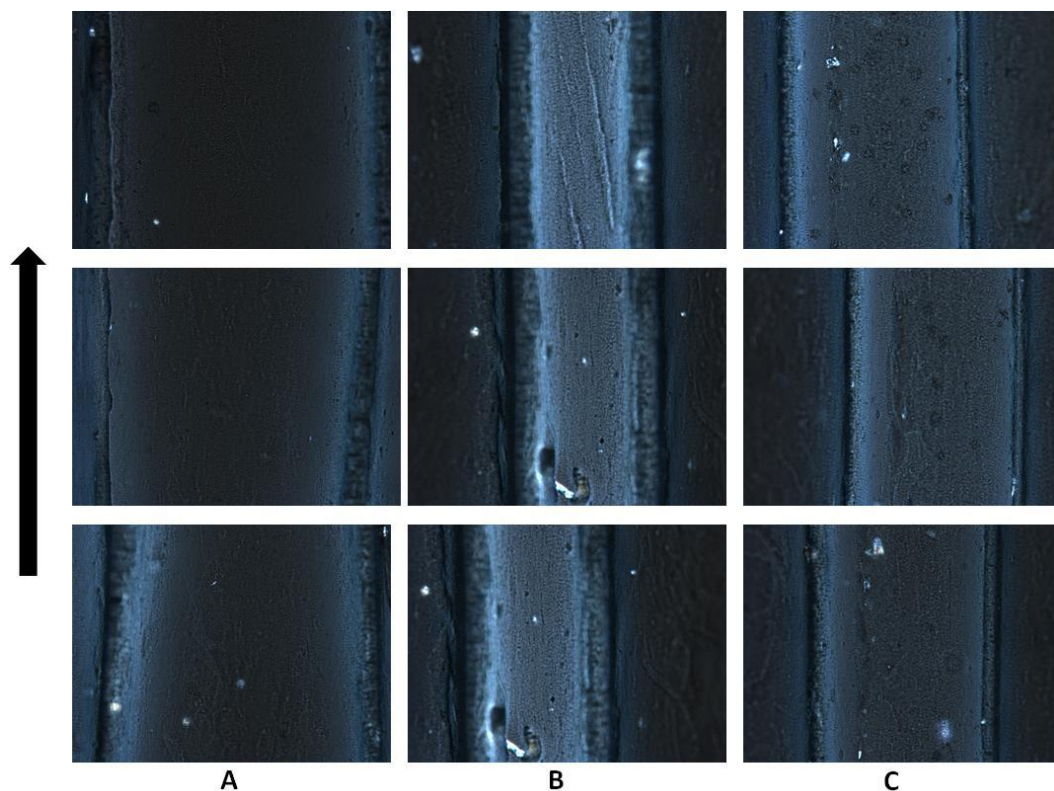
Fig.4.12. Polarized optical micrographs of three 60 mg/ml HAGMa hydrogels crosslinked with 1:1 ratio of PEGPLADa after hydrolytic degradation for 48hrs. Images were captured at the two ends and the middle of the sample. The arrow indicates the direction of flow of the pre-crosslinking solution in the glass mold prior to rapid crosslinking. The retardance for this composition calculated from the captured spectra was 21.15 ± 3.43 nm. The magnification is 20X.

Similarly the second composition, 70 mg/ml HAGMa crosslinked with 1:1 ratio of PEGPLADa, was observed under the POM prior to and after being immersed in PBS at 37°C for 48 hrs. Figure 4.13 shows the optical micrographs for the samples prior to hydrolytic degradation. Each sample was imaged at the two ends and the middle to determine the homogeneity of molecular orientation. The brightness verified the existence of molecular orientation. The average retardance was 23.52 ± 4.57 nm. Samples of the same composition were then degraded and imaged to observe effect of degradation on molecular orientation. Figure 4.14 shows the polarized optical micrographs for the

hydrolytically degraded samples. The retardance values and the observable brightness did not significantly decrease (p >> 0.05), as compared to values obtained from prior to degradation, indicating no significant loss of molecular orientation. The average retardance value post degradation was 24.30 ± 6.54 nm. The magnitude of overall sample shrinkage was not measured during this experiment. Figure 4.15 summarizes the results from the birefringence experiment.
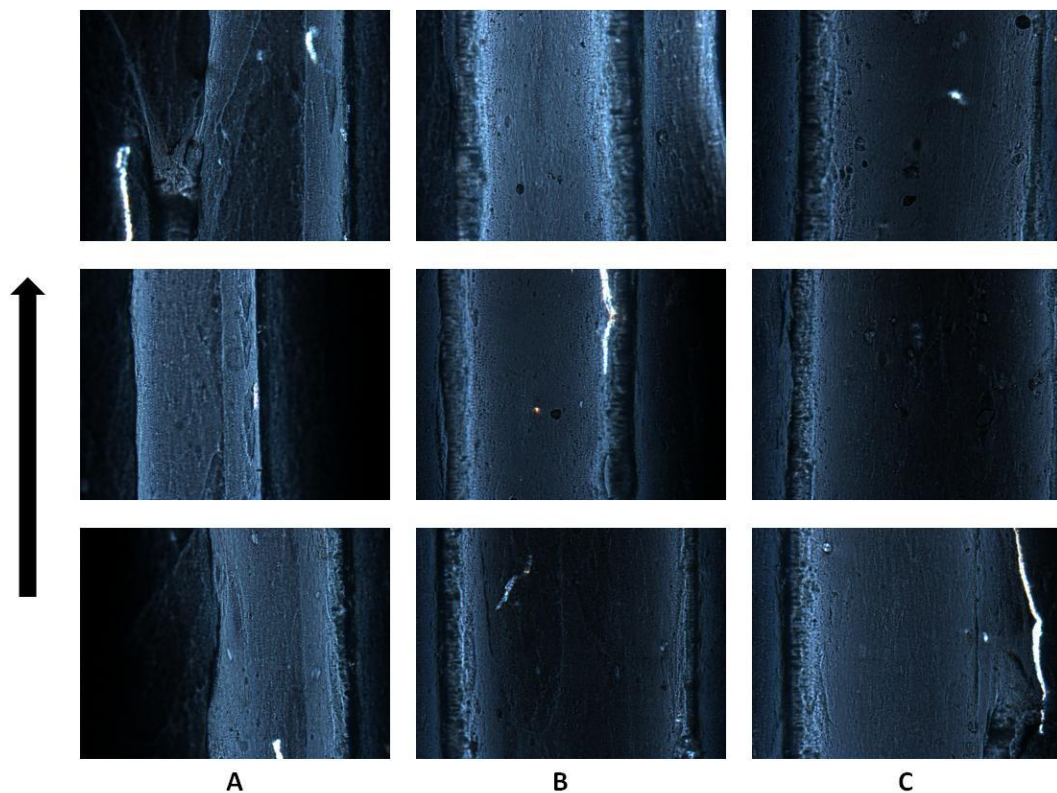
Fig.4.13. Polarized optical micrographs of three 70 mg/ml HAGMa hydrogels crosslinked with 1:1 ratio of PEGPLADa prior to their hydrolytic degradation. Images were captured at the two ends and the middle of the sample. The arrow indicates the direction of flow of the pre-crosslinking solution in the glass mold prior to rapid crosslinking. The retardance for this composition calculated from the captured spectra was 23.52 ± 4.57 nm. The magnification is 20X.
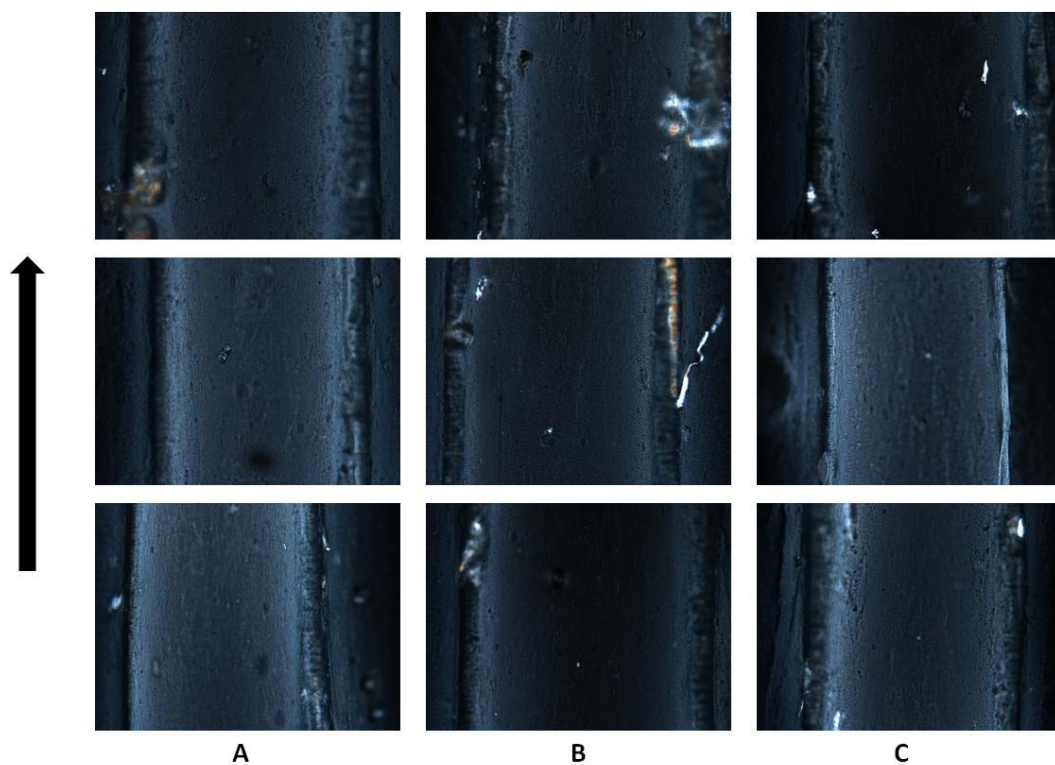
Fig.4.14. Polarized optical micrographs of three 70mg/ml HAGMa hydrogels crosslinked with 1:1 ratio of PEGPLADa post hydrolytic degradation for 48hrs. Images were captured at the two ends and the middle of the sample. The arrow indicates the direction of flow of the pre-crosslinking solution in the glass mold prior to rapid crosslinking. The retardance for this composition calculated from the captured spectra was 24.30 ± 6.54 nm. The magnification is 20X.
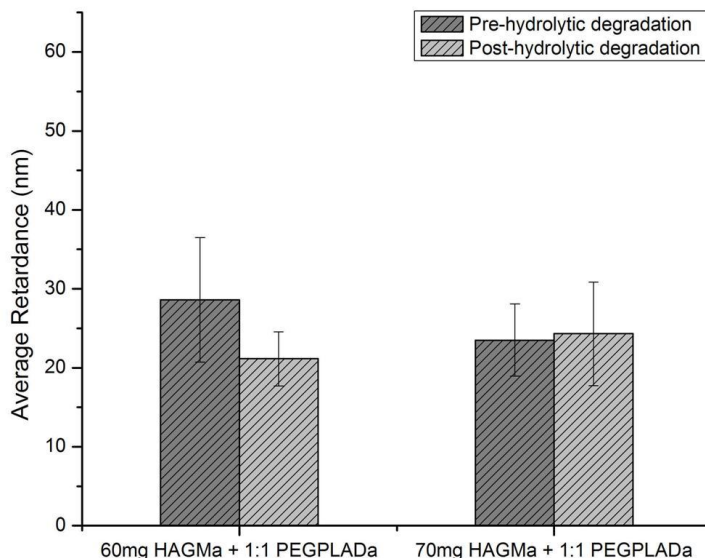
Fig.4.15. Bar graph summarizing the retardance values calculated for the PEGPLADa crosslinked HAGMa hydrogel samples prior to and following hydrolytic degradation. There was no significant decrease in the retardance of samples for the two compositions tested. (n=3)

4.3.5 **Estimation of retractive stress in the hydrogel:** To calculate the crosslink density of the hydrogels, swelling experiments were performed to calculate the swelling ratios. The gels with lower concentration of HAGMa showed significantly higher swelling coefficient. We adapted rubber elasticity theory to estimate the retractive stress stored in a rapidly crosslinked hydrogel. Table 4.1 and Figure 4.18 show the results from this experiment. Increasing the HAGMa concentration did not significantly increase the predicted retractive stress (kPa) stored in the hydrogel network, although the averages seemed to scale with the HAGMa concentration.

Table 4.1. Results from the swelling experiments and retractive stress estimation study

Composition	Swelling Coefficient (Q_m)	Volumetric Swelling Ratio (Q_v)	Crosslink Density $(n \times 10^{-4})$	Stretching Factor (α)	Predicted Retractive stress (σ_{Pr}) kPa
60mg/ml HAGMa + 1:1 PEGPLADa	30.87 ± 4.28	37.71 ± 5.26	5.08 ± 1.49	1.03 ± 0.01	11.22 ± 2.98
70mg/ml HAGMa + 1:1 PEGPLADa	20.95 ± 1.45	25.51 ± 1.78	10.8 ± 1.62	1.02 ± 0.003	13.44 ± 2.11

118

4.3.6 **Hydrolysis driven shrinkage**: HAGMa samples crosslinked with PEGPLADa were degraded hydrolytically. Figure 4.16 shows the 48 hr shrinkage profile for samples of the composition 60 mg/ml HAGMa crosslinked with 1:1 ratio of PEGPLADa. The controls as well as the experimental samples showed shrinkage. The controls shrunk an average of 0.57 mm or 3.57 % before plateauing out. The experimental samples demonstrated a net shrinkage of 21.71 % or 3.07 mm. However the shrinkage was rapid and most of it occurred within the first 4 hrs. Figure 4.17 shows results for the samples of the second composition 70 mg/ml HAGMa crosslinked with 1:1 ratio of PEGPLADa. We did observe some shrinkage (6.8 % or 0.9 mm) in the control sample. This control sample shrinkage could be on account of some residual retractive stress still present in the network as well as molecular chain reorganization as a result of degradation. The experimental samples also demonstrated shrinkage along their long axis which was significantly greater than the control samples. Unlike the samples of the composition 60 mg/ml HAGMa, the 70mg/ml HAGMa samples demonstrated a much more gradual shrinkage profile. The net shrinkage was 14.21 % or 2.04 mm. The shrinkage did not seem to stop by the end of 48 hr.
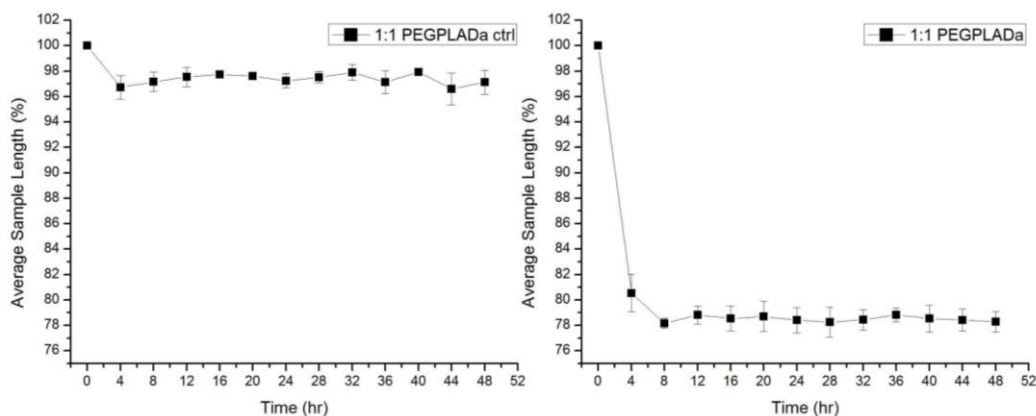
Fig.4.16. Graph showing hydrolysis driven shrinkage profile for hydrogels of the composition 60 mg/ml HAGMa crosslinked with 1:1 ratio of PEGPLADa that were degraded for 48 hrs. The controls were made such that there would be negligible retractive stress in the network. The experimental samples demonstrated 21% shrinkage, however almost all of it occurred within the first 4 hrs. The shrinkage ceased after 8 hrs. In comparison the controls shrunk only 4%. (n=3)
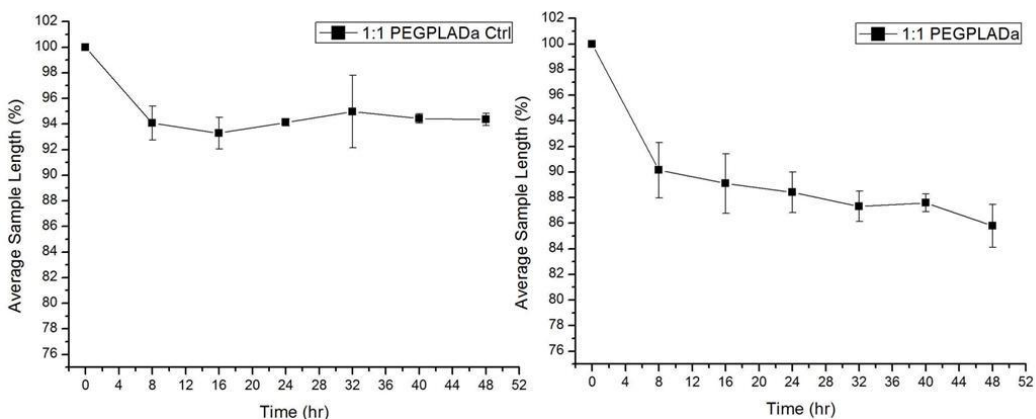
Fig.4.17. Graph showing hydrolysis driven shrinkage profile for hydrogels of the composition 70 mg/ml HAGMa crosslinked with 1:1 ratio of PEGPLADa that were degraded for 48 hrs. The controls had negligible retractive stress in the network. The overall profile of shrinkage was more controlled compared the composition 60mg/ml HAGMa crosslinked with 1:1 PEGPLADa. The net shrinkage after 48 hrs was 14%. The controls showed a net shrinkage of 6.8%. (n=3)

To verify if the networks could produce any more shrinkage, we extended the duration of degradation from 48 hrs to 1 week. Figure 4.18 and 4.19 show the shrinkage

profile results for samples of the two compositions. The 60 mg/ml HAGMa samples did not demonstrate shrinkage beyond 8 hrs. The control samples of the composition 70 mg/ml HAGMa did not show any further shrinkage, however the experimental samples continued to shrink beyond 48 hrs but stopped around 52 hr time point.

We wanted to explore the effect of combining hydrolytic degradation of the networks with enzymatic degradation. PEGPLADa crosslinked samples were exposed to 10 µg/ml concentration of the enzyme hyaluronidase. Figure 4.20 shows the shrinkage profile we obtained from those samples. Adding the enzyme had some interesting synergistic effects on the shrinkage. In case of the 60 mg/ml HAGMa samples, the shrinkage rate was slowed down but the overall magnitude reduced from 21.71 % to 16.89 %. The duration of shrinkage increased from 8 hrs to 20 hrs. The 70 mg/ml HAGMa samples on the other hand showed an increase in the net magnitude of shrinkage from 14.21 % to 20.77 %, however the shrinkage ceased by 52 hrs.
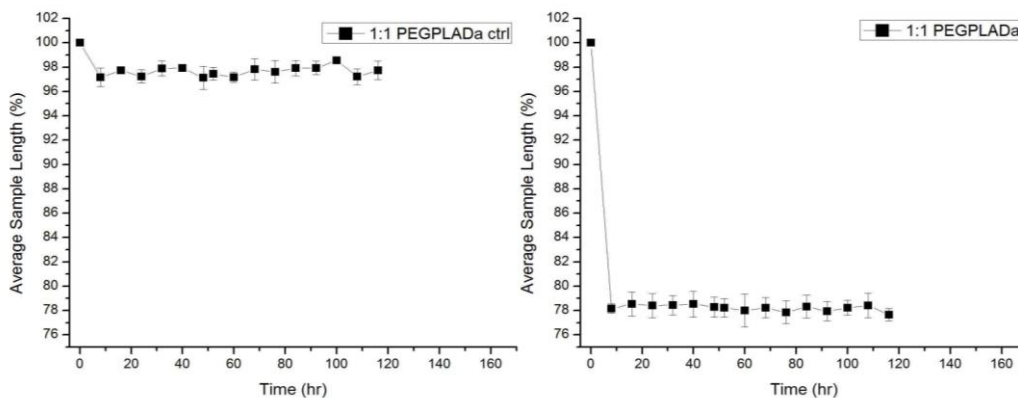
Fig.4.18. Graph showing hydrolysis driven shrinkage profile for hydrogels of the composition 60 mg/ml HAGMa crosslinked with 1:1 ratio of PEGPLADa that were degraded for one week. The controls were made such that there would be negligible retractive stress in the network. The samples did not show any renewed shrinkage after 8 hrs. (n=3)
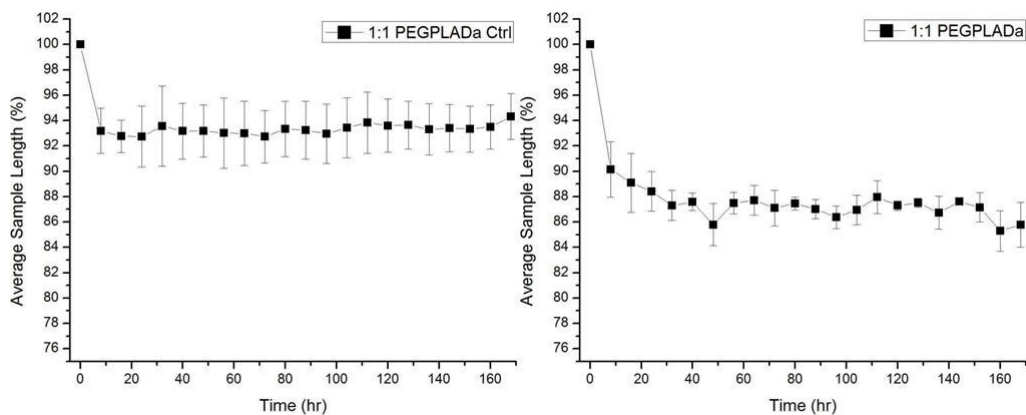
Fig.4.19. Graph showing hydrolysis driven shrinkage profile for hydrogels of the composition 70 mg/ml HAGMa crosslinked with 1:1 ratio of PEGPLADa that were degraded for one week. The experimental samples continued to shrink till 52 hrs and the shrinkage profile then seemed to plateau out. (n=3)
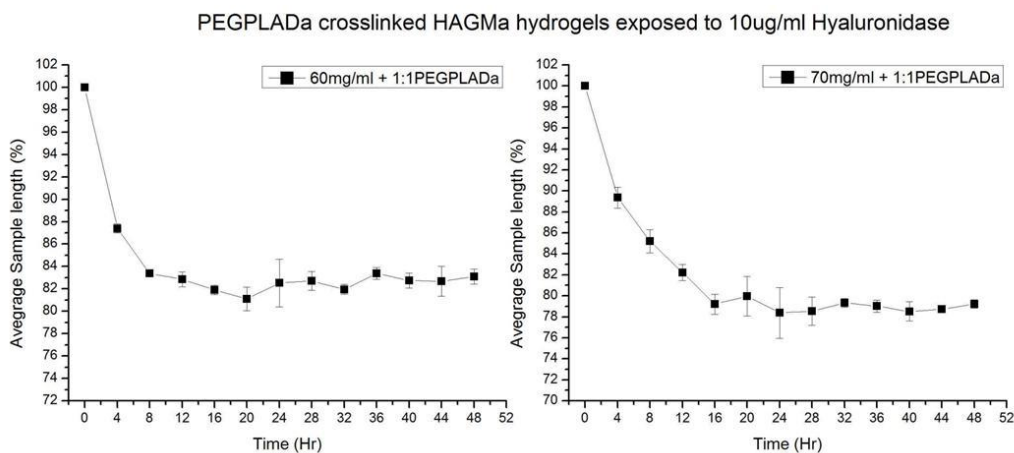
Fig.4.20. Shrinkage profile for samples of the composition 60 mg/ml HAGMa and 70 mg/ml HAGMa crosslinked with 1:1 PEGPLADa that were exposed to 10 µg/ml concentration of hyaluronidase. Combining hydrolytic and enzymatic degradation slowed down the overall shrinkage profile for the 60 mg/ml composition, while increased the net magnitude of 70 mg/ml HAGMa composition when compared to the samples that were only hydrolytically degraded. (n=3)

Figure 4.21 summarizes the shrinkage rates per day that we calculated for the hydrolytically degraded PEGPLADa crosslinked HAGMa samples. The 60 mg/ml HAGMa samples stopped shrinking by the end of 8 hrs with a rate greater than 100

122

μm/hr during that duration. The 70 mg/ml HAGMa samples stopped shrinking by the end of day two. The rate calculated for the first day was 70 μm/hr, which is within the beneficial stretching rate previously reported for axonal elongation (7, 8, 11). Table 4.2 summarizes the degradation induced shrinkage for the PEGPLADa crosslinked samples.
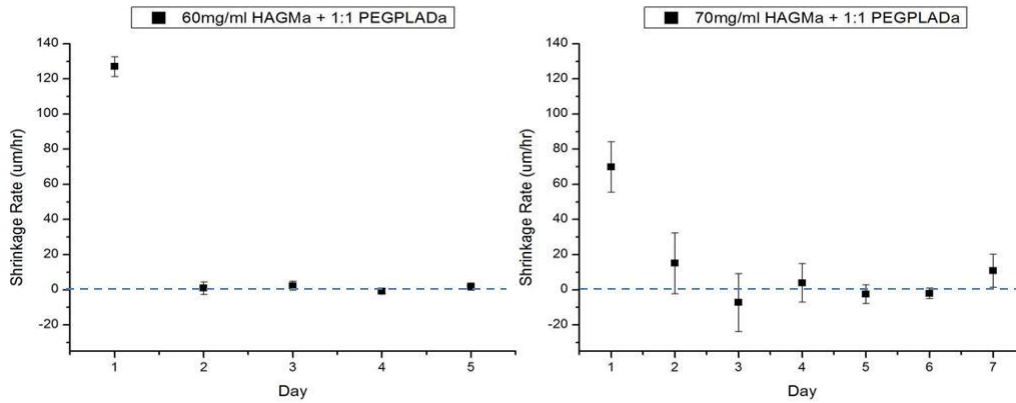
Fig.4.21. Profile of the shrinkage rates for the PEGPLADa crosslinked HAGMa hydrogels that were degraded hydrolytically for a period of 1 week. The shrinkage rates for the first day ranged from 70 μm/hr to 125 μm/hr. The shrinkage gradually ceased by day 2 for all the compositions. (n=3)

Table.4.2. Summary of the average sample shrinkage for the PEGPLADa crosslinked HAGMa hydrogel samples

Condition	Sample Type	60mg/ml HAGMa + 1:1 PEGPLADa		70mg/ml HAGMa + 1:1 PEGPLADa	
		Average Sample Shrinkage (%)	Average Sample Shrinkage (mm)	Average Sample Shrinkage (%)	Average Sample Shrinkage (mm)
Hydrolysis	Control	3.57 ± 0.94	0.57 ± 0.32	6.82 ± 2.06	0.9 ± 0.3
	Experimental	21.71 ± 0.82	3.07 ± 0.19	14.21 ± 1.66	2.04 ± 0.21
Hydrolysis + 10μg/ml Hyaluronidase	Experimental	16.89 ± 0.67	2.32 ± 0.17	20.77 ± 0.39	3.23 ± 0.25

4.3.7 **Effect of solvent diffusion on shrinkage**: Figure 4.22 shows the shrinkage profiles for the samples that were one half the thickness of the regular samples. We observed that the overall profile did not change significantly. Samples of the composition 60 mg/ml

HAGMa still showed rapid shrinkage that lasted 8 hrs. There was a 7% decrease in the net magnitude of shrinkage. The samples of the composition 70 mg/ml HAGMa showed an increase of 4% in the net shrinkage. Thus we did see some effect of sample thickness on the shrinkage. However it was only on the magnitude and not the manner in which they shrink. Reducing thickness meant reducing the source of the shrinkage. We believe that in case of 60 mg/ml samples we reduced the overall potential to shrink while in case of the higher concentration 70 mg/ml HAGMa samples we decreased the density of chains which was restricting efficient reorganization of chains in the first place.
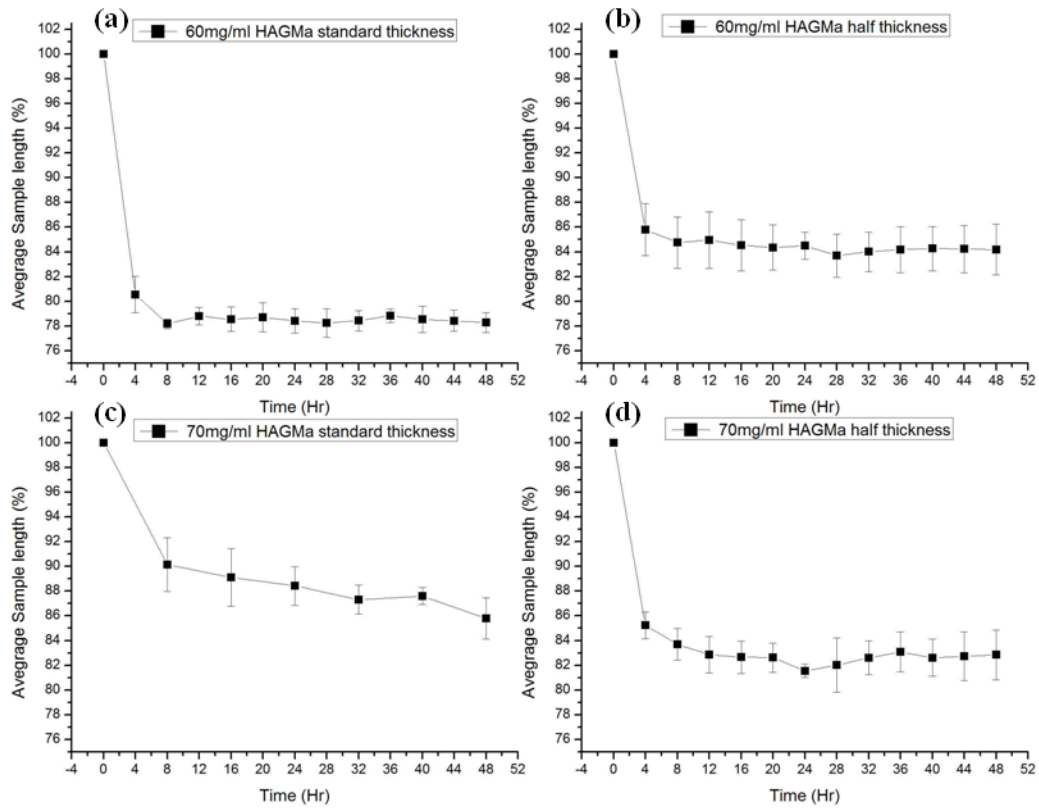
Fig. 4.22. Graph showing the hydrolysis driven shrinkage of PEGPLADa crosslinked HAGMa hydrogels (a, b – 60 mg/ml; c, d – 70 mg/ml), comparing the effect of sample thickness on nature of sample shrinkage. For the 60 mg/ml composition there was a decrease in overall magnitude of shrinkage but the profile remained unchanged. The 70 mg/ml composition demonstrated a 3% increase in the magnitude of shrinkage. (n=3)

4.3.8 **Hydrogel stiffness**: PEGPLADa crosslinked HAGMa samples were indented at random locations prior to and following hydrolytic degradation. The load-displacement curves indicated a linear elastic behavior where the loading and unloading curves overlapped. The stiffness was calculated from the loading portion of the curve. Prior to exposure to degradation the stiffness of gels with the composition 60 mg/ml HAGMa crosslinked with 1:1 PEGPLADa was 2.04 ± 0.10 N/m. After degradation for 48 hrs, the stiffness dropped to 1.14 ± 0.09 N/m. Similarly the stiffness of gels made using 70 mg/ml HAGMa and 1:1 PEGPLADa before hydrolytic degradation was 2.21 ± 0.19 N/m. After degradation, the stiffness decreased to 1.44 ± 0.09 N/m. Figure 4.23 summarizes the results from this experiment. The stiffness values helped us in designing the aluminum cantilevers with stiffnesses specifically matched to the hydrogel composition.
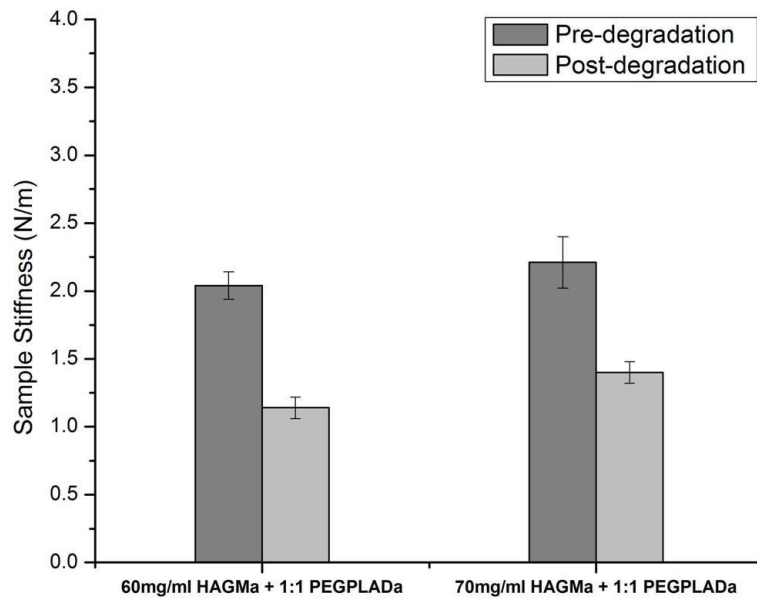
Fig. 4.23. Graph showing the measured stiffness of HAGMa hydrogels crosslinked with PEGPLADa before and after 48hr degradation. The stiffness of the samples decreased significantly ($p \ll 0.05$) following degradation. (n=3)

4.3.9 **Measurement of shrinkage force:** Flexible cantilevers were fabricated based on the stiffness values obtained from the indentation experiments. We selected the stiffness value as 2.01 N/m keeping a fine balance between the stiffness achievable while acquiring sufficient signal from the DVRT-cantilever pair. The cantilever was calibrated using known loads and displacements (see appendix). The test was conducted for 48 hrs and the raw voltage values were converted to appropriate force and displacement values using the calibrations. The DVRT signal was recorded at the rate of one point per second; however the plots display only one point per hour for the purpose of clarity. The cross-section of the hydrogels was 1 mm^2. The force values were converted to corresponding stress (kPa) to corroborate with the predicted stress (σ_{pr}). This was done to determine how much of the stored retractive stress was recovered. Figure 4.24 (a, c, e) shows the force, displacement, and recovered stress curves for hydrogels of the composition 60 mg/ml HAGMa crosslinked with 1:1 ratio of PEGPLADa. The control samples were able to displace the cantilever by 0.24 ± 0.05 mm generating a force equivalent to 0.45 ± 0.1 mN. The cantilever displacement can be equated to the sample's shrinkage; however the sample gets weaker as it degrades, so it will be unable to sustain the cantilever displacement. The sample shrinkage was half that of the unconstrained shrinkage experiments. The experimental samples demonstrated shrinkage of 1.3 ± 0.6 mm exerting a net force of 1.4 ± 0.27 mN on the cantilever. This amounted to a net stress of 1.4 kPa or 12.47 % of the predicted stored retractive stress.

Samples of the second composition, 70 mg/ml HAGMa crosslinked with 1:1 PEGPLADa, were tested in the similar fashion. The control samples shrunk 0.51 ± 0.19

mm with a net force of 0.77 ± 0.26 mN. Once again the shrinkage values were half the values we measured during the unconstrained experiment. The experimental samples shrunk 1.46 ± 0.40 mm while applying a force of 1.00 ± 0.23 mN on the cantilever. This value translated to a net recovered stress of 1 kPa, which was 7.44 % of the predicted stored retractive stress. The constrained condition of the samples in the test device affected the shrinking behavior of the hydrogels. Unlike the unconstrained shrinkage tests, the samples now performed work on another object. Thus even the profile of shrinkage appeared to be more gradual when compared to the profile obtained from the unconstrained shrinkage. Another factor that also probably played a role in the plateau observed in the force and displacement profiles was the fact that the sample strength decreased on account of the degradation. Thus overtime the cantilever stiffness overtook the sample stiffness and was able to compensate for the force the sample was applying on it. Figure 4.25 shows a comparison of between the predicted stored retractive stress in the networks and the measured recovered stress from this experiment. It was evident that a significantly smaller percentage of the stored retractive stress could be recovered which again can be explained by the sample constrainment and loss of sample stiffness.
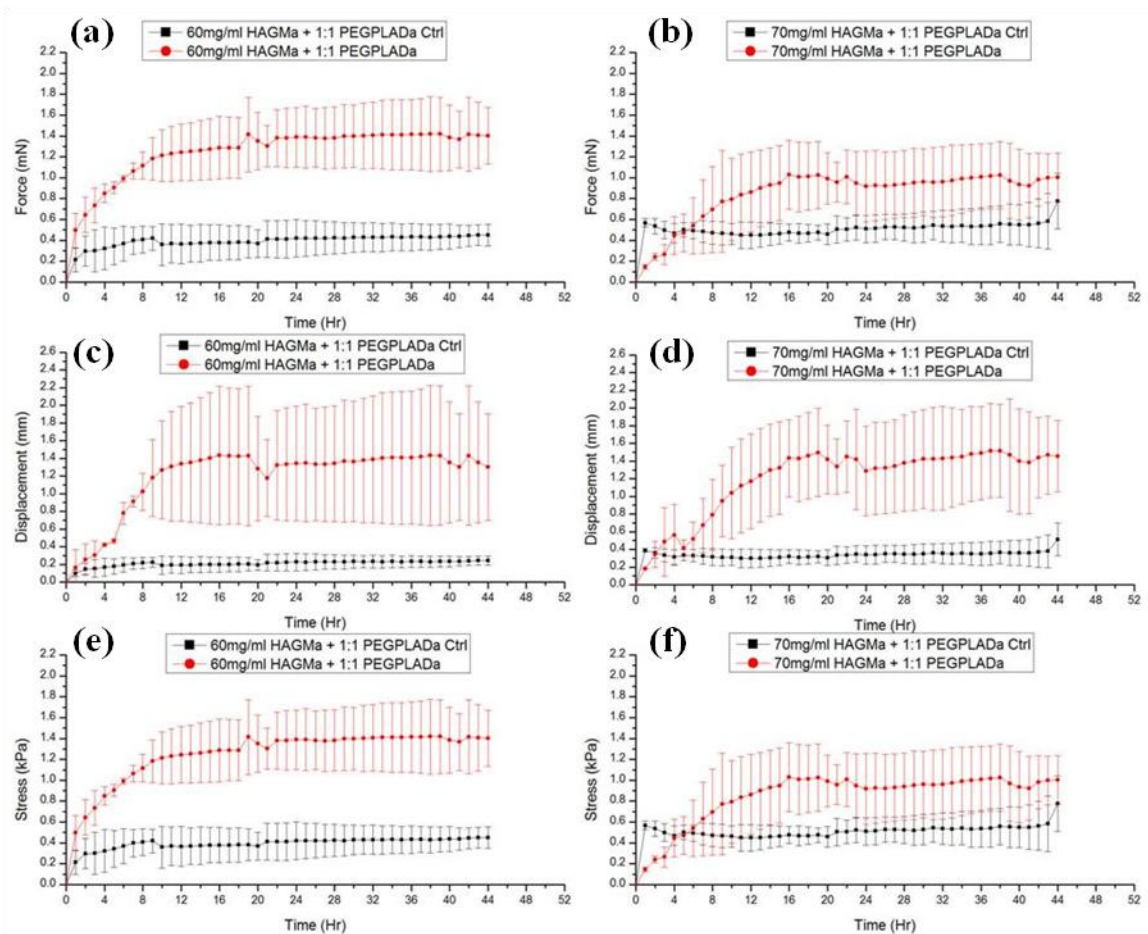
Fig.4.24. Graphs showing the force, cantilever displacement, and recovered stress curves for the PEGPLADa crosslinked HAGMa samples that were hydrolytically degraded while attached in the force measurement device. The control samples showed very minimal shrinkage compared to experimental samples. The stress recovered either composition was significantly lower than what was predicted using rubbery elasticity principles. (n=3)
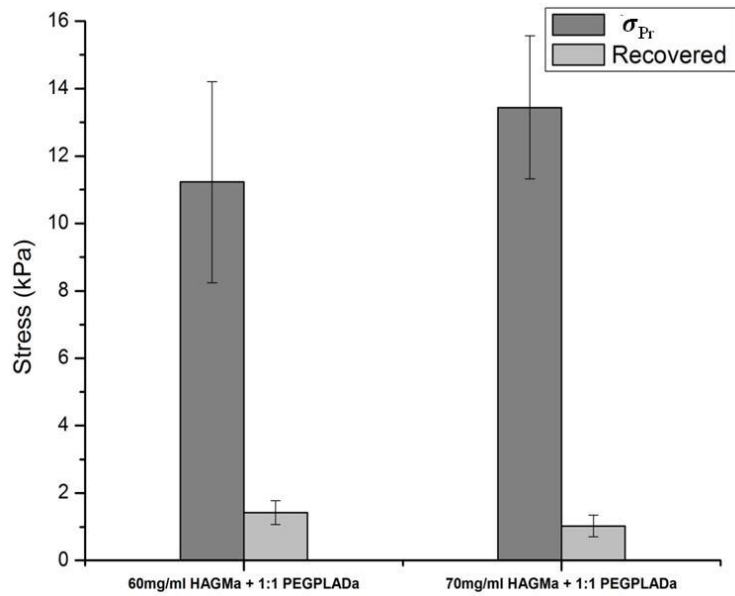
Fig.4.25. Bar graph showing the values of predicted stored and the recovered retractive stress for the two compositions of PEGPLADa crosslinked HAGMa hydrogel samples. The magnitude of the recovered shrinkage was significantly lower than the predicted stored retractive stress. (n=3)

4.4 Discussion

The unique properties of the HA molecule enabled us to design a novel hydrogel that could be programmed to shrink on a time scale relevant for application as a mechanical stimulator of neuronal cells. Birefringence enabled us to verify the success of arresting the shear flow induced molecular chain alignment. Our hypothesis was that increasing the HAGMa concentration would decrease the extent of molecular orientation in the crosslinked network. We increased the HAGMa concentration from 60 mg/ml to 70 mg/ml. The average retardance value decreased from 28.60 nm to 23.52 nm however the standard deviations were high enough to negate any significant difference between the compositions. The retardance values were uniform across the samples for either composition indicating that the crosslinking process maintained similar disentanglement induced state of orientation

throughout the sample. In our previous work, we hypothesized that enzymatic cleavage of HAGMa chains was hampering our ability to extract higher degree of shrinkage. Thus we devised a network where the crosslinks were degraded selectively via hydrolysis. We examined the birefringence of samples that were degraded for 48 hrs. We did not see any significant decrease in the molecular orientation despite the fact we observed shrinkage of the samples. The high concentration of backbone HAGMa chains might be preventing further relaxation of the chains despite the fact that the hydrolysis cleaves the crosslinks. We did not observe a complete degradation within our testing duration. An extended degradation study may be able to shine some light on the duration it takes for the complete network to collapse.

Based on our previous work, we concluded that the magnitude of shrinkage that could be obtained from the novel HAGMa network is limited by the size and concentration of the HAGMa chains. The method we adapted to predict this magnitude of retractive stress stored in the network demonstrated that the retractive stress does seem to scale with the concentration of HAGMa but we did not see any significant difference between the two compositions we tested. Our ability to test higher concentrations was limited by the non-homogenous crosslinking we observed at higher HAGMa concentrations. The higher concentration of HAGMa restricted diffusion of the free radicals through the samples thereby producing unevenly crosslinked samples. A solution to this issue would be to increase the molecular weight of the HAGMa chains which would allow us to reduce the concentrations and may provide us a wider range of compositions to experiment with.

Hydrolytic degradation of the rapidly crosslinked HAGMa hydrogels brought about shrinkage of the gel along its long axis which was also the axis of flow prior to crosslinking. The magnitude and rate of shrinkage were affected by the concentration of HAGMa. As we increased the HAGMa concentration the shrinkage was much more gradual. However the increase in HAGMa concentration also decreased the net magnitude of shrinkage. This result may seem confusing, considering that higher concentration of the HAGMa chains translate to higher potential retractive stress in the network, until we inspect how the network chains behave at the two different concentrations. As the PEGPLADa crosslinks get cleaved, the free volume within the network increases. So the chains can have some long range motion and reorganization which translates to shrinkage of the crosslinked sample. But higher the concentration of the HAGMa, greater is the difficulty for the chains to move past one another to reorganize. Thus it is easier for samples containing 60 mg/ml HAGMa to release the retractive stress via reorganization when compared to those with 70 mg/ml HAGMa. Adding a second mechanism of degradation in the form of an enzyme verified our hypothesis. When the enzyme worked alongside hydrolysis, the HAGMa chains also got cleaved. Thus we saw an increase in the net magnitude of shrinkage in the 70 mg/ml HAGMa samples as more room was created within the network by combining hydrolytic and enzymatic degradation. Cleaving the chains in lower HAGMa concentration composition samples reduced the total potential of an intact chain to recoil and relax. Thus the rate and magnitude of shrinkage were reduced.

The rapid nature of the shrinkage cannot be entirely explained by the hydrolysis alone. The hydrolysis process is a gradual and slow process. Despite the high hydrophillicity of the

131

network due to both HAGMa and PEG, there might be another mechanism at play that may be responsible for the rapid shrinkage. Prior to the testing of the PEGPLADa crosslinked samples, they were swollen in PBS for two hours at 4°C. This was done to allow for swelling while slowing down any hydrolysis. In hindsight this may not have been the optimal experimental design. The change in temperature from 4°C to the test condition 37°C may have caused additional network swelling and network reorganization which led to the rapid shrinkage. To test this hypothesis a shrinkage assay could be performed by completely getting rid of the two hour swelling duration. Instead, the sample can be subjected to 37°C conditions straightaway after the crosslinking process and images of the sample captured at intervals of one hour. The normalized sample length vs time profile will show how the sample swells, when it reaches equilibrium swelling, and when the shrinkage starts and stops. The expected outcome profile may show initial swelling followed by shrinkage and maybe another swelling cycle when the shrinkage stops and hydrolysis increases capacity of the gel to absorb water.

The rate of shrinkage for the samples of the composition 60 mg/ml HAGMa crosslinked with 1:1 PEGPLADa for the first day was over the recommended 100 µm/hr rate that is favorable to elicit axonal elongation by stretch growth (4, 5, 7, 8). Also the shrinkage was very rapid and lasted only 8 hrs. Samples of the 70 mg/ml composition sustained shrinkage for 52 hrs and the rates of shrinkage per day were less than 100 µm/hr. We could not elicit more shrinkage when we extended the degradation to one week indicating that there are still significant limitations to this hydrogel design. Looking at results from the mechanical device designed to measure the force generated by the shrinking hydrogel, it is evident that we are

unable to measure all of the recovered retractive stress. As the samples got weaker on account of the degradation, the cantilever stiffness exceeded that of the hydrogels and the hydrogels were unable to sustain the "tug" on the aluminum cantilever. We could not fabricate cantilevers that were softer than the ones we used. Any further reduction in the size or flexibility of the cantilever hampered our ability to obtain a high enough DVRT signal that was devoid of noise generated by vibrations within the reservoir. Simultaneously, the physical chain entanglements may have prevented complete rearrangement of the network as it degraded.

Comparing the PEGPLADa crosslinked hydrogels with the PEGDa crosslinked hydrogels described in the previous chapter, we can start to appreciate the complex processes that result in the hydrogel network shrinkage. The average retardance of the PEGDa hydrogel compositions prior to shrinkage was significantly higher than any of the PEGPLADa crosslinked gels indicating a greater magnitude of retractive stress stored in the network. This would imply that the former would produce the greatest magnitude of shrinkage. However the magnitude of shrinkage obtained over a period of 2 days from the PEGPLADa hydrogels was higher than the PEGDa gels (2.32 – 3.07 mm vs 1.1 – 2.00 mm). The parameter that is crucial for the intended application of this polymer network is the rate at which the hydrogels shrink and the efficiency of stress recovery from the network. The profile of shrinkage for the PEGDa appears to be more gradual and the shrinkage was sustained for a longer duration when compared with the rapid shrinkage observed with the PEGPLADa hydrogels. Based on the values reported in the literature on axonal stretching this rapid shrinkage with rates greater that 100 µm/hr, as seen with the hydrolytically degraded PEGPLADa crosslinked

gels, could to be detrimental for the application as axonal stretch growth actuators (2, 4, 7, 8, 11, 40). It is crucial to point out that adding a second means of degradation, in the form of the enzyme hyaluronidase, did slow down the rapid shrinkage of the PEGPLADa gels increasing their applicability. Thus after critically analyzing and comparing the data from the array of characterization we performed, the composition 70 mg/ml HAGMa crosslinked with 1:1 PEGPLADa stands out as the most favorable candidate among the PEGPLADa compositions tested.

There is an emerging need for polymeric actuator materials with applications that range from artificial muscles to robotic prosthesis (12). The current technology on actuator polymers includes hydrogel based actuators, shape memory polymers (SMP) and a class of polymers called electroactive polymers (EAP). Swelling/de-swelling of hydrogels is the primary mechanism of hydrogel based actuators and ionic EAP's. However the inverse relationship between the swelling behavior and the ability to generate force presents a challenge in applying some of the currently described systems for mechanical actuation. PNIPAAm based gels are able to produce large values (3-4mm) of displacement/shrinkage due to network collapse (19). Trying to achieve high displacements of the gels invariably leads to gels with low degree of crosslinking which also means a very fast and short actuation response. The gel shrinkage for PNIPAAm gels could not be sustained for more than two hours. Brazel et al. (23) designed a unique PVA based gel that was swollen in DMSO and was able to produce a constant and directionally controlled locomotion in air using a DC electric field. This concept, although very promising, would be very difficult to apply in an *in vivo* biological environment due the obvious application of high voltage and non-

biocompatible elements of the gel. SMP's tend to have high strain recoveries but at rates that are as high as 1.8% to 5% per minute (15, 16). A review of the actuation literature reveals that a majority of current actuator systems have response times that are of the order of minutes to a few hours (12, 14, 16, 19, 22, 23, 41) which would make them unsuitable for slow actuation applications.

Recently Chippada et al. (42) described a DNA crosslinked hydrogel that shows some potential to be a slow actuating polymer system. The DNA-crosslinked polyacrylamide gels have the ability to dynamically contract or swell by the addition of crosslinks or removal of strands respectively. The tendency of these loosely crosslinked gels to contract as their crosslink density was increased is a novel technique to generate a force. The dynamic modulation of the stiffness of the hydrogels by addition of crosslinks caused the tissue scaffold to shrink and this could potentially be used to exert traction on the emerging neurites and physically expand the tissue. The force generated by the DNA crosslinked gel per unit length was approximately equal to 1050 pN/µm. This force was of the same order of magnitude as that observed by Heidemann et al. to elicit stretch growth in individual neurites (4). The PEGPLADa crosslinked hydrogels produced forces that are greater than 90 nN/µm, which is a few orders of magnitude higher. However unlike singular neurites, a bundle of neurites may be able to sustain greater forces. The advantage that our crosslinked networks provide is the ability to produce tensile forces at rates favorable for axonal stretch growth using a trigger that is not damaging (thermal, electrical) to the already injured neurons.

The critical limitation evident from our results was obtaining the correct balance between the concentration of the HAGMa and the crosslinker PEGPLADa to prevent phase separation of the pre-crosslinking solution. A possible solution we believe that would give us a wider range of compositions to test is using a higher molecular weight HA molecule. This would enable us to use lower concentrations of derivatized HA chains while achieving the rheological conditions favorable for trapping disentangled chains in an ordered structure via rapid crosslinking. Fabrication conditions like flow rate prior to crosslinking could be altered to achieve the maximum degree of molecular chain orientation. The hydrogel system needs to be optimized further for application in its desired application as a mechanical stimulator. However this system is a significant step towards building a new class of degradable polymeric actuators that can provide controlled slow and long term actuation.

4.5 Conclusion

Novel PEGPLADa crosslinked hyaluronic acid hydrogels were designed to possess the property of controlled shrinkage for the purpose of use as a potential axonal growth enhancer via the mechanism of stretch growth. The samples were characterized for their ability to shrink and ability to exert a force on account of shrinkage. The composition 60 mg/ml HAGMa crosslinked with 1:1 ratio of PEGPLADa demonstrated the highest magnitude of shrinkage in 48 hrs (21.71 %) but could not sustain it for more than 8 hrs. Samples of the composition 70 mg/ml HAGMa crosslinked with 1:1 ratio of PEGPLADa sustained shrinkage for 52 hrs and the magnitude of shrinkage was 14.21 %. Despite the lower net magnitude of shrinkage, the 70 mg/ml HAGMa composition demonstrated shrinkage rate that

is more conducive for the application of axonal stretch growth. Further optimization of the hydrogel system is necessary to improve on the duration of shrinkage.

References

1. Evans GRD. Peripheral nerve injury: a review and approach to tissue engineered constructs. Anat Rec. 2001;263:396.

2. Schmidt CE, Leach JB. Neural tissue engineering: strategies for repair and regeneration. Annu Rev Biomed Eng. 2003;5(1):293-347.

3. Wang S, Cai L. Polymers for fabricating nerve conduits. International Journal of Polymer Science. 2010;2010.

4. Heidemann SR, Buxbaum RE. Tension as a regulator and integrator of axonal growth. Cell Motil Cytoskeleton. 1990;17(1):6-10.

5. Dennerll T, Lamoureux P, Buxbaum R, Heidemann S. The cytomechanics of axonal elongation and retraction. J Cell Biol [Internet]. 1989;109(6):3073.

6. Goldberg JL. How does an axon grow? Genes & Development. 2003 April 15;17(8):941-58.

7. Smith DH. Stretch growth of integrated axon tracts: Extremes and exploitations. Prog Neurobiol. 2009 11;89(3):231-9.

8. Bray D. Axonal growth in response to experimentally applied mechanical tension. Dev Biol. 1984 4;102(2):379-89.

9. Pfister BJ, Iwata A, Meaney DF, Smith DH. Extreme Stretch Growth of Integrated Axons. The Journal of Neuroscience. 2004 September 08;24(36):7978-83.

10. Pfister BJ, Iwata A, Taylor AG, Wolf JA, Meaney DF, Smith DH. Development of transplantable nervous tissue constructs comprised of stretch-grown axons. J Neurosci Methods. 2006 5/15;153(1):95-103.

11. Smith DH, Wolf JA, Meaney DF. A New Strategy to Produce Sustained Growth of Central Nervous System Axons: Continuous Mechanical Tension. Tissue Eng. 2001 04/01; 2011/05;7(2):131-9.

12. Carpi F, Smela E, editors. Biomedical Applications of Electroactive Polymer Actuators. John Wiley & Sons; 2009.

13. Ionov L. Hydrogel-based actuators: possibilities and limitations. Materials Today. 2014;17(10):494.

14. Ionov L. Polymeric Actuators. Langmuir. 2014;10:1021.

15. Song J, Xu J. Thermal Responsive Shape Memory Polymers for Biomedical Applications. In: Fazel-Rezai R, editor. Biomedical Engineering - Frontiers and Challenges. ; 2011.

16. Sokolowski W, Metcalfe A, Hayashi S, Yahia L, Raymond J. Medical applications of shape memory polymers. Biomed Mater. 2007;2:S23.

17. Miyata T, Jikihara A, Nakamae K, Hoffman AS. Preparation of poly(2-glucosyloxyethylmethacrylate) concanavalin A complex hydrogel and its glucose-sensitivity. Macromolecular Chem , and Phys. 1996;197:1135.

18. Miyata T, Asami N, Uragami T. A reversibly antigen-responsive hydrogel. Nature. 1999;399:766.

19. Hu Z, Zhang X, Yong L. Synthesis and application of modulated polymer gels. Science. 1995;269:525.

20. Topham PD, Ryan AJ. Antagonistic Triblock Polymer Gels Powered by pH Oscillations. Macromolecules. 2007;40:4393.

21. Gutowska A, Bae YH, Feijen J, Kim SW. Heparin release from thermosensitive hydrogels . J Controlled Release. 1992;22:95.

22. Lendlein A, Langer R. Biodegradable, elastic shape-memory polymers for potential biomedical applications. Science. 2002;296:1673.

23. Brazel ES, Peppas NA. Pulsatile local delivery of thrombolytic and antithrombotic agents using poly(N-isopropylacrylamide-co-methacrylic acid) hydrogels. J Controlled Release. 1996;35:57.

24. Cussler EL, Stokar MR, Varberg JE. Gels as size selective extraction solvents. AICHe J. 1984;30:578.

25. Hayashi S, Kondo S, Kapadia P, Ushioda E. Room-Temperature-Functional Shape-Memory Polymers. Plastics Engineering. 1995;51(2):29.

26. Huffman AS, Afrassiabi A, Dong LC. Thermally reversible hydrogels: II. Delivery and selective removal of substances from aqueous solutions. J Controlled Release. 1986;4:213.

27. Knight PT, Lee KM, Qin H, Mather PT. Biodegradable thermoplastic polyurethanes incorporating polyhedral oligosilsesquioxane. Biomacromolecules. 2008;9(9):2458.

28. Kim JS, Singh N, Lyon LA. Displacement-induced switching rates of bioresponsive hydrogel microlenses. Chem Mat. 2007;19:2527.

29. Mano J. Stimuli-responsive polymeris systems for biomedical applications. Adv Engg Mat. 2008;10(6):515.

30. Sakai Y, Matsuyama Y, Takahashi K, Sato T, Hattori T, Nakashima S, et al. New artificial nerve conduits made with photocrosslinked hyaluronic acid for peripheral nerve regeneration. Biomed Mater Eng. 2007;17(3):191-7.

31. Wang K, Nemeth IR, Seckel BR, Chakalis-Haley DP, Swann DA, Kuo J, et al. Hyaluronic acid enhances peripheral nerve regeneration in vivo. Microsurgery. 1998;18(4):270-5.

32. Borland G, Ross J, Guy K. Forms and functions of CD44. Immunology. 1998;93(2):139-48.

33. Lesley J, Hascall VC, Tammi M, Hyman R. Hyaluronan Binding by Cell Surface CD44. Journal of Biological Chemistry. 2000 September 01;275(35):26967-75.

34. Laurent TC, editor. The Chemistry, Biology and Medical Applications of Hyaluronan and its Derivatives. 1st ed. London and Miami: Portland Pr; 1998.

35. Laurent TC, Laurent UB, Fraser JR. Functions of hyaluronan. Annals of the Rheumatic Diseases. 1995 May 01;54(5):429-32.

36. Bader RA, Rochefort WE. Rheological characterization of photopolymerized poly(vinyl alcohol) hydrogels for potential use in nucleus pulposus replacement. Journal of Biomedical Materials Research Part A. 2008;86A(2):494-501.

37. Sawhney AS, Pathak CP, Hubbell J. Bioerodible hydrogels based on photopolymerized poly(ethylene glycol)-co-poly(.alpha.-hydroxy acid) diacrylate macromers. Macromolecules. 1993(4):581.

38. Bryant, S J Nuttelman, C R Anseth,K S. Cytocompatibility of UV and visible light photoinitiating systems on cultured NIH/3T3 fibroblasts in vitro. Journal of biomaterials science. Polymer edition. 2000;11(5):439.

39. Allen NS, editor. Photopolymerization and photo imaging science and technology. 1st ed. New York: Elsevier Science Publishers Ltd; 1989.

40. Schmidt CE, Leach JB. NEURAL TISSUE ENGINEERING: Strategies for Repair and Regeneration. Annu Rev Biomed Eng. 2003;5:293-347.

41. Illeperuma W, Sun J, Suo Z, Vlassak J. Force and stroke of a hydrogel actuator. Soft Matter. 2013;9:8504.

42. Chippada U. Non-intrusive characterization of properties of hydrogels [dissertation]. New Brunswick, New Jersey: The State University of New Jersey; 2010.

Chapter 5

5.1. **Background**

One of the advantages of hyaluronic acid for the current application as a mechano actuator for neuronal cells is its inherent ability to be cell adhesive. CD44 is a major cell surface receptor for HA (1). It is expressed on many different cells, including neuronal cells where it is over expressed following trauma (2, 3). The cell surface receptors for HA are CD44 and receptor for hyaluronan mediated mobility (RHAMM) (1, 4). CD44 is by far the major receptor. CD44 is a ubiquitous multi-structural and multifunctional cell surface adhesion molecule involved in cell-cell and cell-matrix interactions. It shares a 100-amino acid region of homology with other HA-binding proteins known as the "link module" or the "proteoglycan tandem repeat" (1, 5). CD44 differs in important ways from other HA binding proteins. HA binding by CD44 requires sequences outside the common link module and is regulated by cell-specific factors, and requires multiple CD44/HA engagements to achieve a functional affinity. The most significant feature that distinguishes CD44 from other HA-binding proteins is that CD44 binding to HA takes place at the cell surface, where multiple, closely arrayed CD44 receptor molecules interact with the highly multivalent repeating disaccharide chain of HA. The affinity of a single CD44-HA binding domain for HA is likely to be very low (1). It is known that following injury to the central or peripheral nervous system, cell surface receptors like CD44 are over expressed (2, 3). It is believed that the excess cell surface receptors help in guiding the severed or damaged neurites along the matrix to their suitable target for reinnervation (2). Thus the crosslinked HA network has an inherent binding advantage for the eventual

application in a peripheral nerve gap injury during both the phases (active mechano-stimulator and passive bridging scaffold) the hydrogel will exist at the site.

HA has a very short half-life in the body. To increase the feasability of using HA based scaffolds, crosslinking process is the preferred way (6-8). HA can be modified chemically at the hydroxy groups on both the glucoronic and N-acetylglucosamine units or the carboxyl group on the glucoronic acid unit to add a reactive species that can be used in the crosslinking process. However this may have adverse effects on the inherent property of HA to be cell adhesive. Achieving a high degree of derivatization may have effetcs on the charge density of the molecule. The electronegative nature of the HA molecule is favorable for cell and ligand binding. Thus it was imperative to study if the crosslinked hydrogels are still cytocompatible. A live-dead assay was performed to study the cytocompability.

One of the methods we implemented to cause network shrinkage was degrading the HAGMa chains in the network. HA is naturally degraded by the enzyme hyaluronidase (9). The cleavage occurs at the β-N-acetyl-D-glucosaminidic linkages to yield fragments of N-acetylglucosamine at the reducing terminus and glucoronic acid at the non-reducing end (6, 7, 10, 11). We used this enzyme at physiologic and elevated concentrations to simulate *in vivo* degradation at the site of injury. The breakdown products of HA have been shown to modulate wound healing (6, 7, 10, 12). This would be an added advantage of this polymer network system that would aid in repairing the injury site. Hence it was

critical to know the effect of high concentrations of hyaluronidase on primary cortical neurons over the 48 hour duration of the shrinkage / degradation experiment.

The crosslinked HAGMa networks described in Chapters 3 and 4 have properties that would be considered as favorable to be used a mechanical stimulators for axonal stretch growth. As a preliminary step towards eventual *in vivo* application, it is crucial to test this potential *in vitro*. This required designing an experiment wherein the neurons and the gel could interact and the gel would be able to exert extensional forces on the axonal ends. The challenge was of the size scale issue with neurons growing on a 2D substrate and the gel having to be adhered in a way that it is flush with the axonal ends. Moreover restricting the gel in a chamber filled with media and still allowing free shrinkage without any frictional force was a daunting task. To circumvent these problems, we built a mechanical device to simulate the effect of a shrinking hydrogel on stretch growth of axons. Mouse primary cortical neurons were used for all experiments involving neuronal cells. We hypothesize that the crosslinked hydrogel would maintain the inherent cytocompatibility of HA. The potential of the shrinking hydrogels to cause axonal stretch growth can be tested using the custom-built mechanical stretching device. The results from the experiments described in the following sections will allow us to assess if the interfacial bonding between axonal ends and the crosslinked HA network is strong enough to sustain axonal stretch growth. This will help us decide if any additional adhesion sites may be required.

5.2. Materials and Methods

5.2.1. **Effect of Hyaluronidase on primary neurons:** PEGDa crosslinked hydrogels were degraded via the enzyme hyaluronidase to effect shrinkage. The concentrations used for the study simulate the elevated levels of enzyme at the site of neuronal injury. The exact concentration of the enzyme post injury is unknown. It is thus imperative to understand if the hyaluronidase concentration has any effect on the primary neurons. Primary cortical neurons were generously donated by the Hewett lab. The neurons were harvested from day 15 gestation mouse pup embryos. The cells were suspended in serum free primary cortical neuron media and seeded at a density of 200000 cells/well in a tissue culture polystyrene 12 well plate. On day two following seeding, 1 μM solution of anti-mitotic agent Cytarabine (Ara-C) was introduced into the wells to stop the growth of any non-neuronal cells. The media was changed every two days. The testing for the effect of hyaluronidase on primary neurons was conducted on neurons at least six days post seeding. Hyaluronidase at a concentration of 10 μg/ml was added to the wells every four hours. The cells at the center of the wells were imaged every four hours to observe any morphological changes or detachment as a result of the enzyme.

5.2.2. **Live-dead assay of HAGMa hydrogels:** To test cytocompatibility of the crosslinked HAGMa hydrogels, a live-dead assay was performed using NIH MC-3T3 fibroblasts. The gels were crosslinked in the shape of thin cylindrical disks and swollen in DI water before any tests were conducted. The compositions tested were 60 mg/ml HAGMa crosslinked with 3:1 and 4:1 ratio of PEGDa, 60 mg/ml HAGMa crosslinked

with 1:1 ratio of PEGPLADa, and 70 mg/ml HAGMa crosslinked with 1:1 ratio of PEGPLADa. The samples were sterelized under a 30 W, 254 nm wavelength UV lamp for 45 mins. Fibroblasts were seeded on to the hydrogels at the concentration of 10000 cells per sample. The cells were grown on the samples for 24 hours before the live-dead reagents were added. Fluorescent images of the samples were captured to determine the percentage of live and dead cells.

5.2.3. **Cytocompatibility with primary neurons:** Primary neurons were seeded on crosslinked HAGMa hydrogels at density of 400000 cells/sample. Samples were imaged every 24 hours to observe the morphology of the primary neurons that attached to the hydrogels. Day 6, the second media change, was selected as the timepoint to visually observe the shape and arrangement of the neuronal cells. The compositions tested were 60 mg/ml HAGMa crosslinked with 3:1 and 4:1 ratio of PEGDa, 60 mg/ml HAGMa crosslinked with 1:1 ratio of PEGPLADa, and 70 mg/ml HAGMa crosslinked with 1:1 ratio of PEGPLADa.

5.2.4. **Axonal stretch device:** To test the ability of hydrogels to stretch neuronal bundles we designed a mechanical device that would allow us to bypass the difficulties related with a direct *in vitro* test involving interaction of the hydrogel with the neurite ends. In order to directly test the capability of the shrinking hydrogel to stretch the neurons we had to tackle several design challenges. The soft gels needed to be anchored at one location while keeping one or both ends free to interact with axonal ends. Having the gels submerged in a liquid caused them to lift off the surface thereby not actually being on the same plane as the cells. Thus the custombuilt device allowed us to

simulate gel shrinkage at appropriate rates. Two glass surfaces, one bearing axonal ends and the other the HAGMa hydrogel, were aligned so that the axonal ends have an opportunity to interact with the hydrogel on the same plane. The slide bearing the hydrogel was then slowly moved away using a microstepper motor at rates corresponding to the shrinkage rates for the hydrogel composition being tested. This would simulate the situation where the hydrogel shrinks while being attached to axons. Instead of letting the gel shrink we covalently bonded the gels to glass slides and moved them at rates corresponding to the composition's shrinkage rates using the microstepper motor.

5.2.5. **Design of the device**: The axonal stretch device was designed to be a self contained mini incubator. To maintain sterility and superior heat conductivity, the chamber in the device was entirely made out of stainless steel. UV sterelization was chosen to be the best mode to ensure sterelity. This made it imperative to select all the non-metallic components to be resistant to UV degradation. All the raw materials were sourced from McMaster Carr unless stated otherwise. The range of lateral speeds we anticipated for our experiments ranged from 40 µm/hr to just over 100 µm/hr.The candidates to produce such slow motions were piezo electric stages and microstepper motors. The piezo based stage was a custom order design while the microstepper motor was available off the shelf. After comparing the range of motors and controllers available, we selected CRK543AKP-PS25 Microstep Stepper Motor System with Built-in Controller (Stored Program) (24 VDC) manufactured by Oriental Motors Corp. This stepper motor when orperated in microstepper

configuration could produce a linear diaplacement of 1 μm at sufficiently high torque. The motor came with its own controller and a sophisticated graphical user interface (GUI) that permitted need based custom programming of the motor movement. Figure 5.1 shows the GUI.
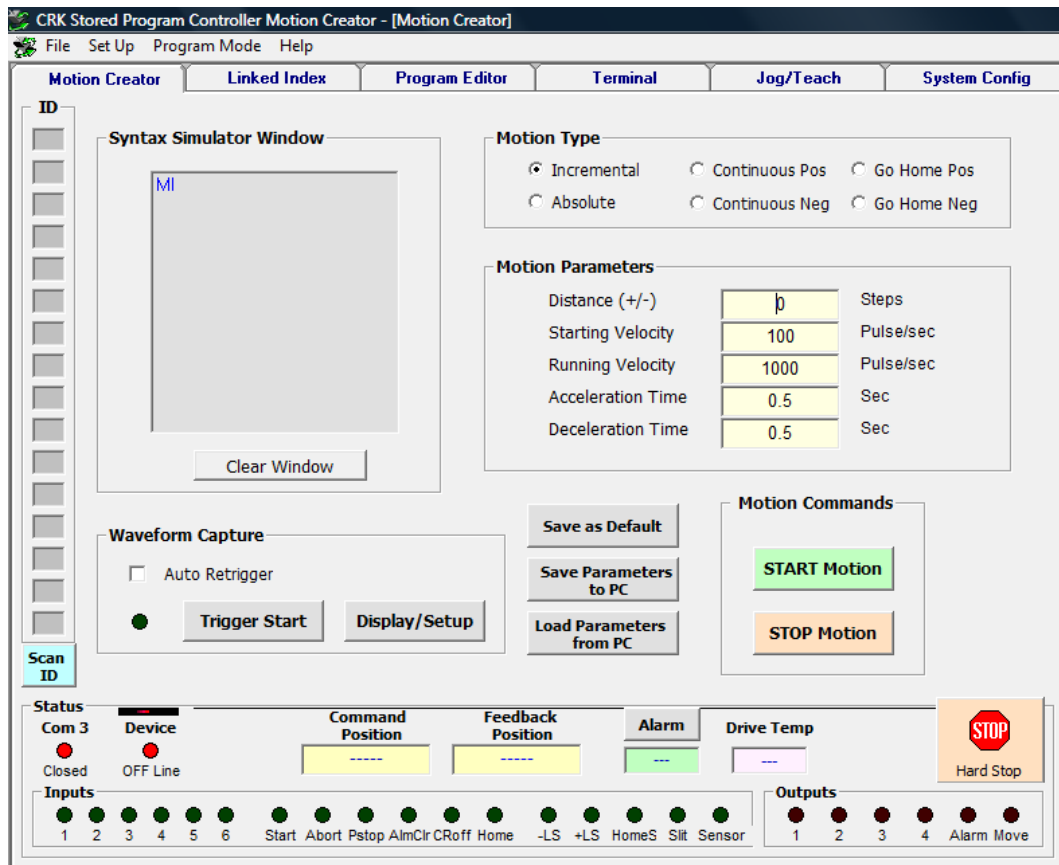
Fig. 5.1. Screen shot of the GUI provided by Oriental Motor Corp. for controlling the steppermotor. The program editor option allows writing custom codes to control the motor movement.

To translate the rotational motion of the motor to linear displacement, we designed and custom ordered a drive chain system from Applied Industrial Tech. The hurdle faced with microstepper motors driving any conveyer belt assembly is that of backlash which is the rotation that the motor shaft undergoes before actually causing motion in the drive belt. The CRK543AKP-PS25 series motor has a very low

147

backlash of 15 arc minutes or 1/21600 of a full shaft rotation. Moreover the tension on the custom ordered berg drive chain belt was adjustable so that there was no lag between the transfer of motion from the motor to the drive chain. The next major component of the motion system was the lead screw. The mobile stage that would bear the hydrogel slide was mounted on the lead screws that were connected to the drive chain assembly. To ensure a smooth motion we used two lead screws. Figure 5.2 shows images of the axonal stretching device. For details of the device schematics please refer the appendix. The input parameters necessary to bring about the motor movement were the motor speed, the acceleration and deceleration duration, and the linear displacement magnitude. These parameters were calculated using the following steps.

Move distance revolutions in Rev = Move distance / (Diameter * 3.14)

Operating Pulses (DIS) = Revs * (pulses/rev)

Pulse speed = Operating pulses / (positioning time – Acceleration time)

TA = Acceleration time

TD = Deceleration time

For micro-stepping function, the maximum gear ratio of 25:1 was selected along with the option of "High Res" in the system configuration tab of the GUI.
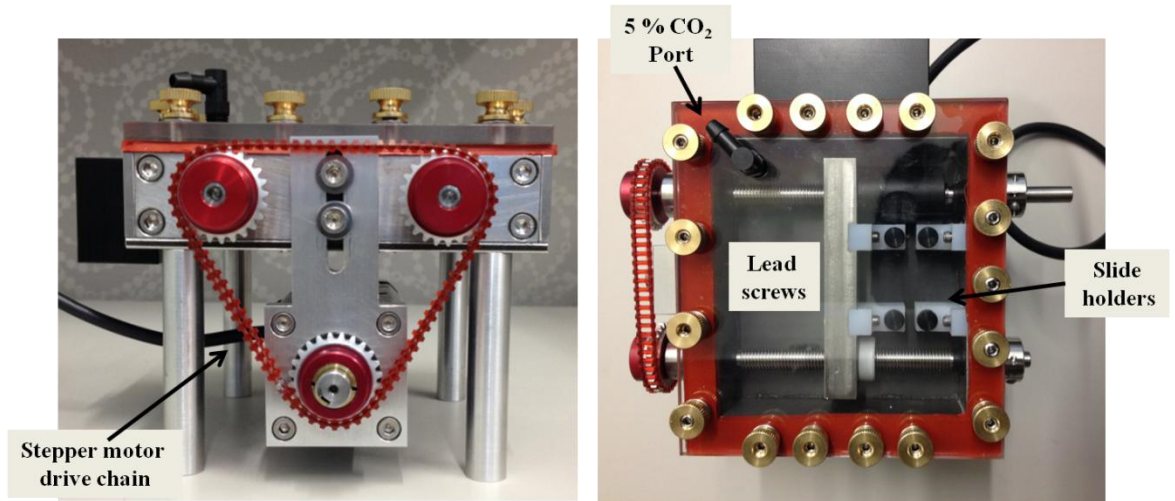
Fig. 5.2. Side view and top view of the axonal stretching device. The twin lead screws are turned using a micro-stepper motor. The device is maintained at 37°C with a port to provide constant flow of 5% CO_2.

The device mandated self-contained incubator condition with precise control over the temperature and CO_2 level. The device was maintained at 37 °C using a heater, two feedback K type thermocouples, and a Model ETR-9090 Microprocessor based SMARTER LOGIC Auto Tune PID Controller. The PID controller has an in-built calibration mode which heats up the target at different rates and constantly compares the desired versus actual temperature detected by the sensors. Thus it determines the ideal rate at which the device can be heated and maintained at the desired temperature. The auto calibration was verified using a mercury thermometer. It was made certain that the temperature at the center and the boundaries of the chamber was at 37°C. A constant stream of 5 % CO_2 was also supplied via the port on the plexiglass lid. The CO_2 was bubbled at a constant speed of two bubbles per second.

5.2.6. **Axonal stretch trials**: Glass slides were scored and cracked into two pieces using a diamond tipped scoring tool. If this process is done correctly the interface of the cracked slides will align perfectly leaving a negligible gap. SEM analysis of the interface was performed to quantify the gap. On one half of the slide, Polyethyleneimine (PEI) was microcontact printed and primary neurons were cultured on the pattern such that bundles of axons were growing towards the interface. The silicone stamp had a pattern consisting of rectangular 10 µm ridges and 5 µm deep grooves. The neurites reached the edge of the slide by day four or five after seeding. The neuronal slides to be used for the experiment were picked on day 6 after the second media change and the corresponding slide of the pair was activated and the hydrogel was crosslinked on it. The second half of the slide, that would bear the hydrogel, was treated with 3-aminoproyltrimethoxysilane to create a self-assembled mono layer (SAM) bearing double bonds. These end groups were covalently crosslinked with the hydrogel during the UV exposure. The activation of the slide was performed using the method described by Wang and co workers (13) (See appendix). The pre-crosslinking solution was pipetted on to the slide and a coverglass was placed on top to reduce exposure to air and minimize oxygen inhibition of the free radicals. The coverglass was treated with surfasil siliconizing fluid which made the surface extremely hydrophobic. This assisted in peeling the top coverslip after the gel was successfully crosslinked. The two slides were firmly mounted in the holders and the interface was aligned by manually turning the lead screws. The steppermotor was operated in the micro-stepper mode and was moved in linear steps of 3.5 µm followed by a pause. By changing the duration of the pause,

effective linear displacement rates ranging from 42 µm/hr to 100 µm/hr could be achieved. Fig 5.3 shows the motion profiles of the different linear displacement rates that the micromotor can produce by incorporation of a pause period between consecutive motor activation signals.
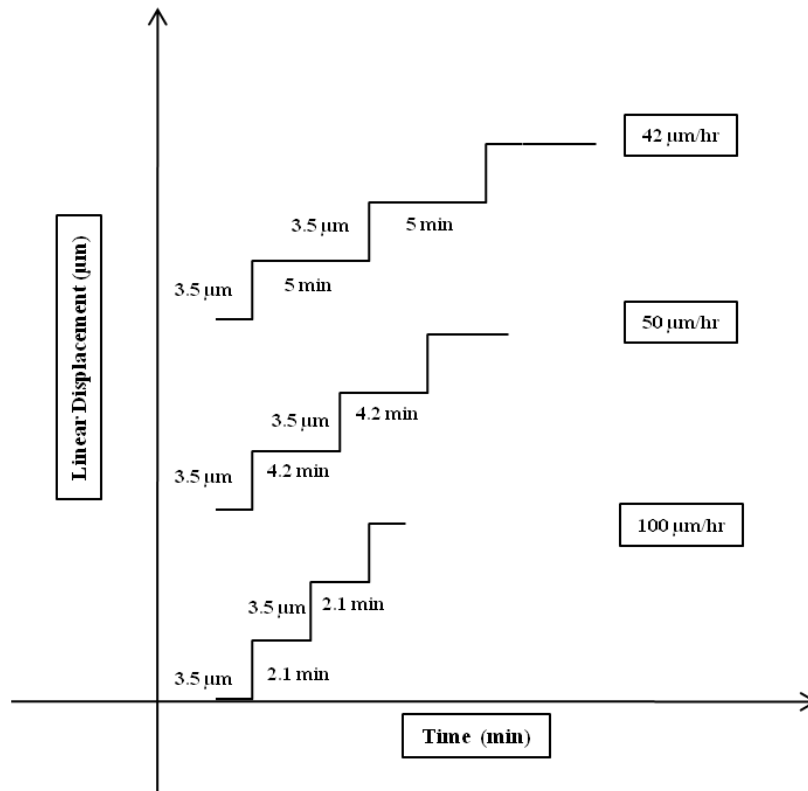
Fig. 5.3. Graph showing how different stretching rates could be produced by the microsteppermotor. The y axis is shifted for the purpose of clarity. By varying the duration of the pause a variety of stretching rates can be achieved.

We tested various conditions to attempt simulated axonal stretching using the hydrogel. Condition 1 consisted of the neuron slide and the hydrogel slide aligned such that the axonal ends have an opportunity to interact with the hydrogel on the same plane. After a 24 hour interaction period, the slide bearing the hydrogel was slowly moved away using the microstepper motor at 42 µm/hr corresponding to the

shrinkage rate for the hydrogel composition being tested. In condition 2 the hydrogel was coated with 10 µg/ml laminin to attract the neurites to cross the interface and attach to the hydrogel. For condition 3, the hydrogel was fabricated with an additonal free floating flap that was placed across the interface directly on the neuronal ends. The hydrogel was coated with 10 µg/ml laminin in this case as well. The neurites at the interface were allowed to interact with the hydrogel for 24 hours before the motor was activated to move at 42 µm/hr for 24 hours. Finally, for condition 4 modifications were made to the slide holders in the device. The slide with the cells was flipped over and placed just at the egde but right on top of the slide with the hydrogel. Thus the hydrogel and the neurites were sandwiched between two glass slides. Once again the cells were given 24 hours to interact with the hydrogel before the motor was moved. The hydrogel composition was 60 mg/ml HAGMa crosslinked with 4:1 PEGDa. We selected the hydrogel composition that showed the best neuronal cell attachment results. Once the experiment was stopped after a total 48 hours, the interface was oberved under a stereomicroscope and an inverted microscope to study the interface.

5.3. Results

5.3.1. Effect of hyaluronidase on primary cortical neurons: Primary neurons were exposed to 10 µg/ml of hyaluronidase for a period of 48 hours. The enzyme was replenished every 4 hours. Figure 5.4 shows the optical micrographs for a control well that was not exposed to any enzyme. The cells demonstrated typical morphologies as seen with primary neurons in high density environments on TCPS substrates. It has been observed that when the density of neurons is not sufficient

these cells tend to form clusters. The density of cells was more than sufficient to avoid cluster formation. On comparing images of cells from wells exposed to hyaluronidase (Figure 5.5) to the controls it was evident that there was no observable difference in the appearance of primary neurons due to the presence of the enzyme.
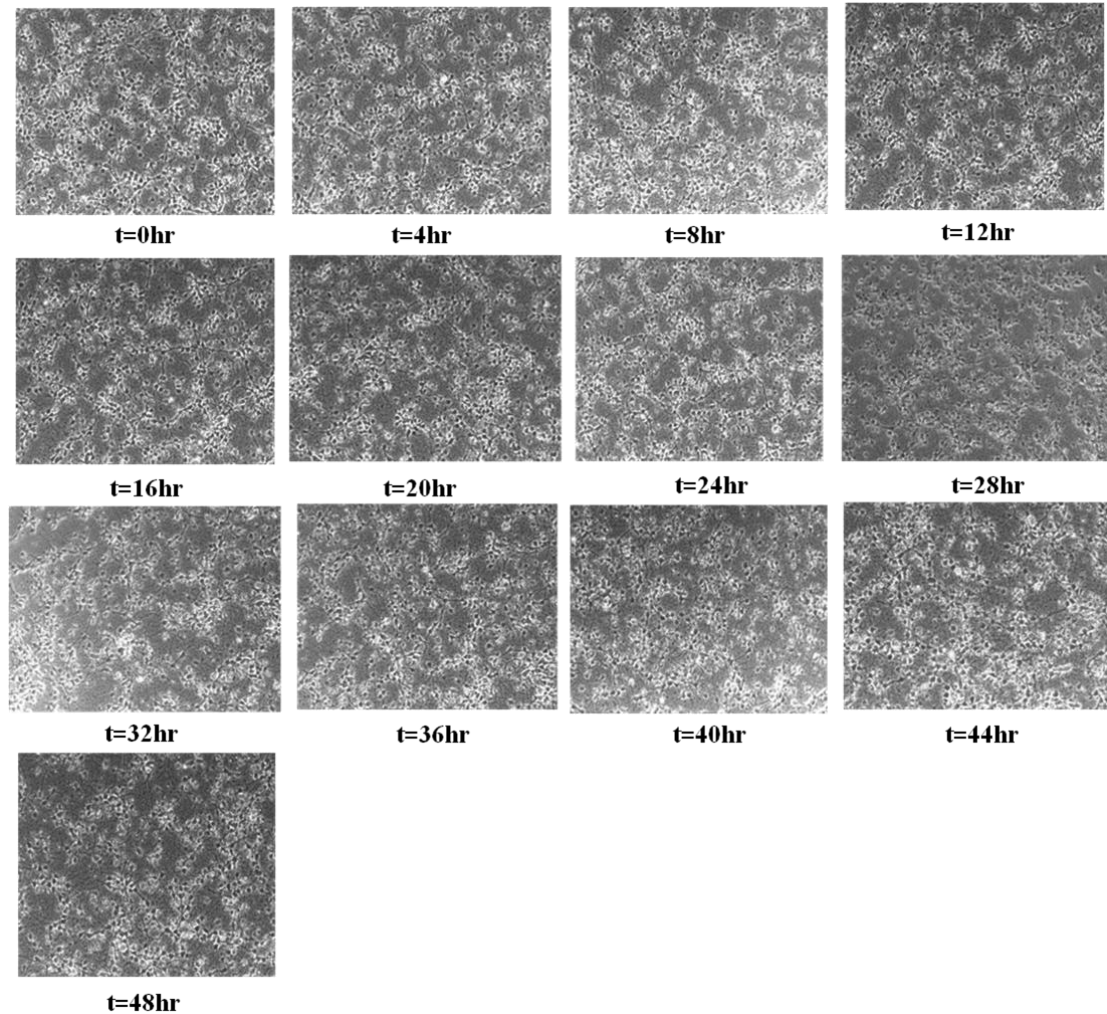
Fig.5.4. Representative optical micrographs of primary cortical neurons seeded in a PEI coated TCPS well that was not exposed to 10 μg/ml hyaluronidase. The images of the center of the well were captured every 4 hours for a period of 2 days. There was no visual difference in the morphology of the cells between the time points which was the expected outcome for these control wells. (n = 3)
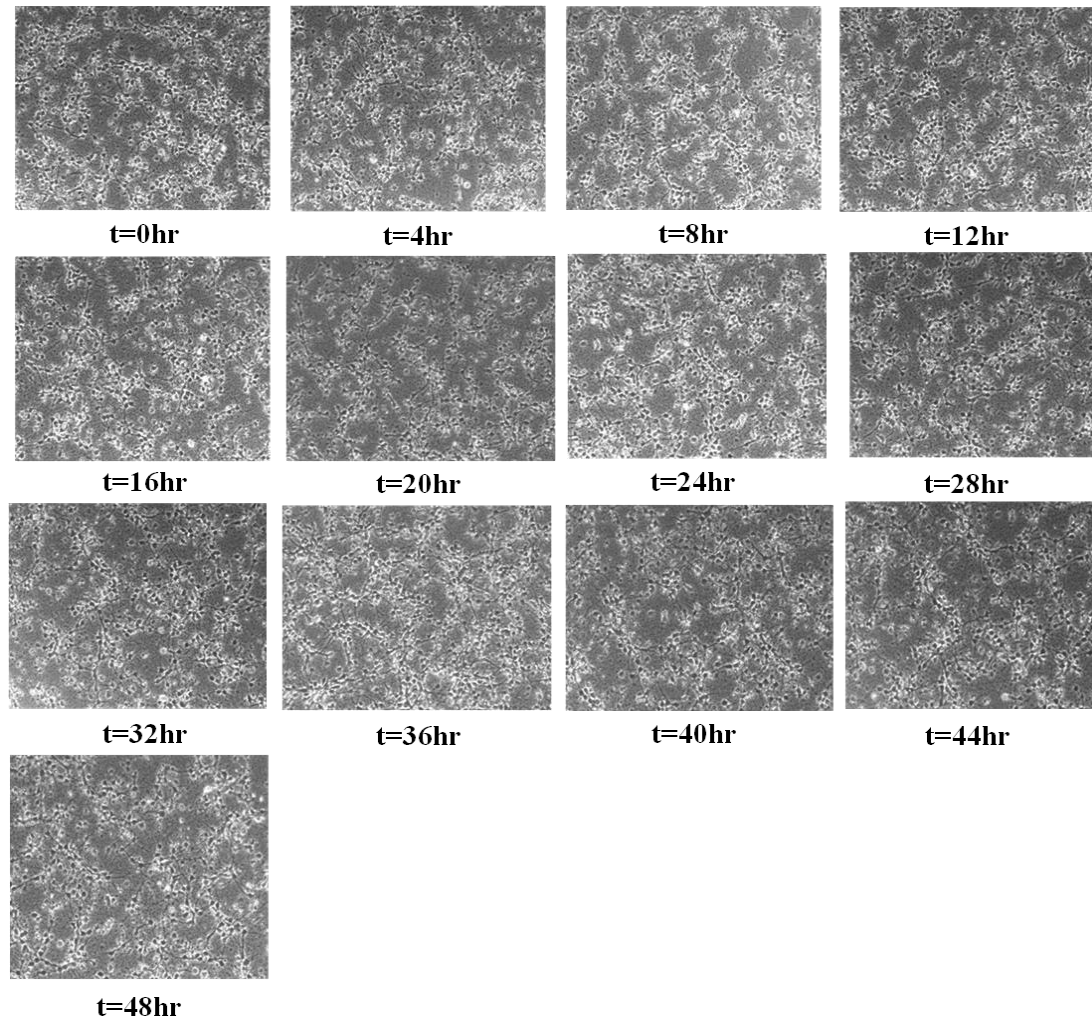
Fig.5.5. Representative optical micrographs of primary cortical neurons seeded in PEI coated TCPS well that was exposed to 10 µg/ml hyaluronidase. The images of the center of the well were captured every 4 hours for a period of 2 days. The enzyme was replenished every 4 hours as well. There was no observable difference in the morphology of the cells between time points. This indicated that the tested concentration of hyaluronidase did not have any effect on the primary neurons. (n = 3)

5.3.2. **Live- Dead assay of the HAGMa hydrogels:** Fibroblasts were seeded on the crosslinked hydrogels for a period of 24 hours following which a live-dead assay was performed. Figure 5.6 shows the fluorescent micrographs for the hydrogels of the compositions 60 mg/ml HAGMa crosslinked with 3:1 and 4:1 ratio of PEGDa

along with control TCPS wells. The number of cells that remained adhered to the hydrogels compared to TCPS controls were low. The hydrated state of the hydrogels may have hampered the attachment of some cells causing them to flow off the surface when fresh media was first introduced into the wells. However over 82% of the cells that adhered to the surface were viable. The fibroblasts demonstrated their typical morphology. There was no significant difference ($p \gg 0.05$) in the percent viability between the PEGDa crosslinked samples when compared to TCPS controls.

Figure 5.7 shows the fluorescent micrographs of the representative samples for the PEGPLADa crosslinked HAGMA samples. Similar to tht PEGDa samples, we observed fewer cells compared to TCPS wells however there was no significant difference in the viability of fibroblasts that were seeded on the hydrogels when compared to the TCPS controls. The cell viability results are summarized in Figure 5.8. The results indicated that the crosslinked hydrogels maintained cytocompatibility although the cell density was reduced compared to TCPS control surface.

Fig.5.6. Representative fluorescent optical micrographs of the TCPS control wells, and the PEGDa crosslinked hydrogels following the live-dead assay. Green indicates live cells while red indicates dead cells. The MC-3T3 fibroblasts demonstrated a high percentage of viability and the morphology of the cell was typical of this cell line. There was no significant difference in the cell viability between the hydrogel samples and the TCPS control surface (p >> 0.05). (n = 6)
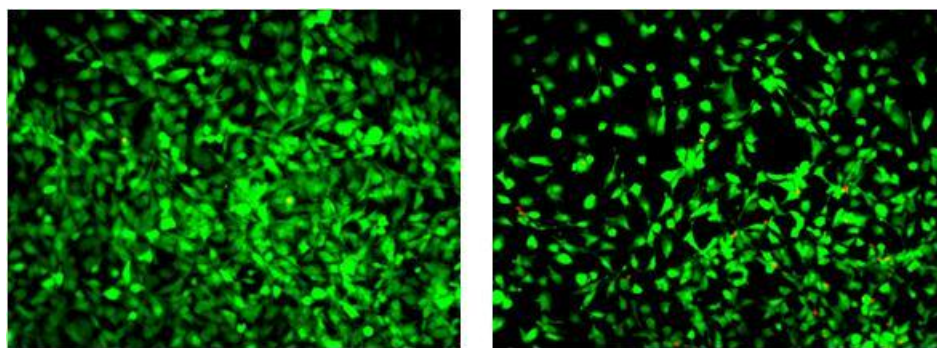
Polystyrene control wells
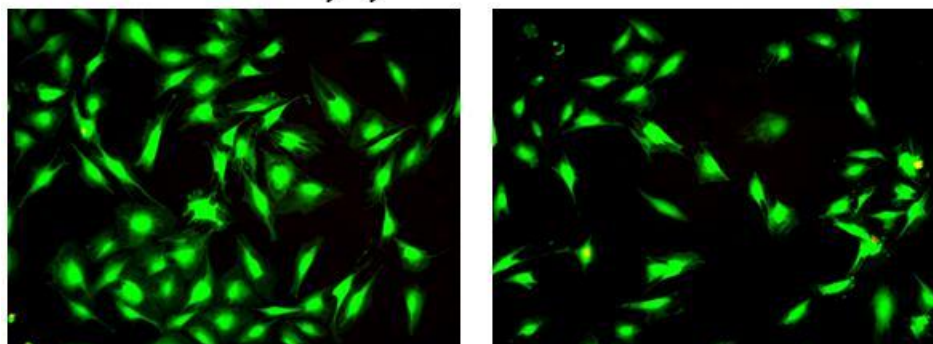
60mg/ml HAGMa crosslinked with 1:1 PEGPLADa
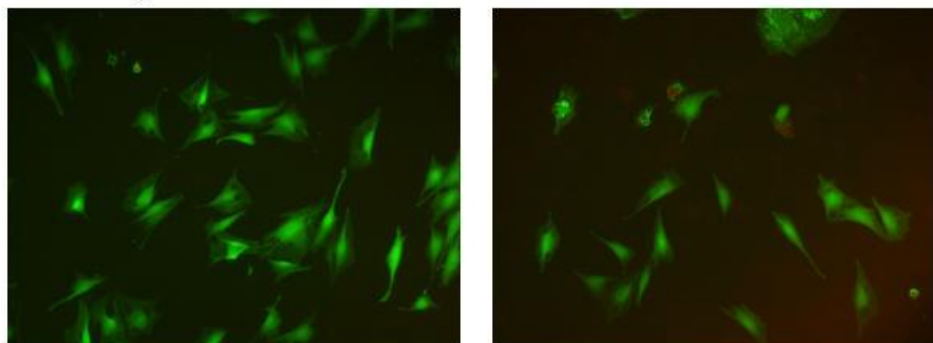
70mg/ml HAGMa crosslinked with 1:1 PEGPLADa

Fig.5.7. Representative fluorescent optical micrographs of the TCPS control well and the PEGPLADa crosslinked hydrogels following the live-dead assay. Green indicates live cells while red indicates dead cells. The MC-3T3 fibroblasts demonstrated a high percentage of viability and the morphology of the cell was typical of this cell line. There was no significant difference in the cell viability between the hydrogel samples and the TCPS control surface ($p \gg 0.05$). (n = 6)
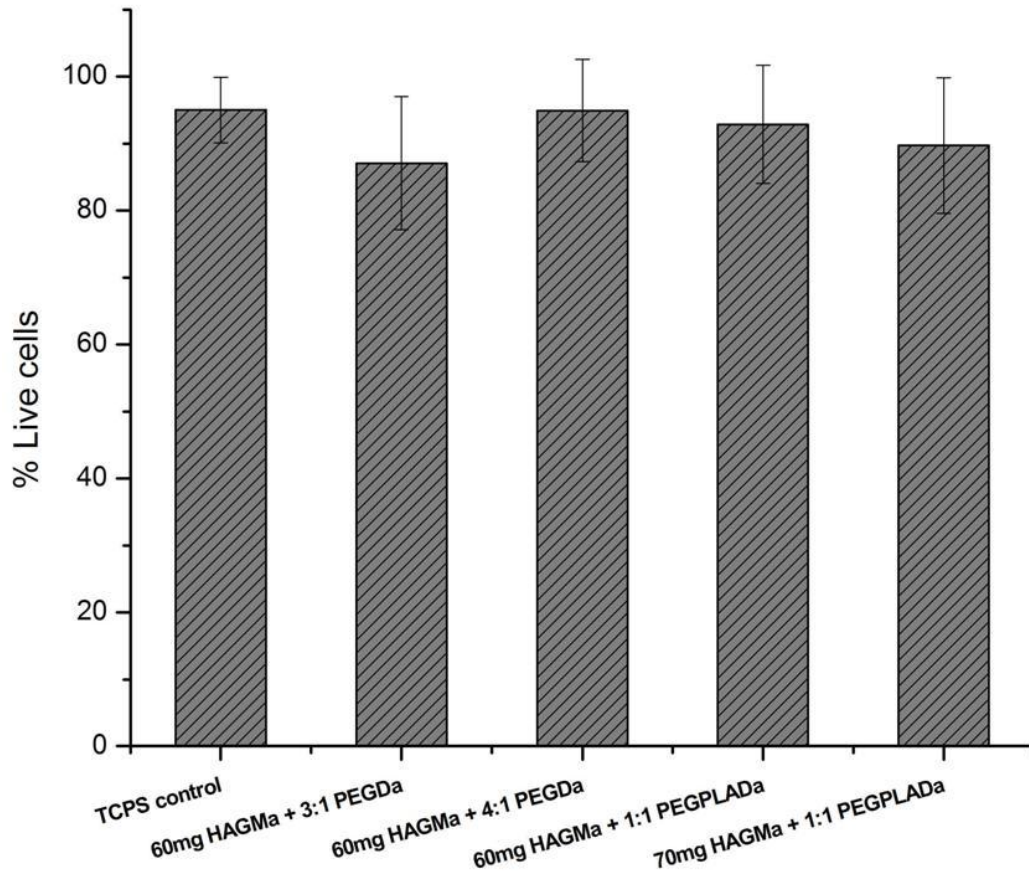
Fig.5.8. Summary of the results for the cell viability experiment conducted on the crosslinked HAGMa hydrogels. There was no significant difference in the percentage of live cells when the controls were compared with each of the tested compositions. (n = 6)

5.3.3. **Cytocomaptibility study with primary neurons :** The cytocompatibility study performed using the MC-3T3 fibroblasts showed very promising results. The crosslinked hydrogels were cytocompatible and fibroblasts were still able to attach to the gels. The next step was to observe how neuronal cells behave on the hydrogel surface. Figure 5.9 (a) shows representative images of neurons on PEI coated TCPS surfaces. These were the control wells. The cells formed dense interconnected networks. The interconnecting neurites were relatively short due to the high density

158

of neurons in the well. Figures 5.9 (b) and 5.9 (c) show micrographs of neurons seeded on hydrogels of the composition 60 mg/ml HAGMa crosslinked with 3:1 and 4:1 ratio of PEGDa respectively. We observed that the cell bodies were forming clusters and then sprouting neurites in all directions akin to a dorsal root ganglion. By day 4 many of these neurites made contact with neighbouring clusters or neurites and formed thriving inter-connecting networks. Figures 5.10 (a) and 5.10 (b) show images of hydrogel samples of the composition 60 mg/ml HAGMa crosslinked with 1:1 PEGPLADa and 70 mg/ml HAGMa crosslinked with 1:1 PEGPLADa. Once again we saw the cell bodies forming clusters and sprouting long neurites which resulted in interconnected networks. The PEGPLADa crosslined hydrogels were slightly more opaque compared to PEGDa crosslinked hydrogels. Hence we treated some samples with the LIVE dye stain calcein to be able to observe the neuronal cells using the inverted microscope. It is in the nature of primary cortical neurons to form interconnected networks. In the absence of a sufficient density of neurons in the near vicinity, these cells have been known to form sattelite clusters and produce long neurites which explore the surroundings. Our observations fall in line with the understanding of this primary cell line.
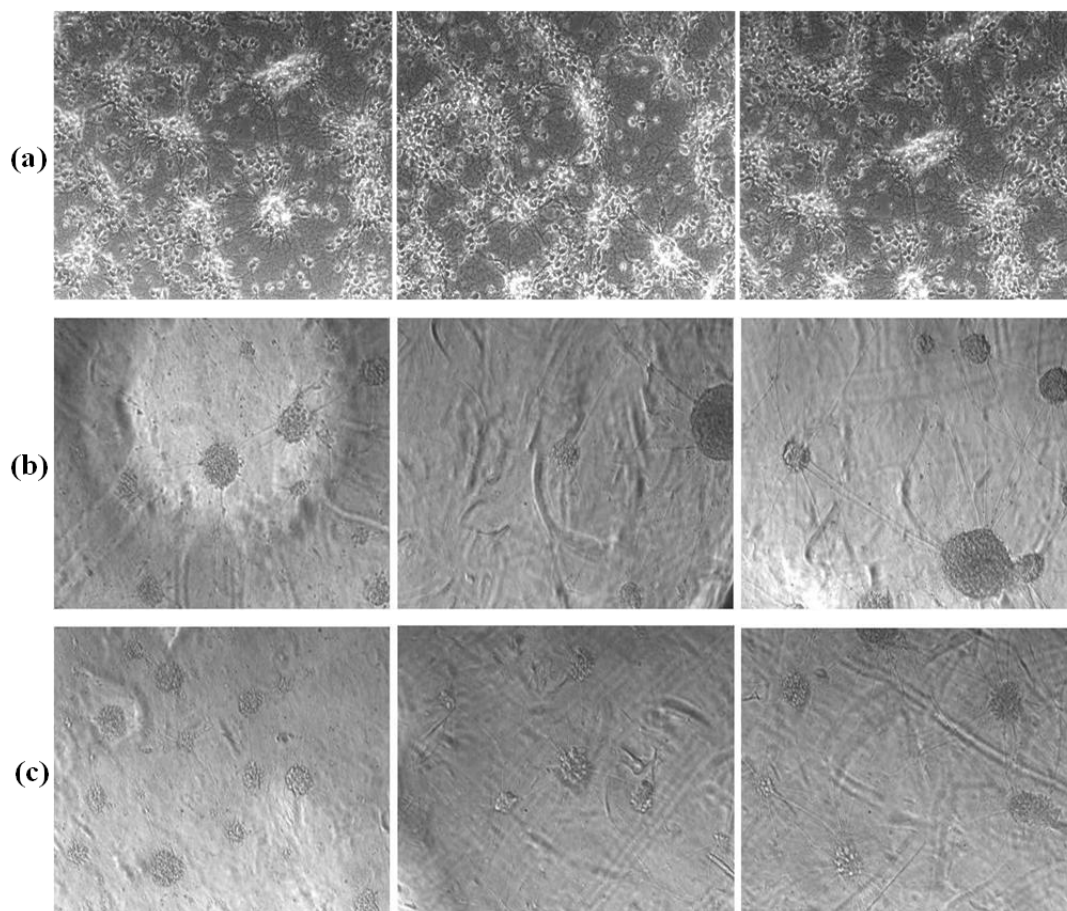
Fig. 5.9. Representative optical micrographs of primary cortical neurons on (a) PEI coated TCPS, (b) on gel composition 60 mg/ml HAGMa crosslinked with 3:1 PEGDa, and (c) on gel composition 60 mg/ml HAGMa crosslinked with 4:1 PEGDa captured on day 6 post seeding. The density was 0.4 million cells/well. The neurons form dense networks on the TCPS surface due to close proximity with other neuronal cells, while on the hydrogel surface they form sparse inter-connected cluster networks due to absence of close proximity with other neuronal cells. Magnification is 10X.
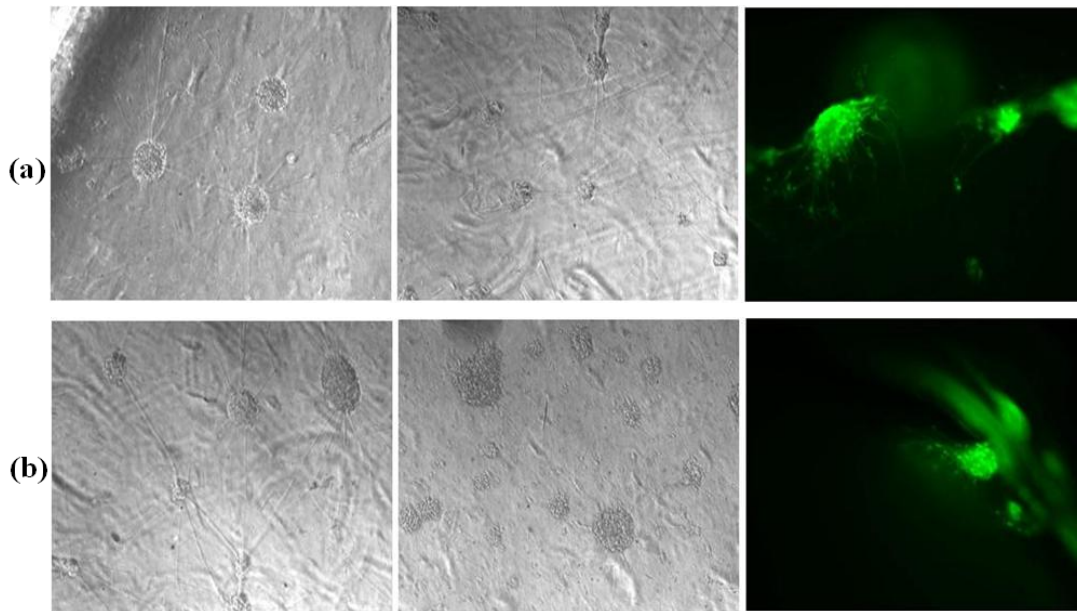
Fig.5.10. Representative micrographs of primary cortical neurons on (a) gel composition 60 mg/ml HAGMa crosslinked with 1:1 PEGPLADa, and (b) on gel composition 70 mg/ml HAGMa crosslinked with 1:1 PEGPLADa captured on day 6 post seeding. The density was 0.4 million cells/well. The neurons formed sparse inter-connected cluster networks similar to those seen for the PEGDa crosslinked hydrogels due to low density of the adhered cells. Magnification is 10X.

5.3.4. **Axonal stretch device:** The custom-built device provided us a way to test the ability of these novel HA networks to facilitate axonal stretch. The device consists of a twin lead screw driven slide holder which is moved using a microsstepper motor. The temperature for the device is maintained using a feedback loop between the heater element and two thermocouples. The PID controller has a self calibrate mode which was used to calibrate the temperature within the chamber. The temperature control was verified using a mercury thermometer. There was a discrepancy with the actual temperature and what the PID display read. Adjustments were made to make sure the temperature within the device is always maintained at 37 °C. The 5% CO_2 was pumped into the device at a rate of two bubbles/second.

Figure 5.11 shows the SEM micrographs of the interface created by score cracking microscope glass slides. Scoring and cracking dislodges material from the slide which may create some imperfections at the interface. Hence we decided to use the reverse side of the glass slide and imaged it to measure the gap distance. Based on the measurements from Image J we observed an average gap distance of 6.7 ± 1.1 µm. This might still seem like a valley for the neurite that approaches the interface, however the presence of a swollen gel might be sufficient to close this small gap. Slide pairs were imaged using the Hirox microscope before being selected for the stretch device experiment. Primary cortical neurons were seeded close to the edge on the slide bearing the PEI micropattern. Figure 5.12 shows representative images of the neurites growing towards the edge of one of such sample slides. The neurites extended from the cell bodies and aligned to the PEI pattern. We observed that on ocassion the neurites at the edge would interconnect with each other to form what looked like a thick branch running perpendicular to the protein pattern. However there were always multiple neurites that were at the edge.The composition of hydrogel tested was 60 mg/ml HAGMa crosslinked using 4:1 PEGDa. The shrinkage rate for this composition for the first day was 42 µm/hr. To obtain this lateral movement, the micromotor was triggered repeatedly such that it turned on for 1 second to cause a 3.5 µm lateral movement followed by a 5 minute pause.
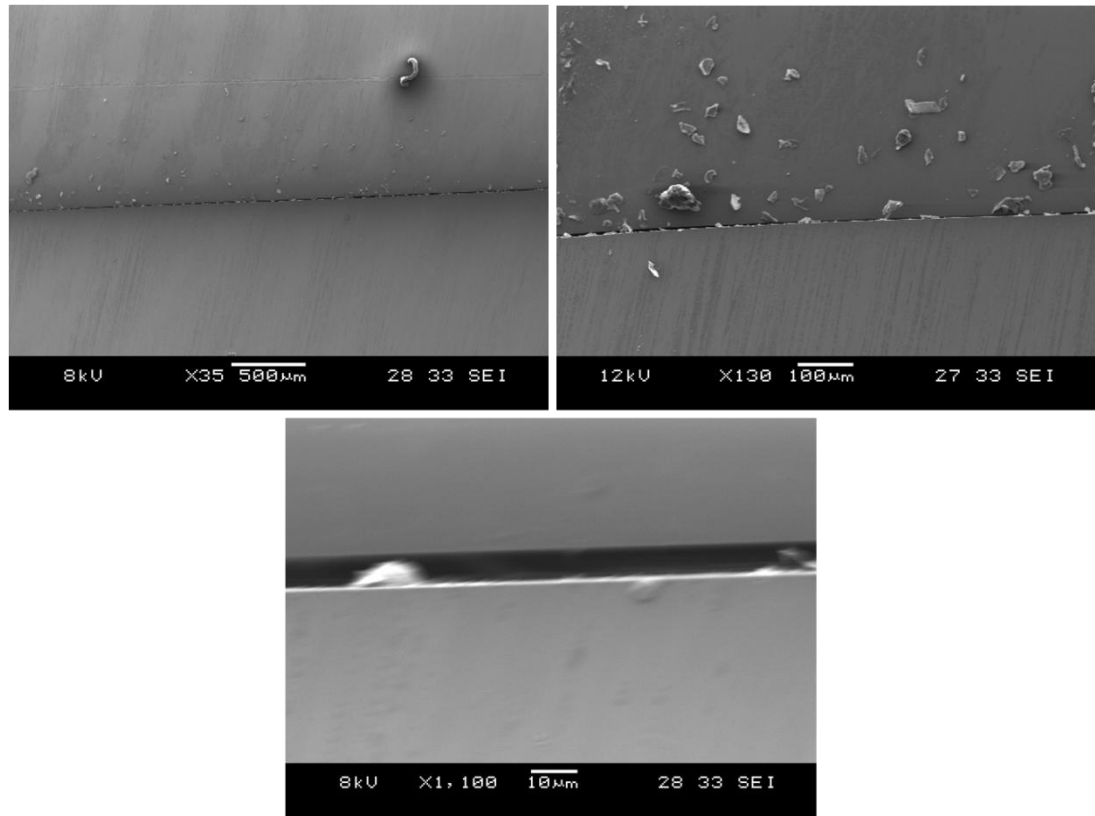
Fig. 5.11. Representative SEM micrographs of the score cracked glass slide interface. The images show the interface is increasing magnification. The gap at the interface was 6.7 ± 1.1 µm.
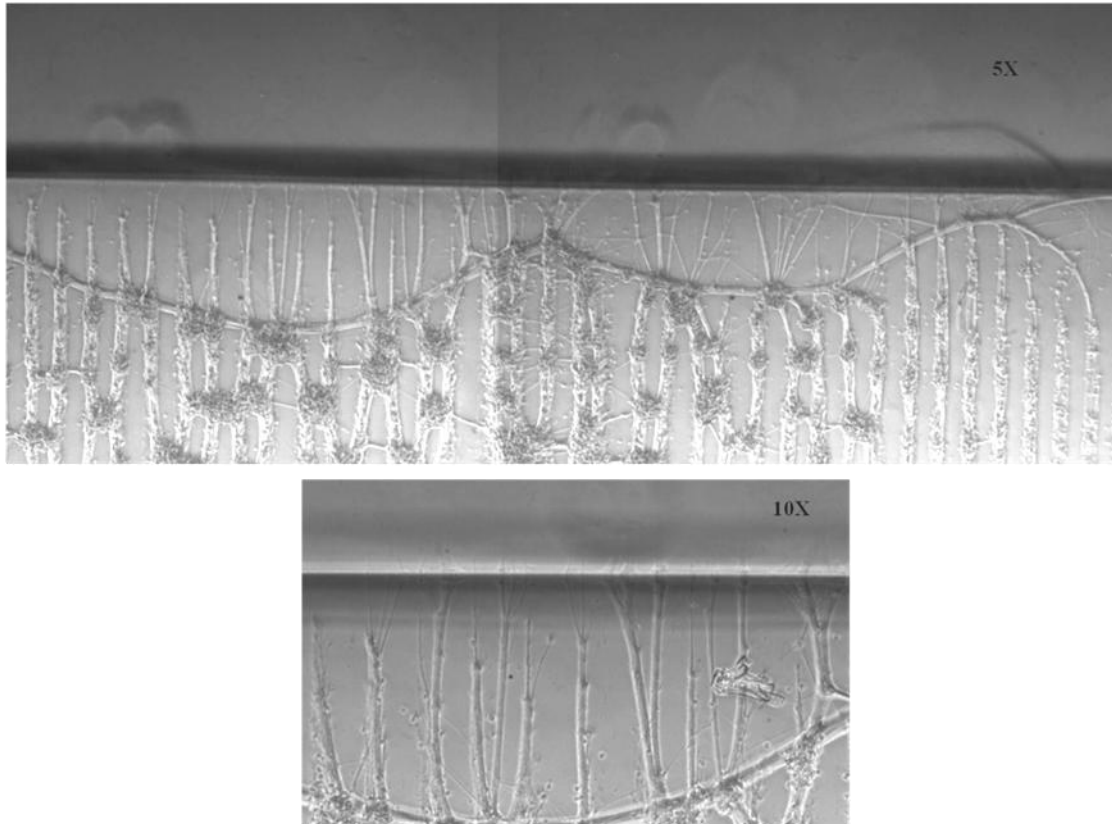
Fig. 5.12. Representative optical micrographs showing the edge of the microcontact printed PEI glass slide at two different magnifications. The primary neurons sprouted neurites that aligned to the PEI pattern. We did observe some neurites interconnecting just near the edge forming a long branch. Despite this there were neurites that reached the edge of the slide.

The main difference between the condition 1 and condition 2 test was the treatment of the hydrogel with 10 µg/ml laminin. Each condition was repeated twice to confirm the observations. The results from either conditions were similar. Figure 5.13 shows stereo micrograph images of the cell-gel interface following an experiment testing condition 2. The interface was only separated at the rate of 42 µm/hr after a 24 hour period of contact. For either condions (1 & 2) we did not observe any neurites spanning the interface. The hydrogels did not show any evidence of neurite attachment either in the form of snapped neurites or deformed hydrogel surface near the interface.

Figure 5.14 shows micrographs of the slide bearing the neurons after one of such experiment. The visual phenotype of the neuronal cells appeared to be normal with no indication of delamination or retraction.
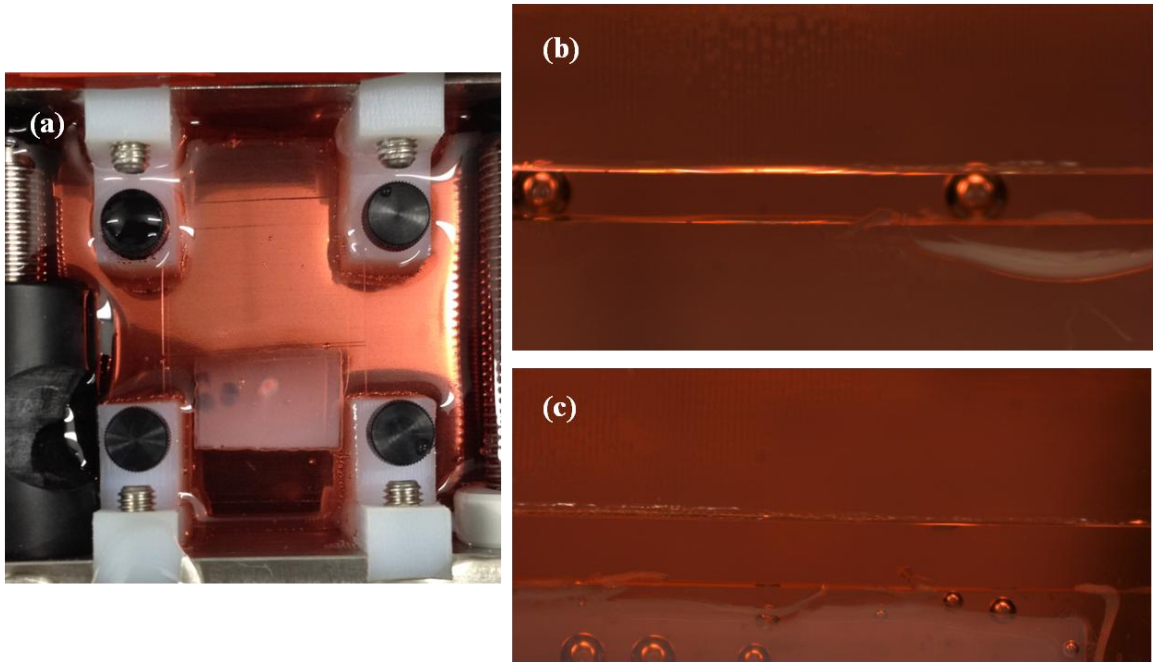
Fig. 5.13. Stereomicrographs of the gel-cell interface (a-c) after a 48 hour experiment. The neurites were allowed to interact with the gel at the interface for 24 hours before the motor was turned on and the interface was separated. The hydrogel was coated with 10 µg/ml laminin. We did not observe any indication of neurites spanning the separated interface.
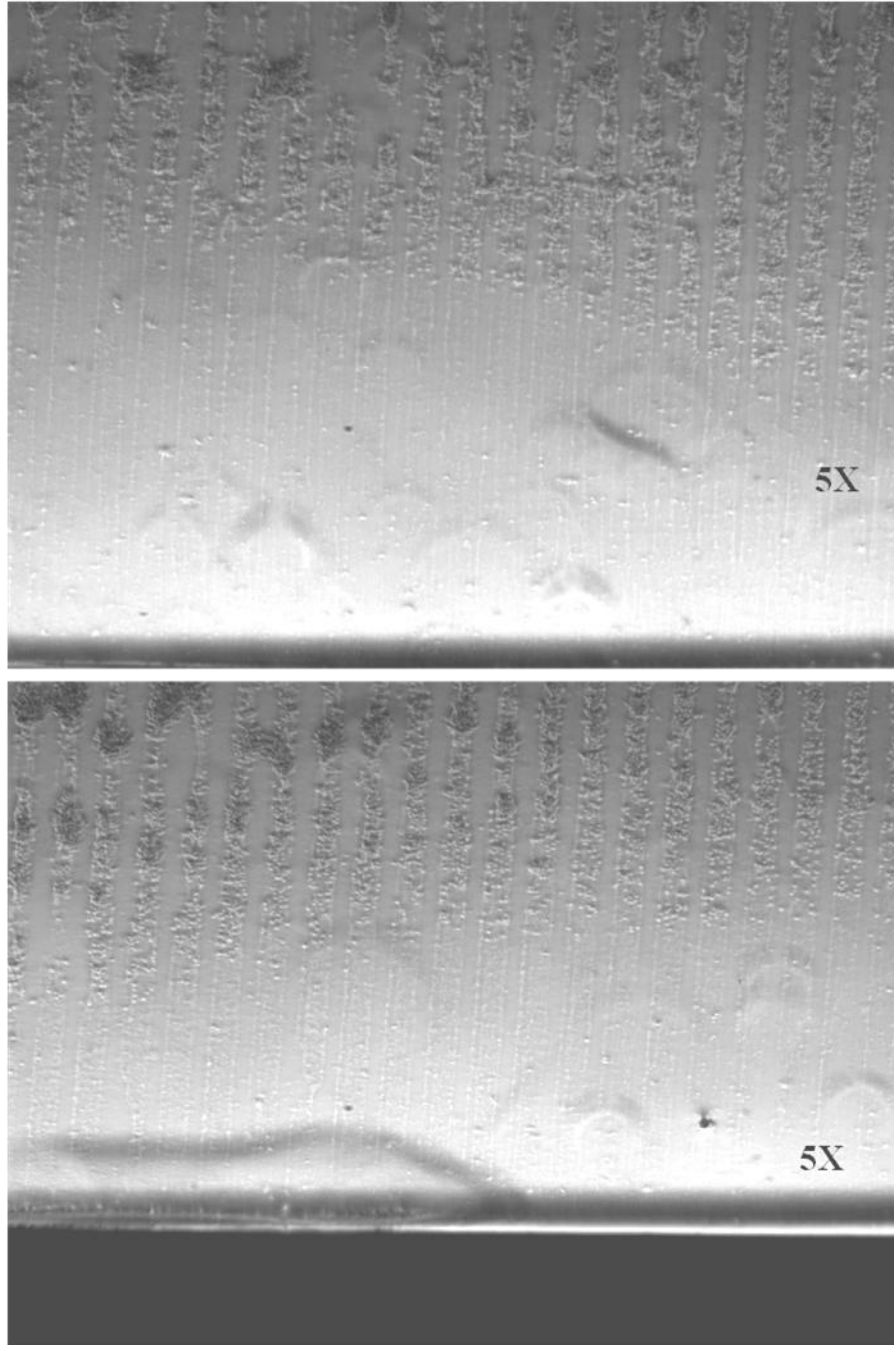
Fig.5.14. Optical micrographs showing the edge of glass slide bearing the primary neurons after a 48 hour experiment in the stretch device. The cells showed normal visual phenotype. The neurites were aligned along the PEI micropattern and did not show any delamination. The magnification was 5X.

The next variation we tested (condition 3) was having an overlapping flap of gel directly on top of the neurite ends. Figure 5.15 shows images of the actual experimental setup in the stretch device. It was a challenge to obtain an extended gel flap extending the entire expance of the gel slide. The gel and cell interface was allowed to interact for 24 hours before the interface was separated at the rate of 42 µm/hr for 24 hours. Once more we did not see any stretched neurites spanning the separated interface. The gel flap however appeared to be still attached to the slide with the neurites. However it had fractured from its connection with the remainder of the hydrogel. We also imaged the slide bearing the neurites after the experiment (Figure 5.16). We observed what appeared to be a boundary created by the gel flap on the area containing the neurites that it rested on. The failure of the gel flap made it impossible to draw any conclusions regarding ability of the gels to stretch neurites. The technical difficulty in fabricating the gel flap led us to test our final variation (condition 4).
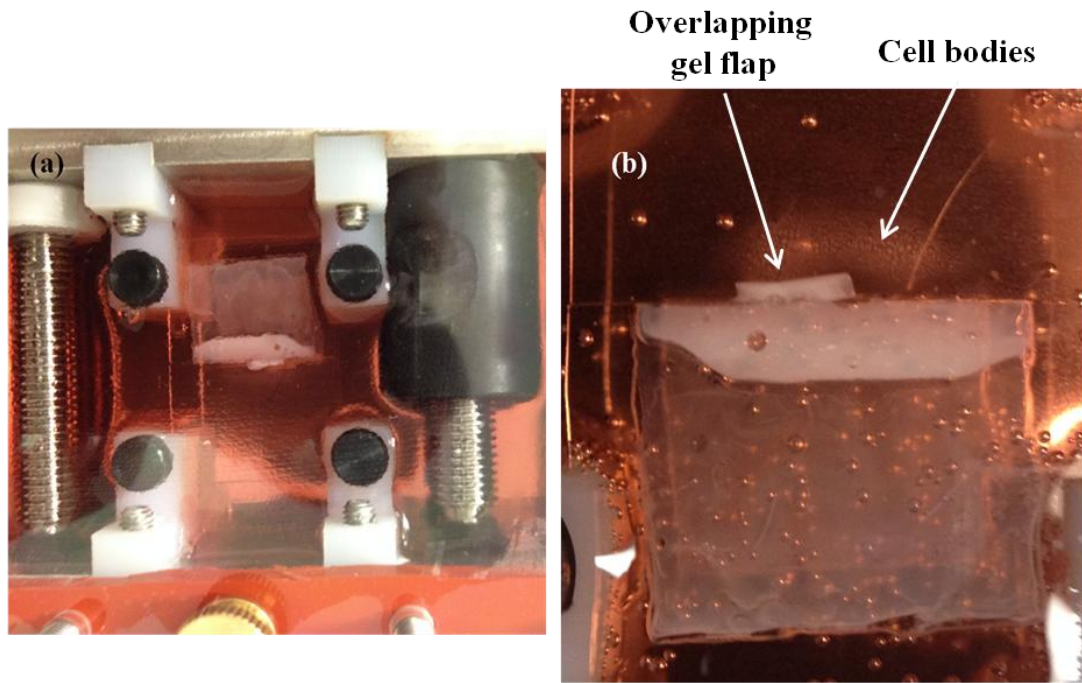
Fig 5.15. Stereomicrgraphs of the experimental setup prior to a stretch experiment for condition 3, where an extra flap of gel was placed directly over the slide bearing neurites. The opacity of the gel was a function of the thickness of the gel layer on the glass slide.
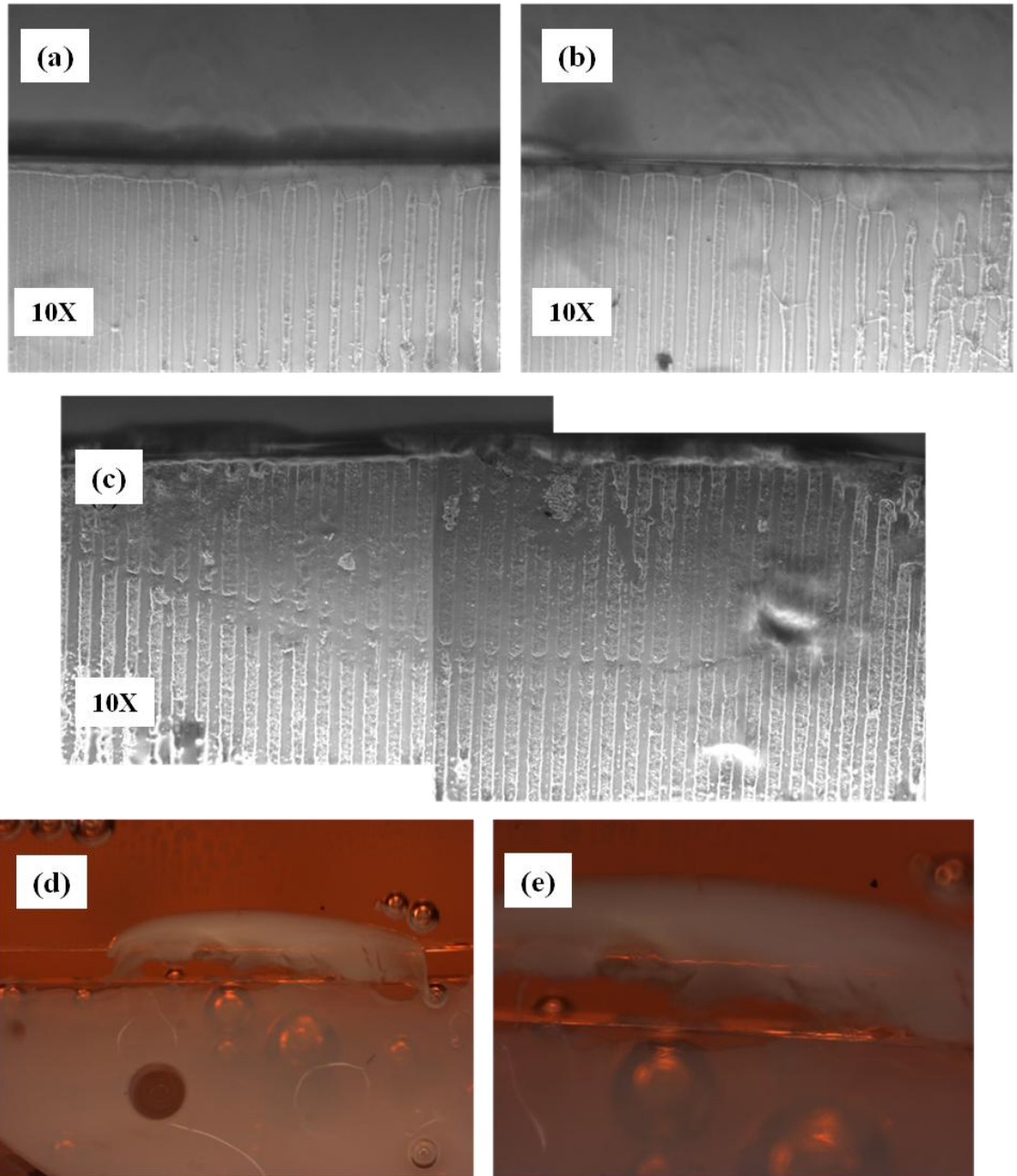
Fig. 5.16. Optical micrographs of the slide bearing neurites prior to (a, b) and post 48 hour stretch experiment (c). Stereomicrographs of the cell-gel interface (d, e) showing the overlapping gel flap. We observed a boundary that the gel flap created on the patterned neurites. The gel flap was still connected to the neurite slide when the motor was stopped, however the gel flap fractured and was pulled apart from the rest of the gel layer.

The final condition we tested (condition 4) entailed flipping of one of the slides

and creating a sandwich of the gel and neurite ends. We made changes to the holders in

the device to accomodate this configuration. Figure 5.17 shows a schematic depicting the arrangement of the glass slides. The cell-gel sandwich was motionless for 24 hours followed by microstepper motor mediated separation at the rate of 42 μm/hr lasting 24 hours. Figure 5.18 shows the actual arrangement inside the device. When the experiment was stopped we did not observe any neurites extending between the gel and the flipped cell slide. When the cell slide was imaged under the microscope we observed the absence of any neurites or cell bodies on the PEI pattern. All that was left was the PEI pattern itself. Figure 5.19 shows images from such a slide. We observed the same end result in the two trials conducted for this condition leading to the hypothesis that either the shearing motion or a lack of sufficient diffusion of nutrients through the gel may have led to cell detachment or delamination.
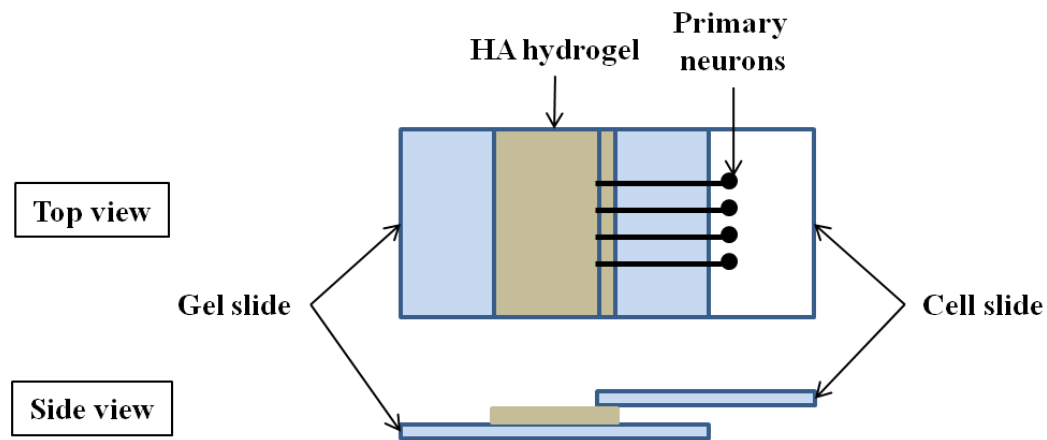
Fig. 5.17. Schematic showing the top view and the side view for the glass slide setup inside the stretch device for condition 4. The slide bearing the neurite ends was flipped and placed in direct contact with the crosslinked HA gel layer.
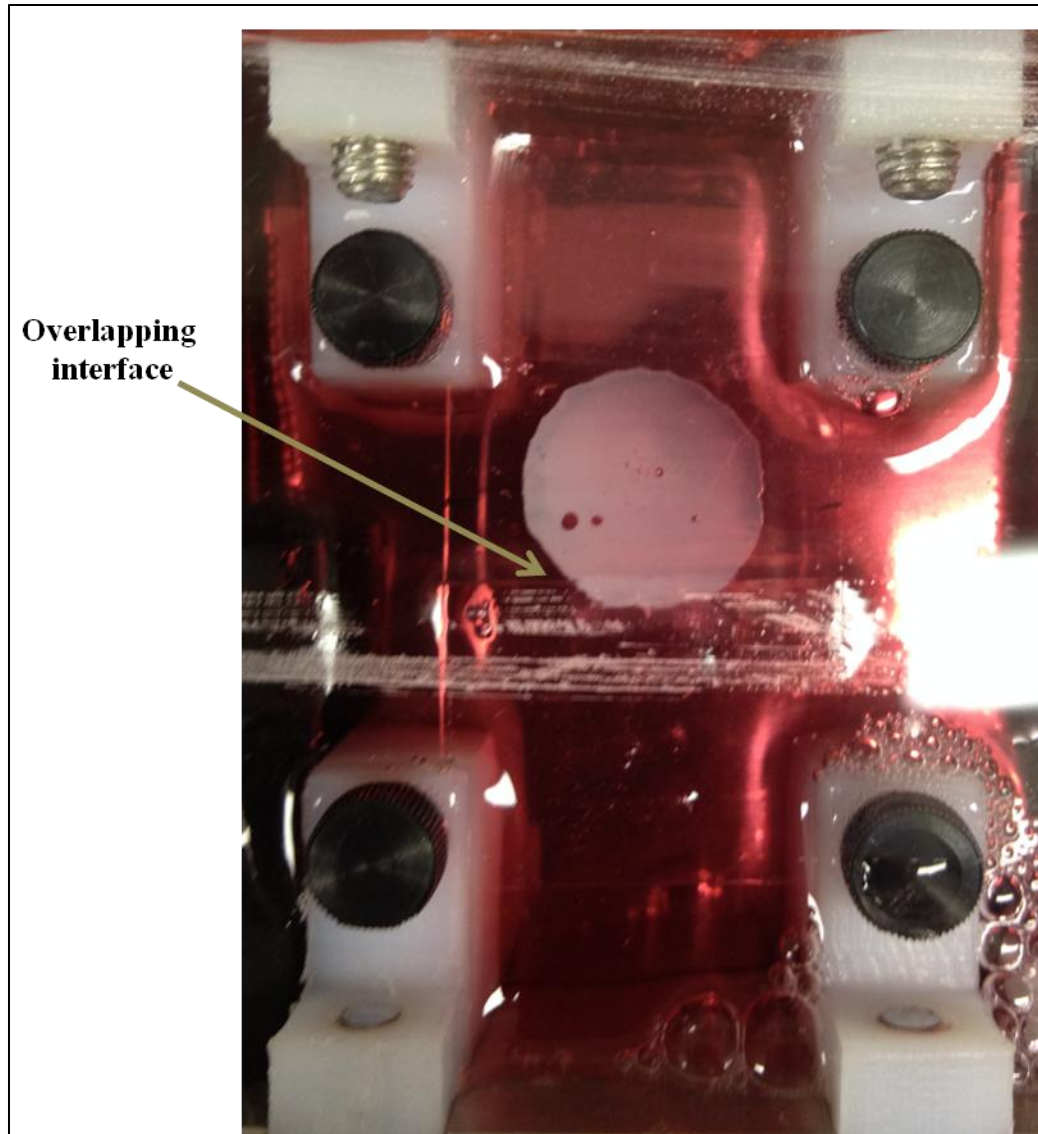
Fig. 5.18. Stereomicrograph of the cell-gel interface prior to start of the stretch device experiment showing the overlapped glass slides. The cell-gel sandwich was maintianed motionless for 24 hours before the motor was switched on to separate the interface at 42 µm/hr.
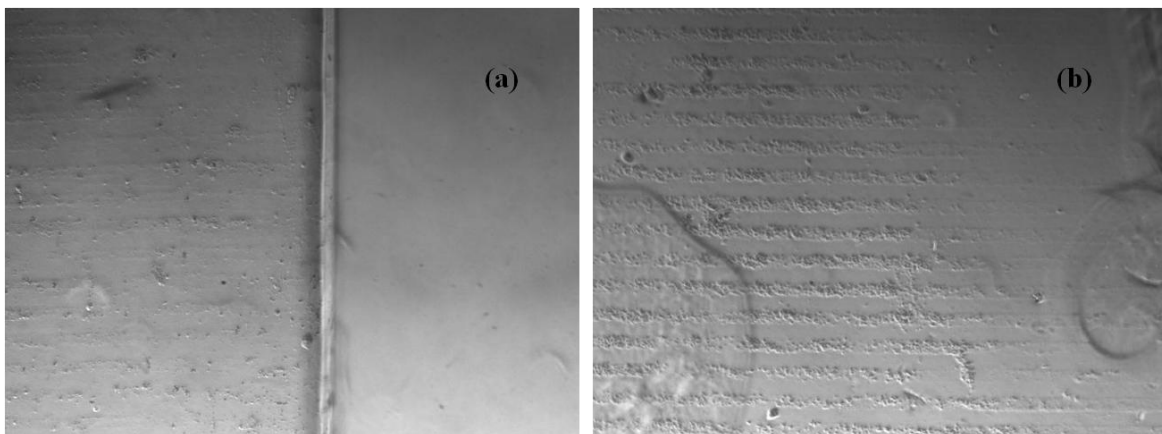
Fig.5.19. Representative optical micrographs showing the slides bearing the neurites after a 48 hour stretch experiment. After the experiment we did not see any neuronal cells still attached to the PEI pattern. The shearing motion seems to have triggered cell death which led to detachment of the cells from the slide surface.

5.4. **Discussion:** The applicability of the novel crosslinked HAGMa networks as axonal stretch growth facilitators depends on their ability to be cytocompatible. The HA molecule was derivatized to incorporate a photoreactive group that was used for crosslinking the network. Both these processess could affect the conformation of the molecule which may make it difficult for cell surface receptors to access the inherent binding sites on the HA molecule. We performed standard LIVE/DEAD assay using MC-3T3 fibroblast and also performed a cell viability study using mouse primary cortical neurons. The high percentage of fibroblast survival ($\geq$ 82%) across all compositions verified that the chemical processess performed on the HA molecule did not affect cytocompatibility of the crosslinked hydrogels. Despite these high survival numbers it is evident from the optical micrographs that the number of cells that bound to the hydrogels were fewer than the control TCPS surface. The hydrophilic nature of hydrogels makes the *in vitro* cell adhesion process challenging. Despite the care taken to make sure the gel surface was

relatively dry during the seeding process, the capillary wicking action draws more liquid to the surface. Thus there may be a layer of media in between the cells and the gel surface making binding difficult. As a consequence when the wells are flodded with media after 30 minutes of binding time, many of them float off the surface into the well. Thus we observed fewer cells on the samples when compared to the TCPS control, however a very high percentage of those cells (fibroblast) that adhered to the surface were live. The primary neurons seeded on the hydrogels showed normal morphology for this cell type on substrates and created an interconnected network between satellite clusters of neuronal cell bodies. The high concentration of hyaluronidase enzyme we used to cause shrinkage of PEGDa gel network did not affect the behavior of the primary neurons that were seeded in TCPS wells. There was no obervable difference between the control group of cell that were not exposed to the enzyme and those that were.

The results from the custom built axonal stretch device were not as we expected. The neurite ends and the hydrogel were allowed to interact on the same plane by precisely aligning the two glass slide that bore the neurons and the gel. Inspite of providing 24 hours for the neurite ends to bind to the hydrogel at the interface we did not observe any evidence of neurite attachment. This may be inferred as either the neurites did not bind at all or that the strength of binding was insufficient to withstand the separation motion that followed. Adsorption of adhesion protein laminin on the hydrogels did not alter the outcome. A possible solution in the future to this issue would be to have a more permanent binding of adhesion molecules to the hydrogel by covalently linking small peptides to the HA molecule itself. To increase the probability of the neurites binding to the gel we

flipped one of the slides so as to have the gel directly on top of the neurites. This trial had the most unexpected outcome. None of the cells remained adhered to the PEI pattern by the time the experiment was stopped. The simplest explaination as to what could have caused this is lack of diffusion of nutrients through the gel. The overlapping of a large section of gel on the entirety of the neurites may have suffocated them and led to their retraction or delamination from the protein pattern. Another cause of this outcome may be the shearing process itself, however there are no studies in the literature at the moment that can support this hypothesis. The most promising result came from trial 3 where a small flap of gel was extended across the interface. After the experiment was stopped, the gel flap was still adhered to the slide with the neurites, however it had almost fractured from the remaining gel. The media in the chamber sloshed from side to side creating ripples in the chamber while being trasnported from the vibration isolation table to the stereo-microscope for imaging after the experiment was stopped. The gel flap adhered to the slide with the neurites was able to sustain these ripples suggesting the bond strength was strong. The low stiffness of the gels posed a challenge to successful fabrication of gel samples with the extended flap. Nevertheless we are hopeful that improvements in fabrication of these delicate gel films in the future may allow us to successfully test our hypothesis that these novel hydrogels can promote and sustain axonal stretch growth. A possible technique that could be beneficial is 3D printing on the glass slide and past the edge under steady nitrogen flow conditions. This technique would allow for accurate fabrication of hydrogels with features in different planes. The nitrogen flow would prevent free radical scavanging by oxygen in the absence of the coverglass sandwich method that

was used to fabricate the gels described above. Thus the gel flap would not be damaged during the fabrication and peeling process.

5.5. **Conclusions**: Derivatization of the HA molecule as well as the crosslinking process did not have any detrimental effect on the cytocompatibility of the hydrogels, however the total number of cells that attached to the hydrophilic gel was lower than control TCPS surface. The high concentration of hyaluronidase enzyme we used to cause shrinkage of PEGDa gel network did not affect the behavior of the primary neurons. There was no obervable difference between the control group of cell that were not exposed to the enzyme and those that were. The observations from the four condtions tested can be interpretted as either the neurite ends were unable to crossover the interface to attach with the hydrogel or they were unable to form strong bonds that could sustain the separation motion. The experiments with the extended gel flap did indicate that the gels was able to form a bond with the slide bearing neurites, however the fracturing of the gel flap from the remainder of the gel made drawing any concrete conculsion difficult.

References

1. Lesley J, Hascall VC, Tammi M, Hyman R. Hyaluronan binding by cell surface CD44. Journal of Biological Chemistry. 2000 September 01;275(35):26967-75.

2. Moon C, Heo S, Sim K, Shin T. Upregulation of CD44 expression in the spinal cords of rats with clip compression injury. Neurosci Lett. 2004 8/26;367(1):133-6.

3. Napoli I, Noon LA, Ribeiro S, Kerai AP, Parrinello S, Rosenberg LH, et al. A central role for the ERK-signaling pathway in controlling schwann cell plasticity and peripheral nerve regeneration In Vivo. Neuron. 2012;73(4):729.

4. Nagy J, Hacking J, Frankenstein U, Turley E. Requirement of the hyaluronan receptor RHAMM in neurite extension and motility as demonstrated in primary neurons and neuronal cell lines. The Journal of Neuroscience. 1995 January 01;15(1):241-52.

5. Knudson CB, Knudson W. Hyaluronan-binding proteins in development, tissue homeostasis, and disease. FASEB J. 1993;7(13):1233.

6. Laurent TC, Laurent UB, Fraser JR. Functions of hyaluronan. Annals of the Rheumatic Diseases. 1995 May 01;54(5):429-32.

7. Laurent TC, editor. The chemistry, biology and medical applications of hyaluronan and its derivatives. 1st ed. London and Miami: Portland Pr; 1998.

8. Collins MN, Birkinshaw C. Hyaluronic acid based scaffolds for tissue engineering - A review. Carbo Poly. 2013;92:1262.

9. Menzel EJ, Farr C. Hyaluronidase and its substrate hyaluronan: Biochemistry, biological activities and therapeutic uses. Cancer Lett. 1998 9/11;131(1):3-11.

10. Price RD, Berry MG, Navsaria HA. Hyaluronic acid: The scientific and clinical evidence. Journal of Plastic, Reconstructive & Aesthetic Surgery. 2007 10;60(10):1110-9.

11. Zhong SP, Campoccia D, Doherty PJ, Williams RL, Benedetti L, Williams DF. Biodegradation of hyaluronic acid derivatives by hyaluronidase. Biomaterials. 1994 4;15(5):359-65.

12. Wakao N, Imagama S, Zhang H, Tauchi R, Muramoto A, Natori T, et al. Hyaluronan oligosaccharides promote functional recovery after spinal cord injury in rats. Neurosci Lett. 2011 1/25;488(3):299-304.

13. Pelham RJ, Wang Y. Cell locomotion and focal adhesions are regulated by substrate flexibility. Proc Natl Acad Sci U S A. 1997;94(25):13661.

<center>**Chapter 6**</center>

6.1. **Summary:** Hyaluronic acid networks were crosslinked using two different bifunctional crosslinkers. This enabled us to degrade them either enzymatically or via hydrolysis to create novel slow-shrinking hydrogels. The shear thinning nature of HA made it possible to shear align the molecular chains of a highly concentrated HA solution. We hypothesized that rapid crosslinking of this configuration would store a retractive stress in the network. The crosslinkers we selected were PEGDa (non-degradable) and PEGPLADa (hydrolytically degradable). Degrading the crosslinked network that had a stored retractive stress afforded the property of macroscopic shrinkage to the hydrogel network. Cleaving the crosslinks or the HAGMa chains increased the free volume of the network. The chains had more room to reorganize or recoil thereby releasing some of the stored retractive stress. The shrinkage was significant along a preselected axis. The four compositions we tested were 60 mg/ml HAGMa crosslinked with 3:1 and 4:1 ratio of PEGDa, 60 mg/ml HAGMa crosslinked with 1:1 PEGPLADa, and 70 mg/ml HAGMa crosslinked with 1:1 PEGPLADa. The hydrogels were characterized using various techniques for their ability to produce shrinkage.

Oriented polymers have the property of optical anisotropy which can be measured as birefringence. Visually, birefringence is observed as brightness or shades of color depending on the kind of anisotropic material. The intensity of the brightness is directly proportional to the degree of molecular orientation. Degrading the network caused the gels to shrink as the network reorganized. This was manifested as a decrease in molecular orientation and thus the birefringence. The decrease in the birefringence value was significant for the PEGDa crosslinked gels when compared to PEGPLADa crosslinked gels. The molecular

<center>177</center>

reorganization in case of the enzymatically degraded gels would be higher on account of directly cleaving the HAGMa chains. Hence the birefringence values post 48 hour degradation decreased significantly when compared to the degraded PEGPLADa hydrogels. We adapted rubber elasticity theory to predict the retractive stress that could be stored in the network. The retractive stress values were in a similar range for all the four compositions. We did not see a significant effect of PEGDa concentration or HAGMa concentration on the magnitude of the stored retractive stress.

Shrinkage of the hydrogels was predominantly along the long axis of the sample which was also the optical axis. The shrinkage along the width of the sample was less than or equal to 5%. The shrinkage profiles obtained were vastly different for all the compositions. The concentration of the enzyme and the crosslinker ratio had the most effect on the shrinkage of the PEGDa crosslinked samples. The shape of the shrinkage profile showed that rate at which the samples shrunk increased when either the enzyme concentration was increased or the crosslinker concentration was decreased. The two day profile of shrinkage was almost linear for samples crosslinked with 4:1 ratio of PEGDa that were degraded with 10 µg/ml hyaluronidase. The shrinkage for the PEGPLADa crosslinked hydrogels could only last for two days for the 70 mg/ml HAGMa composition and the profile was not linear. The 60 mg/ml HAGMa samples crosslinked with PEGPLADa demonstrated very rapid shrinkage within the first 8 hours and thus would not be a good candidate for axonal stretch growth actuator. The shrinkage rates for the first 24 hours were below the desirable 100 µm/hr maximum threshold for all but one composition (60 mg/ml HAGMa crosslinked with 1:1 PEGPLADa). Recovered stress was measured in terms of force applied by the shrinking

178

hydrogel on a flexible aluminum cantilever paired with a non-contact sensor. It was observed that there was significant disparity between the predicted stored retractive stress and the recovered stress. The inability of the flexible cantilever to match with the dynamically decreasing stiffness of the degrading hydrogel along with any opposition to molecular reorganization within the network meant that the extent of the measured recovered stress was significantly lower than the predicted stored stress. The DVRT had a maximum range of 3 mm. Thus even if the cantilever were made more flexible, it would be impossible to test any shrinking gel with a magnitude of shrinkage beyond this range. A solution to that would be to adopt a testing strategy described by Chippada et. al (1). They used a thin brass filament cantilever which was coupled to their shrinking DNA crosslinked gel. Time lapse images were obtained of the position of the cantilever and then by using cantilever theory the force per unit length was calculated. This methodology would require negligible changes to our current setup.

The degradation of the network was performed using two different mechanisms. Enzymatic degradation cleaved the HAGMa chains to cause the molecular reorganization which led to the gel shrinkage. However in doing so, the source of the retractive stress i.e. the long HAGMa chains were cleaved into smaller sections. This reduced the potential that an extended whole chain might possess to recoil once freed from the element holding it in the extended conformation. Thus we expected that the hydrolytically degraded PEGPLADa crosslinked network would produce a greater magnitude of shrinkage and the results confirmed our hypothesis. What we did not expect was the rapid nature of shrinkage. The 60 mg/ml gels crosslinked with 1:1 PEGPLADa shrunk by 3 mm or 21.71% but all the shrinkage occurred within the first 8 hours. This behavior mimicked that of thermoresponsive

179

or pH responsive gels which contract when the threshold trigger is activated (2). The 70 mg/ml HAGMa gels crosslinked with 1:1 PEGPLADa had a slightly more gradual shrinkage profile that extended to almost 2 days with a net shrinkage of 2.04 mm or 14.21%. The concentration of PEGPLADa tested was limited by the hydrophobic-hydrophilic interaction between the crosslinker and polysaccharide. Even though there was no observable phase separation of the pre-crosslinking solution, there might be some effect on the conformation of HAGMa chains that may have an effect on how the gels shrink. Further analysis of the kinetics of PEGPLADa degradation is required to completely understand the cause of the rapid shrinkage. *In vitro* and *in vivo* degradation studies have investigated how gels made entirely of PEGPLADA degrade at 37°C (3, 4). Gels consisting of 23% w/v of PEGPLADa with varying molecular weights of PEG and lactoyl repeat units degraded *in vitro* between two days to four months. The degradation rate of PEGPLADA gels depended on the crosslink density and length of the PEG block. Degradation rate was inversely proportional to the length of the PEG segment. Gels made from lower molecular weight precursor were more tightly cross-linked and thus degraded more slowly than gels made from higher molecular weight precursors. However using the crosslinker to form the HAGMa network may change how the hydrolysis degrades the crosslinker. The rate of degradation may be increased as now there are two hydrophilic elements (PEG and HA) that attract water molecules into the network. This hypothesis may be a possible explanation as to why the shrinkage profile was so rapid. The gels from the one week long term study did not disintegrate completely, however their stiffness appeared to be significantly reduced and visually also looked less opaque. The hydrolysis process is a gradual and slow process. Despite the high hydrophillicity of the network due to both HAGMa and PEG, there might be another

mechanism that may be responsible for the rapid shrinkage. Prior to the testing of the PEGPLADa crosslinked samples, they were swollen in PBS for two hours at 4°C. This was done to allow for swelling while slowing down any hydrolysis. The change in temperature from 4°C to the test condition 37°C may have caused additional network swelling and network reorganization which led to the rapid shrinkage. The new set of swelling experiments suggested in section 6.4 might shed more light on the exact cause of the rapid shrinkage.

The HA molecule has inherent sites which allow binding with cell surface receptors like CD44 and RHAMM. It was inevitable to make chemical modification to the molecule in order to form crosslinked networks. These processes may alter the conformation of the molecule in the crosslinked network thereby making it difficult for the cells to bind. Our observations from the cytocompatibility study with MC-3T3 fibroblasts and primary cortical neurons assured us that there was no significant effect on the viability of these hydrogels as cytocompatible materials. However the number of cells that adhered to the hydrogel samples was severely lower than control TCPS wells. Seeding cells on a wet or semi-dry hydrogel is always a challenge. If a thin film of liquid exists between the cells and the gel surface, the cells do not get the opportunity to make contact with the gel surface and bind. Thus on flooding of the sample wells with media many cells get washed off. However, of the cells that adhered to the gels, a majority were alive and thriving. The main sites on the HA molecule that bind to cell receptors like CD44 are the carboxylic (-COOH) groups (5, 6). Successful derivatization of HA using epoxides like GMa primarily occurs at the (-COOH) groups along with some reversible methacrylation at the hydroxyl (-OH) groups (5). Besides

the hindrance in cell binding due to hydrophillicity of the gel, a higher degree of modification may have decreased the ability of the HA network to present sites for neuronal cells to bind. We adsorbed laminin on the HAGMa hydrogels in order to promote enhanced binding but failed to see any benefit. Covalent binding of adhesion molecules like RGD peptides could provide a boost to the binding capability and strength of the bond.

We custom built a mechanical device that allowed us to indirectly test the binding of the gels with neurons and the potential of these gels to cause axonal elongation. There was no indication of neurites binding to the hydrogel across the interface. Despite providing an additional chemical cue in the form of laminin, it was not possible to get the neurites to bind to the hydrogel. The only promising observation was made for condition 3 where an extra gel flap crossed the interface and was laid directly in contact with the neurites. The gel flap demonstrated bonding with the slide bearing neurites as it was still connected when the motor was stopped after 24 hours. However the gel flap fractured from the remainder of the gel which made it difficult to make concrete conclusions regarding the ability of the gels to facilitate axonal stretch growth. Furthermore there were fabrication challenges with the gel extension flap. Thus the next progression was to flip one of the slides and sandwich the neurites and the gel so they are in direct contact. However we observed that at the end of the experiment there were no cells left attached to the PEI pattern. This was an intriguing outcome as it suggested that lack of sufficient nutrient diffusion or the shearing of neurites led to their retraction / delamination. Further investigation into different hydrogel fabrication techniques may help in increasing the probability of the gel flap not fracturing from the rest of the gel and possibly elongating neurons. Primary cortical neurons were generously

donated by the Hewett lab. These neurons are multi-polar neurons. Growing these neurons along a protein pattern forced them to extend neurites along two directions. However the density of neurites that reach the edge of the glass slides could be improved by using dorsal root ganglion (DRG) explants. The benefit of using DRG's over primary neurons is their direct clinical relevance. DRG's are routinely used to study peripheral nerve system neuropathies (7). The density of neurites emanating from the explant are significantly greater compared with primary cortical neurons. The main advantage that DRG's would provide is culture longitivity due to presence of support cells and microglia. The primary cortical neurons were ready to be used around day 6 post seeding and the optimal shelf life was 8 to 10 days post seeding.

To be considered as a suitable actuator material for axonal stretching, the biomaterial should be able to produce shrinkage at rates that can sustain development of neo-axoplasm. Thus while selecting the compositions which would be feasible candidates, the rate of the shrinkage and profile of shrinkage are more critical than the net magnitude of shrinkage. We conclude that among the compositions tested here, 60 mg/ml HAGMa crosslinked with 4:1 PEGDa and 70 mg/ml HAGMa crosslinked with 1:1 PEGPLADa were the best compositions with the potential to be used as axonal stretch growth actuators. The ability to shrink in a controlled fashion as a response to a trigger made this network system an addition to a special class of polymers known as polymeric actuators.

There are several successful examples of polymeric actuator materials in the literature which have applications ranging from coatings on medical devices, artificial muscles, to drug

delivery vehicles (8-10). Each of these materials has a trigger that causes a change in shape or volume that is exploited for the desired application. These triggers are generally a change in temperature, electric field, or ionic balance. The success of a polymer actuator is judged on time of response, the magnitude of the contractile force, and the actuation strain. Almost all of the electroactive polymers (EAP) have a response rate that would be unsuitable for sustained stress application problems such as stretching axons. Uragami and co-workers synthesized a semi-interpenetrating network (semi-IPN) hydrogel containing both grafted antigens and their corresponding specific antibodies (11). An antigen-antibody semi-IPN hydrogel was prepared by the copolymerization of the vinyl (rabbit IgG), acrylamide, and N,N-methylenebisacrylamide (MBAA) as a cross-linker in the presence of the polymerized goat anti-rabbit (GAR) IgG. Antigen-antibody binding reaction caused the formation of cross-links within the polymer. Free antigens were then added to the solution around the hydrogel creating competition between the grafted antigens leading to a decrease in cross-linking density. This caused an increase in swelling of the hydrogel. This increase in swelling was reversible. By removing the hydrogel from the antigen solution and washing, the polymer would return to approximately its original volume. This change in volume caused shrinking of the hydrogel as well as change in permeability of the hydrogel. The authors used the hydrogel as a selective permeable membrane for transport of drugs, however there is potential for use as a mechanical actuator. This gel could be implanted in the nerve gap and subsequently triggered to shrink after sufficient time has been provided for neurite ends to attach. There are however some operational disadvantages in the actuation mechanism that may limit its applicability beyond serving as a selective permeable membrane. The main advantage our hydrogel networks have over the networks synthesized by Uragami and

184

coworkers is the feasibility of the concept to be implemented *in vivo*. Maintaining the concentration of the free antigen in a hostile injury environment filled with debris clearing macrophages would be extremely difficult. On the other hand, shrinking a crosslinked HAGMa hydrogel by cleaving the network using hyaluronidase or via hydrolysis or both is much more realistic for *in vivo* application.

Recently a novel crosslinked hydrogel system has been described by Lin et al. and Chippada et al. (1, 12). A DNA crosslinked hydrogel was fabricated that demonstrated potential to be used for stretching axons. The DNA-crosslinked polyacrylamide gels have the ability to contract or swell by the addition of crosslinks or removal of strands respectively. The tendency of these loosely crosslinked gels to contract as their crosslink density was increased is a novel technique to generate a force. The dynamic modulation of the stiffness of the hydrogels by addition of crosslinks caused the tissue scaffold to shrink and this could potentially be used to exert traction on the emerging neurites and physically expand the tissue. The force potential was measured by two techniques that used linear elasticity principles. The force generated by the DNA crosslinked gel per unit length was approximately equal to 1050 pN/µm, at room temperature testing conditions, which is in the range reported by Heidemann and coworkers (13) for successful axonal stretching. However the potential of the DNA crosslinked gels as axonal stretch inducers is vastly reduced by the fact that the force potential drops almost three times at 37°C. The HAGMa hydrogels described here generated forces ranging between 600 nN/µm and 2300 nN/µm. Despite the fact that these values are significantly higher than those reported in the axonal stretch literature, it is important to note that the literature values are for the stresses a single neurite

can successfully sustain to elongate. It is known that a bundle of neurites can sustain stretch rates that are 100 times more than what a single neurite can sustain (14). We could draw a parallel analogy and expect that a neurite bundle may be able to sustain higher stretch forces as well.

Thus except for the DNA crosslinked polyacrylamide hydrogels there is an absence of a polymer system that can successfully demonstrate controlled slow transformation that could be exploited for actuation purposes. EAP's and SMP's have been designed to exhibit multi-functionality in terms of biocompatibility, biodegradability, quick transitioning / shape changing phenomenon, and mechanical tunability (15). The transformation of the SMP networks after the transition temperature is reached is very rapid, usually ranging between 1.8% to 5% per minute depending on the size of the monomer used to form the crosslinked network (9, 10, 15). Thus there is an alarming absence of slow transforming (shrinking) polymer actuators. The polymer system discussed in this dissertation is the first of its kind. We have been able to demonstrate controlled slow shrinkage of the hydrogel network via two different mechanisms of degradation that is sustained for at least two days. We admit that there is still potential room for optimization; however this network system fills a void that is present in the current available polymeric actuator materials by creating a new class of biologically relevant slow actuators.

6.2. **Limitations of the polymer system:** We demonstrated that a novel hyaluronic acid based network system can be designed to shrink along a preferred axis of the sample. All but one composition of the gel produced shrinkage rates that are compatible to be used for the

186

application of stretching axons (14, 16, 17). The shrinkage however could only be sustained for three days at the most. Despite the fact that this hydrogel system is unique, this short duration of shrinkage is a potential drawback. Optimizing this gel system will further increase the applicability of the hydrogel. High degree of derivatization of HA at the (-COOH) groups may have reduced the number of available sites for cells to bind. An alternative strategy that has been described in literature is covalently binding the methacrylate moiety to the (-OH) groups. HA esterification with methacrylic anhydride can be performed in ice cold water at pH 8 for 24 hours to obtain methacrylated HA (18). This photoactive HA polymer can then be crosslinked with PEGDa and PEGPLADa to form hydrogels as described in earlier sections. Having the (-COOH) groups free may increase the number of viable sites for cell surface receptors and improve cell binding. Moreover we can further enhance the binding potential of the gels by covalently adhering small peptide molecules. Carrying on with the theme of improving the neurite binding probability, DRG explants can be cultured on a PEI microcontact printed glass slide. Using the hydrogels described above along with the DRG explants in the axonal elongation device might provide the best chance of successfully stretch elongating the axons. The following sections describe a few future investigations that may help further improve our understanding of the polymer network system and prolong the shrinkage magnitude and duration.

6.3. **Further variables to investigate:** Some of the variables that can affect the extent of molecular orientation but were not investigated as part of this dissertation include molecular weight of the HA chains, injection flow rate prior to crosslinking, and pH similar to the injury site.

6.3.1. **Increasing the molecular weight of HA:** Degradation caused the shear aligned HA chains to recoil and release the stored retractive stress. The magnitude of the retractive stress in the network is dependent on how long the HA chain was i.e. the molecular weight of HA. For the PEGPLADa crosslinked composition we observed that increasing the ratio of the crosslinker caused phase separation of the solution. Increasing the molecular weight of HA might allow us to reduce the final concentration of HA in the solutions at the same time maintaining viscosity conditions necessary for getting relaxation time greater than crosslinking time. Besides this possible advantage, higher molecular weight would increase the magnitude of retractive stress that can be stored in the crosslinked network.

6.3.2. **Flow rates:** The shear thinning property of HA molecule made it possible for us to shear align some of the molecular chains and store retractive stress in the network via rapid crosslinking. We maintained the injection rate at 0.5 ml/min. The effect of varying the flow rate of the pre-crosslinking solution on the degree of molecular orientation and the effective magnitude of retractive stress in the crosslinked network will be a valuable addition to our knowledge of this polymer system in order to increase the applicability of the hydrogels as mechanical stimulators for axonal elongation.

6.3.3. **Varying pH during degradation:** The pH that was maintained during both enzymatic and hydrolytic degradation was neutral. The enzyme hyaluronidase is at optimum activity at neutral pH. However following nervous system injuries, the pH at the site of injury has been observed to be slightly acidic on account of the

immune system response. It will be critical to understand how the shrinkage profile is affected at varying levels of acidic pH values ranging between neutral and 3.

6.4. **Swelling studies for PEGPLADa crosslinked hydrogels:** The current testing protocol followed during the shrinkage study of the hydrolytically degraded hydrogels involved swelling the hydrogel for two hours at 4°C prior to any testing. This was done to minimize any hydrolysis and allow for swelling. However there is not sufficient evidence that the gel reached equilibrium swelling. To understand the equilibrium swelling and if and how it affected the shrinkage profile observed for the PEGPLADa crosslinked hydrogels, the following set of experiments should be explored.

A long term swelling study at room temperature and 4°C should be performed to understand the swelling behavior of the hydrogel. At least three samples of the PEGPLADa crosslinked gels should be weighed every hour and a profile of swelling ratio vs time should be established. Simultaneously a shrinkage assay should be performed by completely getting rid of the two hour swelling duration. Instead, the sample can be subjected to 37°C conditions straightaway after the crosslinking process and images of the sample captured at intervals of one hour. The normalized sample length vs time profile will show how the sample swells, when it reaches equilibrium swelling, and when the shrinkage starts and stops. Also, the samples will be taken to complete or near complete hydrolytic breakdown. The expected outcome profile may show initial swelling followed by shrinkage and maybe another swelling cycle when the shrinkage stops and hydrolysis increases capacity of the gel to absorb water.

6.5. **Viscosity measurement to determine mechanism of hydrolytic degradation driven shrinkage**: The shrinkage observed for the PEGPLADa crosslinked hydrogels that were exposed to 37°C was rapid. The mechanism we posit for shrinkage is hydrolysis driven cleavage of the crosslinks that permit recoiling of the HA chains. The initial rapid shrinkage observed is confusing since the hydrolysis process is described to be a slow process. To investigate further what is actually happening in the hydrogels we can measure overtime the viscosity of the solvent that the gels are degraded in. The main degradation byproducts of the gel hydrolysis that have the potential to increase viscosity of the degradation solvent are PEG and HAGMa. The smaller PEG molecule is more likely to be diffused out before considerable degradation would enable the large HAGMa molecule to escape. HAGMa will have a greater effect on the viscosity as compared to PEG. With a sensitive setup (GPC or Ubbelohde capillary viscometer) the viscosity of the degradation solvent could be measured. Standard curves for both the components at various concentrations would allow us to determine which component is diffusing out of the gel and at what time along the degradation process. Correlating this data with the shrinkage profile would help us formulate a hypothesis and possibly explain the true mechanism of shrinkage and the rapid nature of the shrinkage.

6.6. **Hydrogel fabrication techniques:** New strategies in hydrogel fabrication can be explored to improve probability of neuronal ends crossing the interface and binding to the hydrogel. Figure 6.1 shows a couple of strategies worth exploring. Creating a ramp [6(a)] for the neuronal ends to adhere to instead of presenting them with an interface in the form of a wall might compel them to traverse the interface successfully. Crosslinking a gel with aligned

190

channels fabricated by implementing the principles used in fabricating foams would produce substrates could improve the cell-gel interaction at the interface. The idea is once again the same of replacing the gel wall at interface with a more inviting gel interface.
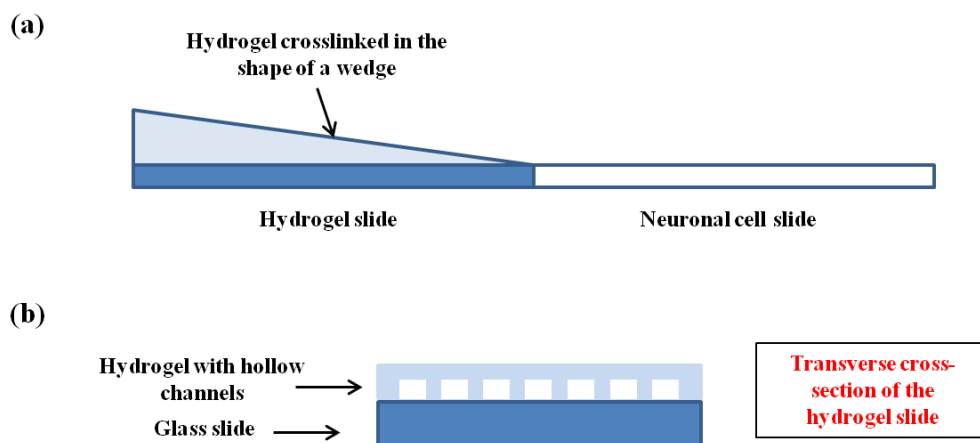
Fig. 6.1. Schematics showing alternative fabrication strategies to create a better hydrogel-cell interface. (a) Gel crosslinked as a wedge on the glass slide with the tapering edge at the interface. (b) Hydrogel with aligned hollow channels.

6.7. **Double crosslinking:** The shrinkage profile we obtained for the compositions tested were unimodal; meaning there wasn't as second stint of sample shrinkage after the shrinkage plateaued. It would be an added advantage to have multiple levels of shrinkage. This could be achieved by crosslinking the hydrogels twice either using same crosslinker or different crosslinkers. Figure 6.2 shows schematic for a proposed method to achieve that. A pre-crosslinking solution containing HAGMa and a crosslinker would be injected in to the glass mold and rapidly crosslinked. Then a slight extensional pressure would be applied via a vacuum line connected to the mold. While this pressure exists another solution containing crosslinker and photoinitiator will be pipetted at the end across from the vacuum port. The pressure might facilitate in slightly stretching the crosslinked gel as well as diffusion of the second crosslinker. The mold would be exposed to UV source to crosslink a second time.

191

Degradation of such a double crosslinked hydrogel could increase the duration of shrinkage as well as introduce multiple levels in the shrinkage profile.
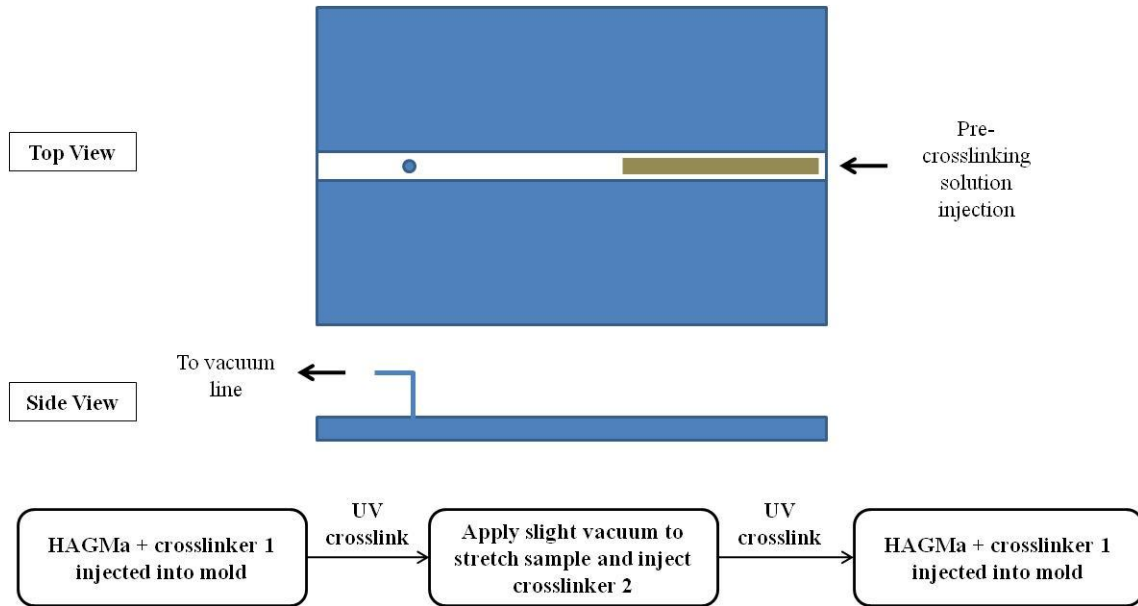
Fig. 6.2. Schematic showing the proposed double crosslinking method. For the first stage of crosslinking the pre-crosslinking solution is injected into mold and rapidly crosslinked. Then a slight pressure will be created using vacuum line and the second=d crosslinker is introduced followed by UV exposure.

6.8. **Magnetic bead study:** Magnetic beads have been employed to study tractional behavior and microrheology of a variety of cell lines. The technique utilizing magnetic beads to study microrheology was pioneered half a decade earlier by Crick and Hughes (19). Since then it has been improved upon by introduction of beads smaller than 5 μm which has enabled researchers to study the viscoelastic properties of the cytoplasm once the beads were phagocytized. Sackmann et al. (19) have developed a magnetic bead microrheometer capable of generating forces in the nano-newton range on supermagnetic and ferromagnetic beads with diameters smaller than 5 μm. This technique could be used to further understand and test the axon-hydrogel interface. The device that was built to test the interface had its limitations. The magnetic beads can be modified so as to covalently bind a thin layer of

192

hyaluronic acid hydrogel. The beads could then be introduced in a well containing primary neurons that have been cultured on a microcontact printed PEI pattern along the axonal end. The size scale match between the axonal ends and the beads would be a definite advantage over the glass slide interface tested earlier as it would give us a chance to position them at neurite ends and test the direct bond between the neurite end and the gel. Using appropriate calibrations the beads could be moved in desired directions at speeds coinciding with the shrinkage rate of the hydrogel composition coated on them. Thus we may be better able to study and quantify the strength of the bond between the growth cone of the axon and the hydrogel and the effect of applying the mechanical stimulation on the stretch growth of the axons.

References

1. Chippada U. Non-intrusive characterization of properties of hydrogels [dissertation]. New Brunswick, New Jersey: The State University of New Jersey; 2010.

2. Ionov L. Polymeric Actuators. Langmuir. 2014;10:1021.

3. Sawhney AS, Pathak CP, Hubbell J. Bioerodible hydrogels based on photopolymerized poly(ethylene glycol)-co-poly(.alpha.-hydroxy acid) diacrylate macromers. Macromolecules. 1993(4):581.

4. Kim BS, Hrkash JS, Langer R. Biodegradable photo-crosslinked poly(ether-ester) networks for lubricious coatings. Biomaterials. 2000;21:259.

5. Schante CE, Zuber G, Vandamme Tf. Chemical modifications of hyaluronic acid for the synthesis of derivatives for a broad range of biomedical applications. Carbo Poly. 2011;85:469.

6. Laurent TC, editor. The Chemistry, Biology and Medical Applications of Hyaluronan and its Derivatives. 1st ed. London and Miami: Portland Pr; 1998.

7. Melli G, Hoke A. Dorsal Root Ganglia Sensory Neuronal Cultures: a tool for drug discovery for peripheral neuropathies. Expert Opin Drug Discov. 2009;4:1035.

8. Carpi F, Smela E, editors. Biomedical Applications of Electroactive Polymer Actuators. John Wiley & Sons; 2009.

9. Davis KA, Burke KA, Mather PT, Henderson JH. Dynamic cell behavior on shape memory polymer substrates. Biomaterials. 2011;32(9):2285.

10. Song J, Xu J. Thermal Responsive Shape Memory Polymers for Biomedical Applications. In: Fazel-Rezai R, editor. Biomedical Engineering - Frontiers and Challenges. ; 2011.

11. Miyata T, Asami N, Uragami T. A reversibly antigen-responsive hydrogel. Nature. 1999;399:766.

12. Lin DC, Yurke B, Langrana NA. Inducing reversible stiffness changes in DNA-crosslinked gels. Journal of Materials Research. 2005;20(6):1456.

13. Heidemann SR, Buxbaum RE. Tension as a regulator and integrator of axonal growth. Cell Motil Cytoskeleton. 1990;17(1):6-10.

14. Smith DH. Stretch growth of integrated axon tracts: Extremes and exploitations. Prog Neurobiol. 2009 11;89(3):231-9.

15. Knight PT, Lee KM, Qin H, Mather PT. Biodegradable thermoplastic polyurethanes incorporating polyhedral oligosilsesquioxane. Biomacromolecules. 2008;9(9):2458.

16. Smith DH, Wolf JA, Meaney DF. A New Strategy to Produce Sustained Growth of Central Nervous System Axons: Continuous Mechanical Tension. Tissue Eng. 2001 04/01; 2011/05;7(2):131-9.

17. Pfister BJ, Iwata A, Meaney DF, Smith DH. Extreme Stretch Growth of Integrated Axons. The Journal of Neuroscience. 2004 September 08;24(36):7978-83.

18. Burdick JA, Chung C, Jia X, Randolph JA, Langer R. Controlled Degradation and Mechanical Behavior of Photopolymerized Hyaluronic Acid Networks. Biomacromolecules. 2005;6:386.

19. Bausch AR, Moller W, Sackmann E. Measurement of Local Viscoelasticity and Forces in Living Cells by Magnetic Tweezers. Biophys J. 1999;76:573.

APPENDIX

7.1. NMR of Hyaluronic acid molecule modified with 10X glycidyl methacrylate

23Nov11HAGMa10x

49.05% modification
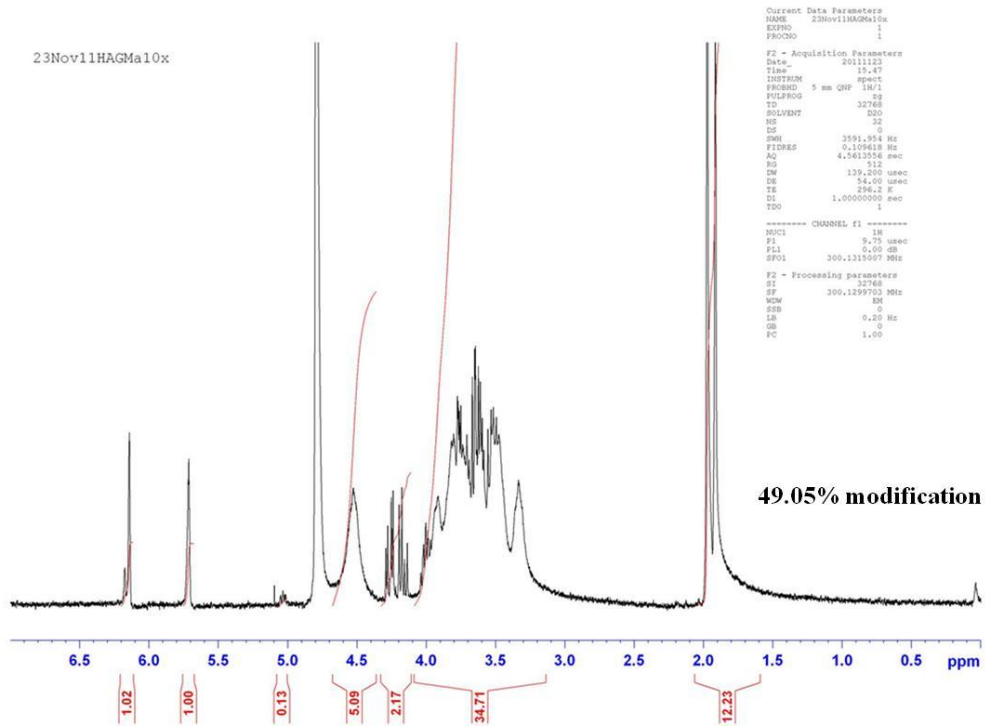
7.2. NMR of pre-dialysis and post-dialysis HAGMa solution

23Nov11HAGMa20x_predial_200mgj

Pre-dialysis residual GMa

14Nov11HAGMa20x_200mgj

Current Data Parameters
NAME   14Nov11HAGMa20x_200mgj
EXPNO   1
PROCNO   1

F2 - Acquisition Parameters
Date_   20111114
Time   11.10
INSTRUM   spect
PROBHD   5 mm QNP 1H/1
PULPROG   zg
TD   32768
SOLVENT   D2O
NS   32
DS   0
SWH   3591.954 Hz
FIDRES   0.109618 Hz
AQ   4.5613556 sec
RG   512
DW   139.200 usec
DE   54.00 usec
TE   295.2 K
D1   1.00000000 sec
TDO   1

======== CHANNEL f1 ========
NUC1   1H
P1   9.75 usec
PL1   0.00 dB
SFO1   300.1315007 MHz

F2 - Processing parameters
SI   32768
SF   300.1299703 MHz
WDW   EM
SSB   0
LB   0.20 Hz
GB   0
PC   1.00

Post dialysis GMa
filtered out

7.3. Measuring sample dimensions using Image J

1. The sample images were captured using an iPhone camera from a fixed distance.

2. A reference scale was placed underneath the wells before imaging the samples as shown below.

3. The images were opened in Image J and the measuring tool was calibrated using the reference scale present in the image.

4. The sample dimensions were measured at least 3 times and the average value was reported as the actual dimension of the sample.
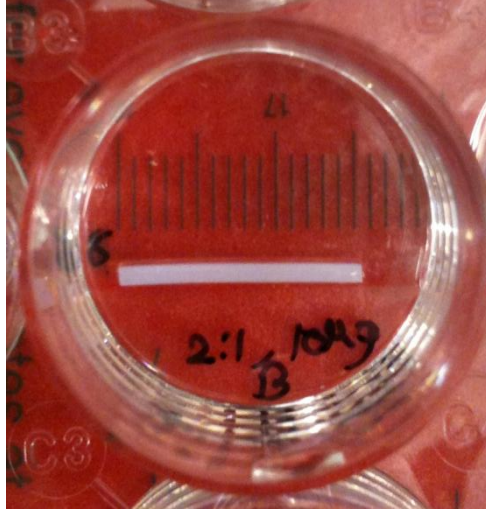
7.4. Analysis of birefringence spectra

1. The spectrum obtained from the optical spectrophotometer gets stored as an excel file. The first column being the wavelengths and the second is the intensity data.

2. Select the data between 480nm and 700nm. Using the dark and bright reference spectra, normalize the intensity spectrum using the formula given below.

$$T = \frac{I - I_0}{I_d - I_0}$$

3. Next construct a column using the standard equation using an arbitrary retardance value. Perform non-linear regression to fit the actual data with the standard equation to find the best fit and extract the retardance value.

7.5. Activation of glass slides for crosslinking hydrogel

Chemical activation of the glass coverslip is done following the procedure used by Pelham and Wang.

Reagents:

- Coverslips, square (No. 1, 18 x 18mm; Fisher)

- 0.1N NaOH

- 3-Aminopropyltrimethoxysilane (Sigma Aldrich)

- 0.5% Glutaraldehyde in Phosphate buffered saline (PBS) (Polysciences, Inc.)

Procedure:

1. Pass the coverslips briefly through the flame of the Bunsen burner.

2. Pipette out 100ul of 0.1N NaOH on the coverslip and smear it across the surface of the coverslip till it forms a layer. Aspirate the excess after 5 minutes and air dry the coverslip. The coverslip surface should be covered with a film of dried NaOH. Mark the untreated surface with a marker.

3. Pipette 100-200ul of 3-aminopropyltrimethoxysilane evenly on the treated side of the glass surface with the Pasteur pipette. Allow the coverslip to sit for 4 minutes.

4. Soak the treated side of the coverslip with deionized (DI) water and let it sit for 5 minutes. Rinse thoroughly with DI water and air dry.

5. Transfer the coverslips into petri dishes, treated side up, and cover the surface with 0.5% glutaraldehyde. Incubate at room temperature for 20-30 minutes.

6. Wash the coverslip extensively with DI water and then let it air dry. The treated coverslips should be used for gel attachment within 48 hours after activation.

7.6.Activation of top glass slides: Chemical activation of the glass coverslip is done following the procedure suggested by the manufacturer.

Reagents:

- Coverslips, square (No. 1, 22 x 22mm; Fisher)

- 0.1N NaOH

- SurfaSil Siliconizing Fluid (Pierce Biotechnology)

- Acetone

- Methanol

Thorough cleaning of glassware ensures maximum coating. Clean glassware before siliconizing. Use of acid or base to prepare glassware etches glass and exposes more sites with which the siliconizing agent can react.

1. Clean glassware with standard laboratory cleaner.

2. Thoroughly rinse glassware with DI water to remove residue. Dry the surface in an oven at 200°C for at least 15 minutes. Multiple layers of silane can form on the glass surface if water is not completely removed.

SurfaSil Siliconizing Fluid: Immersion Technique:

1. Dilute SurfaSil Siliconizing fluid in a non-polar organic solvent such as acetone. Working   concentration is 10% volume to volume.

2. Completely immerse the coverslip to be coated in the diluted SurfaSil Solution for at least 5-10 seconds. Agitate the solution to ensure a uniform coat. A thin film will immediately coat the object's surface.

3. Rinse the coverslip with acetone.

4. Rinse the coverslip with methanol. This rinse is required to prevent interaction of the SurfaSil Coating with water and thus, reversing siliconization.

5. Air-dry the object for 24 hours or heat at 100°C for 20-60 minutes.

6. SurfaSil Siliconizing Fluid evolves HCl as a by-product during coating. Use a fume hood and vented explosion-proof ovens.

7.7. MC3T3 Fibroblast cell culture

MC3T3 fibroblast cell lines are good models for studying in vitro osteoblast differentiation, particularly ECM signaling. They have behavior similar to primary calvarial osteoblasts. They need to be grown and expanded in culture until they reach confluence and then passaged 2-3 times before using them for cell culture experiments.

Following is the procedure for culturing undifferentiated cells:

1. Remove a vial of stored MC3T3 cells from the liquid N_2 tank. A vial should have approximately $1x10^6$ cells in 1mL of media.

2. Rapidly thaw the vial of cells by placing it in your palm for about 5 minutes.

3. Once thawed, transfer the aliquot into a 15mL conical tube and add 9mL of culture medium.

4. Form a pellet of cells by spinning them down in a centrifuge at 1000 RPM for 5 minutes. This is to remove the DMSO used during cryopreservation.

5. Remove the supernatant and resuspend the cell pellet in 10mL of fresh culture medium. Transfer this solution to a T-75 flask ($75mm^2$) and place the flask in the incubator at 37°C with 5% CO_2. Change media every alternate day until cells reach confluence. Once the cells reach about 80% confluence they are ready to be passaged. Cells usually split 1:3.

Materials:

- 1X Trypsin EDTA
- 1X PBS
- Cell Culture Medium
- 2, T-75 flasks

Procedure:

1. Aspirate the culture medium from the T-75 flask that needs to be passaged.

2. Add 10mL of 1X PBS and gently tap the flask. This is done to remove dead and poorly attached cells. Aspirate off the PBS and add 1mL of 1X trypsin.

3. Make sure to cover the entire surface of the flask with trypsin. Put the flask into the incubator at 37°C for 3 minutes.

4. Add 9mL of culture media and rinse the cells off of the flask. When most of the cells are off the flask, suck up all of the media and transfer it to the 15mL conical tube.

5. Add 7mL of fresh media in 2 new T-75 flasks as well as in the flask from which we passaged cells.

6. Spin down the cells in the conical tube in the centrifuge for 5 minutes at 1000 RPM. Aspirate the supernatant and resuspend the pellet of cells in 10mL of fresh culture media.

7. Add 3mL of media and cells to each of the T-75 flasks. Place all the three flasks in the incubator. Change media every alternate day until cells are needed for passaging or cryopreservation.

MC3T3 Fibroblast Media

Media Constituents

- Advanced Minimum Essential Medium AMEM

- Fetal Bovine Serum (FBS)

- Penicillin Streptomycin Glutamine (PSG)

Remove FBS and PSG from freezer and thaw to room temperature.

For making 200ml media

20ml of FBS

2ml PSG

178ml AMEM

7.8. Hemocytometry

A hemocytometer is used for counting cells. Remove the hemocytometer, clean with DI water and 70% Ethanol, dry thoroughly and assemble it for counting cells.

1. Obtain 10ul of the sample of the cell suspension in media and dispense it onto the hemocytometer

2. Focus on the grid under the microscope and count cells in 16 boxes at 4 corners of the hemocytometer (16 boxes x 4 squares = 64 boxes).

3. Divide the total number of cells from 64 boxes by four to get the number of cells per square.
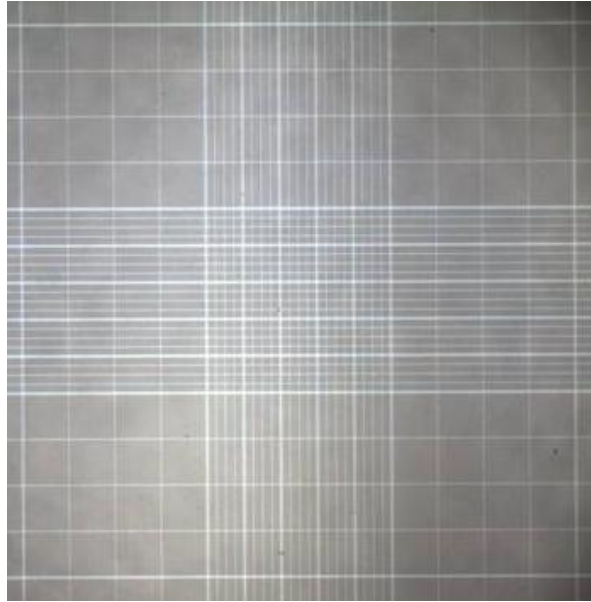
4. Multiply the number of cells/square by 10,000 to get the number of cells/mL of media

5. Multiply number of cells/mL by the total amount of media you have (about 10mL) to get the total number of cells in your media.

6. For freezing or splitting cells you normally need about $1\text{x}10^6$ cells in 1mL of media, so you divide $1\text{x }10^6$ by the number of cells/mL to get the amount of media that needs to be removed to get $1\text{x}10^6$ cells

Example:

200 cells were counted in the 64 boxes

200 cells/4 = 50 cells/square

50 cells/square x 10,000 = 500,000 cells/mL

500,000 cells/mL x 10 = 5,000,000 cells in total suspension of media

We need $1\text{x}10^6$ cells, thus

$1\text{x}10^6$/ 500,000 cells/mL = 2mL of cell-suspension contains 1 million cells

Thus we extract 2mL of cell-media suspension for the process we need to perform.

7.9. Cryopreservation of cells

PC12 cells can be cryopreserved and stored for future usage. The method for preserving cells is called cryopreservation. After passaging cells when all three T-75 flasks are confluent and you do not need all the cells we can freeze them down.

1. Follow steps 1-4 from the cell passaging procedure stated earlier for two T-75 flasks.

2. Pipette out 10ul of media and cells onto the hemocytometer to count the number of cells. We want to freeze down around 1x 10^6 cells in 1mL.

3. Pellet down the cells in the conical tube using the centrifuge for 5minutes at 1000 RPM. Aspirate off the supernatant and resuspend the pellet of cells in 10 mL of 1X PBS.

4. Spin down the cells again for 5 minutes in the centrifuge, and resuspend the pellet of cells in 10 mL of fresh culture media containing 10% dimethyl sulfoxide (DMSO), a cryopreservative.

5. Aliquot out 1mL of media containing about 1x 10^6 cells into 2mL cryovials. Put the vials in Mr. Frosty which is filled with 250 mL of isopropyl alcohol and leave them for 24 hours in the -80°C freezer for controlled freezing (1°C/min).

6. Remove Mr. Frosty from the freezer and store the vials in the liquid nitrogen tank (-120°C) for future use.

7.10. Primary Cortical Neuron Media

Media constituents:

- B-27 supplement

- L-Glutamine

- Penicillin/ Streptomycin

- Neurobasal Media

Remove the B-27 supplement, L-glutamine, and penicillin/streptomycin from the freezer and let it thaw.

For making 200mL of Neurobasal media add:

4 mL of B-27 supplement

1mL of L-glutamine

2mL of Penicillin/ Streptomycin (1:100 dilutions)

193 mL of Neurobasal Media

The media can be stored in the refrigerator at 4°C until required.

7.11. Live –Dead Assay

1. Wash the cells prior to the assay to remove or dilute serum esterase activity generally present in serum-supplemented growth media (serum esterases could cause some increase in extracellular fluorescence by hydrolyzing calcein AM). Wash adherent cells gently with 500–1,000 volumes of Dulbecco's phosphate-buffered saline (D-PBS)

2. Remove the LIVE/DEAD® reagent stock solutions from the freezer and allow them to warm to room temperature.

3. Add 20 μL of the supplied 2 mM EthD-1 stock solution (Component B) to 10 mL of sterile, tissue culture–grade D-PBS, vortexing to ensure thorough mixing. This gives an approximately 4 μM EthD-1 solution.

4. Combine the reagents by transferring 5 μL of the supplied 4 mM Calcein AM stock solution (Component A) to the 10 mL EthD-1 solution. Vortex the resulting solution to ensure thorough mixing.

5. The resulting approximately 2 μM Calcein AM and 4 μM EthD-1 working solution is then added directly to cells. The final concentration of DMSO is ≤ 0.1%, a level generally innocuous to most cells.

6. Note that aqueous solutions of Calcein AM are susceptible to hydrolysis (see Storage and Handling of Reagents). Aqueous working solutions should therefore be used within one day.

7. Incubate the cells for 30–45 minutes at room temperature. A shorter incubation time may be used if the dye concentrations or incubation temperature are increased.

7.12. 4% Paraformaldehyde

Paraformaldehyde is used for fixing cells once the experiment is complete.

Media Constituents:

- Monobasic Sodium Phosphate Anhydrous (Soln. A) (0.2M)

- Dibasic Sodium Phosphate Anhydrous (Soln. B) (0.2M)

- Paraformaldehyde granules

- NaOH (1M)

For making 500mL of solution, dissolve 24 grams of monobasic sodium phosphate anhydrous in 1000mL of DI water (soln A). Dissolve 28.4 grams of dibasic sodium phosphate anhydrous in 1000mL of DI water (soln B). Dissolve 20 grams of paraformaldehyde granules in 250mL DI water at 55-60°C while adding 10-15 drops of 0.1M NaOH to it until solution is clear. For the 500mL of 4% paraformaldehyde solution, take a 500 mL glass bottle and from the above prepared solutions add 250mL of paraformaldehyde solution, 47.5mL of solution A and 202.5 mL of solution B. This will yield a 4% fixing solution which should be stored in the refrigerator at 4°C until needed.

7.13. Microindentation Device

- Fill the liquid cell with either DI water or PBS. Load the sample into the test setup.

- Get the sample close to the tip.

- Switch on the power supply (First Elenco then Topward)

- Press the "Acquire" button to check if all sensors are in proper range. (refer table for trace information)

- Press "Stop acquire".

- Enter the file name ("_filename"), scan dimensions, and indent spacing. (select linear profile if testing gradient samples)

- Enter the maximum load to be reached in uN .

- Press "Snap location". Enter number of indents in the manual over ride box if you intend to perform a specific number of indents.

- Press "Scan" button.

- A message box pops up after the test is finished.

209

Trace color	Description
Yellow	DVRT voltage (has to between -1 to +1 volt. If voltage >2 volts tip might be in contact with sample or cantilever is bent towards the DVRT
Green	Z – LVDT voltage (has to be between 5 & 6 volts for optimal performance)
Pink	Displacement LVDT (has to be between -3 & 1 volts for best performance)
Red	X motor LVDT voltage
Blue	Y motor LVDT voltage
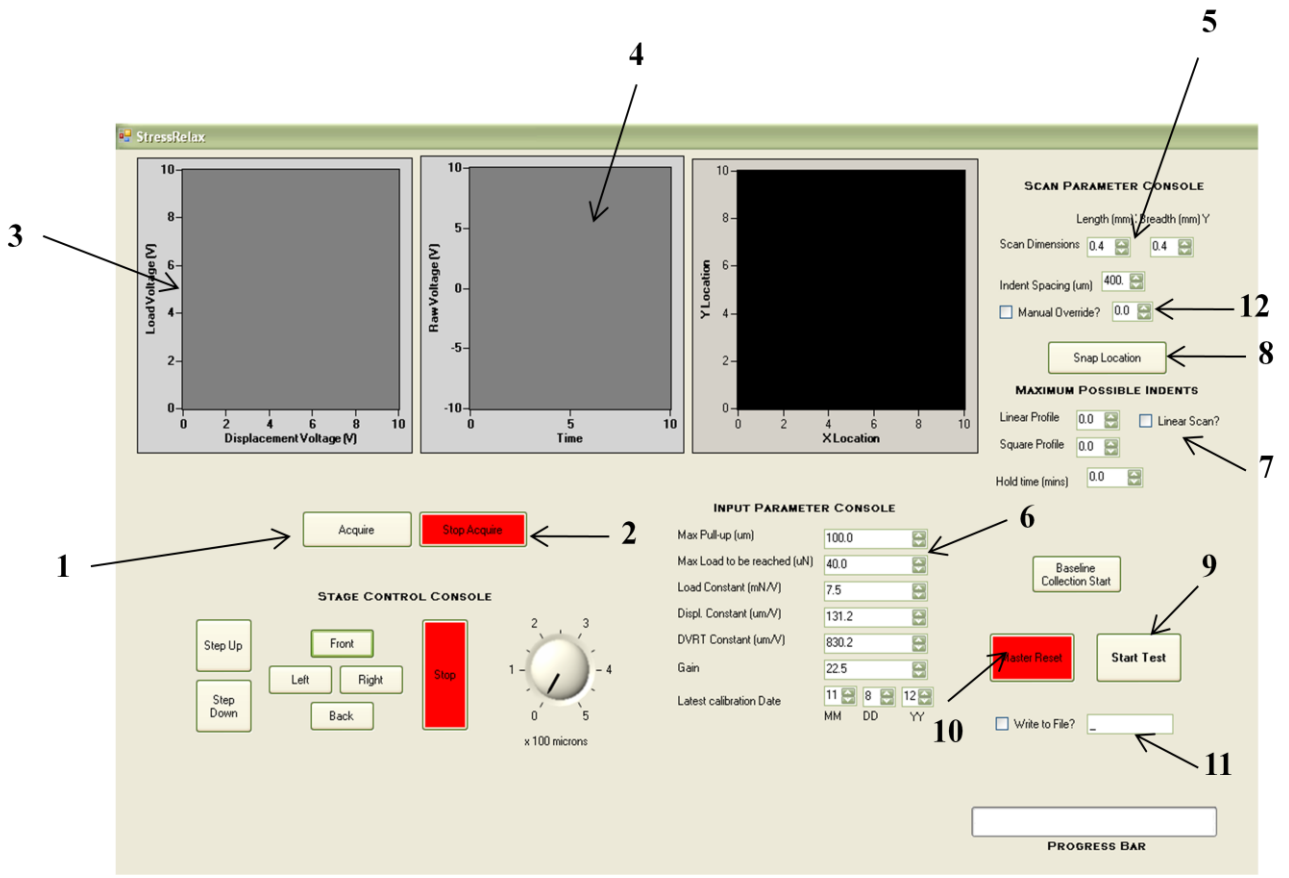
#	Button Name	Description
1	Acquire	On clicking this control button the strip chart above the button will *acquire and show* the current voltages on the various LVDT sensors and the DVRT
2	Stop Acquire	On clicking this control button the strip chart above the button will *stop acquiring* the current voltages on the various LVDT sensors and the DVRT
3	Current status Voltage Chart	It displays the current voltage state of the sensors. (refer the table 1)
4	Test status Voltage Chart	This chart displays the DVRT voltage Vs displacement LVDT voltage during the test.
5	Test area dimension	Enter the length and breadth of the region you wish to test.
6	Indent Spacing	Enter the distance between two indent locations. Minimum distance being 2 times radius of the tip.

7	Linear scan select	On checking this box the test will be done in a straight line across the sample as per the dimensions entered in 5
8	Snap Location	This control takes a snapshot of the voltages at the start of test. The test is run comparing these conditions as baseline.
9	Scan	Clicking this control starts the test
10	Reset	Click this button at the end of test to get the system back to pre-test conditions
11	Filename	The format for entering the filename is "_name_date". The underscore is important as the test is automated and the software increments the counter and every indent is stored as a separate file automatically. Always remember to check he write to file box
12	Manual Over ride	Enter the number of indents if you wish to indent at fewer locations than calculated by the program.

***********Code for microindenter************

```vb
Option Strict Off
Option Explicit On
Imports Excel = Microsoft.Office.Interop.Excel
Public Class StressRelax

    Const z_down As Short = 1 'assign integers to these actions
    Const z_up As Short = 2
    Const y_front As Short = 3
    Const y_back As Short = 4
    Const x_left As Short = 5
    Const x_right As Short = 6
    Const x_left1 As Short = 7
    Const x_right1 As Short = 8
    Const y_back1 As Short = 9
    Const z_down1 As Short = 10 'assign integers to these actions
    Const z_up1 As Short = 11
    Const x_right2 As Short = 12
    Const x_left2 As Short = 13
    Const y_front2 As Short = 14
    Const y_back2 As Short = 15

    Dim gbWriteHeader As Boolean

    Dim vdif As Object
    Dim lconst As Object
    Dim dconst As Object
    Dim ldconst As Object
    Dim ifile As Short
    Dim teststart As Object
    Dim maxload As Object
    Dim testend As Object
    Dim indentnum As Object

    Dim vdata As Object
    Dim label As Single
    Dim Voltage1 As Object
    Dim Voltage2 As Object
    Dim Voltage3 As Object
    Dim z As Object
    Dim i As Object
    Dim i1 As Object
    Dim j1 As Object
    Dim j As Object
    Dim bv As Object
    Dim t As Object
    Dim vqdata As Object
    Dim vwdata As Object
    Dim vedata As Object
    Dim vzdata As Object
    Dim vddata As Object
    Dim nvdata As Object
    Dim nvddata As Object
    Dim zv As Object
    Dim dzv As Object
```

```vb
        Dim zref As Object
        Dim zdata As Object
        Dim zddata As Object
        Dim zdata0 As Object
        Dim zddata0 As Object
        Dim ldata0 As Object
        Dim lndata As Object
        Dim zcoord As Object
        Dim xcoord As Object
        Dim ycoord As Object
        Dim maxindents As Short
        Dim maxindents1 As Short
        Dim maxindents2 As Short
        Dim totalindents As Short
        Dim totalindents1 As Short
        Dim indentlocationx As Object
        Dim indentlocationy As Object
        Dim progress As Short
        Dim progressincr As Short
        Dim Llocation As Short
        Dim Blocation As Short
        Dim XL As Short
        Dim XXL As Short
        Dim YL As Short
        Dim YYL As Short
        Dim XXLmax As Short
        Dim YYLmax As Short

        Dim fs As Object
        Dim fc As Object
        Dim order As Object
        Dim ldata1 As Object

        Dim ltempdata As Object
        Dim ltempdata2 As Object
        Dim dtempdata As Object
        Dim ltempdata3 As Object
        Dim dtempdataX As Object
        Dim ltempdataX As Object
        Dim dtempdata3 As Object
        Dim imax As Object
        Dim ldata(9000000) As Object
        Dim ddata(9000000) As Object
        Dim load_ldata(9000000) As Object
        Dim unload_ldata(9000000) As Object
        Dim load_ddata(9000000) As Object
        Dim unload_ddata(9000000) As Object
        Dim disp(9000000) As Object
        Dim load1(9000000) As Object


    Private Sub DaqTaskComponent1_DataReady(ByVal sender As System.Object,
ByVal e As ContinuousAcquire.DaqTaskComponentDataReadyEventArgs) Handles
DaqTaskComponent1.DataReady
        Dim acquiredData() As NationalInstruments.AnalogWaveform(Of Double) =
e.GetData
```

```vb
        WaveformGraph2.PlotWaveforms(acquiredData)

    End Sub


    Private Sub DaqTaskComponent1_Error(ByVal sender As System.Object, ByVal
e As NationalInstruments.DAQmx.ComponentModel.ErrorEventArgs) Handles
DaqTaskComponent1.Error
        'TODO: Handle DAQ errors.
        Dim message As String = e.Exception.Message
        MessageBox.Show(message, "DAQ Error", MessageBoxButtons.OK,
MessageBoxIcon.Warning)

    End Sub


    Private Sub AcquireVoltages_Click(ByVal sender As System.Object, ByVal e
As System.EventArgs) Handles AcquireVoltages.Click
        DaqTaskComponent1.StartRead()
    End Sub


    Private Sub StopAcquireVoltages_Click(ByVal sender As System.Object,
ByVal e As System.EventArgs) Handles StopAcquireVoltages.Click
        DaqTaskComponent1.StopRead()
    End Sub


    Private Sub Button1_Click(ByVal sender As System.Object, ByVal e As
System.EventArgs)
        Dim up((Pointout_XmotorComponent1.NumberOfChannelsToWrite) - 1) As
Double
        up(0) = -3
        Pointout_XmotorComponent1.Write(up)
    End Sub


    Private Sub Pointout_XmotorComponent1_Error(ByVal sender As
System.Object, ByVal e As
NationalInstruments.DAQmx.ComponentModel.ErrorEventArgs) Handles
Pointout_XmotorComponent1.Error
        'TODO: Handle DAQ errors.
        Dim message As String = e.Exception.Message
        MessageBox.Show(message, "DAQ Error", MessageBoxButtons.OK,
MessageBoxIcon.Warning)
        Pointout_XmotorComponent1.StopTask()

    End Sub


    Private Sub start_Click(ByVal sender As System.Object, ByVal e As
System.EventArgs) Handles start.Click
        indentlocationx = 0
        indentlocationy = 0
        If CheckBox2.Checked = True Then
            linearscan()
        Else
            squarescan() 'add creep call here
        End If

        MsgBox("Test Done  Press Reset")
    End Sub
```

```vbnet
    Private Sub masterreset_Click(ByVal sender As System.Object, ByVal e As
System.EventArgs) Handles masterreset.Click

        vqdata = Pointread_ZlvdtComponent1.Read
        vwdata = Pointread_YlvdtComponent1.Read
        vedata = Pointread_XlvdtComponent1.Read

        zcoord = -1
        xcoord = 0.2
        ycoord = 3

        If vqdata(0) > zcoord Then
            Run((z_down1)) 'move the stage toward z down (see section Run for
detail)
        Else
            Run((z_up1)) 'move the stage toward z up (see section Run for
detail)

        End If

        If vedata(0) < xcoord Then
            Run((x_left2)) 'move the stage left (see section Run for detail)
        Else
            Run((x_right2)) 'move the stage right (see section Run for
detail)
        End If

        If vwdata(0) < ycoord Then
            Run((y_back2)) 'move the stage back (see section Run for detail)
        Else
            Run((y_front2)) 'move the stage front (see section Run for
detail)
        End If
        MsgBox("Master Reset Done")
    End Sub

    Private Sub halt_Click(ByVal sender As System.Object, ByVal e As
System.EventArgs) Handles halt.Click


        Dim hlt((Pointout_ZmotorComponent1.NumberOfChannelsToWrite) - 1) As
Double
        hlt(0) = 0
        Pointout_ZmotorComponent1.Write(hlt)
        Dim hlt1((Pointout_YmotorComponent1.NumberOfChannelsToWrite) - 1) As
Double
        hlt1(0) = 0
        Pointout_YmotorComponent1.Write(hlt1)
        Dim hlt2((Pointout_XmotorComponent1.NumberOfChannelsToWrite) - 1) As
Double
        hlt2(0) = 0
        Pointout_XmotorComponent1.Write(hlt2)

    End Sub
    Private Sub yback_Click(ByVal sender As System.Object, ByVal e As
System.EventArgs) Handles yback.Click
```

```vb
        Run((y_back)) 'move the stage toward y back (see section Run for
detail)
    End Sub

    Private Sub xright_Click(ByVal sender As System.Object, ByVal e As
System.EventArgs) Handles xright.Click
        Run((x_right)) 'move the stage toward x right (see section Run for
detail)
    End Sub
    Private Sub xleft_Click(ByVal sender As System.Object, ByVal e As
System.EventArgs) Handles xleft.Click
        Run((x_left)) 'move the stage toward x left (see section Run for
detail)
    End Sub

    Private Sub yfront_Click(ByVal sender As System.Object, ByVal e As
System.EventArgs) Handles yfront.Click
        Run((y_front)) 'move the stage toward y front (see section Run for
detail)
    End Sub
    Private Sub zdown_Click(ByVal sender As System.Object, ByVal e As
System.EventArgs) Handles zdown.Click
        Run((z_down))
    End Sub

    Private Sub zup_Click(ByVal sender As System.Object, ByVal e As
System.EventArgs) Handles zup.Click
        Run((z_up))
    End Sub
    Private Sub NumericEdit3_AfterChangeValue(ByVal sender As System.Object,
ByVal e As NationalInstruments.UI.AfterChangeNumericValueEventArgs)

    End Sub

    Private Sub NumericEdit2_AfterChangeValue(ByVal sender As System.Object,
ByVal e As NationalInstruments.UI.AfterChangeNumericValueEventArgs)

    End Sub

    Sub Run(ByRef RunMode As Single) 'this section defines motion for the 3D
stage x(right,left), y(front,back),and z(up,down)
        Dim zdata As Object
        Dim zdata0 As Object
        Dim ydata As Object
        Dim ydata0 As Object
        Dim xdata As Object
        Dim xdata0 As Object
        Dim nvdata As Object


        Select Case RunMode
            Case z_down
                vdata = Pointread_ZlvdtComponent1.Read
                zdata0 = vdata
                zdata = zdata0
```

```vb
                    Do While System.Math.Abs(zdata(0) - zdata0(0)) <
(Gauge1.Value * 0.7918)
                        nvdata = Pointread_ZlvdtComponent1.Read
                        zdata = nvdata

                        Dim
stgdwn((Pointout_ZmotorComponent1.NumberOfChannelsToWrite) - 1) As Double
                        stgdwn(0) = -5
                        Pointout_ZmotorComponent1.Write(stgdwn)

                    Loop

                    Dim
stgdwn1((Pointout_ZmotorComponent1.NumberOfChannelsToWrite) - 1) As Double
                        stgdwn1(0) = 0
                        Pointout_ZmotorComponent1.Write(stgdwn1)


                Case z_up

                    vdata = Pointread_ZlvdtComponent1.Read
                    zdata0 = vdata
                    zdata = zdata0

                    Do While System.Math.Abs(zdata(0) - zdata0(0)) <
(Gauge1.Value * 0.7918)
                        nvdata = Pointread_ZlvdtComponent1.Read
                        zdata = nvdata

                        Dim
stgup((Pointout_ZmotorComponent1.NumberOfChannelsToWrite) - 1) As Double
                        stgup(0) = 5
                        Pointout_ZmotorComponent1.Write(stgup)

                    Loop

                    Dim
stgup1((Pointout_ZmotorComponent1.NumberOfChannelsToWrite) - 1) As Double
                        stgup1(0) = 0
                        Pointout_ZmotorComponent1.Write(stgup1)


                Case x_right
                    vdata = Pointread_XlvdtComponent1.Read
                    xdata0 = vdata
                    xdata = xdata0

                    Do While System.Math.Abs(xdata(0) - xdata0(0)) <
(Gauge1.Value * 0.0946)
                        nvdata = Pointread_XlvdtComponent1.Read
                        xdata = nvdata

                        Dim
stgrt((Pointout_XmotorComponent1.NumberOfChannelsToWrite) - 1) As Double
                        stgrt(0) = 5
                        Pointout_XmotorComponent1.Write(stgrt)
                    Loop
```

219

```vb
                        Dim
stgrt1((Pointout_XmotorComponent1.NumberOfChannelsToWrite) - 1) As Double
                        stgrt1(0) = 0
                        Pointout_XmotorComponent1.Write(stgrt1)


                Case x_left
                        vdata = Pointread_XlvdtComponent1.Read
                        xdata0 = vdata
                        xdata = xdata0

                        Do While System.Math.Abs(xdata(0) - xdata0(0)) <
(Gauge1.Value * 0.0946)
                                nvdata = Pointread_XlvdtComponent1.Read
                                xdata = nvdata

                                Dim
stglft((Pointout_XmotorComponent1.NumberOfChannelsToWrite) - 1) As Double
                                stglft(0) = -5
                                Pointout_XmotorComponent1.Write(stglft)
                        Loop

                        Dim
stglft1((Pointout_XmotorComponent1.NumberOfChannelsToWrite) - 1) As Double
                        stglft1(0) = 0
                        Pointout_XmotorComponent1.Write(stglft1)

                Case y_front
                        vdata = Pointread_YlvdtComponent1.Read
                        ydata0 = vdata
                        ydata = ydata0

                        Do While System.Math.Abs(ydata(0) - ydata0(0)) <
(Gauge1.Value * 0.0853)
                                nvdata = Pointread_YlvdtComponent1.Read
                                ydata = nvdata

                                Dim
stgfrnt((Pointout_YmotorComponent1.NumberOfChannelsToWrite) - 1) As Double
                                stgfrnt(0) = -5
                                Pointout_YmotorComponent1.Write(stgfrnt)
                        Loop

                        Dim
stgfrnt1((Pointout_YmotorComponent1.NumberOfChannelsToWrite) - 1) As Double
                        stgfrnt1(0) = 0
                        Pointout_YmotorComponent1.Write(stgfrnt1)

                Case y_back

                        vdata = Pointread_YlvdtComponent1.Read
                        ydata0 = vdata
                        ydata = ydata0

                        Do While System.Math.Abs(ydata(0) - ydata0(0)) <
(Gauge1.Value * 0.0853)
```

220

```vbnet
                    nvdata = Pointread_YlvdtComponent1.Read
                    ydata = nvdata

                    Dim
stgbk((Pointout_YmotorComponent1.NumberOfChannelsToWrite) - 1) As Double
                    stgbk(0) = 5
                    Pointout_YmotorComponent1.Write(stgbk)
                Loop

                Dim
stgbk1((Pointout_YmotorComponent1.NumberOfChannelsToWrite) - 1) As Double
                    stgbk1(0) = 0
                    Pointout_YmotorComponent1.Write(stgbk1)


            Case x_left1

                    vdata = Pointread_XlvdtComponent1.Read
                    xdata0 = vdata
                    xdata = xdata0

                    Do While System.Math.Abs(xdata(0) - xdata0(0)) <
((NumericEdit_indentspacing.Value / 100) * 0.0946)
                    nvdata = Pointread_XlvdtComponent1.Read
                    xdata = nvdata

                    Dim
stglft((Pointout_XmotorComponent1.NumberOfChannelsToWrite) - 1) As Double
                    stglft(0) = 10
                    Pointout_XmotorComponent1.Write(stglft)
                Loop

                Dim
stglft1((Pointout_XmotorComponent1.NumberOfChannelsToWrite) - 1) As Double
                    stglft1(0) = 0
                    Pointout_XmotorComponent1.Write(stglft1)


            Case x_right1

                    vdata = Pointread_XlvdtComponent1.Read
                    xdata0 = vdata
                    xdata = xdata0

                    Do While System.Math.Abs(xdata(0) - xdata0(0)) <
((NumericEdit_indentspacing.Value / 100) * 0.0946)
                    nvdata = Pointread_XlvdtComponent1.Read
                    xdata = nvdata

                    Dim
stgrt((Pointout_XmotorComponent1.NumberOfChannelsToWrite) - 1) As Double
                    stgrt(0) = -10
                    Pointout_XmotorComponent1.Write(stgrt)
                Loop

                Dim
stgrt1((Pointout_XmotorComponent1.NumberOfChannelsToWrite) - 1) As Double
```

221

```vbnet
                stgrt1(0) = 0
                Pointout_XmotorComponent1.Write(stgrt1)



            Case y_back1
                vdata = Pointread_YlvdtComponent1.Read
                ydata0 = vdata
                ydata = ydata0

                Do While System.Math.Abs(ydata(0) - ydata0(0)) <
((NumericEdit_indentspacing.Value / 100) * 0.0853)
                    nvdata = Pointread_YlvdtComponent1.Read
                    ydata = nvdata

                    Dim
stgbk((Pointout_YmotorComponent1.NumberOfChannelsToWrite) - 1) As Double
                    stgbk(0) = 10
                    Pointout_YmotorComponent1.Write(stgbk)
                Loop

                Dim
stgbk1((Pointout_YmotorComponent1.NumberOfChannelsToWrite) - 1) As Double
                stgbk1(0) = 0
                Pointout_YmotorComponent1.Write(stgbk1)


            Case z_down1

                vdata = Pointread_ZlvdtComponent1.Read
                zdata0 = vdata
                zdata = zdata0

                Do While zdata(0) > zcoord
                    nvdata = Pointread_ZlvdtComponent1.Read
                    zdata = nvdata

                    Dim
stgdwn((Pointout_ZmotorComponent1.NumberOfChannelsToWrite) - 1) As Double
                    stgdwn(0) = -5
                    Pointout_ZmotorComponent1.Write(stgdwn)

                Loop

                Dim
stgdwn1((Pointout_ZmotorComponent1.NumberOfChannelsToWrite) - 1) As Double
                stgdwn1(0) = 0
                Pointout_ZmotorComponent1.Write(stgdwn1)


            Case z_up1
                vdata = Pointread_ZlvdtComponent1.Read
                zdata0 = vdata
                zdata = zdata0

                Do While zdata(0) < zcoord
                    nvdata = Pointread_ZlvdtComponent1.Read
```

```vbnet
                        zdata = nvdata

                        Dim
stgup((Pointout_ZmotorComponent1.NumberOfChannelsToWrite) - 1) As Double
                        stgup(0) = 5
                        Pointout_ZmotorComponent1.Write(stgup)

                    Loop

                        Dim
stgdwn1((Pointout_ZmotorComponent1.NumberOfChannelsToWrite) - 1) As Double
                        stgdwn1(0) = 0
                        Pointout_ZmotorComponent1.Write(stgdwn1)

                Case x_right2
                    vdata = Pointread_XlvdtComponent1.Read
                    xdata0 = vdata
                    xdata = xdata0

                    Do While xdata(0) > xcoord
                        nvdata = Pointread_XlvdtComponent1.Read
                        xdata = nvdata

                        Dim
stgrt((Pointout_XmotorComponent1.NumberOfChannelsToWrite) - 1) As Double
                        stgrt(0) = -10
                        Pointout_XmotorComponent1.Write(stgrt)
                    Loop

                        Dim
stgrt1((Pointout_XmotorComponent1.NumberOfChannelsToWrite) - 1) As Double
                        stgrt1(0) = 0
                        Pointout_XmotorComponent1.Write(stgrt1)


                Case x_left2
                    vdata = Pointread_XlvdtComponent1.Read
                    xdata0 = vdata
                    xdata = xdata0

                    Do While xdata(0) < xcoord
                        nvdata = Pointread_XlvdtComponent1.Read
                        xdata = nvdata

                        Dim
stglft((Pointout_XmotorComponent1.NumberOfChannelsToWrite) - 1) As Double
                        stglft(0) = 10
                        Pointout_XmotorComponent1.Write(stglft)
                    Loop

                        Dim
stglft1((Pointout_XmotorComponent1.NumberOfChannelsToWrite) - 1) As Double
                        stglft1(0) = 0
                        Pointout_XmotorComponent1.Write(stglft1)

                Case y_front2
                    vdata = Pointread_YlvdtComponent1.Read
```

223

```vbnet
                ydata0 = vdata
                ydata = ydata0

                Do While ydata(0) > ycoord
                    nvdata = Pointread_YlvdtComponent1.Read
                    ydata = nvdata

                    Dim
stgfrnt((Pointout_YmotorComponent1.NumberOfChannelsToWrite) - 1) As Double
                    stgfrnt(0) = -10
                    Pointout_YmotorComponent1.Write(stgfrnt)
                Loop

                Dim
stgfrnt1((Pointout_YmotorComponent1.NumberOfChannelsToWrite) - 1) As Double
                    stgfrnt1(0) = 0
                    Pointout_YmotorComponent1.Write(stgfrnt1)


            Case y_back2
                vdata = Pointread_YlvdtComponent1.Read
                ydata0 = vdata
                ydata = ydata0

                Do While ydata(0) < ycoord
                    nvdata = Pointread_YlvdtComponent1.Read
                    ydata = nvdata

                    Dim
stgbk((Pointout_YmotorComponent1.NumberOfChannelsToWrite) - 1) As Double
                    stgbk(0) = 10
                    Pointout_YmotorComponent1.Write(stgbk)
                Loop

                Dim
stgbk1((Pointout_YmotorComponent1.NumberOfChannelsToWrite) - 1) As Double
                    stgbk1(0) = 0
                    Pointout_YmotorComponent1.Write(stgbk1)



        End Select
    End Sub

    Private Sub getcoordinates_Click(ByVal sender As System.Object, ByVal e
As System.EventArgs) Handles getcoordinates.Click
        ' get the current location of the tip w.r.t stage and use as origin
value

        zcoord = -1
        xcoord = 0.2
        ycoord = 0.6

        maxindents2 = ((NumericEdit_scanlength.Value * 1000 /
NumericEdit_indentspacing.Value))
        NumericEdit_linearindents.Value = maxindents2
```

```
        Llocation = NumericEdit_scanlength.Value * 1000 /
NumericEdit_indentspacing.Value
        Blocation = NumericEdit_scanbreadth.Value * 1000 /
NumericEdit_indentspacing.Value
        maxindents = Llocation * Blocation
        NumericEdit_squareprofile.Value = maxindents

        MsgBox("Do you want to proceed with the test?")
        MsgBox("Press Start button")

    End Sub


    Private Sub linearscan()
        progress = 0
        indentnum = 0
        totalindents = 0
        XL = (Llocation - Llocation)
        YL = Llocation
        ' scanning in x direction
        If CheckBox1.Checked = True Then
            maxindents1 = NumericEdit_override.Value
        Else
            maxindents1 = maxindents2
        End If

        'progressincr = 100 / maxindents1

        Do While totalindents < (maxindents1)

            If CheckBox2.Checked = True Then

                Do While indentnum < ((maxindents2)) ' defining number of
indents per scan line

                    Scannsave()
                    'ProgressBar1.Value = progress
                    indentlocationx = indentlocationx + 1
                    vzdata = Pointread_ZlvdtComponent1.Read
                    XL = XL + 1
                    ScatterGraph2.PlotXYAppend(XL, YL)
                    If vzdata(0) > zcoord Then
                        Run((z_down1)) 'move the stage toward z down (see
section Run for detail)
                    Else
                        Run((z_up1)) 'move the stage toward z up (see section
Run for detail)
                    End If
                    Run((x_right1)) 'move the stage and sample toward x left
(see section Run for detail)

                    bv = 0
                    While bv < 2000 ' 120 sec pause to lets ripples settle
                        bv = bv + 1
                    End While
                    bv = 0
```

```vb
                Loop

                indentnum = 0
            End If
        Loop
    End Sub


    Private Sub squarescan()
        Dim marker As Object

        progress = 0
        indentnum = 0
        marker = 0
        totalindents = 0
        XXL = ((Llocation - Llocation) + 1)
        XXLmax = Llocation
        YYLmax = Blocation
        YYL = Blocation + 1
        Dim pointer As Object = 0
        'progressincr = 100 / maxindents

        If CheckBox1.Checked = True Then
            maxindents1 = NumericEdit_override.Value
        Else
            maxindents1 = maxindents
        End If

        ' scanning in x direction
        Do While totalindents < maxindents1

            If marker = 0 Then

                Do While indentnum < ((maxindents2)) ' defining number of
indents per scan line
                    indentlocationx = indentlocationx + 1

                    If XXL > XXLmax Then
                        pointer = 1
                        YYL = YYL - 1
                        XXL = XXL - 1
                    End If

                    If XXL < 2 Then
                        pointer = 0
                        YYL = YYL - 1
                    End If

                    Scannsave()
                    'ProgressBar1.Value = progress
                    ScatterGraph2.PlotXYAppend(XXL, YYL)

                    If pointer = 0 Then
                        XXL = XXL + 1
                    Else
```

```
                        XXL = XXL - 1
                    End If

                    vzdata = Pointread_ZlvdtComponent1.Read

                    If vzdata(0) > zcoord Then
                        Run((z_down1)) 'move the stage toward z down (see
section Run for detail)
                    Else
                        Run((z_up1)) 'move the stage toward z up (see section
Run for detail)
                    End If

                    Run((x_right1)) 'move the stage and sample toward x left
(see section Run for detail)

                    bv = 0
                    While bv < 2000 ' 120 sec pause to lets ripples settle
                        bv = bv + 1
                    End While
                    bv = 0

                Loop
                marker = 1
                indentnum = 0


            End If

            Run((y_back1)) 'move the stage and sample toward y back away from
user(see section Run for detail)
            indentlocationy = indentlocationy + 1

            If marker = 1 Then

                Do While indentnum < (maxindents2) ' defining number of
indents per scan line

                    indentlocationx = indentlocationx - 1

                    If XXL > XXLmax Then
                        pointer = 1
                        YYL = YYL - 1
                        XXL = XXL - 1
                    End If

                    If XXL < 2 Then
                        pointer = 0
                        YYL = YYL - 1
                    End If

                    Scannsave()


                    'ProgressBar1.Value = progress
                    ScatterGraph2.PlotXYAppend(XXL, YYL)
```

227

```vb
                    If pointer = 0 Then
                        XXL = XXL + 1
                    Else
                        XXL = XXL - 1
                    End If

                    vzdata = Pointread_ZlvdtComponent1.Read

                    If vzdata(0) > zcoord Then
                        Run((z_down1)) 'move the stage toward z down (see
section Run for detail)
                    Else
                        Run((z_up1)) 'move the stage toward z up (see section
Run for detail)
                    End If


                    Run((x_left1)) 'move the stage and sample toward x right
(see section Run for detail)

                    bv = 0
                    While bv < 2000 ' 120 sec pause to lets ripples settle
                        bv = bv + 1
                    End While
                    bv = 0

                Loop
                marker = 0
                indentnum = 0


            End If
        Loop

    End Sub


    Private Sub Scannsave()

        fs = 100
        fc = 1
        order = 1

        ltempdata = Pointread_dvrtComponent1.Read

        ldata0 = ltempdata
        lndata = ldata0

        i = 0
        j = 0
        t = 0

        dconst = NumericEdit_dconst.Value 'microns/volt
        ldconst = NumericEdit_ldconst.Value / NumericEdit_gain.Value
'microns/volt
        lconst = NumericEdit_lconst.Value / NumericEdit_gain.Value
```

```vb
        Do While lndata(0) < (ldata0(0) + (NumericEdit_maxload.Value) / (1000
* lconst)) ' micro newton

            Dim stgdwn((Pointout_ZmotorComponent1.NumberOfChannelsToWrite) -
1) As Double
            'stgdwn(0) = -3
            stgdwn(0) = -2.5
            Pointout_ZmotorComponent1.Write(stgdwn)


            ltempdata2 = Pointread_dvrtComponent1.Read
            lndata = ltempdata2
            ldata(i) = lndata(0)
            load_ldata(i) = ltempdata2
            dtempdata = Pointread_displlvdtComponent1.Read
            ddata(i) = dtempdata(0)
            load_ddata(i) = dtempdata

            ScatterGraph1.PlotXYAppend(ddata(i), ldata(i)) 'plot the acquired
data on trace monitor

            i = i + 1
            j = j + 1
            t = t + 1

        Loop

        i1 = i
        j1 = 0
        bv = 0




        Dim stg((Pointout_ZmotorComponent1.NumberOfChannelsToWrite) - 1) As
Double
        stg(0) = 0
        Pointout_ZmotorComponent1.Write(stg)

        vddata = Pointread_ZlvdtComponent1.Read
        zddata0 = vddata
        zddata = zddata0

        dconst = NumericEdit_dconst.Value 'microns/volt
        ldconst = NumericEdit_ldconst.Value / NumericEdit_gain.Value
'microns/volt
        lconst = NumericEdit_lconst.Value / NumericEdit_gain.Value


        'highlight from here to get rid of pause for stress relaxation

        ' While bv < (holdtime.Value * 9000)      '1500 = 10 sec


        'Dim stg9((Pointout_ZmotorComponent1.NumberOfChannelsToWrite) - 1) As
Double
        'stg9(0) = 0
        'Pointout_ZmotorComponent1.Write(stg9)
```

```vbnet
        'ltempdata2 = Pointread_dvrtComponent1.Read
        'lndata = ltempdata2
        '' ldata(i) = lndata(0)
        'load_ldata(i) = ltempdata2
        'dtempdata = Pointread_displlvdtComponent1.Read
        'ddata(i) = dtempdata(0)
        'load_ddata(i) = dtempdata

        'ScatterGraph1.PlotXYAppend(ddata(i), ldata(i)) 'plot the acquired
data on trace monitor



        ' bv = bv + 1
        'i = i + 1
        'j = j + 1
        'gbWriteHeader = True
        'End While



        'i1 = i
        'j1 = 0
        'bv = 0
        'highlight till here to get rid of pause for stress relaxation


        dconst = NumericEdit_dconst.Value 'microns/volt
        ldconst = NumericEdit_ldconst.Value / NumericEdit_gain.Value
'microns/volt
        lconst = NumericEdit_lconst.Value / NumericEdit_gain.Value

        Do While System.Math.Abs(zddata(0) - zddata0(0)) <
((NumericEdit_pullup.Value / 100) * 0.7918) 'telling z-motor to move up
integer*100 microns
            nvddata = Pointread_ZlvdtComponent1.Read
            zddata = nvddata

            Dim stg1((Pointout_ZmotorComponent1.NumberOfChannelsToWrite) - 1)
As Double
            'stg1(0) = 3
            stg1(0) = 2.5

            Pointout_ZmotorComponent1.Write(stg1)

            ''highlight from here for stress relaxation

            ltempdata = Pointread_dvrtComponent1.Read
            ldata(j) = (ltempdata(0) - 0.0953)
            unload_ldata(j1) = ltempdata

            dtempdata = Pointread_displlvdtComponent1.Read
            ddata(j) = dtempdata(0)
            unload_ddata(j1) = dtempdata
```

```vb
            ScatterGraph1.PlotXYAppend(ddata(j), ldata(j)) 'plot the acquired
data on trace monitor

            j = j + 1
            j1 = j1 + 1
            t = t + 1
            gbWriteHeader = True

            ''highlight till here for stress relaxation

        Loop

        Dim stg2((Pointout_ZmotorComponent1.NumberOfChannelsToWrite) - 1) As
Double
        stg2(0) = 0
        Pointout_ZmotorComponent1.Write(stg2)

        ' bfldata = CWDSP1.BwLPF(ldata, fs, fc, order) ' butterworth
filtering load data for an order n
        ' bfdata = CWDSP1.BwLPF(ddata, fs, fc, order)
        ' load_bfdata = CWDSP1.BwLPF(load_ldata, fs, fc, order)
        'unload_bfdata = CWDSP1.BwLPF(unload_ldata, fs, fc, order)
        'time1.Value = t

        imax = j
        ifile = FreeFile()
        If CheckBox3.Checked = True Then
            FileOpen(ifile, "D:/Mesomechdata/" & totalindents &
inputfilename.Text & ".csv", OpenMode.Append)
        End If
        For i = 0 To (j - 1)
            WriteLine(ifile, ddata(i), ldata(i))

        Next i
        FileClose(ifile)

        ltempdata(0) = 0
        dtempdata(0) = 0
        Dim hlt((Pointout_ZmotorComponent1.NumberOfChannelsToWrite) - 1) As
Double
        hlt(0) = 0
        Pointout_ZmotorComponent1.Write(hlt)

        Dim hlt1((Pointout_XmotorComponent1.NumberOfChannelsToWrite) - 1) As
Double
        hlt1(0) = 0
        Pointout_XmotorComponent1.Write(hlt1)

        Dim hlt2((Pointout_YmotorComponent1.NumberOfChannelsToWrite) - 1) As
Double
        hlt2(0) = 0
        Pointout_YmotorComponent1.Write(hlt2)
        indentnum = indentnum + 1
        totalindents = totalindents + 1
        progress = progress + progressincr

    End Sub
```

231

```vb
    Private Sub Baselinecollection_Click(ByVal sender As System.Object, ByVal
e As System.EventArgs) Handles Baselinecollection.Click
        ifile = FreeFile()

        If CheckBox3.Checked = True Then
            FileOpen(ifile, "D:/Mesomechdata/" & inputfilename.Text & ".csv",
OpenMode.Append)
        End If
        For i = 0 To 10000
            ltempdataX = Pointread_dvrtComponent1.Read
            dtempdataX = Pointread_displlvdtComponent1.Read
            WriteLine(ifile, dtempdataX(0), ltempdataX(0))
        Next i
        FileClose(ifile)
        MsgBox("Baseline collected")
    End Sub




    Private Sub NumericEdit_pullup_AfterChangeValue(ByVal sender As
System.Object, ByVal e As
NationalInstruments.UI.AfterChangeNumericValueEventArgs) Handles
NumericEdit_pullup.AfterChangeValue

    End Sub

    Private Sub NumericEdit_dconst_AfterChangeValue(ByVal sender As
System.Object, ByVal e As
NationalInstruments.UI.AfterChangeNumericValueEventArgs) Handles
NumericEdit_dconst.AfterChangeValue

    End Sub

    Private Sub Form1_Load(ByVal sender As System.Object, ByVal e As
System.EventArgs) Handles MyBase.Load

    End Sub

    Private Sub NumericEdit_scanlength_AfterChangeValue(ByVal sender As
System.Object, ByVal e As
NationalInstruments.UI.AfterChangeNumericValueEventArgs) Handles
NumericEdit_scanlength.AfterChangeValue

    End Sub

    Private Sub NumericEdit_lconst_AfterChangeValue(ByVal sender As
System.Object, ByVal e As
NationalInstruments.UI.AfterChangeNumericValueEventArgs) Handles
NumericEdit_lconst.AfterChangeValue

    End Sub
```

```
    Private Sub NumericEdit_ldconst_AfterChangeValue(ByVal sender As
System.Object, ByVal e As
NationalInstruments.UI.AfterChangeNumericValueEventArgs) Handles
NumericEdit_ldconst.AfterChangeValue

    End Sub

    Private Sub NumericEdit_maxload_AfterChangeValue(ByVal sender As
System.Object, ByVal e As
NationalInstruments.UI.AfterChangeNumericValueEventArgs) Handles
NumericEdit_maxload.AfterChangeValue

    End Sub

    Private Sub NumericEdit_gain_AfterChangeValue(ByVal sender As
System.Object, ByVal e As
NationalInstruments.UI.AfterChangeNumericValueEventArgs) Handles
NumericEdit_gain.AfterChangeValue

    End Sub

    Private Sub Pointread_dvrtComponent1_ReadCompleted(ByVal sender As
System.Object, ByVal e As
ContinuousAcquire.Pointread_dvrtComponentReadCompletedEventArgs) Handles
Pointread_dvrtComponent1.ReadCompleted

    End Sub

    Private Sub Label23_Click(ByVal sender As System.Object, ByVal e As
System.EventArgs) Handles Label23.Click

    End Sub

    Private Sub NumericEdit2_AfterChangeValue_1(ByVal sender As
System.Object, ByVal e As
NationalInstruments.UI.AfterChangeNumericValueEventArgs) Handles
NumericEdit2.AfterChangeValue

    End Sub
End Class
```

Mesoindenter calibration

The custom built indentation system has following components that need to be calibrated in order to measure the modulus accurately;

- X & Y motor stage LVDT's

- Stage displacement LVDT

- Z displacement LVDT

- Cantilever (load) calibration

The calibration should be done in the order given below.

Materials:

- Dial gauge

- 2 x Digital multimeter (DMM)

Displacement LVDT Calibration:

- Place the dial gauge such that the measuring pin rests on the stage.

- Connect the DMM between terminal 28 and ground (GND) on the SCB 68 board.

- Press the master reset button on the GUI. Note the reading on the dial gauge in inches and the DMM reading. Dial gauge reading changes in steps of 0.001 inches. E.g. if the arrow is at 2 and goes down by 2 marks ➔ 1.998.

- Now move the stage in steps of 100 microns using the software till the DMM reading goes to 10 volts.

- Convert the dial gauge readings from inches to microns and plot displacement vs voltage and find the slope of the linear regression for the curve (μm/V).

- Repeat it a couple of times and average the values to get the "dconst".

Z LVDT calibration:

- Placement of the dial gauge is same as the previous calibration. DMM is now connected between pin 68 and GND.

- Follow the same procedure as the displacement LVDT calibration and find the slope of the linear regression line. This is "zconst".

Load calibration:

- Remove the tip from the cantilever and flatten out any bumps in cantilever caused during removal of the tip.

- Invert the Z stage such that the tip face of the cantilever faces the ceiling.

- Connect the DMM between the actual DVRT output voltage and not the amplified voltage and GND.

- Measure weights of paper disks punched out of standard bond paper in grams. Now place the disks one by one on top of each other every time noting the voltage. Calibrate for a change of 0.5 volts.

- Plot the Load vs. Volt (mN/volt) curve and get slope of the linear regression which gives you the load constant "lconst".

7.14. Force measurement device

- Based on the stiffness of the sample, select aluminum cantilever of appropriate dimension.

- Glue the sample on one end to the cantilever and other end to the adjustable stage.

- Pipette a few drops of PBS around the sample and gently move the stage to test if the sample is not glued to the base. Add PBS to submerge the sample and the DVRT.

- Enter the duration of the test in mins and the voltage on the smaller Elenco voltage supply. This is a backup to verify the signal captured is of the DVRT.

- The design schematics of the device are shown below.

1.000   .750   2" nom.   1.375

1.000

.250

0-Rings
I.D.

R=1/8"

.752

.700
.875

1.875

2.125

3.000

3.250

3.500

Pashqar
PSvarde
@syl.edu

1.335
.187   1.600
.250   oal.
.700   10-32

.500
.250   .793

sliding shoe

2-115
O-Ring

1.625

1.375

O

.375
.500
.750
.875

3/8

1.100

1.750

R   small hole .032" &

1.250   1.218"

Dick Chase

1-19-12

236

tap 4-40

tap 2-56

1.500

x 1/4 thk.
acrylic

.50

.250

1.125

.125

clear + c'bore
4-40 slits

1.375

1.875

2.000

.753"∅

top
clear
4-40

x 1/4" thk.
aluminum
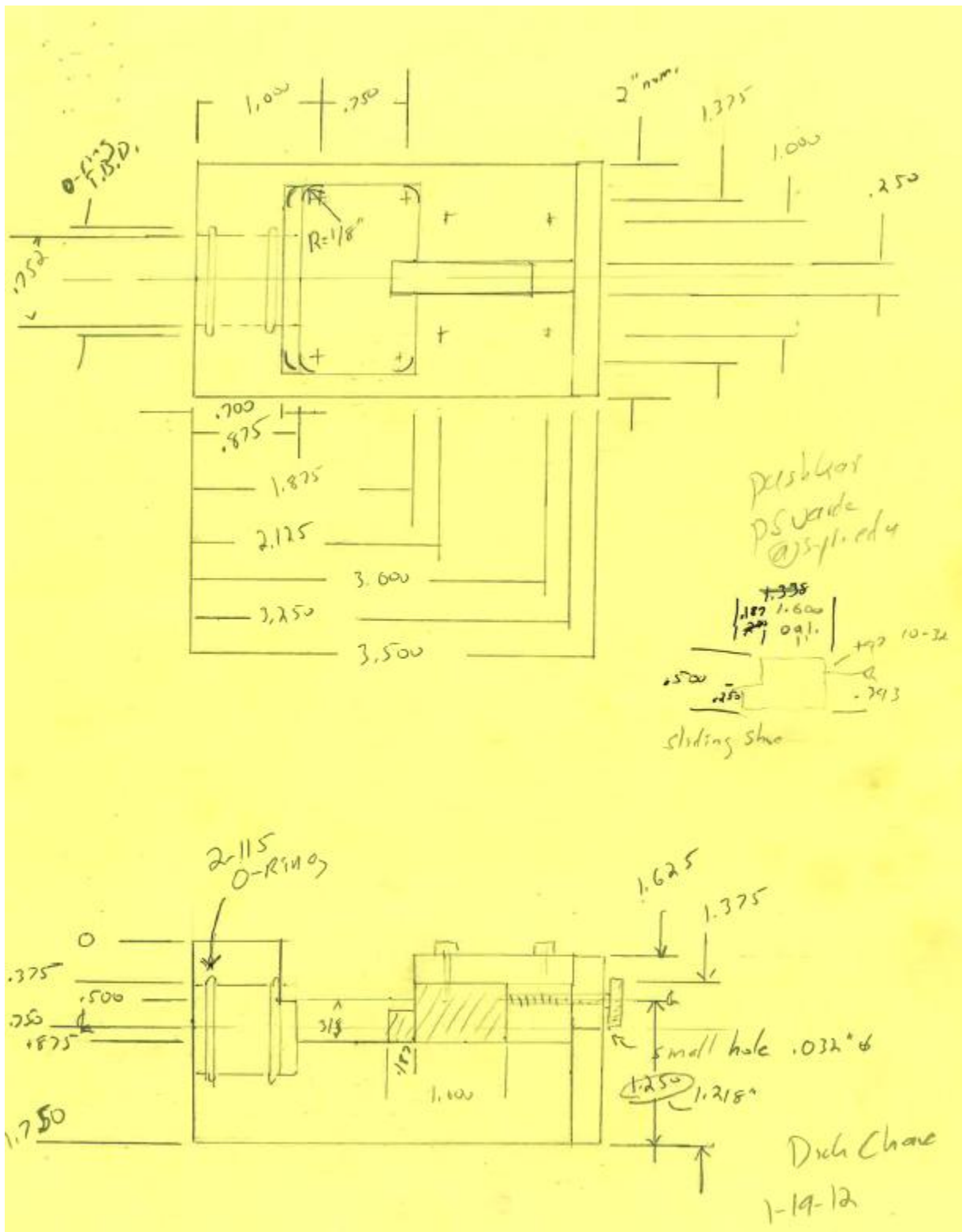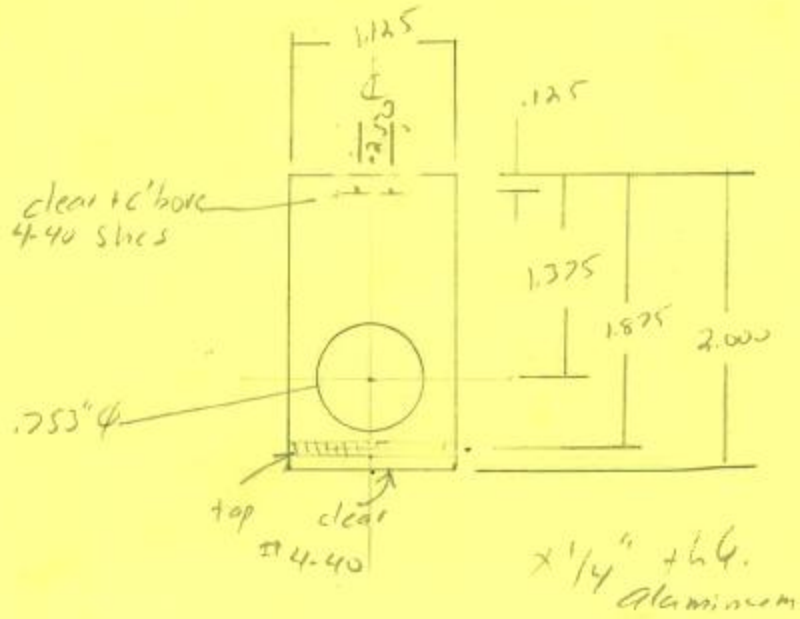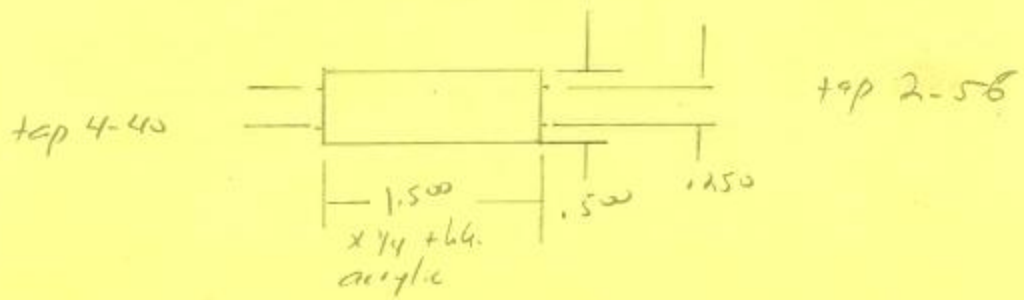
Pushkar / Golbert

new clamp   2-15-12

Drill Chuck
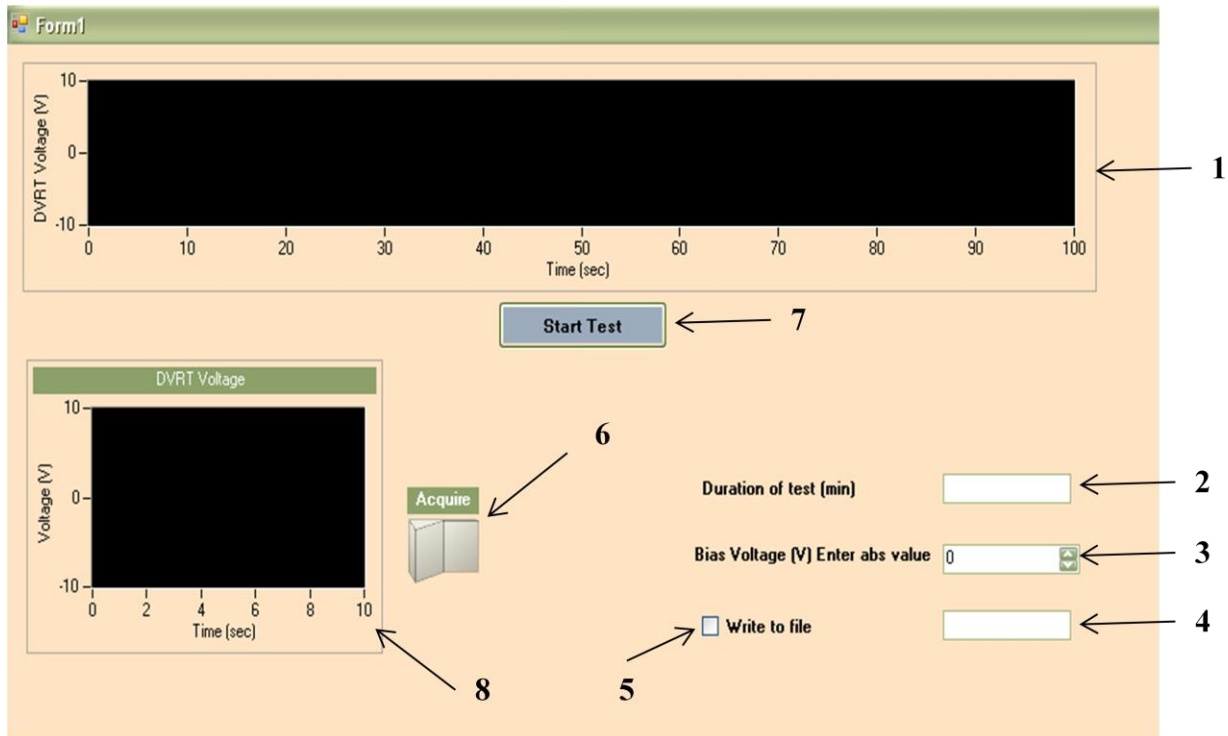
Button #	Name	Description
1	Graph 1	Displays the live force voltage signal
2	Test duration	Enter the total duration of test in minutes
3	Bias voltage value	Voltage from the elenco bioa power supply
4	File name	Enter the file name starting with " _ "
5	Write to file	Select this to ensure the file gets created
6	Acquire	This button will activate graph 2 and show the raw voltage level
7	Start test	Pressing this button will start data acquisition
8	Graph 2	Shows the raw voltage level

************Code for Force measurement device***********

```vb
Public Class Form1
    Dim dvrtdata As Object
    Dim dvrtdata1 As Object
    Dim dvrttempdata As Object
    Dim dvrtRawdata As Object
    Dim dvrtRawdata1 As Object
    Dim dvrtRawtempdata As Object
    Dim datapoint As Object
    Dim biasvoltage As Object
    Dim i As Object
    Dim p As Object
    Dim k As Object
    Dim ifile As Short
    Dim stopwatch As New Stopwatch()
    Dim elapsedTime As Object
    Dim elapsedTimeArray(90000) As Object
    Dim dataArray(90000) As Object
    Dim dataArrayRaw(90000) As Object
    Dim datapointnumber(90000) As Object

    'Private Sub Switch1_StateChanged(ByVal sender As System.Object, ByVal e
As NationalInstruments.UI.ActionEventArgs) Handles Switch1.StateChanged
    'Try
    'If Switch1.Value Then
    ' DaqTask2Component1.StartRead()
    'Else
    '    DaqTask2Component1.StopRead()
    'End If
    'Catch ex As NationalInstruments.DAQmx.DaqException
    'MessageBox.Show(ex.Message, "DAQ Error", MessageBoxButtons.OK,
MessageBoxIcon.Warning)
    'Switch1.Value = False
    'End Try
    'End Sub

    ' Private Sub DaqTaskComponent1_DataReady(ByVal sender As System.Object,
ByVal e As DaqApplication1.DaqTask2ComponentDataReadyEventArgs) Handles
DaqTask2Component1.DataReady
    'Dim acquiredData() As NationalInstruments.AnalogWaveform(Of Double) =
e.GetData
    'WaveformGraph1.PlotWaveforms(acquiredData)
    'End Sub

    Private Sub Start_Test_Click(ByVal sender As System.Object, ByVal e As
System.EventArgs) Handles Start_Test.Click
        'Stopwatch timer starts when the DVRT begins reading data'
        stopwatch.Start()

        datapoint = 0
        i = 0
        k = 1
        p = 0

        'Stopwatch elapsed time is read'
```

239

```vbnet
        elapsedTime = stopwatch.Elapsed.TotalSeconds

        'The DVRT reads data as long as the elapsed stopwatch time that was
just read is within the amount of time entered by user'
        While elapsedTime <= (testduration.Text * 60)

            elapsedTime = stopwatch.Elapsed.TotalSeconds 'Stopwatch elapsed
time is read'
            'DVRT data is recorded along with elapsed time approximately
every second'
            If ((elapsedTime > (0.99 * k)) AndAlso (elapsedTime < (1 * k)))
Then

                elapsedTime = stopwatch.Elapsed.TotalSeconds 'elapsed time
recorded'

                If (p = 4) Then

                    dvrttempdata = DVRT_pointread.Read 'DVRT data recorded'
                    dvrtRawtempdata = RawDVRT_pointread.Read 'RawDVRT data
recorded'

                    biasvoltage = biasvolt.Value

                    dvrtdata = dvrttempdata
                    dvrtRawdata = dvrtRawtempdata

                    dataArray(i) = (dvrtdata(0) / 22.55) + biasvoltage 'Array
records all DVRT data'
                    dataArrayRaw(i) = dvrtRawdata(0) 'Array records all DVRT
data'

                    datapointnumber(i) = datapoint
                    elapsedTimeArray(i) = elapsedTime 'Array records all
elapsed time data'

                    'collected DVRT and elapsed time data are graphed on the
user interface'
                    ScatterGraph2.PlotXYAppend(elapsedTimeArray(i),
dataArrayRaw(i))
                    p = 0
                    i = i + 1
                End If

                k = k + 1

                p = p + 1

            End If
            datapoint = datapoint + 1
            elapsedTime = stopwatch.Elapsed.TotalSeconds
            'Stopwatch elapsed time is read so it can be used in the while
loop'

        End While
        stopwatch.Stop() 'At the end of collection, stopwatch is stopped and
reset to 0'
```

```vb
        stopwatch.Reset()

        'Write to file'
        ifile = FreeFile()
        If CheckBox1.Checked = True Then
            FileOpen(ifile, "D:/Mesomechdata/" & filename.Text & ".csv",
OpenMode.Append)
        End If
        For i = 0 To (i - 1)
            WriteLine(ifile, elapsedTimeArray(i), dataArray(i),
dataArrayRaw(i))

            'Written file closed/saved and user is alerted of test end'
        Next i
        FileClose(ifile)
        MsgBox("Test Done. File is saved")

        datapoint = 0
        i = 0

    End Sub

    Private Sub CheckBox1_CheckedChanged(ByVal sender As System.Object, ByVal
e As System.EventArgs) Handles CheckBox1.CheckedChanged

    End Sub

    Private Sub Label2_Click(ByVal sender As System.Object, ByVal e As
System.EventArgs) Handles Label2.Click

    End Sub


    Private Sub DVRT_pointread_ReadCompleted(ByVal sender As System.Object,
ByVal e As DaqApplication1.DaqTask1ComponentReadCompletedEventArgs) Handles
DVRT_pointread.ReadCompleted

    End Sub

    Private Sub DaqTask2Component1_ReadCompleted(ByVal sender As
System.Object, ByVal e As
DaqApplication1.DaqTask2ComponentReadCompletedEventArgs) Handles
DaqTask2Component1.ReadCompleted

    End Sub

    Private Sub RawDVRT_pointread_ReadCompleted(ByVal sender As
System.Object, ByVal e As
DaqApplication1.DaqTask3ComponentReadCompletedEventArgs) Handles
RawDVRT_pointread.ReadCompleted

    End Sub
End Class
```

7.15. Mechanical stretch device

The device design is shown below. The GUI is provided free by the manufacturer of the stepper motor. The unit containing the temperature control PID (Gilbert Lab) is the only floating piece of equipment. Check availability before planning experiment. Perform the following steps in the same order as below to effectively get the device operational.

- Make sure all the power cables are disconnected.

- Place the device on the vibration isolation table on a paper towel mat to soak media if any leak occurs.

- Connect the Serial cable from the temperature control PID to the device and power the controller.

- Next switch on the PID supply (red button) which will turn the display on which should show the current and desired temperatures.

- Turn the 5% CO2 tank regulator on. It should be set to 4-5 psi for the output valve pressure. This should provide a CO_2 flow of 2 bubbles / second. Insert the tube into the port on the device after confirming steady flow of CO_2.

- Next connect the motor control cable to the motor controller module.

- Connect the 20V 3A supply cable to the controller.

- Connect the USB to RS485 adapter to the PC and plug the other end of RS485 into the motor controller module. Turn power on for the power supply.

- Click on the "CRK motion creator" icon on the desktop to launch the GUI.

- Select the proper COM port (Currently set to 3) and that should connect the device to the PC.

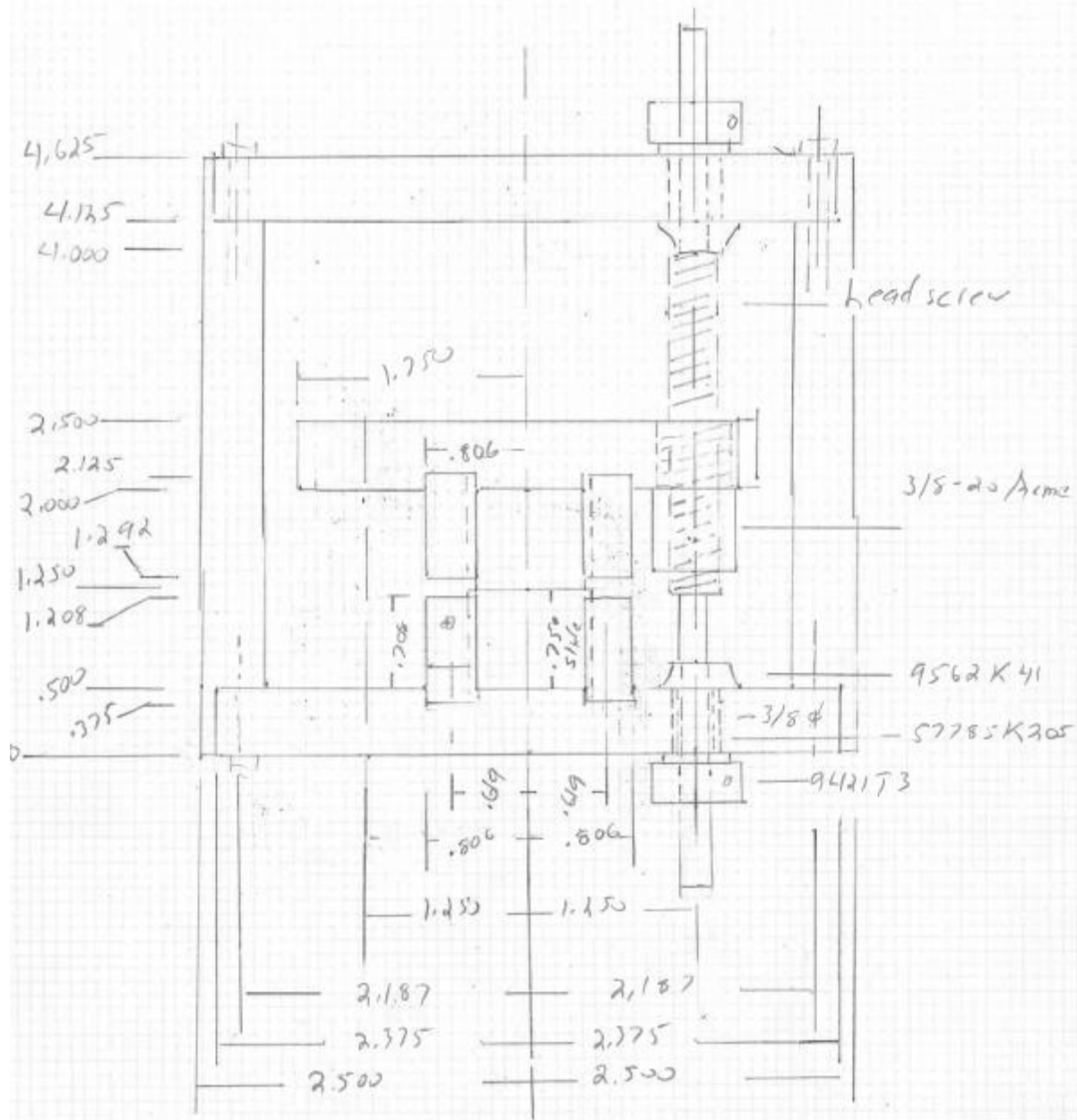- The GUI should read connected for both port and motor.

Pushkar Varde Device

Drill Chuck 6-11-14

$842.14
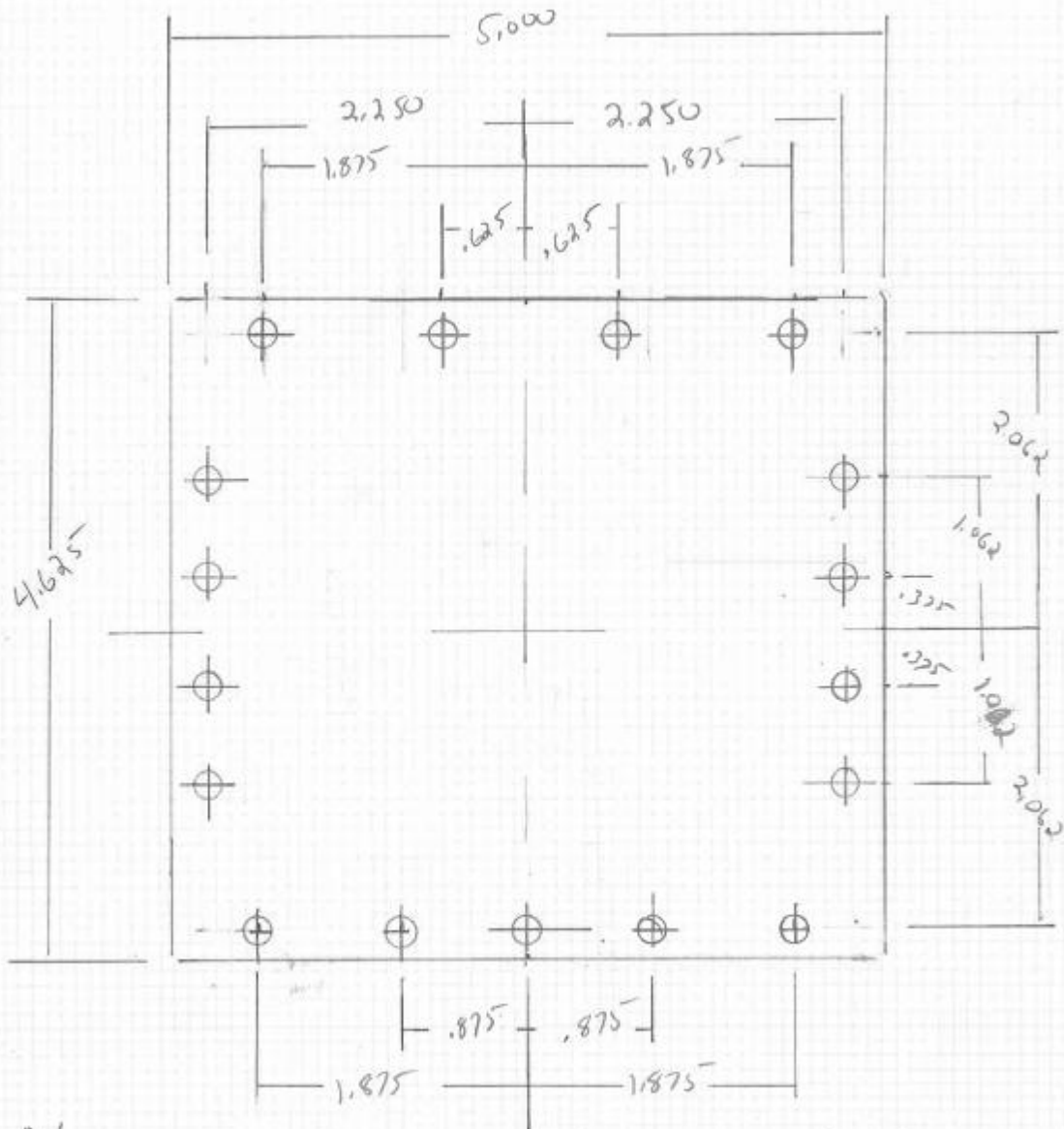
1/2 x 1" S.S. Frame

Lead screw

3/8-20 Acme

9562 K 41

57785 K 305

9421 T 3

4.625
4.125
4.000
1.750
2.500
2.125
2.000
1.292
1.250
1.208
.500
.375
0

.806

-3/8 ∅

.69   .69
.806   .806
1.250 1.250
2.187 2.187
2.375 2.375
2.500 2.500

243
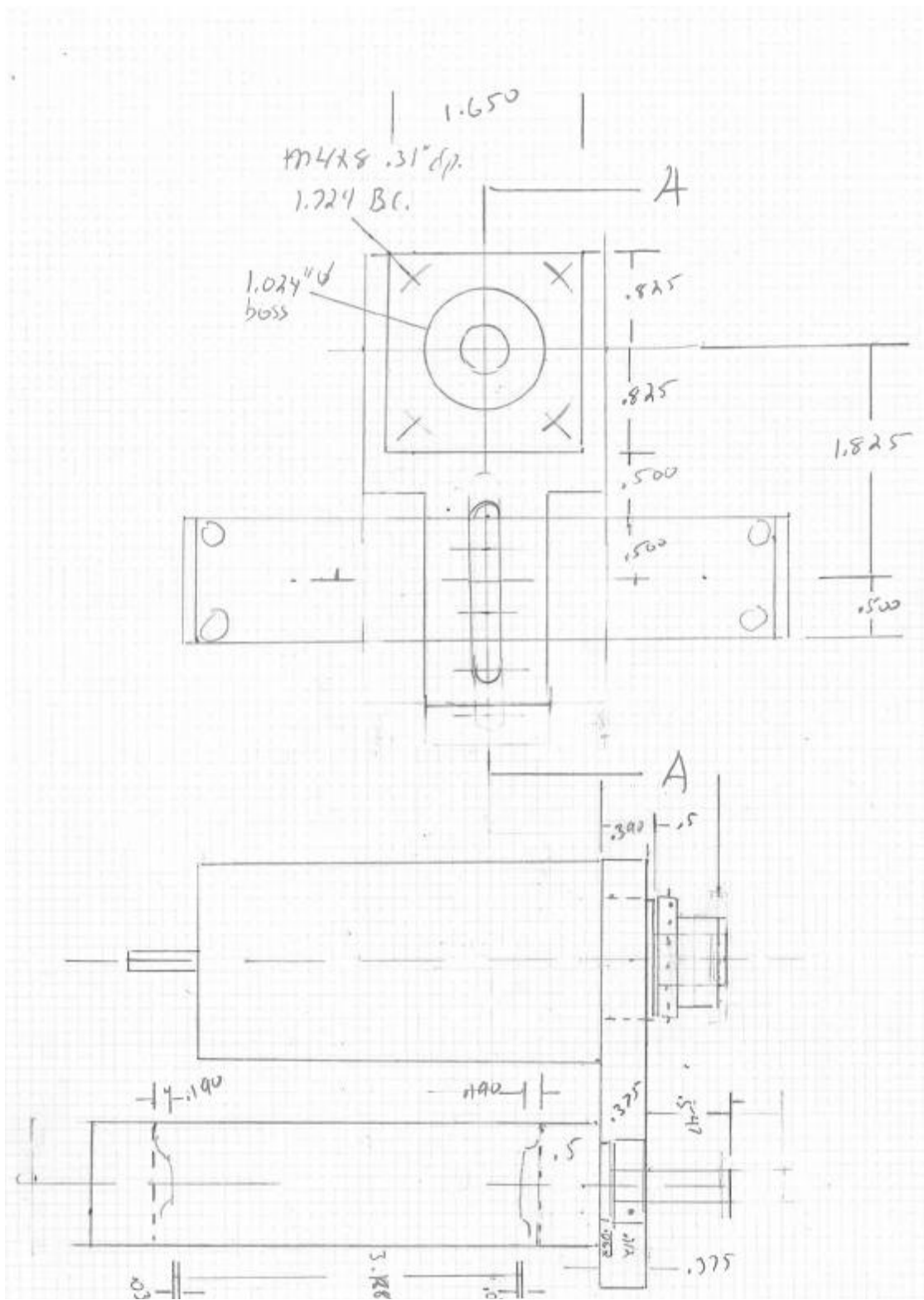
Pushkar Device
Polycarbonate & Al. Covers

5.000

2.250   2.250
1.875   1.875
.625 .625

2.062
1.062
.335
.335
1.062
2.062

4.625

Note: C'sink bottom-side for #10 Flathead
on anodized al. plate

Dick Chase   9-9-14

.875   .875
1.875   1.875

Use the following steps to calculate the parameters to feed into the GUI to control the motor speed.

**Move distance revolutions in Rev = Move distance / (Diameter * 3.14)**

Operating Pulses (DIS) = Revs * (pulses/rev)

Pulse speed = Operating pulses / (positioning time – Acceleration time)

TA = Acceleration time

TD = Deceleration time

For micro-stepping function make sure to select "High Res" and gear ratio as "25" in the system config tab. For further information check out the live demos on the website for Oriental Motor Corp.
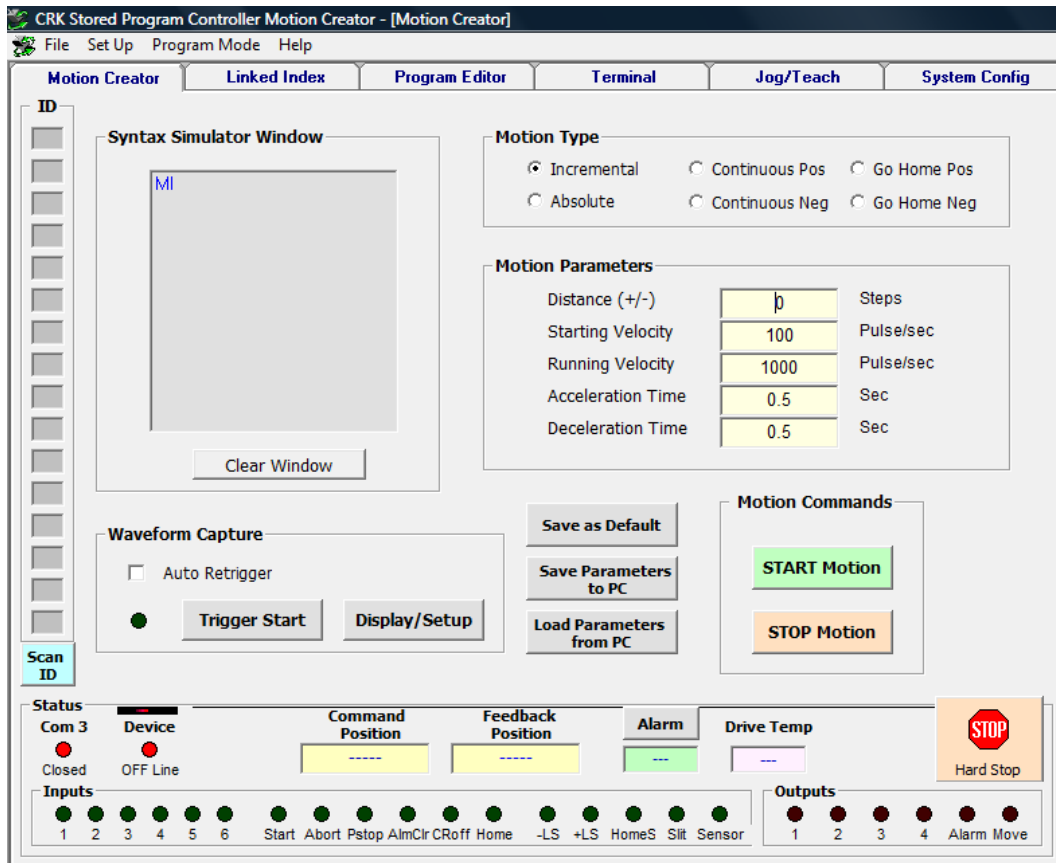
7.16. Microcontact printing of proteins using PDMS stamp

Materials:

- Silicon master

- Sylgard™ 184 (Dow Corning)

- Acetone

- Methanol

Method:

- Clean the silicon master with acetone and methanol to remove any residues.

- Dry the silicon master in a vacuum over at 100° C for 15 min.

- Mix the resin and curing agent in the ratio of 10:1 by volume using a spatula and then carefully sonicate the mixture to remove the air bubbles making sure the mixture does not contact water at any time.

- Pour this mixture on the silicon master and place it in the vacuum oven at 100° C for 1 hr.

- Remove the chip from the oven and cool it to room temperature and peel the silicone stamp off the master.

The steps performed to print the protein pattern on to the substrate are illustrated in Figure below.

- The stamps were sonicated in 70% ethanol for 30 minutes and dried under a stream of nitrogen gas.

- A 10 µg/mL laminin solution was poured onto the stamp and the inking process was carried out for 30 minutes.

- The excess protein solution was washed off and the stamps were dried under a stream of nitrogen gas and quickly brought into contact with the pre-desiccated flat surface of the polyacrylamide samples. The efficiency of pattern transfer decreases with an increase in the time between drying and stamping.

- The stamps were kept in contact with the polyacrylamide sample surface for 10 minutes and then peeled off.

- Pattern integrity was verified using fluorescent light microscopy as the protein was tagged with FITC.
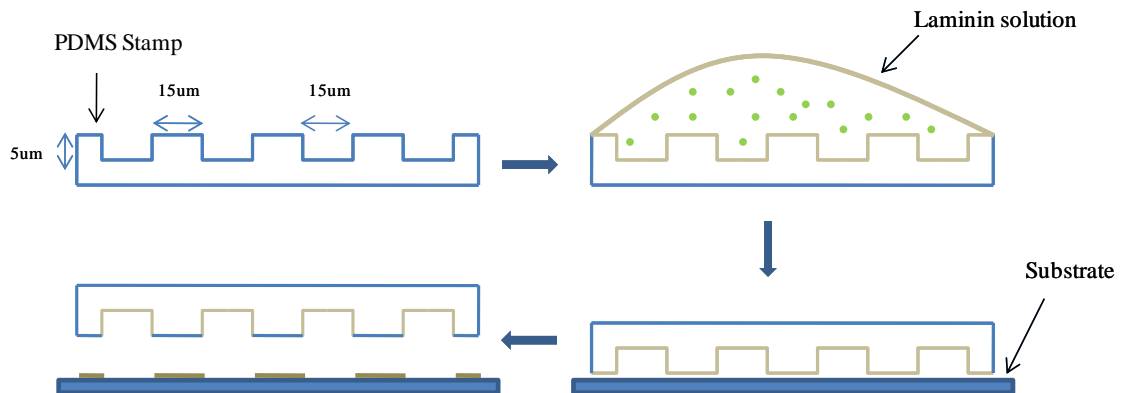
Pushkar S. Varde

Email: psvarde@syr.edu
16 Kings Court, Apt 10, Camillus, NY 13031

Ⓒ: 315-560-3666

OBJECTIVE: Researcher with over 6 years of hands-on experience in designing & characterizing natural and synthetic polymeric biomaterials seeking full time position as Scientist / Research & Development Engineer / Polymer Applications Scientist in the biomedical device and pharmaceutical industry.

EDUCATION

Ph.D. in Biomedical Engineering

Syracuse University, Syracuse, NY (GPA: 3.81/4.0)   **Feb 2015**

M.S. in Biomedical Engineering

Syracuse University, Syracuse, NY (GPA: 3.78/4.0)   **Dec 2009**

B.E. in Biomedical Engineering

Mumbai University, Mumbai, India   **May 2006**

- First class with distinction, ranked 5/120 in the graduating class.

TECHNICAL SKILLS

- Extensive experience in polymeric physics and design
- Polymer synthesis/chemistry and Polymer modification
- Proficient in material characterization techniques (SEM, EDS, ^{1}H NMR, GPC, DSC, FTIR, AFM, Rheometry)
- Expertise in designing surface and bulk mechanical characterization devices
- Six Sigma Green Belt Certification
- Experienced in analyzing mammalian cell-material interaction and polymer biocompatibility
- Fluorescence microscopy
- Statistical analysis (OriginPro, Minitab)
- Programming languages: C, C++, CVI 6.0, MATLAB, Visual Basic.
- Tools: MS office, Origin Pro., Sigma Plot, ChemDraw, SmartDraw.

PROFESSIONAL EXPERIENCE

Syracuse Biomaterials Institute, Syracuse University, NY

Research Assistant   2009-2015

- Designed a novel degradable slow shrinking hyaluronic acid based shape memory polymer hydrogel network to perform function as a mechanical actuator for soft tissue applications.
- Designed mechanical devices to measure the bulk modulus and the potential of the actuator gel network to perform work.

Syracuse Biomaterials Institute, Syracuse University, NY

Research Assistant   2006-2009

- Modified the surface mechanics and topography of polyacrylamide based hydrogels to optimize neurite outgrowth of nerve growth factor treated *pheochromocytoma* (PC-12) cells.
- Optimized a custom built sophisticated surface indentation test system to indent soft hydrogels and rat spinal cords to ascertain their elastic moduli.

- Embedded astrocytes in a 3D agarose gel matrix to mimic the astroglial scar and investigate effect of reactive astrocytes on mechanical properties of the gel matrix. Study indicated that reactive astrocytes made the 3D matrix more viscoelastic due to over secretion of ECM glycoproteins.

Bhabha Atomic Research Centre (BARC), Mumbai, India
Student Intern 2005 -2006
- Led a team in successfully designing an AI based GUI and fabricating operational hardware for a 3-channel Holter Monitoring System.

LEADERSHIP SKILLS

Hasenwinkel Lab Manager
Syracuse University, NY 2010-2015
- General lab maintenance and managing vendors to procure consumables while maintaining GMP compliance.

Syracuse Biomaterials Institute Safety Committee Representative
Syracuse University, NY 2013-2014
- Designed and implemented chemical and biological safety training protocols specific to the Institute.
- Designed and implemented entry protocols and policy for new graduate and undergraduate researchers.

Six-Sigma Green Belt Certification
Syracuse University, NY Spring 2008
- Applied Six Sigma strategies to improve correspondence efficiency and reduce communication lags at Syracuse University Project Advance, a division of the university offering advanced college level courses to local high school students.
- As the team leader, ensured the successful completion of the project with an improvement in response rate of correspondence from 60% to 90%.

Founding Member
Society for Biomaterials Student Chapter at Syracuse University
- Co-authored chapter bylaws and supervised organization of Biomaterials day at Syracuse University

TEACHING SKILLS

Graduate Teaching Assistant
BEN 468/668: Biomaterials and Medical Devices Spring 2013
BEN 231/CEN 231: Mass and Energy Balance Fall 2012
BEN 300/BIO 300/PHI 300/REL 300: Stem Cells and Society Spring 2012

LANGUAGES: Fluent in English, Hindi, and Marathi.

PROFESSIONAL AFFILIATIONS
- Society for Biomaterials (SFB)
- American Association of Pharmaceutical Scientists (AAPS)

PUBLICATIONS / CONFERENCE PROCEEDINGS / PODIUM PRESENTATIONS

Novel Crosslinked Hyaluronic Acid Based Polymeric Actuators, **Varde P**, Hasenwinkel J *(in preparation)*

Development of an Injectable Hyaluronic Acid Based Hydrogel to Facilitate Stretch Growth of Axons, **Varde P**, Hasenwinkel J, Society for Biomaterials, Denver CO, April 2014 *(**Podium presentation**).*

Crosslinked Hyaluronic Acid Hydrogel Networks Designed as Mechano-stimulators, **Varde P**, Hasenwinkel J, Conference proceedings of Society for Biomaterials, Boston MA, April 2013.

Effect of Young's Modulus Gradient on Neurite Extension in PC12 Cells, **Varde P**, Hasenwinkel J, Conference proceedings of Society for Biomaterials, Seattle WA, April 2010.

Mesoindentation of Polyacrylamide: Effects of Sample Thickness, Tip Size, Tip Geometry and Load on Young's Modulus, Saxena T, **Varde P**, Gilbert J, Hasenwinkel J, Conference proceedings of Society for Biomaterials, San Antonio TX, April 2009.

Photopolymerization and mechanical testing of polyacrylamide hydrogel scaffolds with a linear gradient in modulus, **Varde P**, Hasenwinkel J, Syracuse Biomaterials Institute offsite meeting, Syracuse, August 2008.